NTNU

Norwegian University of
Science and Technology

Integration and Stability of a Large Offshore Wind Farm with HVDC Transmission in the Norwegian Power System

Fabien Renaudin

Master of Science in Electric Power Engineering
Submission date: February 2009
Supervisor: Terje Gjengedal, ELKRAFT

Norwegian University of Science and Technology
Department of Electrical Power Engineering

Problem Description

In 1998, with the Kyoto protocol, the European states made the commitment of reducing their CO2 emissions for 2012. Based on this point of view, Norway has the goal of no net CO2 emissions for 2050. The production of electricity is one of the more polluting sectors and improvements have to be made to reduce its CO2 emissions. One of the alternatives to the classical electricity production is wind power. Norway has a great potential in this domain due to its long coasts on the North Sea. Nevertheless the exploitation of this resource implies the building of large offshore wind farms. Statkraft has great ambitions in the development wind power in Norway and the construction of a large offshore wind farm is one of its goals.

In this thesis, the emphasis will be put on the integration of a 1000MW offshore wind farm connected to the Norwegian grid with a VSC-HVDC link. Simulations will be done with different connection configurations Furthermore different connection points along the Norwegian coast will be use. Thereby an investigation on the impacts of the offshore wind farm on the onshore power system will be made in order to find the best scenario in regard of the stability and the behaviour of the grid.

Assignment given: 28. September 2008
Supervisor: Terje Gjengedal, ELKRAFT

ABSTRACT

In the last decades, due to the environmental concerns and the increase of energy demand, wind power has strongly penetrated the field of electricity generation. Today, because of the lack of onshore sites and visual and noise nuisances, the development of wind farms turns more and more to offshore and Norway has a great potential of offshore wind power.

This thesis investigates the impact of the integration of an offshore 1000MW wind farm on the Norwegian power system. Two different transmissions are used, one HVAC transmission system and one HVDC transmission system. They are installed in four different configurations which represent the possible cases of wind farm integration regarding the distance from the shore. Two different connection points have been chosen regarding the load flow simulations. The first one is situated in the region of Bergen in the West Norway and the other one is situated between Kristiansand and Stavanger in the south Norway.

In order to investigate the power stability and the behaviour of the system, simulations are performed under both steady-state and dynamic conditions by using PSS^{TM}E. Disturbances are applied in different locations on the system both near the connection point and on the offshore wind farm. The results show that the power system with large offshore wind power remains stable after the different faults. The requirements of the Norwegian Transmission System Operator, Statnett, are respected after the integration of a large offshore wind farm in the Norwegian power system.

PREFACE

The research work of this thesis has been carried out in the Department of Electrical Power Engineering of the Norwegian University of Science and Technology as part of the Electrical Power Engineering International Master program and in cooperation with Statkraft.

First I would like to thank my supervisor, Professor Terje Gjengedal for giving me the chance to write this thesis and for his help, guidance and encouragements.

I want to thank all the persons at SINTEF and Statkraft who helped me all along the advancement of my thesis. I also want to thank Knut Sommerfelt and Tobias Aigner for the time they took to help me with PSS^{TM}E.

I would like to thank all my Norwegian friends, and particularly my office workmates, who helped me for the language problems and who supported me during 5 months.

I would like to thank my French friends, Maxime and Raphaël, who supported me throughout my work.

Finally I thank my family for supporting me all the time and giving me the chance to study in Norway.

CONTENTS

LIST OF FIGURES

LIST OF TABLES

1 INTRODUCTION

In the last decades, due to the global warming, the environmental concerns and the reduction of the CO2 emissions became a priority. Norway is in this process of reduction of CO2 emissions and has the goal of no net CO2 production in 2050. Furthermore, since few years, Norway is in shortage of electrical power production and new plants have to be installed. Classical electricity generation is one of the more polluting sectors and alternative types of generation have to be found. Wind power is one of these alternatives.

Norway has a great potential in this domain due to its long coasts on the North Sea and the goal of 20TWh of annual wind generation for 2020 is realistic. Nevertheless the exploitation of this resource implies the building of large wind farms offshore. The problem with the Norwegian coast is the important depth of the sea near the coast. Actually, the technologies do not permit the construction of offshore wind farms within this range of depths. However several concepts of floating windmills, like HyWind, are under development.

With the increase of the size and distance from the shore of the offshore wind farm project, the question of connection became very important. Utilisation of offshore wind power requires a reliable and efficient transmission system. Because the offshore wind farms and the grids are AC system, the easiest transmission solution is to use High Voltage Alternative Current (HVAC) transmission systems. The advantages of this solution are that it is easy to install, it is a well-known technology and it is cost efficient. Nevertheless, the large amount of reactive power produced by the AC cables becomes a limit of this kind of transmission systems for distance superior to 75km. The solution of this problem is to use High Voltage Direct Current (HVDC) transmission systems. Two types of HVDC are available, the Line Commutated Converter HVDC (LCC-HVDC) and the Voltage Source Converter HVDC (VSC-HVDC). The first one is a well-known technology and is very used for power transmission onshore. However, the important footprint of the converters makes this transmission system not suited for offshore applications. VSC-HVDC converters based on IGBTs require less space and can be built offshore. Furthermore, in the last years, the improvements in power electronic permit to develop VSC-HVDC systems with large capacities, up to 1000MW.

The purpose of this thesis is to investigate the impact of the integration of large offshore wind farm on the dynamic behaviour of the Norwegian power system. Firstly an overview of the different transmission systems and of the wind power technology will be made. Secondly, both steady-state and dynamic simulations will be done in order to study the behaviour of the power system. Two different possible connection points in the west and south coast of Norway will be investigated. The offshore wind farm will be connected to the grid with four different configurations. These represent possible solutions of connection in regard of the distance from the shore and the size of the wind farm. All the simulations will be made with the software PSS^{TM}E from Siemens.

2 TRANSMISSION SYSTEMS FOR OFFSHORE WIND FARMS

2.1 INTRODUCTION

To transmit larges amount of power between two points, for example, a generation point and a grid or between two national grids, three main technical solutions exist, i.e. HVAC transmission, LCC-HVDC transmission and VSC-HVDC transmission. Each of these technologies has its advantages and its drawbacks.

2.2 HVAC TRANSMISSION

HVAC is the simplest technique to transmit power and today it is the most used solution for transmission power systems. HVAC is a passive system, in the meaning that the current produced by the generator is directly transmitted to the grid via a transformer if a stepping up or down is needed. This system permits a power transmission and operations in the both directions.

An HVAC system is composed of:

- HVAC cables.
- Transformers at both ends.
- Reactive power compensation units.

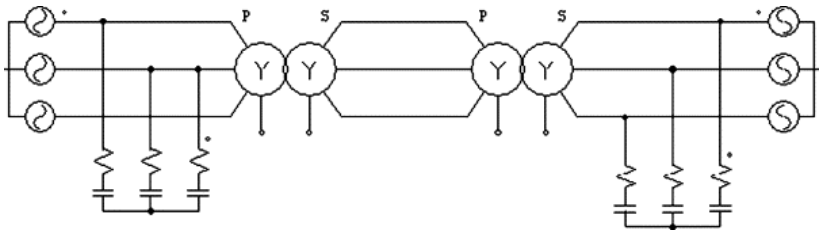

Figure 2-1: HVAC transmission system

The main limitation for a HVAC system is the production of large amount of reactive power by the cables, which leads to the need of large reactive compensation units.

2.3 HVDC CABLES

In an HVDC power transmission system, cable is one of the most important items and its choice has a direct impact on the installation and the cost of the system. Today three types of cables are available:

- Mass Impregnated Cable (MI).
- Low Pressure Filled Cable (LPOF).
- Polymeric Insulating Cable (XLPE).

2.3.1. CABLE STRUCTURE

All kinds of cables have the same composition. There are three major parts in a cable:

- The core.
- The semiconductor screen.
- The insulation.

The main difference between the different sorts of cables is the type of material utilised for the insulation.

The core of a cable is the part which carries the current. It is composed of threaded wires which forming a circular section. This part of the cable is usually made with copper, even if construction with aluminium is possible. Aluminium has advantages that it is lighter and cheaper than copper. Nevertheless, this material has not as good conduction and thermal proprieties as the copper. This leads to higher losses in the cable. A core made of aluminium requires a bigger cross-section area than copper to conduct the same amount of current. Furthermore, aluminium corrodes more easily than copper in presence of water, which is a problem for undersea applications. Typically, cables with core made of aluminium fit more with small voltage applications onshore whereas cables with copper core fit better in medium and high voltage applications, and particularly in offshore conditions.

The area of the core, and so its carrying capacities, can be up to 2000mm^2. For example the 600MW cable use in the SwePol Link has a copper cross-section of 2100mm^2 for a voltage of 450kV.[2] The carrying capacities of the core depend on many parameters: the line voltage, the rated power, the length of the cable, electrical losses and the environment of the cable (burying depth, soil type, on/offshore…).

The semiconductor screen has a role of protection of the cable. Usually it is made of polyethylene materials which have a high percent of black carbon. Typically one screen is placed directly one the core (inner screen) and one other is placed at the exterior of the insulation material (outer screen). Due to the modifications on the electric field distribution, cables are submitted to space charges accumulations which are the source of partial discharges. Partial discharges damage the insulation and finally conduct to the breakdown of the cable. Because of their poor dielectric proprieties, screens have a large resistivity and so the electric field is not able to penetrate the insulation material. Nevertheless if the semiconductor has some imperfections, or if its conductivity is to low, field concentrations may occur and severe damages can be caused to the insulation, leading to the breakdown of the cable. Thus, this is a very important part of the cable.

The main role of the insulation is to insulate electrically the cable from its environment. The electrical field distribution in a cable is radial, but contrary to AC cables, the distribution in a DC cable is governed by the resistivity of the insulation. Furthermore, this same resistivity is dependant of the temperature and the electric field, and generally expressed by the empirical formula [1]:

$$\rho_T = \rho_0 e^{-(\alpha T + \beta E)} \tag{2.1}$$

where, ρ_T is the resistivity of the material at a temperature T, ρ_0 is the resistivity of the material at a reference temperature, T is the temperature, E is the electric field, α and β are respectively the temperature and the electric field coefficient.

If this resistivity of the insulation is too low, because of a too high temperatures or a too strong electric field, there is a risk of space charges formation and stress inversion. Stress inversion is the phenomenon that transfers the maximum electric stress from the conductor to the outer insulation. The consequence of this phenomenon is non uniform electric field distribution, which leads, as said, to partial discharges. It can also limit the transmitted power.

The insulation of the cable is also subject to thermal stress, principally caused by the Ohmic losses in the conductor. This stress coupled with the electrical stress has for effect to reduce the maximum operating voltage of the cable, and so leads to premature failures.

So, the optimum characteristics for an insulating material are:

- Constant insulation resistivity, insensitive to temperature changes and electrical field changes.
- Minimal thermal resistivity.
- Small capacity of storing space charges.
- High dc breakdown strength insensitive to temperature rises.

2.3.2. MASS IMPREGNATED CABLE (MI)

This kind of cable is use since the early days of the transmission systems at the end of the 19th century. Today, it is still the most used technology. With this kind of cables, it is possible to transmit up to 1000MW per cable at a voltage level of 600kV through very long distances. The NorNed cable, between Feda in Norway and Eemshaven in the Netherlands, represents the longest cable in the world with 580 km, but also the most powerful with a capacity of 700MW at 450kV. [2]

The MI cable is composed of a conductor core, an inner semiconductor screen, insulation material made of impregnated paper, an outer semiconductor screen, mechanical protections and anti-corrosion protections.

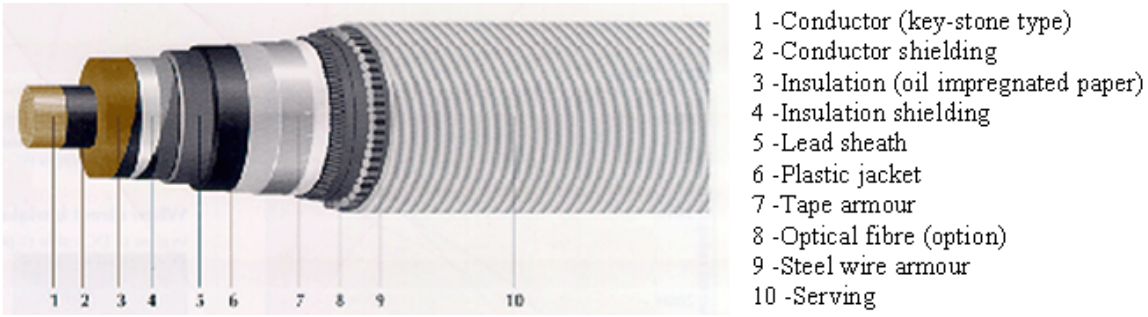

Figure 2-2: Construction of a MI cable

In this kind of cable, the insulation part is made of impregnated paper. The paper is impregnated with resin and high-viscosity oil. Paper ribbons are wrapped around the conductor core with a pitch angle. There is a displacement between each layer which avoids creation of continuous oil canals where partial discharges could occur.

This technology of cable can be installed for submarines applications at depth up to 1000 m. The length of the cable is almost unlimited.

2.3.3. LOW PRESSURE FILLED CABLE (LPOF)

The first Low Pressure Filled cables were introduced in 1917 by Luigi Emanueli. The first installation using this type of cable was between Chicago and New York in 1927. Today many cables are installed around the world.

The design of this cable is similar to the Mass Impregnated cable, but an oil duct is inserted in the centre of the core. The insulation material is also paper but impregnated with low viscosity oil. Oil under pressured between 10 and 15 bars is flowing in the pipe. This last one is connected to oil tanks

that maintain the oil under pressure. When the current circulates in the cable, the temperature rise. This conducts to a dilatation of oil and insulating material. The surplus of oil is forced out of the cable into the storage tanks and reverse flow takes place on cooling. [3] Thus all voids are filled and the possibilities of partial discharges are considerably reduced.

However, this technology presents some problems. First, working with these pressures means that the cable has to be reinforced in order to resist to the mechanical constraints. This additional protections induce this kind of cable is heavier than the mass impregnated technology. Furthermore, due to the oil flow along the cable, the length of the cable is limited. Another problem, especially in subsea applications, is the possibility of oil leaks. If the cable is damaged oil can flow out of the cable and contaminate its environment. Finally, the auxiliary installations, which permit to keep the oil under pressure, are not easy to install and most of the time are very bulky.

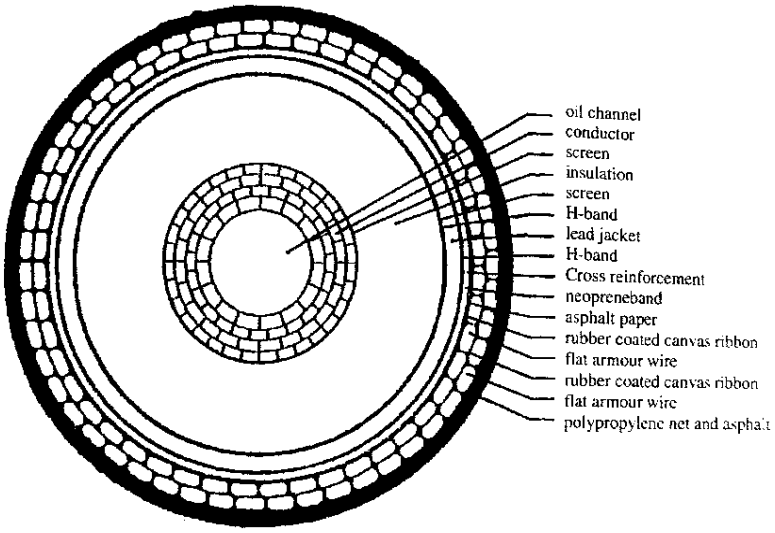

Figure 2-3: Construction of a LPOF cable.

2.3.4. POLYMERIC INSULATING CABLE (XLPE)

Polymeric materials are used as insulation since the 1940s. The first material used, was polyethylene. Its high electric strength and its poor dielectric properties but also its ease of processing and its low cost, made it the perfect client for power cable. However the low melting point of polyethylene, around 110°C, limited the maximum current rating, overload and short-circuit temperatures. But cross-linking the polyethylene, using electron beam processing, permits to increase the thermal properties of the polyethylene. The cross-linked polyethylene is called XLPE. New thermal properties allow conductor temperature around 90°C with emergency capacities up to 140°C. XLPE also has excellent dielectric proprieties for insulation applications. A XLPE cable has a similar design than a Mass Impregnated cable.

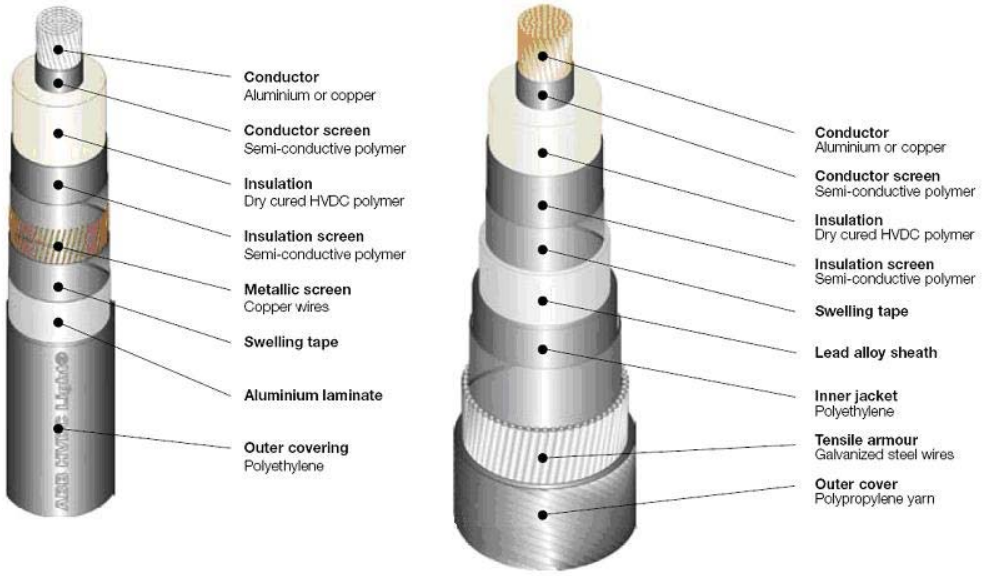

Figure 2-4: Construction of polymeric underground cable (left) and sea cable (right)

Due to the XLPE intrinsic properties, Polymeric Insulating cables are lighter than Paper Insulating cables. Furthermore, the very good insulating properties of this material lead to less insulation material, so smaller dimensions of the cable. In DC applications, the breakdown strength of the cable is around 75kV/mm with a working stress of 25kV/mm whereas, for a paper insulated cable, the breakdown strength is around 40kV/mm with a working stress of 10 to 15kV/mm.

Another advantage of this kind of cable is the mechanical properties of the XLPE. The bending capabilities and the mechanical resistance are higher than other cables, which permits an easier installation and less maintenance. Likewise the absence of oil circulation requires fewer joints along the cable and no risk of contamination for the environment.

XLPE insulating cable can handle lower temperatures than paper insulating cable, and so can be used in cold conditions, for example in cold waters, like in Norway or Russia.

2.4 HVDC TRANSMISSION

AC is dominant in industrial and domestic uses. Nevertheless, in the domain of power transmissions, AC shows limitations especially for long distances. For these kinds of applications, the use of DC shows more advantages.

The idea in an HVDC system is to transform AC into DC with a rectifier, transmit this DC with a HVDC cable, and convert it back to AC with an inverter. In the past, mercury arc valves assured the conversion part but the evolution of the technologies and the apparition of semi-conductive devices, like thyristor and IGBT, gave new perspectives to the conversion part. Today, there are two fundamentally different technologies to convert AC and DC for HVDC applications, based on the type of the switching technology and the place of the main storage element. The first one and the oldest is the LCC Source Converter based on the thyristors. The second one is the VSC, based on the IGBT transistors.

2.5 LCC-HVDC

2.5.1. INTRODUCTION

The first commercial use of thyristors in a converter was in a converter station in the island of Gotland, Sweden, in 1970. Today, many HVDC transmission systems based on LCC technology have been installed around the world with success. So now, this is a mature technology. This kind of technology fits very well in applications where the transmission should be made over long distances (more than 100 km) and high voltages (up to 800kV). The current technologies permit LCC-HVDC systems in the range of 1GW onshore and 500MW offshore.

2.5.2. COMPOSITION OF LCC-HVDC TRANSMISSION SYSTEMS

A typical LCC-HVDC transmission system is mainly composed of:

- AC and DC filters.
- Converter transformers.
- Convertors based on thyristor valves.
- Smoothing reactors.
- Capacitors banks or STATCOMs.
- DC cable and return path.
- Auxiliary power set.
- Protection and control devices.

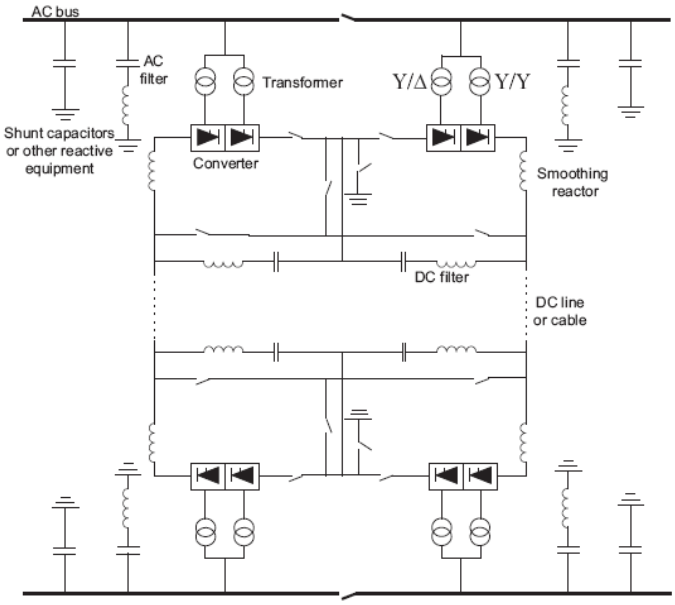

Figure 2-5: Typical configuration of a LCC-HVDC system

2.5.3. THYRISTOR PRESENTATION

As said, the basis of this type of technology is the use of thyristors as switching components. A thyristor is a solid-state semiconductor device made of highly pure mono-crystalline silicon [6]. It is comparable to a diode, but with an extra electrode called the gate. As a diode, the current can only flow in one way, from the anode to the cathode. The gate permits to control the trigger of the device

during a chosen instant in the AC cycle. By applying a current at the gate with a positive voltage between the anode and the cathode, the thyristor turns on and the current through it is positive. It stops conducting when the voltage between the anode and the cathode becomes null because of its diode behaviour. It is also possible to command thyristors not with current, and so electrons, but with light, and so photons. These kinds of thyristors, called Light-Triggered Thyristors (LTT), are commanded with fibre optic cables. Today, the existing thyristors can stand voltages of 8 kV and DC currents up to 4kA.

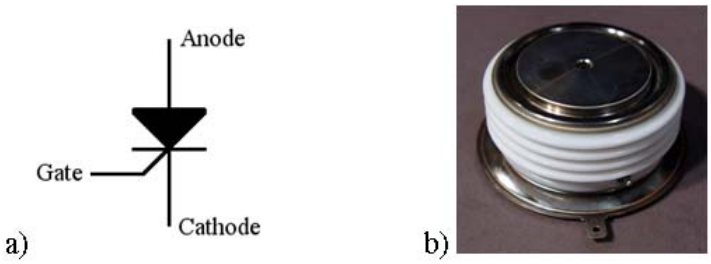

Figure 2-6: a) Thyristor symbol b) Thyristor module

To be able to work with voltage above 8 kV, many thyristors are connected in series in an installation called thyristor valve. Thyristor valves are equipped with cooling systems and fire protections. Most of the time valves are suspended in a building in order to avoid seismic perturbations. By using LTT technology, the number of components is reduced up to 80%.

2.5.4. CONVERTERS

The typical arrangement of the thyristors for a three-phase system is the Graetz bridge configuration (Figure 2-7). This configuration uses six thyristors, and so each of them switches exactly once per line cycle which involves a phase angle of sixty degrees for each thyristor due to the arrangement of them. The AC side inductors serve as the main energy storage elements, resulting in a continuous current. Thus, the LCC can be seen as a current source converter [4].

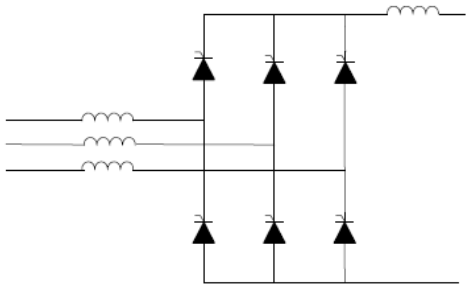

Figure 2-7: Graetz bridge configuration

As the trigger, and so the conduction, of thyristors can be controlled by the gate, it is possible to control the average value of the DC voltage and so the power transmits from the AC side to the DC side. For a three-phase system, the DC voltage and the transmitted power are:

$$V_{DC} = 1.35 V_{LL} \cos\alpha \tag{2.2}$$

And:

$$P = I_{DC} V_{DC} = 1.35 I_{DC} V_{LL} \cos\alpha \tag{2.3}$$

with V_{DC} the average value of the DC side voltage, V_{LL} the rms value of the line to line voltage of the AC side, α the firing delay angle of thyristors, P the power and I_{DC} the average value of the DC side current

From equations (2.2) and (2.3), it can be noticed that the average value of the DC voltage and so the amount of transmitted power depends on one unique parameter, the firing delay angle. This kind of control is called phase control.

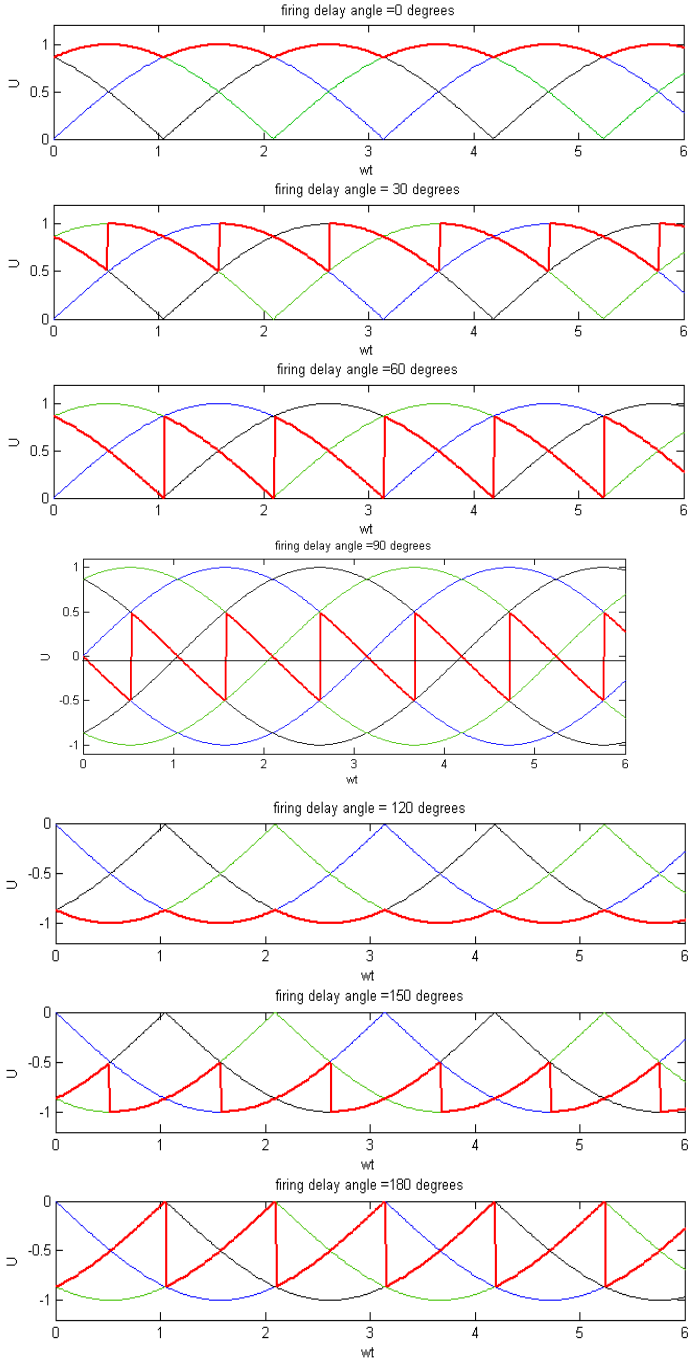

Figure 2-8: DC voltage of the Graetz bridge in function of α

Due to the nature of the switching elements, the current in the DC side is always in the same direction, and the DC side can be considered as a current source. On the Figure 2-8, it can be seen that for a firing delay angle of 90°, the average value of the DC voltage is null, so the transmitted power is also null. For angles between 0° and 90°, the average value of the DC voltage is positive. Thus the power is positive and flows from the AC to the DC side. The converter is in rectifier mode. For angles

between 90° and 180°, the average value of the DC voltage is negative. Thus the power is negative and flows from the DC side to the AC side. The converter is in inverter mode.

The typical operating $U_{DC}I_{DC}$ plan for a converter operating on a zero-impedance AC system is given in the Figure 2-9.

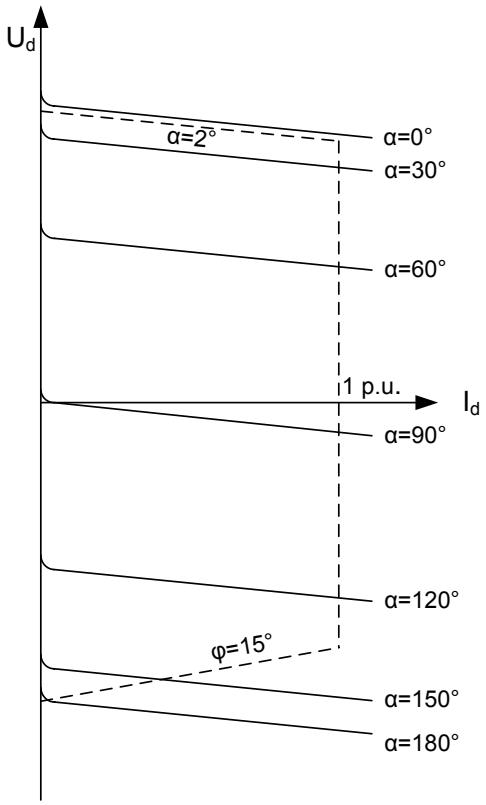

Figure 2-9: Basic firing delay angle characteristics for a constant AC voltage

In this figure, γ represents the extinction angle and is the complementary of the firing delay angle. The doted lines represent the area of operation of the converter. The negative voltage part is the inverter mode operation and the positive voltage part is the rectifier mode operation. Due to the thyristors, natural boundary exists; thus the DC current can not be negative and the firing delay angle is between 0° and 180°. In other words, it means that the thyristors are fired when their anode-cathode voltage is negative. Other boundaries are stepped up for the good operation of the converter. The minimum firing delay angle is limited at 2° to insure the good firing of the thyristors. Minimum extinction angle is set up at 15° to avoid commutation failures. The DC current is limited in order to not exceed thermal characteristics of the system components. In these boundaries, every DC voltage/current characteristics can be achieved by controlling the firing delay angle. [14]

However the 60° phase propriety involves considerable harmonics on the AC side and voltage ripple in the DC side of the converter. Due to high power levels transferred in a HVDC system, the harmonic performances of the converters should be very good in order to avoid large losses. A solution to this problem is to use a configuration with twelve valves known as a 12-pulse converter.

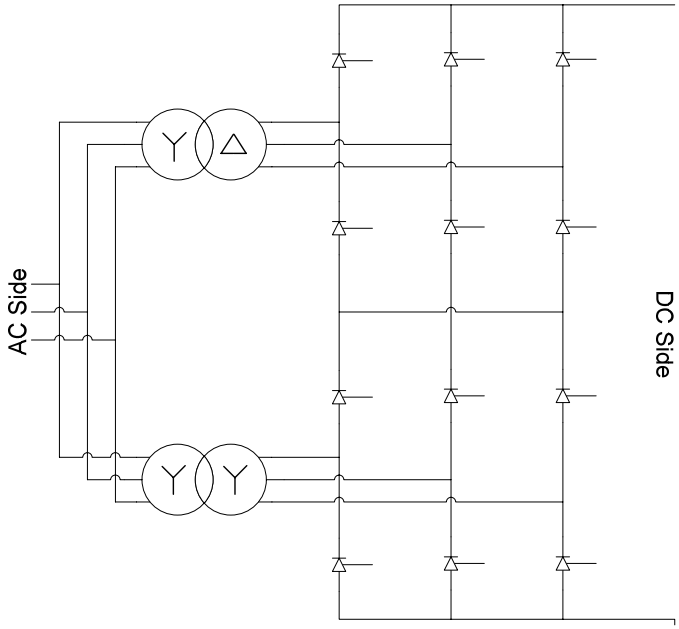

Figure 2-10: 12-Pulse arrangement

Two Graetz bridges are connected in parallel through a Y-Y and a Δ-Y transformer on the AC side and in series in the DC side. With this arrangement, the AC input of the rectifier is split in two three-phase supplies. It permits with the action of transformers, to establish a 30 degrees phase shift between the two AC sets. This value of phase shift permits to reduce considerably the harmonics as the AC current and the DC voltage harmonics have frequencies of 12n±1 and 12n respectively [5].

2.5.5. OTHER ELEMENTS IN THE SYSTEM

The other elements on a LCC-HVDC system are: the filters, the smoothing reactors, the transformers, the STATCOMs and the cable.

The HVDC converters generate many harmonic currents. The need to reduce harmonic effects, and so have the cleanest DC current as possible, is really important. To this end, AC filters are connected to the AC side of the system. DC filters in association with smoothing reactors are also used in order to avoid the effect of the voltage ripple on the DC voltage which can create circulation of AC current in the DC cable. However, the size of these filters is considerably reduced by using a 12-pulse converter.

The smoothing reactors are commonly large inductances, which are placed in series with each DC cable. Their sizes are between 100 to 300mH for long distance transmission and between 30 to 80mH for back-to-back converters. Their role is to prevent the current interruption when the load is minimal but also to limit the DC fault currents, avoid phenomena of resonance and reduce, in association with DC filters, the harmonic currents.

As the voltage levels between the DC line transmission and the ends of the HVDC system are not the same, the use of transformers is imperative in order to raise the voltage to the necessary level. Furthermore, in a 12-pulse converter, two transformers are needed: one with a Y-Y connection and the other one with a Δ-Y connection. Thus the 30 degrees phase shift can be achieved. The transformers used in this kind of systems have a more complicated design than for a normal application because they must provide isolation as well at the AC side as at the DC side to allow the connection of the two converters in series. Transformers need also to be equipped of on-load tap-changers for providing the necessary voltage to the converters.

Due to the control of the thyristors, the current and the line voltage are not in phase and a LCC-HVDC system needs reactive power in order to operate properly. This reactive power can not be provide by the grid due to stability problems. The balance in the reactive power must be achieved. AC and DC filters contribute to supply a part of this reactive power to the converter but larger equipments are needed. Capacitor banks are one solution. It consists in several capacitors connected in parallel to the transformer. A most improved but most expensive solution is the use of STATCOM. STATCOM is a power electronic device based on Voltage Source Converter (VSC). It acts like a producer or a consumer of reactive power, so it permits to compensate the reactive power demand of the thyristors.

For LCC-HVDC systems, both types of cables seen in paragraph 2.3 are usable. However, depending on the characteristics of the project (distance of transmission, environment, on/offshore…), the choice of the cable is very important.

2.5.6. CONFIGURATIONS

As it can be seen on
Figure ***2-11***, different arrangements can be used for a LCC-HVDC power transmission depending of its application.

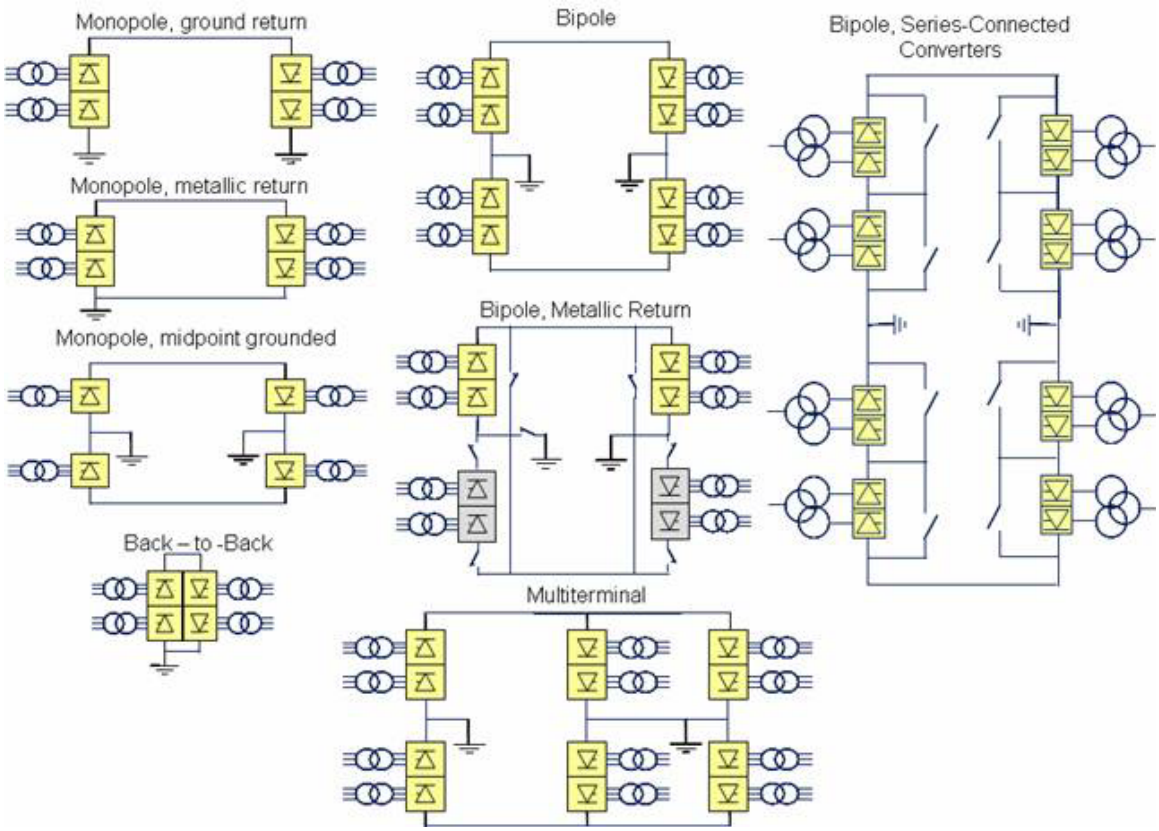

Figure 2-11: HVDC configurations and operating modes

There are four main categories of configuration:

- Monopolar configuration.
- Bipolar configuration.
- Back-to-Back configuration.
- Multiterminal configuration.

2.5.6.1 MONOPOLAR CONFIGURATION

This configuration, the easiest one, uses the ground or the sea as return path. In case of very long distances transmission or subsea transmission, this arrangement is the most feasible solution. Two converters are used and are linked by a single-core cable. Electrodes are commonly used to return the current via sea water or ground. One advantage of this technique is to keep the losses very low due to the good conductivity, and so the small resistance, of sea water or earth. As just one cable is used, the cost of the installation is reduced.

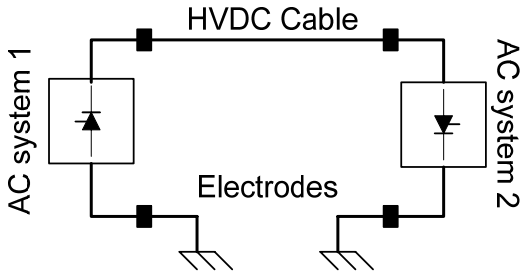

Figure 2-12: Monopolar configuration with ground return path

However this method includes two main problems. First, on its return route, the current can pass through metallic object like gas or oil pipes which can be prone to corrosion. Thus risky objects on the link rout should be protected. Return current can also cross distribution systems with multiple earth points, which leads to an increase of the DC component on the AC grid and so to a DC magnetization of the transformers. Secondly, the electrodes react with sea water which leads to the creation of substances unfriendly for the environment.

One solution to this problem is to use a metallic return path. The electrodes are removed, and the two converters are linked in a close circuit by a second cable. This one uses low DC voltage (around 5kV). This solution cancels the problem of corrosion and bad environmental effects of the electrodes but it also increases the costs and the losses of the project.

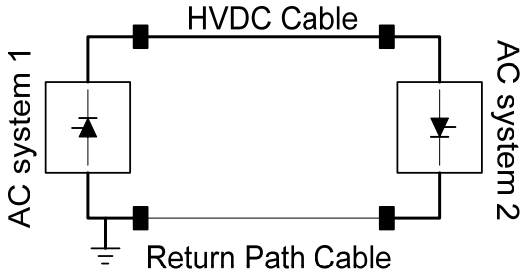

Figure 2-13: Monopolar configuration with metallic return path

In both arrangements (sea water/ground return and metallic path return), one solution to reduce cable costs and losses is to use two DC cables to insure the power transmission. Thus the current as well as the losses in each cable are lower. Nevertheless, the voltage in the converter should be larger than in a normal arrangement. This scheme has been used in the NorNed power transmission.

2.5.6.2 BIPOLAR CONFIGURATION

A bipolar arrangement is a combination of two monopolar systems in such a way that one is at positive polarity and the other one at the negative polarity with respect to the ground.

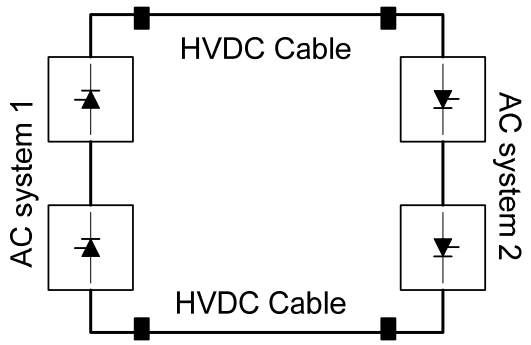

Figure 2-14: Bipolar configuration

This kind of arrangement acquaints the advantage that the power transmitted can be doubled in a respect of a monopolar system. It is often used when the required transmission capacity exceed the capacity of a single monopolar system. Another advantage is that if one of the poles is out of service, due to problem or maintenance, the half of transmission capacity is still available. Thus each pole can work independently from the other one.

There are three schemes possible for the return current, with ground return path, with dedicated metallic return path, and without dedicated metallic return path. [6]

The first solution, i.e. bipole with ground return path, provides the highest degree of flexibility to the system. If there is a single-pole fault in one of the converters or in one of the cables, the current of the second pole will be return by the ground path. If a single-pole fault happens to one of the converters, the cable associated to this pole will play the role of metallic return path for the return current of the second converter. In the two cases, half of the power can still be transmitted, during the fix of the problem.

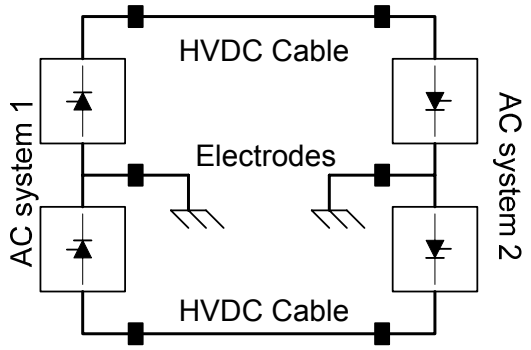

Figure 2-15: Bipolar configuration with ground return path

The second solution, i.e. bipole with metallic return path, presents the same advantages than the above solution, but it is more expensive due to the low voltage DC metallic return path. However, in some situations, the use of electrodes is forbidden thus this scheme is the solution.

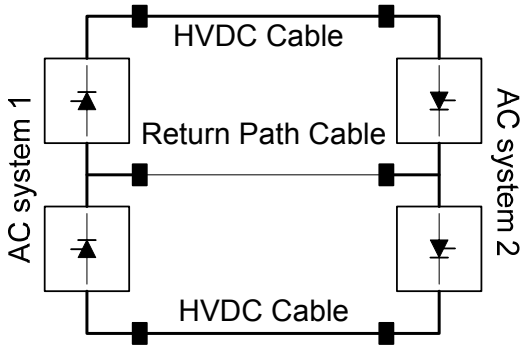

Figure 2-16: Bipolar configuration with metallic return path

The last solution, i.e. bipole without dedicated return path, is the cheapest one. No electrodes or metallic return paths are used. During a converter pole problem, monopolar operation is possible by bypass switches, but if something happens in a cable, all the system is out of service.

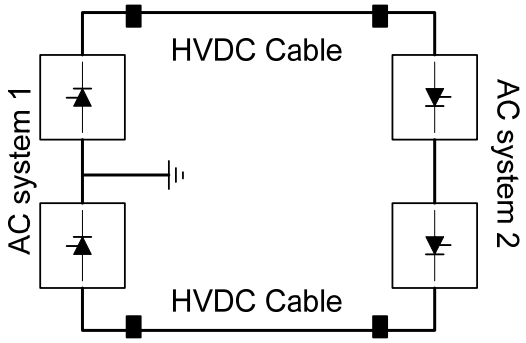

Figure 2-17: Bipolar configuration without return path

2.5.6.3 BACK-TO-BACK CONFIGURATION

This arrangement is mainly used to connect to AC grids which are not synchronized. The frequency between the two grids can be similar or different. The two converters, inverter and rectifier, are located in the same place. Thus the transmission distance is very small so no cables are necessary to connect the two converters.

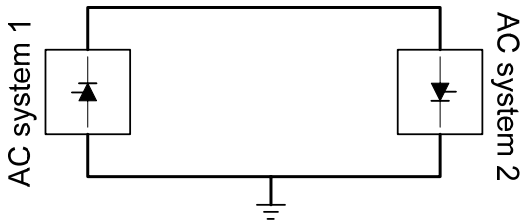

Figure 2-18: Back-to-back configuration

2.5.6.4 MULTITERMINAL CONFIGURATION

When more than two converters are needed for the transmission system, a multiterminal configuration is required. For three converters, two approaches are possible: parallel and series connections. [4]

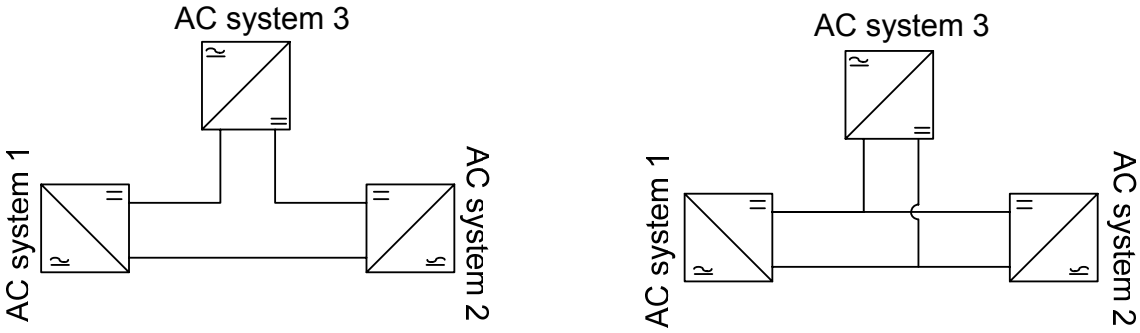

Figure 2-19: Series and parallel multiterminal configurations

With more than three converters, hybrid schemes can be used, in combining series and parallel connections. Such a configuration can be useful in case of very high DC voltages above 500kV, i.e. 600kV or 800kV. Converters are connected in series which permits to reduce the energy unavailability for individual converter outages or partial cable insulation failures. [5] Future applications can also lead to connect an offshore wind farms to an existing HVDC cable.

2.6 VSC-HVDC

2.6.1. INTRODUCTION

VSC-HVDC is a new technology. The first power transmission system based on this technology was built in 1997 by ABB between Hellsjön and Grängesberg in Sweden. However this small project was just a full-size test of the new technology. The system is 10km long and can transmit a maximum of 3MW at 10kV.

The first major VSC-HVDC project was built in 1999 in the Gotland Island in Sweden. The 70km long system permits to link the town of Visby and a 40MW wind farm on the south of the Gotland Island. It has a capacity of 50MW and at a voltage of 80kV.

Today, two companies are pioneer in the development of this technology: ABB with the HVDC Light and Siemens with the HVDC PLUS. Improvements have been made since last years and the transmission capacities reach 1200MW and 320kV.

2.6.2. COMPOSITION OF VSC-HVDC TRANSMISSION SYSTEM

A VSC-HVDC transmission system is composed of two main parts, the converters, at both ends of the system, and the cable between them. The main components of these two parts are similar to the LCC-HVDC system, with some differences:

- AC and DC side harmonic filters.
- Converter transformers.

- Converters based on IGBT valves.
- Phase reactors.
- DC cable.
- Auxiliary power set.
- Protection and control devices.

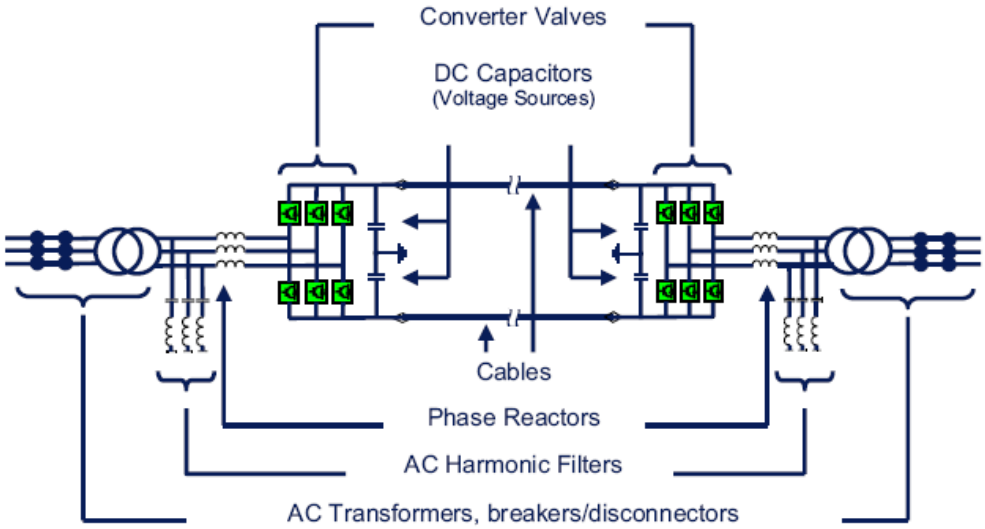

Figure 2-20: Typical configuration of a VSC-HVDC system

2.6.3. IGBT PRESENTATION

VSC-HVDC converters use Insulator-Gate Bipolar Transistors (IGBT) as switching device. IGBT is a recent technology. First-generation of IGBTs was used in the 1980s but was slow and presented problems in operation. A second generation, appeared in the 1990s, resolved these problems and permitted a faster switching time than the first-generation. In the 2000s, new IGBTs appeared with very good performances for high current and voltage.

Due to the process of production similar to printed circuit, IGBTs have a small size (around 1cm^2). Thus many IGBTs connected in parallel, gives to IGBT modules the capability to handle current up to 2.4kA with blocking voltage up to 6.5kV.

An IGBT is the combination of a Bipolar Junction Transistor *PNP* (BJT) and a MOSFET. Thus it takes the advantages of both devices: low conduction losses for the BJT and fast commutation for the MOSFET.[7]

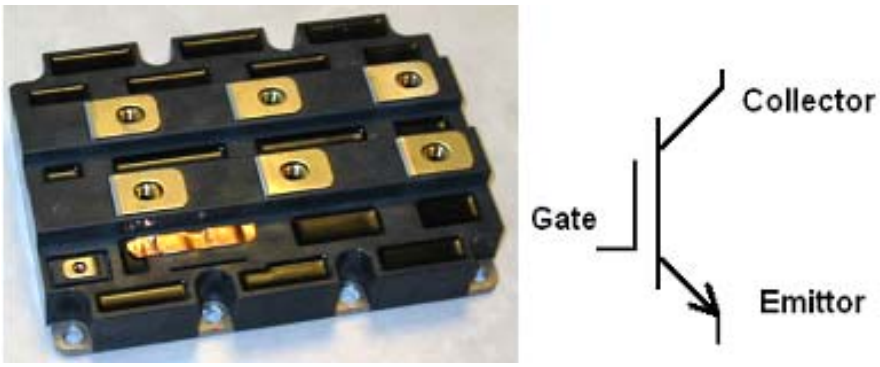

Figure 2-21: Power IGBT (3300V, 1200A) and symbol

An IGBT can be compared to a switch, its conduction and blocking states are commanded by the gate. When the voltage between the gate and the emitter (V_{GE}) is inferior to threshold tension ($V_{GE(TH)}$), the IGBT is in blocking state. Thus the voltage between the collector and the emitter (V_{CE}) is positive and the current flowing in the IGBT (I_{CE}) is null. If V_{GE} become superior to $V_{GE(TH)}$, then the IGBT goes to the conductive mode and I_{CE} flows through it.

This capability of control permits to switch at high frequency which allows the use of Pulse Width Modulation (PWM). High frequency switching also reduces harmonics and thus the number of filters used. A project like Tjæreborg in Denmark is designed with a switching frequency of 1950Hz.

As for the thyristors, the blocking voltage of an IGBT module does not allow the operation within high-voltage levels. To avoid this problem, many modules are connected in series in valves.

2.6.4. CONVERTERS

In a VSC-HVDC converter, the IGBT are commanded by Pulse Width Modulation (PWM). The idea of PWM is to compare a sinusoidal wave with a triangular wave.

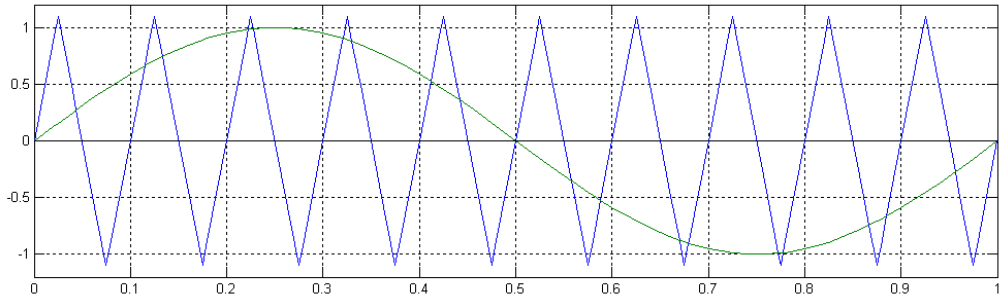

Figure 2-22: PWM switching signal

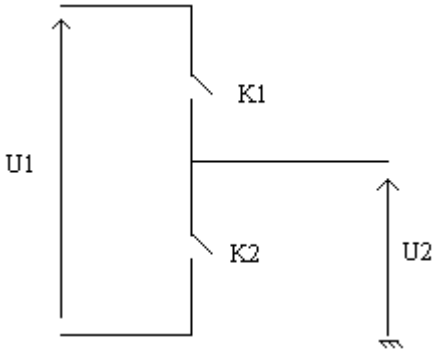

Figure 2-23: Basic circuit for PWM

In the system on Figure 2-23, the switches *K1* and *K2* are commanded with PWM. When the amplitude of the sinusoidal wave is higher than the amplitude of the triangular wave, *K1* conducts and the voltage *U2* is equal to *U1*. When the amplitude of the triangular wave is higher than the amplitude sinusoidal of the wave, *K2* conducts and the voltage *U2* is equal to *–U1*.

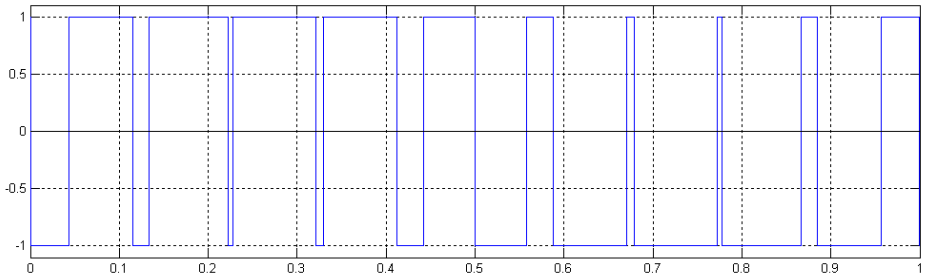

Figure 2-24: Output with PWM command

This signal is composed of many harmonics but its fundamental is a sinusoidal wave. Thus by filtering the signal with a low pass filter, the AC voltage is obtained. The amplitude modulation ratio is defined as [12]:

$$m_a = \frac{\hat{V}_{\sin control}}{\hat{V}_{tri}} \tag{2.4}$$

where $\hat{V}_{\sin control}$ is the peak amplitude of the sinusoidal control signal of the PWM and $\hat{V}_{tri}$ is the peak amplitude of the triangular signal of the PWM which is generally kept constant. Then the peak amplitude of the fundamental sinusoidal wave can be expressed as [12]:

$$V_0 = m_a \frac{V_d}{2} \tag{2.5}$$

where V_d is the amplitude of the signal on Figure 2-24. Any phase angle and amplitude of the output voltage can be achieved by modifying the PWM parameters, i.e. frequency and amplitude of the triangular and the sinusoidal control waves.

When the converter is a three-phase converter, three PWM signals 120 degrees shifted are applied to the legs of the converter. The line to line voltage of one the converter can be expressed as [12]:

$$V_{LL} = \frac{\sqrt{3}}{\sqrt{2}}(V_0) = \frac{\sqrt{3}}{2\sqrt{2}} m_a V_d \simeq 0.612 m_a V_d \tag{2.6}$$

So far two types of converter have been used in the existent VSC-HVDC transmission systems: the two-level and the three-level converters. The two-level converter is the simplest configuration. It consists on 6 valves arranged like a Graetz bridge. It generates two voltage levels, ± $0.5U_{DC}$.

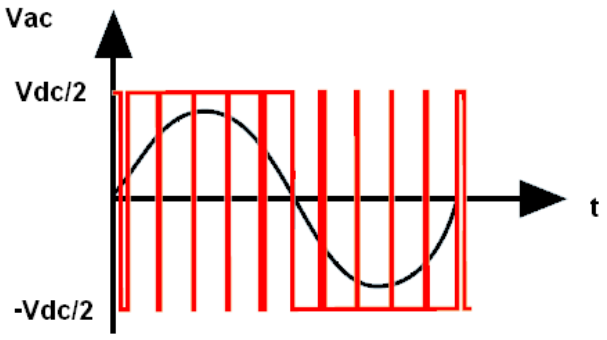

Figure 2-25: Output with PWM command of a two-level converter

The three-level converter consists in 12 valves, but contrary to the 12-pulse converter, this converter is not composed of two 6-valves converters. Each arm of the three-level converter is composed of four valves. With this arrangement, it is possible to generate three levels of voltage, ± $0.5U_{DC}$, as the two-level converter, but also 0.

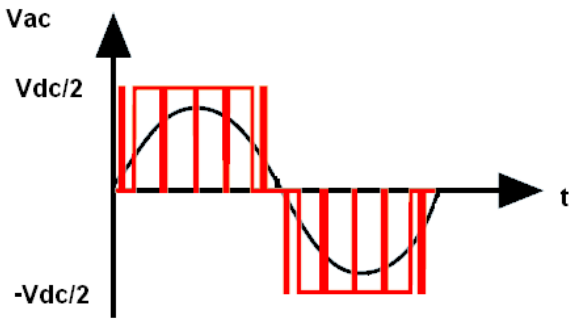

Figure 2-26: Output with PWM command of a three-level converter

The benefit of using a three-level converter is that its harmonic performances are better than a two-level converter. With this last converter, the output current and voltage are strongly distorted and the Total Harmonic Distortion (THD) is very poor, which implies high losses in the converter. The use of a three-level arrangement leads to lower losses (44% less than a two-level arrangement). Thus the converter, and so the transmission system, have a better efficiency. However the three-level converter is 27% more expensive than the two-level converter. [8]

Notwithstanding the harmonic effects are still a major problem even with a three-level converter and filters are required to avoid them. A new approach to reduce the harmonics is the multilevel converter. Several sub-modules, composed of IGBTs, diodes and capacitors, are connected in series and each one are commanded separately. Every sub-module generates a small voltage step and a capacitor in it defines the level of the voltage step. Thus, by controlling each step, an almost sinusoidal voltage (made of steps) is created and so the level of harmonic is very low. Siemens developed a Multilevel Converter which avoids the use of harmonic filters. [9]

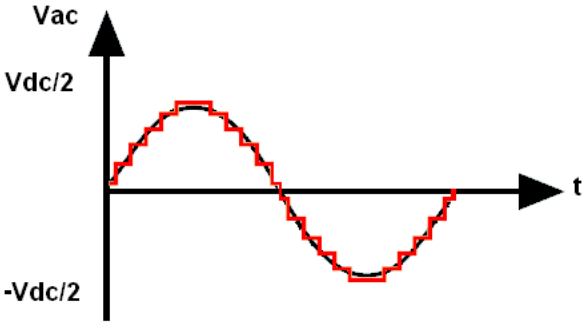

Figure 2-27: Output with PWM command of a multilevel converter

The multilevel approach permits also to reduce the switching frequency of the IGBTs, and thus to reduce the losses in the converter.

The VSC-HVDC converters can control both active and reactive power independently. This is achieved by controlling the phase angle and the amplitude of the AC voltage. As shown on the Figure 2-28, the converter is modelled as a voltage source on the AC side and as a current source on the DC side.

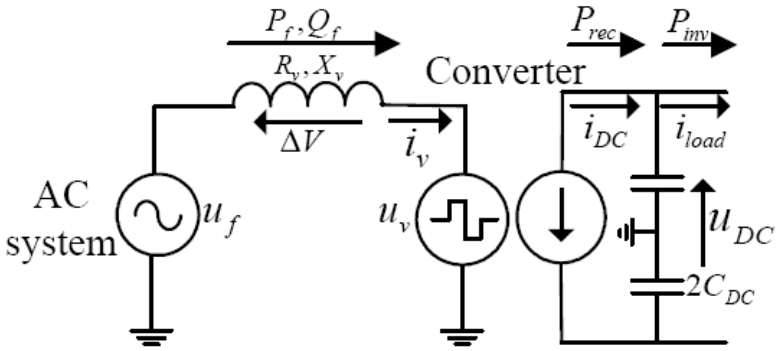

Figure 2-28: Equivalent circuit of the converter

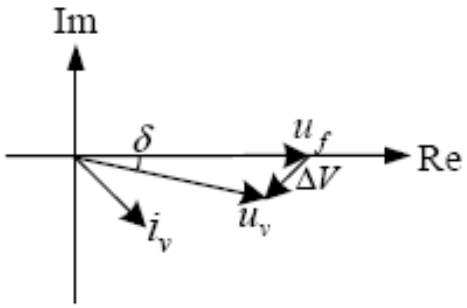

Figure 2-29: Phase diagram of the converter

The voltages u_f and u_v are not on the same phase due to the reactor and u_v lags u_v with the angle δ. By considering a power flow from the AC side to the converter and neglected the losses on the reactor, the power delivered by the AC system can be defined as:

$$\overline{S} = P_f + jQ_f = \overline{U_f}.\overline{I_v}^* = \overline{U_f}\left(\frac{\overline{U_f} - \overline{U_v}}{jX_v}\right) = U_f\left(\frac{U_f - U_v\cos(\delta) - jU_v\sin(\delta)}{jX_v}\right) \quad (2.7)$$

Then the active power is defined as:

$$P_f = \frac{U_f U_v \sin(\delta)}{X_v} \quad (2.8)$$

And the reactive power:

$$Q_f = \frac{U_f(U_f - U_v\cos(\delta))}{X_v} \quad (2.9)$$

Then it can be seen that the converter has two variables, the phase angle δ and the voltage magnitude U_v, which can control the active and reactive power. So, the converter can operate in all four quadrants of the P/Q diagram as seen on Figure 2-30. Active power can flow in both directions with simultaneous generation of inductive or capacitive reactive power.

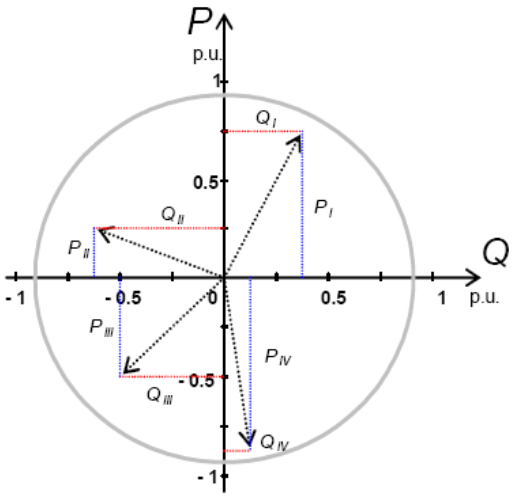

Figure 2-30: P/Q diagram for VSC-HVDC converters

2.6.5. CONTROL PRINCIPLE

According to the application, different control modes can be used for a VSC-HVDC transmission link. As said, the phase angle δ and the amplitude of the voltage U_v permit to control the active power and reactive power of the converters. These two variables are directly linked to the PWM command. The phase angle δ can be modified by changing the phase angle of the sinusoidal control signal $V_{sin\ control}$ and the amplitude of the voltage U_v can be modified by changing the amplitude modulation ratio m_a.

In normal operation, the sent active power must be equal to the received active power. The balance between the two ends is achieved by keeping a constant DC voltage at the receiving end of the transmission i.e. the inverter. For example, when the sent power increases the DC voltage will also increase. The inverter will detect this augmentation and will increase the phase angle of its $V_{sin\ control}$. Thus, the phase angle δ of the AC voltage on the inverter side will increase which, according to equation (2.8), leads to the augmentation of the power flowing to the AC system without changes on the sent power. Then the DC capacitors on the inverter will discharge and the DC voltage will regain its reference value. On its part, the rectifier will control the active power flowing on the DC link in respect of a set point. On the AC side, the converters can either regulate the AC voltage by adjusting their production of reactive power or operate with a constant production of reactive power [13].

However, for wind power applications, the control strategy is different. Indeed, as the wind is not blowing constantly, the amount of power which has to be transfer in the DC line is not constant. Furthermore, the whole production of the wind farm has to be transfer in the grid because it can not be stock. When the wind increases the frequency on the wind farm side will increase. The rectifier will detect this change and will increase the phase angle of the AC voltage. More power will flow through the converter and consequently the frequency will return to its reference value. By regulating the angular frequency on the wind farm side, the power absorption of the rectifier will be maximal according to the wind speed [13].

In a VSC-HVDC transmission for wind power applications, the rectifier will control the active power flow by adjusting the phase angle of the AC side and the inverter will control the DC voltage by adjusting the phase angle of the AC voltage. Both converters control the AC voltage by regulating the amplitude modulation ratio m_a. If the AC voltage generated is lower than a reference value, m_a is increased and inversely.

2.6.6. OTHER ELEMENTS IN THE SYSTEM

Due to the VSC converters, there is less elements on a VSC-HVDC transmission system than in a LCC-HVDC system. The other elements on a VSC-HVDC system are: the transformers, the AC filters, the phase reactors, the DC capacitors and the DC cables

As for a LCC-HVDC system, transformers are needed in a VSC-HVDC system. On the other hand, no special design is necessary in this system and normal transformers can be used. As the harmonics are low in a VSC-HVDC system, the stress and the losses due to harmonic currents are reduced on the transformer so standard windings can be used. The role of the transformers is to transform the AC grid voltage to the required voltage for the operation of the converters. Furthermore as there is no need of phase shifting for the VSC converters, only one transformer is needed at both ends of the system

Even if they are lower than in a LCC converter, the switching of the IGBTs in the converters creates harmonics in the currents and voltages. These currents and voltages are composed by a fundamental frequency plus other harmonics. However, due to the high switching frequency (around 2000Hz) these last have high frequencies. To delete the effects of harmonics, passive high-pass filters are used. As there is no need of reactive compensation in a VSC converter, filters are placed in the secondary of the transformer; thus the currents and voltages are “clean” for the converter.

The phase reactors permit to control the active and reactive power flow. In order to assure this function, the current flowing through them is regulated. As the waveform at the output of the converters is a sinusoidal made of steps, the reactor serves to extract the fundamental of this “raw” waveform. It also plays a role in the suppression of the harmonics. These reactors are made of air core devices which are housed in an aluminium enclosure. [2]

The DC capacitors should be appropriately chosen in order to control the current waveform and to insure the sinusoidal form. The possible ripples in this DC voltage caused by harmonic in the AC current have to be suppressed. The role of the capacitors is to avoid the creation of such ripples. In case of transient states, it also provides an energy buffer which insures that a good power balancing of the system will be keep. The dimensioning of these capacitors is an important phase of the project.

For VSC-HVDC systems, both types of cables presented in part 2.3 are usable. Even they have problem of space charge and stress distribution due to their thermal properties, polymeric cables are preferred. ABB solves this problem with their HVDC Light cable. A VSC-HVDC system is by nature bipolar so the cable operated in bipolar mode, one cable with positive polarity and one cable with negative polarity. The cables are installed close in bipolar pairs with anti-parallel currents and thus eliminating magnetic fields.[2] Furthermore the mechanical strength, the flexibility and the low weight of this kind of cables make it really adapted for the power transmission, especially in subsea environment.

2.7 UHVDC

The power demand during the last years has known a big growth. The need of large bulk power leads to the transmission of higher power level, exceeding 4GW, on longer distances, up to 2000km. This evolution in power grids introduces high voltage level above 600kV.Thus power transmission systems should be adapted.

HVDC technology is well fitted for the transmission of bulk power. However the important voltage levels needed to transmit large amount of power overstep the limit of classical HVDC system and create new problems. High requirements of for insulation, clearance and corona effect are a challenge for design companies. [9] Ultra-HVDC (UHVDC) is similar to HVDC but many

improvements on the elements of the systems have been made regarding these problems. The elements on a UHVDC system have enormous sizes in order to allow good operation. For example, transformers rated power can exceed 300MVA and a weight of 400 tons or smoothing reactor can be made for DC current of 3.3kA with a coil size of 100mH and a high of 14m. [10]

Today, the biggest system is installed in Itaipu, in Brazil. The power transmitted is 6300MW over 1500km with a voltage level of 600kV. The Chinese under construction project of Xiangjiaba-Shanghai link, planned for 2010, should transmit 6400MW over 2071 km with a voltage of 800kV. [2]

2.8 REACTIVE POWER CONSIDERATION

2.8.1. REACTIVE POWER IN GRIDS

The use of AC current and voltage implies two types of power, the active power P and the reactive power Q. The active power is transformed on mechanical and thermal power. The reactive power refers to the circulating power which is not useful for work and it is used to magnetize the magnetic circuits of the equipment.

The AC voltage $v(t)$ and the AC current $i(t)$ applied on a electric system, can be defined as:

$$v(t) = V\sin(\omega t) \tag{2.10}$$

$$i(t) = I\sin(\omega t - \varphi) \tag{2.11}$$

where V is the rms value of the voltage, I is the rms value of the current, ω is the pulsation and φ is the phase angle between the voltage and the current.

It is possible to represent the voltage and the current in a vector diagram:

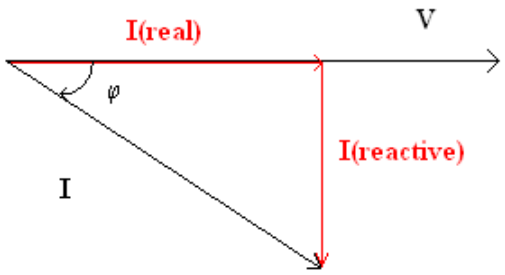

Figure 2-31: Vector diagram of voltage and current

The current can be divided into two parts, the real current and the reactive current which can be defined as:

$$I_{real} = I\cos\varphi \tag{2.12}$$

$$I_{reactive} = I\sin\varphi \tag{2.13}$$

If these current are multiplied by the voltage the active power and the reactive power are obtained:

$$P = VI\cos\varphi = VI_{real} \tag{2.14}$$

$$Q = VI\sin\varphi = VI_{reactive} \tag{2.15}$$

$$S = VI \tag{2.16}$$

where S is the apparent power.

These powers can also be represented in a vector diagram:

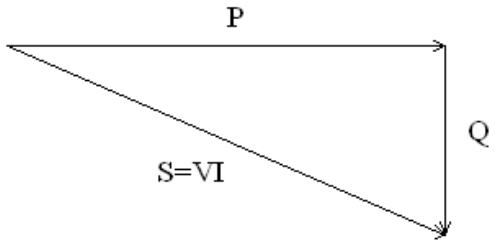

Figure 2-32: Vector diagram of active and reactive power

The sign of the reactive power depends of the phase angle between the current and the voltage. If the current lags the voltage, the phase angle is negative and the reactive power is negative too. So the impedance of the circuit is inductive and so the reactive power is consumed. If the voltage lags the current, the phase angle and so the reactive power are positive. The total impedance is capacitive and the circuit produces reactive power.

If the following two nodes system is considered:

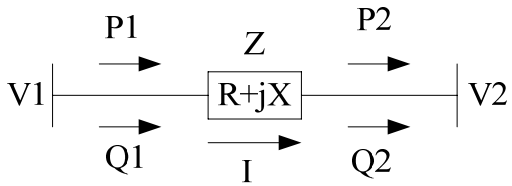

Figure 2-33: Two nodes system.

The voltage drop between the ends will be:

$$\begin{aligned} \Delta V &= V_2 - V_1 \\ &= ZI \\ &= (R\cos\varphi + X\sin\varphi)I \\ &= RI\cos\varphi + XI\sin\varphi \end{aligned} \tag{2.17}$$

So if this expression is linked with the reactive power:

$$\Delta V = \frac{RP_1 + XQ_1}{V_1} = \frac{RP_2 + XQ_2}{V_2} \tag{2.18}$$

But for transmission lines in the grids $R<<X$. So:

$$\Delta V = V_2 - V_1 \approx \frac{XQ_1}{V_1} \approx \frac{XQ_2}{V_2} \tag{2.19}$$

The flow of reactive power Q is determined by ΔV. If $V_1 > V_2$ then the Q flows from the node 1 to node 2 and in the case of $V_2 > V_1$ the flow is reverse. In other words, if there is a lake of reactive power in one point of the system, the rest of the system should provide the necessary reactive in order

to equilibrate the power balance. Otherwise the voltage at the node in deficit can collapse. In the opposite, a surplus in the power balance leads to a rise of the voltage. This can lead to a major breakdown of the whole grid. The stability of a system is linked on the flow of reactive power and it is obvious that a good power balance of the system should be made.

But flow of reactive power through the grid creates extra losses due to the nature of the transmission lines and the capacities of active power transmission are reduced. The losses on transformers are also increased by the flow of reactive current. In another hand, motors need reactive power to produce the magnetic fields required for their operation. To avoid the circulation of reactive power through the grid even as furnishing it to the consumer, compensation is used. Thus the production is made near the consumer and the consequences of the reactive flow are reduced.

2.8.2. REACTIVE POWER AND HVDC

An LCC-HVDC needs a synchronous voltage in order to commutate. Furthermore, as it can be seen on Figure 2-9, converters operate only with positive firing delay angle and positive currents due to the nature of the commutating devices. Thus converters are always consumer of reactive power. The need of reactive power depends of the active power transmitted. The higher is this active power, the higher is the consumption of reactive power. At full load, the requirement of reactive power for the good operation of the converters is about the half of the transmitted active power. A common requirement to a converter station is compensation or overcompensation at rated load.

The balance of reactive power in the system can not be assured by the grid due to considerations made in the previous paragraph. STATCOMs and filters, as explain earlier, supply converters with reactive power. In inverter mode, the reactive power is required not only for the operation of the converter but also for maintaining an acceptable voltage level on the AC system. Additional sources of reactive power can be used to achieve that, like shunt capacitors. The following figure shows the demand of reactive power of the converter, the reactive power compensation and the exchange with the AC system in function of the transmitted power.

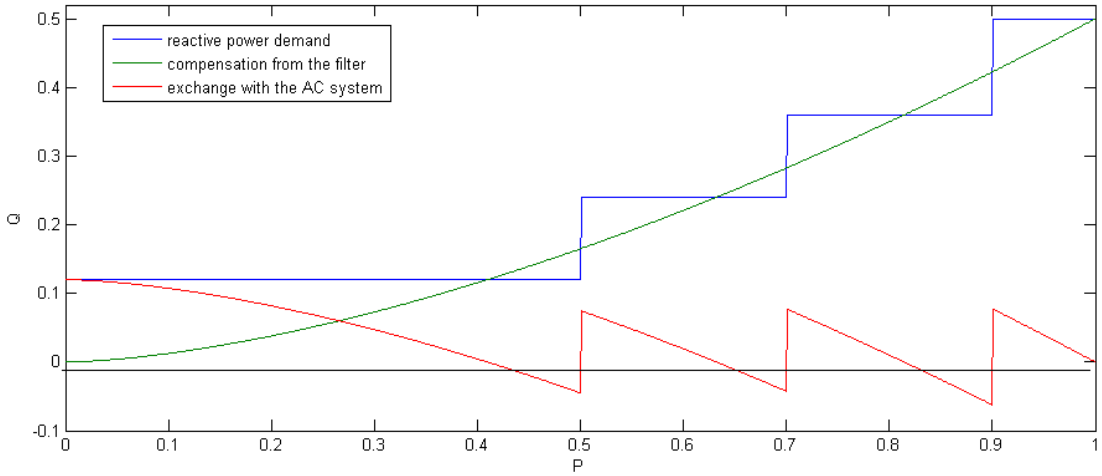

Figure 2-34: Demand and compensation of reactive power for a LCC-HVDC converter.

As said, VSC-HVDC uses IGBTs as commutating devices. These latter, due to their full controllability, have no reactive power demand to operate. Thus the converter can control very quickly both active and reactive power. It can either absorb or generate reactive power. Thus it has a voltage stability role. Each end of a VSC-HVDC power transmission can supply the AC grid with reactive power if the latter is in deficit or absorb reactive power if there is an excess of it. The following figure shows the typical power operating range of a VSC-HVDC transmission. The use of compensation system is not required since the converter insure itself this task.

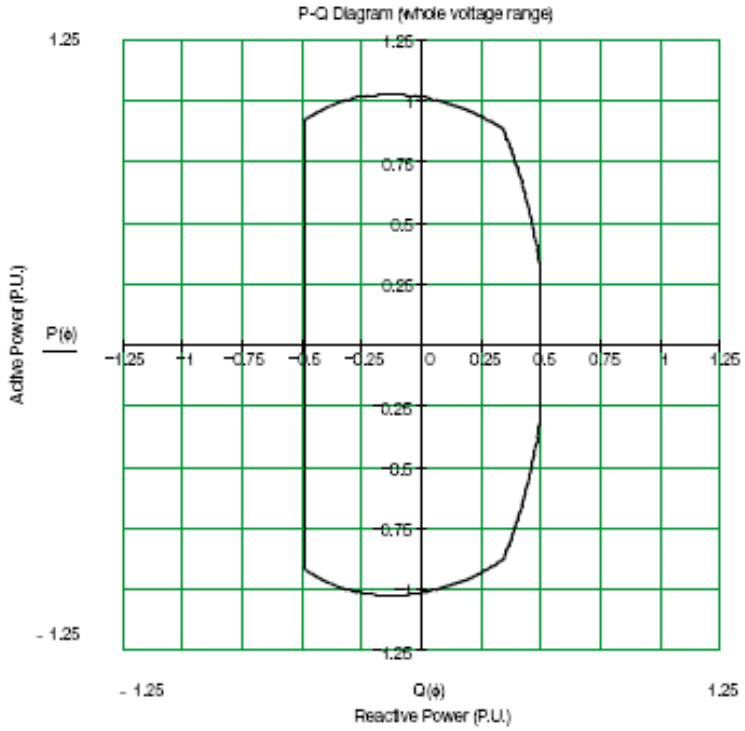

Figure 2-35: Typical P/Q diagram for HVDC Light converter. [45]

2.9 ADVANTAGES AND DISADVANTAGES OF TRANSMISSION SYSTEMS

2.9.1. HVDC AND HVAC

By using a transformer, the conversion of AC voltage is very simple. This equipment allows high power and has relatively low losses. Furthermore, a synchronous generator has better performance than a DC generator. For these reasons, HVAC technology is the simplest way to connect two different power systems, and today it is the most used technology. However, the current requirements of power systems and the improvements of technology, especially in power electronic, have shown limits of HVAC systems.

The most important limit of a HVAC system is the transmission distance. Inductive and capacitive elements on the cable, which are proportional to the length, lead to charging current in the cable. These last, as well as useful currents are quarried in the cable and the transmission capabilities of the cable are reduced. The creation of large amount of reactive power is also an important limiting factor. This implies large and expensive compensation system at the ends of the cable and losses increase consequently. Furthermore, the number of cables is more important with HVAC system as the connection should be done with three phases.

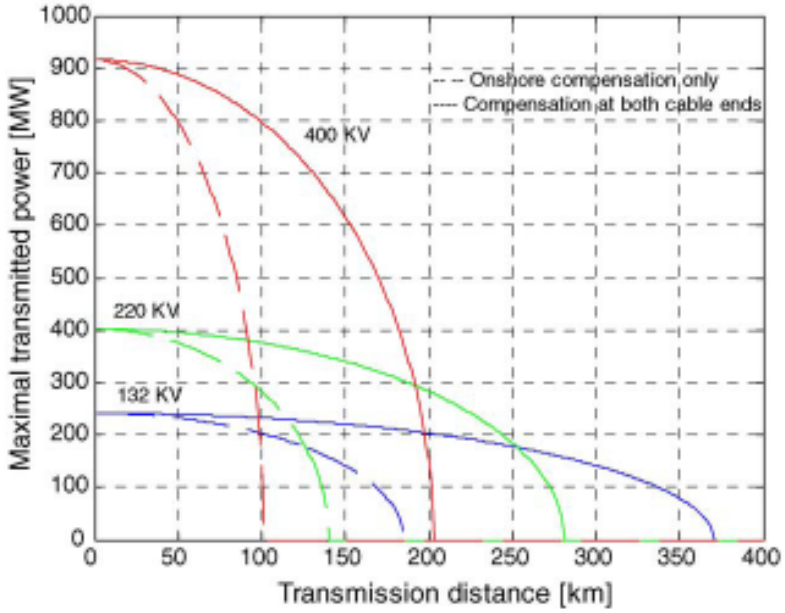

Figure 2-36: Transmission capacity of HVAC cables for different voltage and compensation modes

HVDC systems do not present length limitation. The effect of inductive and capacitive elements is inexistent due to the DC current, so there is no charging current or skin effect. The only source of losses in a HVDC cables is the DC resistance which is constant. Although converters create losses, losses are considerably reduced in a HVDC system compare to a HVAC system.

One other advantage of HVDC system is that synchronous operations are not required. Both ends of the system can work at different frequencies because they are decoupled by the DC link. This is very advantageous, especially for offshore systems like wind farms because it gives more flexibility in the design of the generators. Moreover, each interconnected system is not affected by fault and frequency variation in the other one.

The construction of an HVAC transmission link implies that the short-circuit current in the linked systems will be higher. This is not the case with HVDC systems because they do not contribute to the short-circuit current of interconnected systems.

The investment cost of a transmission system depends of the distance of transmission. A HVDC transmission line is cheaper than a HVAC line. However converters are needed for HVDC and their costs make HVDC more expensive than HVAC in a certain distance range. But from a certain distance, called “break-even distance” this trend is reverse. The “break-even distance” depends on different factors as the type of transmission (overhead line or cable), permits and cost of local labour [11]. The typical “break-even distance” is between 600 and 800km for an onshore system. For an offshore system, it is considerably reduce to 75 km because of the use of cables.

The major advantages of a HVDC link are [2]:

- Lower investment costs.
- Longer distances.
- Lower Losses.
- Possibility of asynchronous connections.
- Limitations of short-circuit current.
- Better controllability.

2.9.2. LCC-HVDC AND VSC-HVDC

Today, the majority of HVDC power transmission systems are based on the LCC technology. However, VSC-HVDC systems present many advantages compare to the LCC-HVDC systems.

For high power levels (above 250MW) LCC-HVDC is more cost effective than VSC-HVDC but this trend tends to change with the improvements made on VSC-HVDC. [2]

One of the main advantages of VSC-HVDC technology is that the controls of active power and reactive power are independent. The system can operate in the four quadrants of the PQ-plan. In a LCC-HVDC system, a limited control of reactive power can be achieved but it require additional expensive equipments. The use of PWM in VSC-HVDC systems permits to achieve any amplitude and phase angle, and so the control of active and reactive power can be made independently without additional equipments. The AC voltage in the network can be controlled while the transmitted active power is constant. The reactive power balance can be achieved by using the reactive power generated or consumed by the converters (within the rating of the latter). The independent control is very advantageous for connection of weak AC grids, were stability is very important.

Another good point for VSC-HVDC technology is that it is independent of the AC network. The converters can create an AC voltage at any frequency, and without the presence of generator in the network. Thus passive networks can be connected with VSC-HVDC technology.

In contrary of LCC-HVDC systems which can not operate at low power, VSC-HVDC systems are able to operate at very low power, even null power. As active power and reactive power are controlled independently, if the active power is null, the reactive power can be fully utilized. This characteristic also allows the active power to be reverse very quickly by changing the direction of the DC current and not the DC voltage as in a LCC-HVDC system.

By using IGBTs, which are self commutating device, the risk of commutation failures is considerably reduced. The high AC voltage level needed for thyristors is not requiring for IGBT technology. The stability of the systems is better.

A VSC-HVDC system is easier to design because of the fewer components. Harmonic filters, STATCOMs or capacitor banks are not needed and the transformer has a normal design. Thus the converter stations for a VSC-HVDC application have a smaller footprint than for a LCC-HVDC application. For example a 600MW converter station requires 14000m^2 for a LCC-HVDC application and only 3000m^2 for a VSC-HVDC application. For offshore application, this is very important.

3 GENERALITIES ABOUT WIND POWER

3.1 STATUS OF OFFSHORE WIND POWER IN EUROPE

In 2007, the offshore wind power installed capacity was around 1100MW divided in 25 offshore wind farms in 5 European countries. The installed capacity represented 1.8% of the total wind power installed capacity but it produced 3.3% of the electricity from the wind [28]. Denmark has always been the leader in offshore wind power with an installed capacity of 427MW but since the opening of the 194MW Lynn and Inner Dowsning wind farms in 2008, UK became the first offshore wind power producer with an installed capacity of 598MW. Furthermore, Belgium opened in 2008 the first 30MW phase of Thornton Bank wind farm. In the future the total capacity of this farm will be 300MW. This offshore wind farm is the first one in the world where 5MW turbines were installed.

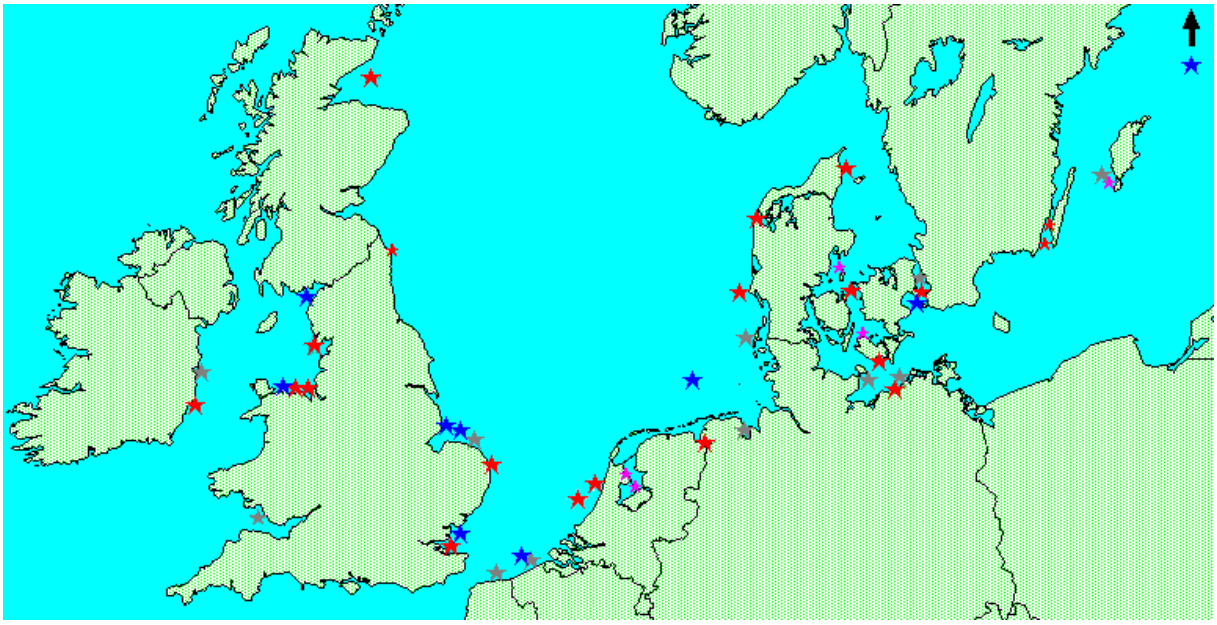

Figure 3-1: Offshore wind farms in Europe in September 2008. Red = builtMW turbines, purple =built small turbines, blue = under construction, grey = planned.[1]

[1] *Notice that the Lynn and Inner Dowsning wind farms are under construction in this map. However they have been open in October 2008.[29]*

Name	Country	Turbine Manufacturer	Number of Turbines	Turbines Rated Power (MW)	Wind Farm Installed capacity (MW)	Sea Depth (m)	Distance to the Shore (km)
Beatrice	UK	REpower	2	5	10	45	25
Blyth	UK	Vestas	2	2	4	6-11	0.8
Barrow in Furness	UK	Vestas	30	3	90	21-23	7
Burbo	UK	Siemens WP	25	3.6	90	1-8	6.4
North Hoyle	UK	Vestas	30	2	60	10-20	6
Scorby Sands	UK	Vestas	30	2	60	4-8	2.3
Kentish Flats	UK	Vestas	30	3	90	5	8.5
Inner Dowsning	UK	Siemens WP	27	3.6	97.2	6-13	5
Lynn	UK	Siemens WP	27	3.6	97.2	6-13	5
Arklow Bank	Ireland	GE Wind	7	3.6	25.2	2-5	10
Thornton Bamk (Phase 1)	Belgium	REpower	6	5	30	29	27
Princess Amalia	Netherlands	Vestas	60	2	120	20-24	23
Egmond ann Zee	Netherlands	Vestas	36	3	108	19-22	10
Lely	Netherlands	Nedwind	4	0.5	2	5-10	0.75
Irene Vorrink	Netherlands	NordTank	28	0.6	16.8	5	0.02
Ems-enden	Germany	Enercon	1	4.5	4.5	3	0.04
Breitling	Germany	Nordex	1	2.5	2.5	2	0.5
Nysted	Denmark	Bonus	72	2.3	165.6	5-9.5	10
Samsø	Denmark	Bonus	10	2.3	23	20	3.5
Frederikshavn	Denmark				10.6	4	0.2
		Vestas	2	3	6		
		Bonus	1	2.3	2.3		
		Nordex	1	2.3	2.3		
Ronland	Denmark				17.2	1	0.2
		Bonus	4	2.3	9.2		
		Vestas	4	2	8		
Horns Rev	Denmark	Vestas	80	2	160	6-12	14-20
Middelgrunden	Denmark	Bonus	20	2	40	3-6	3
Vindeby	Denmark	Bonus	11	0.45	4.95	3-5	1.5
Tuno Knob	Denmark	Vestas	10	0.5	5	3-5	6
Yttre Stengrund	Sweden	NEG-Micon	5	2	10	6-10	5
Utgrunden	Sweden	GE WindEnergy	7	1.425	9.975	7-10	8
Bockstigen-Valor	Sweden	Windwolrd	5	0.5	2.5	6	3

Table 3-1: Built offshore wind farm in Europe [29]

As it can be seen in Figure 3-1 many offshore projects are under construction or are planned in Europe. Denmark expects for 2009, two offshore farms with a capacity of 200MW, Horns Rev II and Rødsand. These two farms will produce 4% of the Danish electricity. In UK, around 500MW are under construction and 2556MW are approved with the 1000MW London Array project. [30] Although Germany is the country were the installed capacity of wind power is the more important in the world, it has only experimental offshore wind farms but the government has a target of 17000MW offshore wind power approved [31]. Furthermore countries like The Netherlands, Belgium, Ireland, Spain and France have under construction or planned projects. Today, Norway has no operational offshore wind farms but plans have been made in this perspective. Statkraft develops the possibility to build a 1000MW offshore wind farm on the Norwegian coast in 2012.

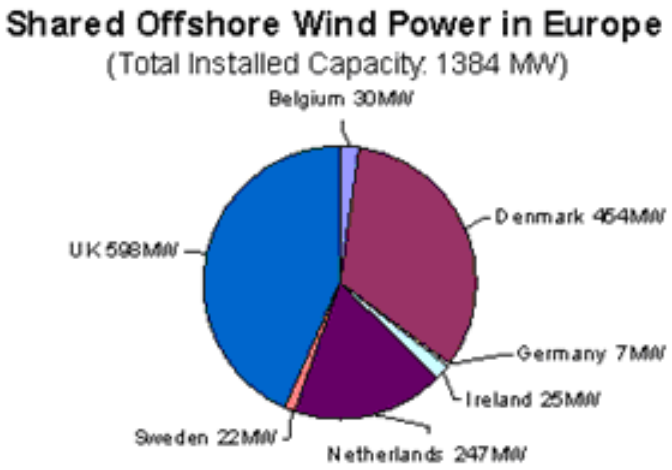

Figure 3-2: Installed capacities of offshore wind power in European countries

3.2 RESOURCES IN NORWAY

3.2.1. STATUS OF WIND POWER IN NORWAY

The installed wind power capacity in Norway is 380MW divided in 15 wind farms which represents 1.25% of the total installed production capacity, and in 2007, the wind plants electricity generation represented 0.65 % of the total generation with 910GWh [15]. However Norway has a great potential for wind power and its goal is to exploit this energy source. NVE (Norwegian Water Resources and Energy Directorate) plans a generation of 3000GWh in 2010, 5000-7000GWh in 2015 and 7000-20000GWh in 2020 with wind power. [16].

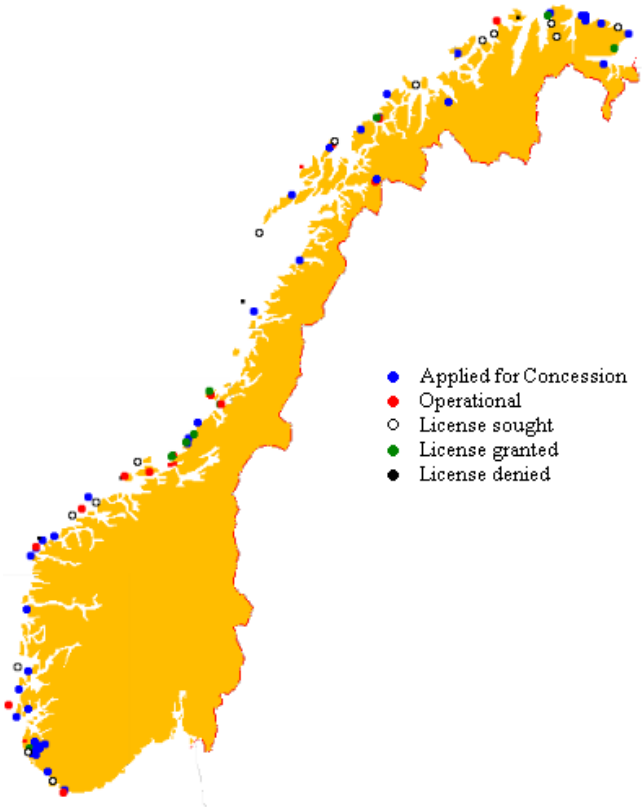

Figure 3-3: Wind farms situation in Norway [33]

3.2.2. THE NORWEGIAN POTENTIAL FOR WIND POWER

The potential of wind in Norway onshore and offshore is clear and scenarios bank on a generation of 20TWh for 2020. This production will require 6000-7000MW installed capacity within an area of 600 km^2 which is very small compare to the 304280 km^2 of the Norwegian territory. The investments on this scenarios and with the current prices will be around 90 billions of NOK but the CO2 saving will represent 15Mtons/years.

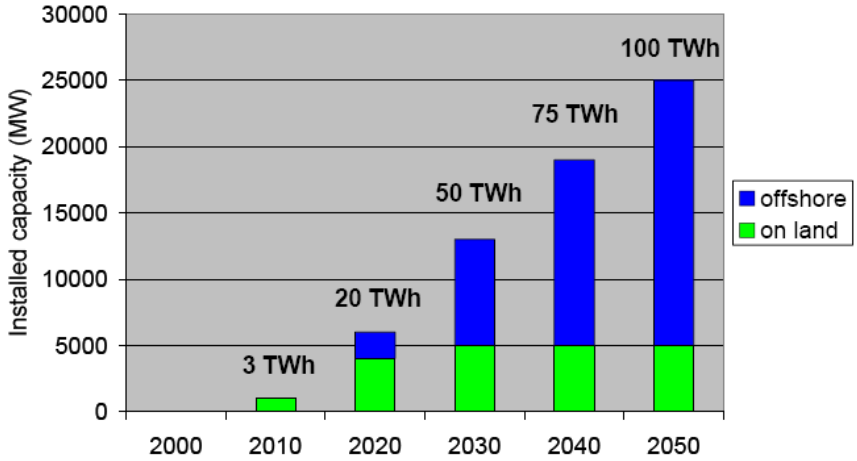

Figure 3-4: Scenario for the evolution of the installed capacity of wind power in Norway until 2050 [18]

Norway is an ideal candidate for Wind power. The wind map in Figure 3-5 shows the great wind potential for onshore sites.

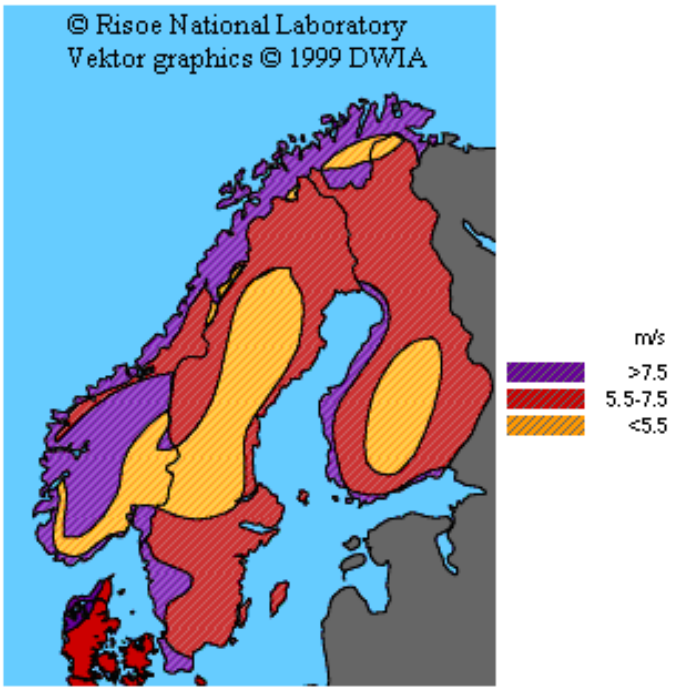

Figure 3-5: Wind map of northern Europe [17]

NVE made a study on the Norwegian wind potential. The study concerned the Norwegian coasts and the offshore areas with a depth less than 50 meters. The conclusions of this study are resumed on the following tables [19]:

Wind speed (m/s)	>6	>7	>8	>9
Area (km^2)	26559	17754	7859	2509
Energy production (TW/h) with an installed capacity of 15MW/km^2	1165	876	444	156

Table 3-2: Area and energy production according to minimum average wind speed for onshore [19]

Sea depths (m)	-10	-20	-30	-40	-50
Area (km^2)	4707	8739	12543	16139	20151
Energy production (TW/h) with an installed capacity of 15MW/km^2	181	345	504	656	829

Table 3-3: Area and energy production according to minimum average sea depths for offshore [19]

These tables show the enormous potential of the Norwegian wind power generation, both onshore and offshore. The goal of 3000GWh in 2010 can be achieved by erecting wind turbines in an area of 60 km^2 [19].

3.2.3. WIND POWER CHARACTERISTICS

Furthermore, studies made on possible onshore implantation sites show that the annual utilization time at full load is typically superior to 3000 hours. The cost of operation for wind power is around 30øre/kWh and with the development of the technologies, this cost tends to reduce.

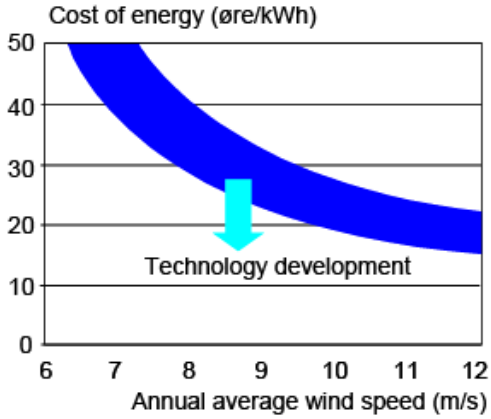

Figure 3-6: Cost of on-land generation as a function of the average wind speed.[20]

An other important fact in the Norwegian case is that the power system is based on hydro power which gives very good regulation capabilities to the power system. Thus the introduction of wind power in the system is easier than in a thermal or nuclear based power system. Wind power and hydro power are a very good combination of generation types for several reasons. Firstly the correlation between wind and hydro generation is small which leads to a stable system. Secondly the wind power generation is normally more important in winter than in summer and as it can be seen on Figure 3-7 wind plant generation follows the consumption. In the opposite, water inflows are essentially in summer. Thus there is a good balance between the two generation types. Finally wind generation varies less than hydro generation Figure 3-8. Studies show that the variations of the mean power of wind over 20 years are around 10% [24] while variations for hydro power are around 20%. Wind is then more predictable and constant than water inflows so generation plans can be more accurate.

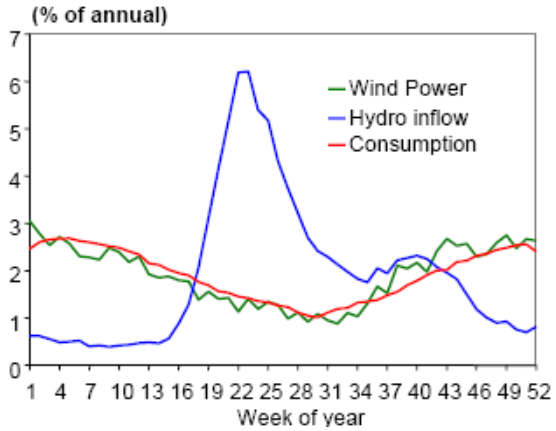

Figure 3-7: Normalized weekly hydro power inflow compared with wind power production and consumption [21]

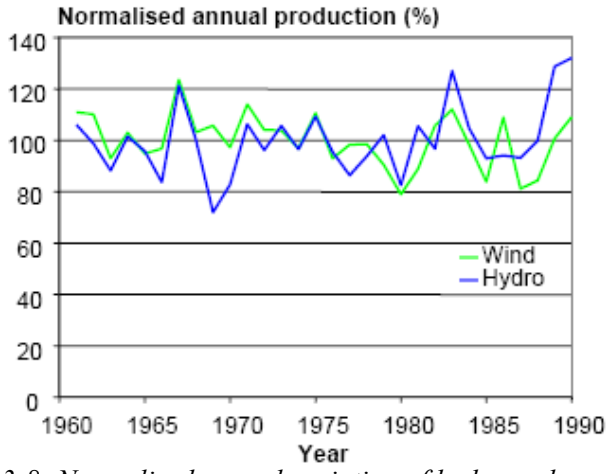

Figure 3-8: Normalized annual variation of hydro and power [21]

3.3 WIND POWER TECHNOLOGY

3.3.1. INTRODUCTION

Using wind energy is not a new idea. Traces of utilization of wind for different goals are found on the human history, in every culture and since a long time. However utilization of wind energy as a reliable source of electrical energy generation is quite recent and with the reduction of the fossil fuel reserves and the increase of the environmental concerns, it becomes more and more considered. Furthermore, since the 1980s and the beginning of wind power industry, wind energy technology knew a big evolution (Figure 3-9).

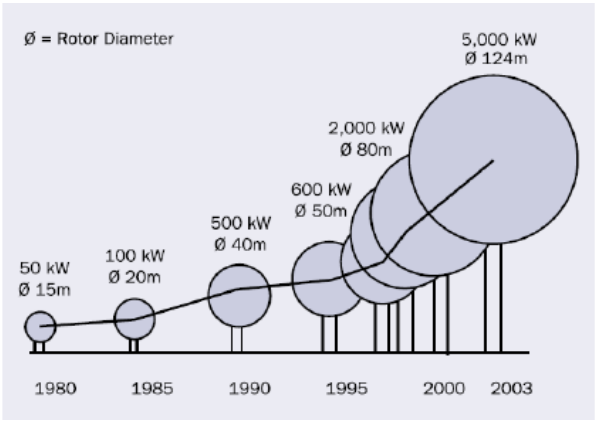

Figure 3-9: Evolution of wind turbines' rated power and rotor diameters since 1980.[22]

Today the wind power industry is one of the thriving industries in the electrical energy production sector. In 2007 the global turnover of the wind power industry was estimated to be 160MNOK. The leaders of the market are Vestas (Denmark), Gamesa (Spain), GE Wind (USA), Enercon (Germany), Suzlon (India) and Siemens (Germany).

Figure 3-10: Manufacturer World Market Shares in 2005 and 2006 [23]

3.3.2. WIND TURBINE

Wind turbine consists in a nacelle fixed on a tower where a vertical rotor blade rotates and transforms wind energy in electrical energy. The nacelle houses electrical and mechanical parts of the wind turbine. The number of blades can vary from one to twenty or more but typically there are three blades on a wind turbine. With this number of blades the performances of the wind turbine are the best for the production of electricity. The diameter of the rotor reaches 124m and the tower sizes are from 30m to up to 100m. Today, wind turbines power is rated between 2 and 5MW but as it can be seen on Figure 3-9 rated power evolutes quickly and turbines with a bigger rated power are under development.

Wind is created by the difference of temperatures between air masses in the atmosphere. The mechanical power from the wind (P_W) is given by:

$$P_W = \frac{1}{2}\rho A V^3 \tag{3.1}$$

with ρ the air density, A the area swept by the rotor blades and V the velocity of the air. However a wind turbine is not able to extract all the power from the wind. Indeed, a part of the wind will be completely stopped by the rotor area. According to Betz, the maximal wind power that can be converted in mechanical power by a wind turbine is [25]:

$$P_{\max} = \frac{1}{2}\rho A V^3 C_{p\max} = \frac{1}{2}\rho A V^3 \times 0,59 \tag{3.2}$$

where C_p is the power coefficient of the rotor or the rotor efficiency. Thus a theoretical maximum of 59% of the wind power can be used if the system has no losses. Today, for a modern three-blade wind turbine, C_p ranges between 0.4 and 0.5.

For a given wind speed, the rotor efficiency is a function of the tip speed ratio, λ. This one is defined as the ratio between the tip of the blade speed and the wind speed:

$$\lambda = \frac{V_{tip}}{V_{wind}} = \frac{\omega R}{V_{wind}} \tag{3.3}$$

where V_{tip} is the speed of the tip of the blade, V_{wind} is the wind speed, ω is the rotational speed of the rotor and R is the radius of the rotor. The maximum rotor efficiency occurs at one tip speed ratio.

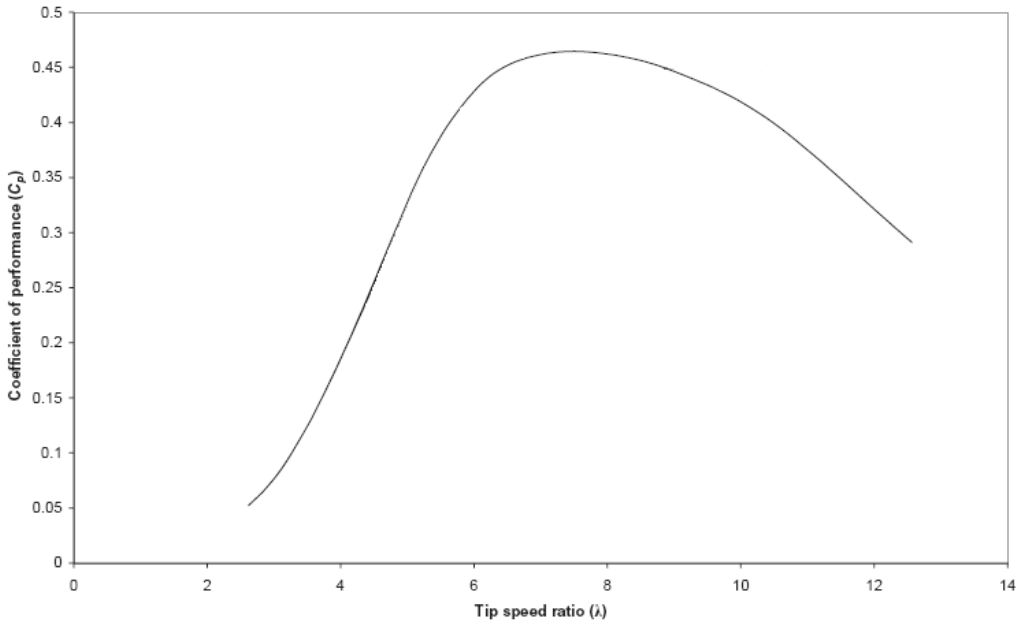

Figure 3-11 Typical rotor efficiency (C_p)- tip speed ratio (λ) Curve

3.3.3. PERFORMANCE CURVE AND REGULATION

Figure 3-12 shows the typical wind turbine power curve. The wind turbine starts producing at the cut-in speed i.e. around 4-5m/s. Below this speed, it is not efficient to start the production. Between the cut-in speed and wind speeds around 13m/s, the wind turbine is producing at its maximum efficiency. When the wind turbine reaches its rated power, the production becomes constant independently of the wind speed until a certain limit. This limit is the cut out speed. When the wind speed is too important, the wind turbine risks to be damaged. Thus, the production is stopped in order to protect the blades and the wind turbine in general. The cut-out speed corresponds to winds with a

speed around 25m/s. Three options are used in the wind turbine design in order to control the power output.

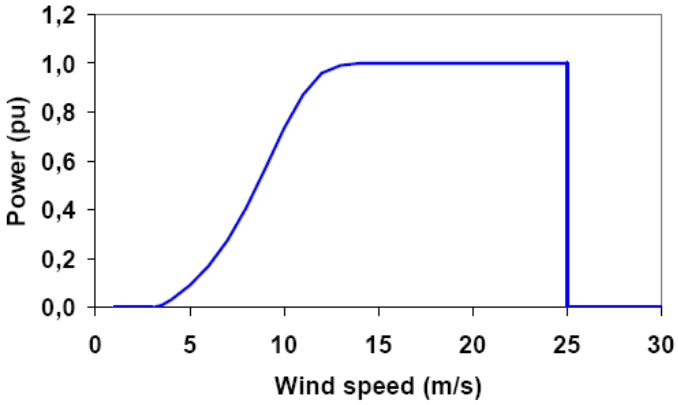

Figure 3-12: Typical Wind Turbine Power Curve.

The first option is called stall regulation. The principle is, with wind speeds superior to a certain limit, to achieve a constant rotor speed independently of the wind speed. Blades are design to created turbulences when the wind reaches the speed limit. Thus the aerodynamic forces on the blades are reduced and the output power too. Furthermore, stall effect permits to protect blades from mechanical overstress but also to protect generators from overloading and overheating [25]. The advantage of this technique is that blades are fixed so it avoids moving part in the rotor and complex control systems. However, the aerodynamical design of the blades is very complex and some vibrations due to the stall effect can cause problems in the whole wind turbine. [26]

The second option is called pitch regulation. In this concept, the blades can turn on their longitudinal axis. As for a plane wing, the rotation modifies the aerodynamical profile of the blades and then the forces applied on them can be controlled. A control system adjusts the angle of each blade independently from the other and then the output power can be maintained constant. [11,12] Pitch-control gives to the wind turbine a better yield for low wind speed than stall-control, as blades can be kept at the optimum angle every time.[22]

The last option is a combination of the two other control options and it is call active stall regulation. For low wind speeds, the blades are pitched like in a pitch regulation hence a better efficiency is achieved. When the turbine reaches its rated power, the angle of attack of the blade is increased in order to create a stall effect on the blades but in the opposite direction from the pitch regulation. An advantage of this regulation is that the output power can be controlled more accurately compare to a stall regulation. Furthermore, the control system is simpler than pitch regulation.

3.3.4. CONVERSION OF ENERGY: THE DIFFERENT TYPE OF GENERATORS

The mechanical power created by the rotor has to be transform in electrical power. However, in order to be injected on the grid, the output power of the wind turbine must have the same frequency as the grid. Several alternatives are possible.

3.3.4.1 *FIXED SPEED CONCEPT*

The wind turbine can operate at fixed speed (Figure 3-13). Once started, the turbine will rotate at the same speed independently of the wind speed. Operating at a fixed speed simplifies the electrical system of the wind turbine, as the frequency of the output power is the same as the frequency in the grid. However, as it can be seen on Figure 3-11, the maximum efficiency of the turbine corresponds to only one tip speed ratio. Thus the energy captured is not maximal with a fixed speed operation. This concept was historically the first one to used. It is based on a squirrel cage asynchronous generator (SCIG). Due to the low rotating speeds of the blades, the rotor of the generator is connected to the turbine with a gearbox. The stator is directly connected to the gird.

An improvement of the fixed speed operation is the two-speed operation. The asynchronous generator is composed of two independent sets of winding. Thus, the wind turbine can operate at two different fixed speeds. The performances of the wind turbine are improved and its noise is reduced for low wind speeds. Fixed speed wind turbines (one or two speed) represent 30% of the European market [27].

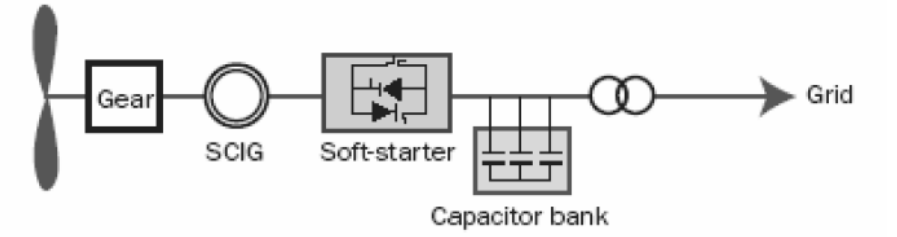

Figure 3-13: Fixed Speed wind turbine [27]

3.3.4.2 *LIMITED VARIABLE SPEED CONCEPT*

The wind turbine can operate at a limited variable speed or also called variable slip operation. The generator is a wound rotor induction generator (WRIG) with a variable resistance in series with the rotor circuit. The slip speed and the air-gap torque of the generator can be controlled by changing the series resistance with power electronics. Hence it is possible to control the speed of the turbine and generator. However the speed variations are limited in a range of ±10%. Limited variable speed wind turbines represent 10% of the European market. [27]

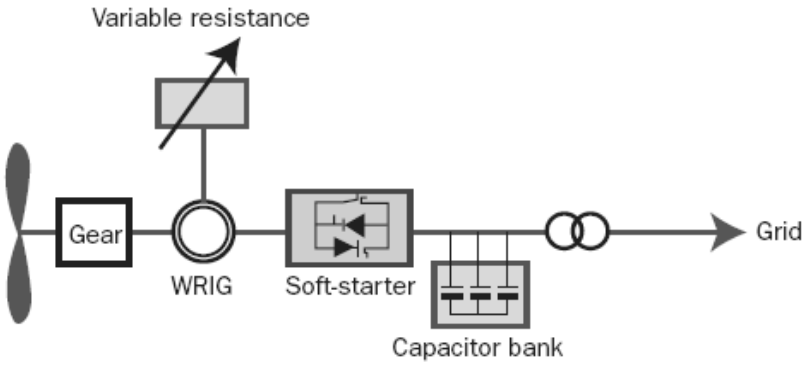

Figure 3-14: Limited variable speed wind turbine [27]

3.3.4.3 VARIABLE SPEED CONCEPT

The third type of system is the variable speed wind turbine. In this concept the generator is a wound rotor induction generator (WRIG) but by introducing a frequency converter between the generator and the network, it is possible to decouple the mechanical and the electrical frequency of the rotor. The stator of the generator is connected directly to the grid and the windings of the rotor are connected to the frequency converter. Then the rotor windings are fed with decoupled frequencies currents. Thus the rotor speed is allowed to vary and then variable wind speed operations are allowed. This kind of generator is called Double Feed Induction Generator (DFIG). One advantage in this kind of operations is that the turbine speed can vary with the wind speed, below the rated speed. Then the turbine operates at the maximum rotor efficiency and the production is higher. Another advantage is that reactive and active power can be controlled, so the power factor can be maintained at a constant value. It is also possible to use wind turbine as a compensator of reactive power in weak networks. Variable speed with DFIG wind turbines represent 45% of the European market. [27]

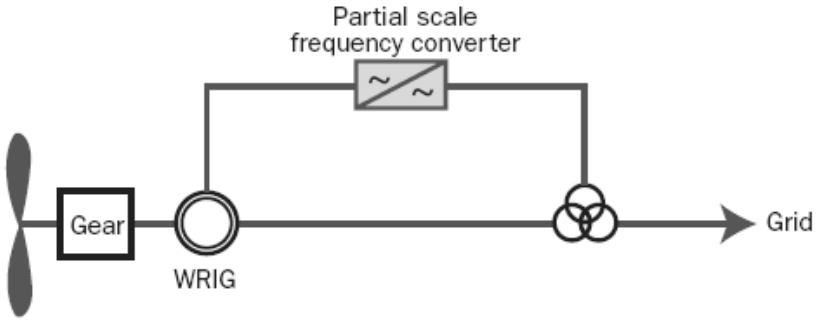

Figure 3-15: Variable speed with DFIG wind turbine [27]

3.3.4.4 DIRECT DRIVE CONCEPT

All the previous wind turbine concepts presented used a gearbox in their structure. However, gearboxes are sources of big mechanical losses and need a high maintenance. In order to avoid gearboxes in wind turbines, the generator can run at a slow speed which is the same as the turbine speed. Different types of generators can be used for example synchronous generator with wounded rotor, permanent magnet generator or squirrel cage induction generator. The generator is connected to the grid via a frequency converter. Thus the generator is completely decoupled from the grid and by controlling the frequency converter, every speed is allowed for the generator. A disadvantage is that the generator needs many poles for working at low rotational speeds and thus its dimensions are important. Another version of the direct-drive concept is the hybrid concept. A gearbox is use to increase the low speed of the turbine to

medium speed for the generator. Thus the number of pole needed is reduced as well as the dimensions of the generator. Direct drive wind turbines represent 15% of the European market. [27]

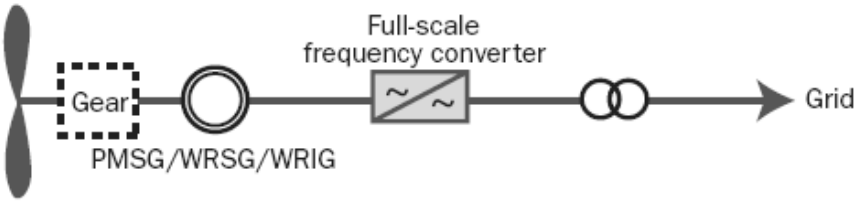

Figure 3-16: Direct drive wind turbine [27]

Until 2000, the fixed speed models were dominant in the market but with the evolution of technologies, particularly improvements of power electronic, it is more common to use variable speed models today. For example the annual share of variable speed models was 42% in 1998 and increased to 80% in 2004 [27]. DFIG models are the most common installed models today.

3.3.5. SHALLOW WATER FOUNDATIONS

Wind power is more expensive offshore than onshore. Thus, to build an offshore wind farm, an important point is the costs, and subsea foundations are a major part of these costs.

3.3.5.1 *MONOPILE FOUNDATION*

Today the most common solution used for offshore wind farms is monopile foundations [34]. A pile is a steel tube with a diameter between 3.5 to 4.5 m. It is pushed into the sea bed at a depth of 10 to 20m by using vibration or a pilling hammer. The tower of the wind turbine is then installed on the pile. It is a simple solution which can be used on water depth ranges to 25m. One advantage of this solution is that the seabed has not to be prepared before the installation.

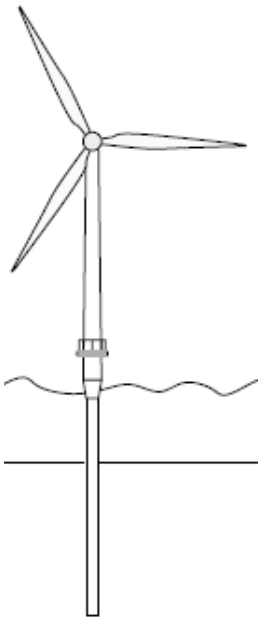

Figure 3-17: Monopile wind turbine foundation

3.3.5.2 GRAVITY BASED FOUNDATION

Another common solution is the gravity based foundation. The gravity force of a concrete caisson maintains the wind turbine in the right position. The caisson is build onshore and carries by floating to the park site offshore. Then it is filled up with sand and gravels. The wind turbine is mounted on the caisson. The caisson has a conical form in order to break the possible pack ice in sea [26]. However a disadvantage of this concept is that the caisson become heavier with water depth and so it is more expensive. This concept is avoided for water depth superior to 10m.

An alternative is the steel gravity base. The method is the same but as steel is lighter than concrete, the installation is easier to install. A flat steel box filled with a dense mineral called olivine, lies down on the seabed. A steel tube is fixed on the flat box and the tower of the wind turbine is mounted on the tube. [26]

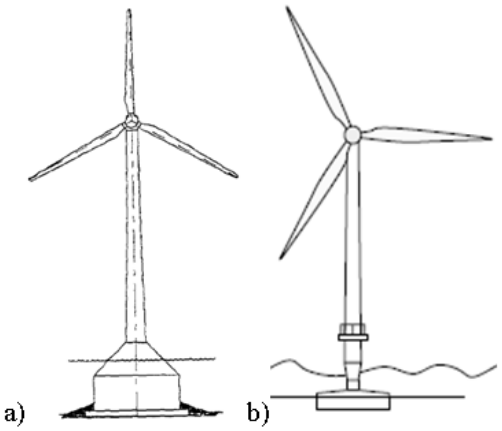

Figure 3-18: Gravity based foundation: a) concrete foundation; b) steel foundation

3.3.5.3 TRIPOD FOUNDATION

For deeper water and heavier turbines, monopole and gravity based solutions can not be use. The tripod structure is the solution for these situations. The structure is made of a central column which carries the tower while three arms which support the central column are fixed to the sea bed with pile push in the soil. An alternative to pile is to use small caissons similar to the gravity based foundation. The tripod structure is used on two experimental turbines in Beatrice field in Scotland [34].

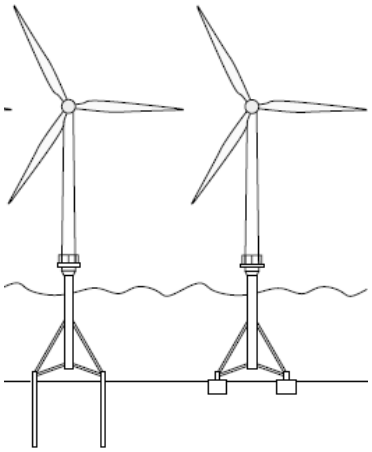

Figure 3-19: Tripod structure

3.3.6. DEEP WATER FOUNDATIONS

The previous technologies are limited technologically and economically by the sea depth (maximum around 50m). However, a great potential of wind exists far from the coast, which means deeper sea. In the case of Norway, the sea depth increase rapidly near the coast. Thus development of new support structures iare needed. Floating option seems to be the more adapted solution. The different concepts investigated can be divided in three categories in regard of physical principle and technology used to achieve wind turbine stability [35], the ballast concept, the mooring lines concept and the buoyancy concept

.

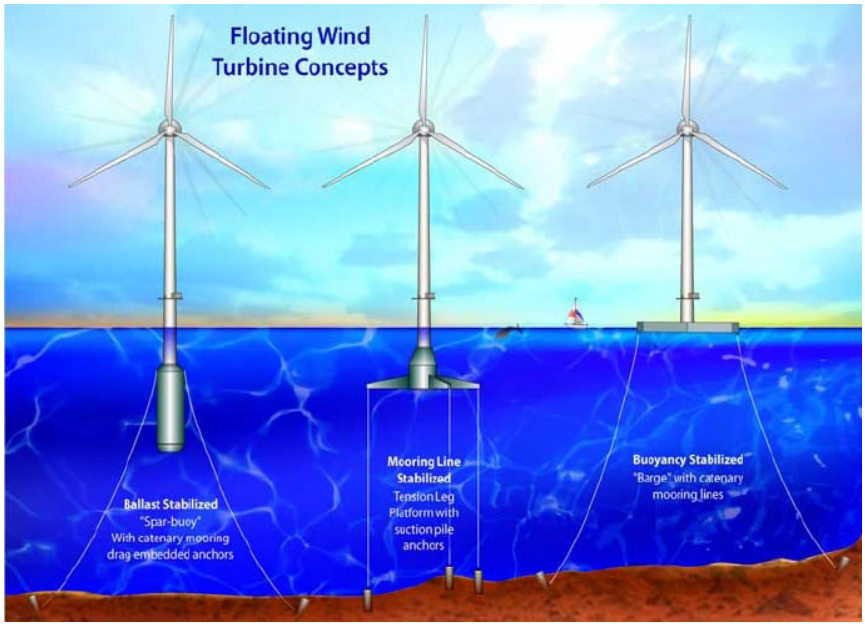

Figure 3-20: Floating Wind Turbine Concepts [35]

3.3.6.1 *BALLAST CONCEPT*

The ballast concept consists in a ballast fixed on the bottom of the tower of the wind turbine. The ballast permits to put the wind turbine gravity centre below the floating point of the structure, thus the stability is ensured. Furthermore, the wind turbine is anchored in the seabed with mooring lines. Statoil-Hydro developed a prototype of this concept called HyWind. It consists in a 2.3MW wind turbine with a rotor diameter of 80m lying 65m under the water and attached to a 100m spar-buoy. The technology is similar to the one used in offshore platform. The turbine is moored to the seabed using three anchor points which can be at a depth between 120 and 700m. Simulations have been made with success on a reduced prototype (scale 1/47) in a water tank. Statoil plans to install the wind turbine in autumn 2009 in the south east of Norway. The sea depth will be 210 m. [36]

Figure 3-21: The HyWind Project [36]

3.3.6.2 *MOORING LINES CONCEPT*

In the mooring line concept, the wind turbine is mounted on a platform buoy. This last one is anchor to the seabed with mooring lines which are tensed. Thus the stability of the structure is ensured. This concept also called Tension Leg Platform (TLP) has been investigated by the American National Renewable Energy Laboratory (NREL). The platform is designed for 60 to 200 m sea depths and for a 5MW wind turbines. Simulations have already been made with concluding results [37]. Another design is the Dutch tri-floater developed by the Delft University. The central tower is attached to three semi-submersible buoyancies in periphery. The structure is then anchor to the seabed.

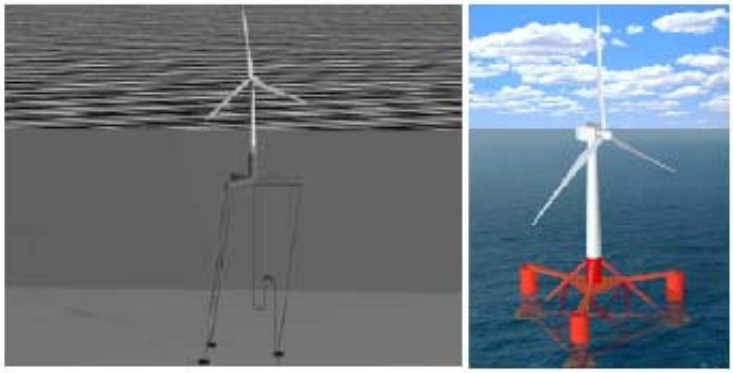

Figure 3-22: Two mooring line concept, the NREL TLP and the Dutch tri-floaters.

3.3.6.3 *BUOYANCY CONCEPT*

The last concept, the buoyancy concept, consists in a large buoy platform floating near the surface on which the wind turbine is fixed. The structure is held in place by mooring cables. This concept is also investigated by the NREL. However it seems less stable than the two other in extreme wave conditions.

3.3.6.4 ADVANTAGES AND DISADVANTAGES OF THE DIFFERENT CONCEPTS

The advantages and disadvantages of each concept are resumed in the following table [35].

	Floating Platform Technical Challenges		
	Platform Stability Classifications		
Platform Design Challenge	Buoyancy (Barge)	Mooring Line (TLP)	Ballast (Spar)
Design Tools and Methods	-	+	-
Buoyancy Tank Cost/Complexity	-	+	-
Mooring Line System Cost/Complexity	-	+	-
Anchors Cost/Complexity	+	-	+
Load Out Cost/Complexity (potential)	+	-	
Onsite Installation Simplicity (potential)	+	-	+
Decommissioning & Maintainability	+	-	+
Corrosion Resistance	-	+	+
Depth Independence	+	-	-
Sensitivity to Bottom Condition	+	-	+
Minimum Footprint	-	+	-
Wave Sensitivity	-	+	+
Impact of Stability Class on Turbine Design			
Turbine Weight	+	-	-
Tower Top Motion	-	+	-
Controls Complexity	-	+	-
Maximum Healing Angle	-	+	-

Table 3-4: Advantages and disadvantages of the different floating concept. Advantage (+); Disadvantage (-); Neutral (blank)

4 THE NORWEGIAN POWER SYSTEM

4.1 NORWEGIAN PRODUCTION AND CONSUMPTION

Today 99.6% of the Norwegian electricity is produced with renewable energies of which are hydro power (98.5% of the total generation), wind power (0.6% of the total generation), biofuel (0.3% of the total generation) and wastes (0.2% of the total generation). The rest of the generation is ensured by thermal plants with natural gas [38]. In 2007, the installed capacity[2] of production in Norway was 30313MW and the available production capacity[3] was 24480MW. However the consumption peak was 21588MW on 14 December 2007. Figure 4-1 summarizes the average and maximum production and consumption for the last 5 years:

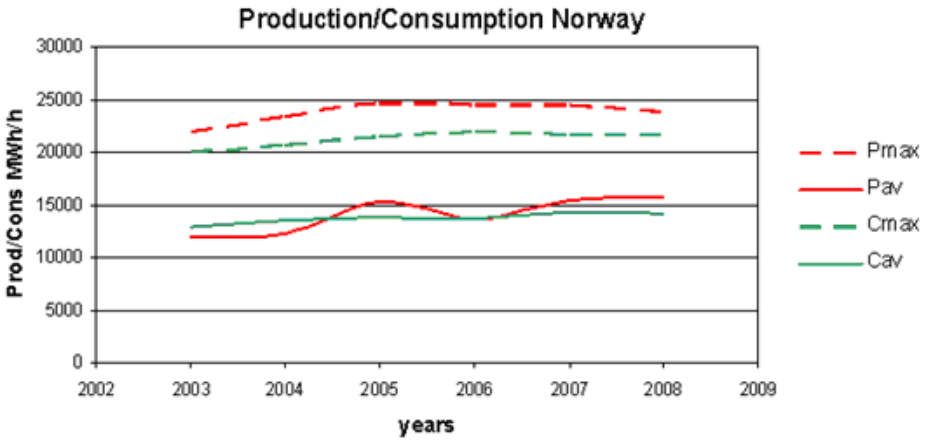

Figure 4-1: Production and consumption in Norway the last 5 years

Table ***3-1*** shows the Norwegian power balance for years between 2002 and 2007.

Year	2002	2003	2004	2005	2006	2007
Generation	130591	107122	110545	137948	121715	137387
Net Supply	120918	115008	122040	125908	122572	127352
Net import	-9673	7886	11495	-12040	857	-10035

Table 4-1: Total electricity balance in Norway between 2002 to 2007(GWh)[39]

It can be noticed from the Figure 4-1 and Table 4-1 that the generation capacity varies significantly from year to year. This is explained by the fact that the dominating supply of Norwegian electricity is hydropower which is very dependant of the precipitations.

4.2 IMPORTATIONS AND EXPORTATIONS

Norway can import/export power with its neighbour countries. The general tendency shows that Norway export power. However since few years this tendency tends to reverse. The mains exchanges are between Sweden and Norway with a transmission capacity around 3000MW. But

[2] *The installed capacity is the sum of rated net capacity of each individual power plant. This capacity does not represent the available capacity at any single time*

[3] *The available production capacity is estimated by Nordel. It represents available production capacity for the market at peak on a cold winter day (10-year winter)*

connections exist with Denmark, the Netherland, Russia and Finland. Most of the time for this two last connections, Norway imports power because of the weakness of the grid and the low production on the northern Norway, but the transmission capacity is small (170MW). Connections with Denmark and The Netherlands are ensured with two HVDC links, the 1000MW Skagerrak connection with Denmark and the 700MW NorNed connection with the Netherlands.

Figure 4-2: Main cross border transmission capacities inn 2008(aggregated capacities)

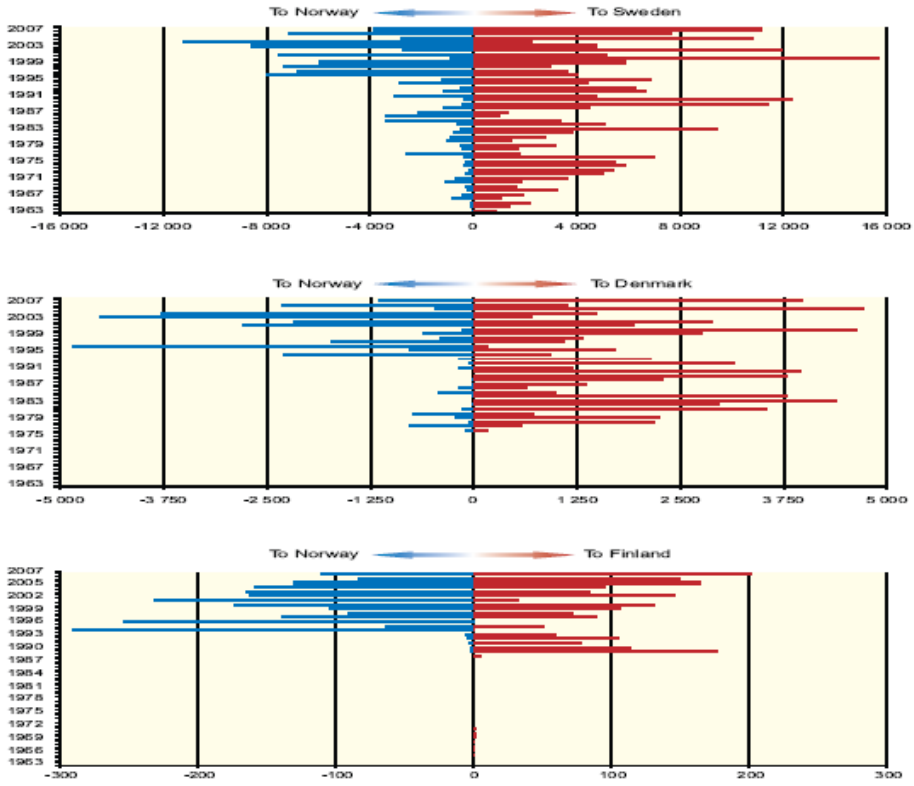

Figure 4-3: Importations and exportations of Norway with its neighbours (MWh/h). [38]

Concerning the exchanges with Russia, Statnett gives a net import of 878.5GWh in the last 5 years i.e. an average of 20,1MWh/h. Concerning the NorNed connection, since its opening the 6th May 2008, the net export given by Statnett is 3064.5MWh i.e. 534,25MWh/h.

4.3 POWER MARKET

The Norwegian power market is open and Norway forms a part of Nordpool. Nordpool is a multinational exchange for trading supply and demand of electric power. The last one is bought and sold between different participants. The hourly price of electricity is called spot price. This one depends on several parameters like weather forecast, transmission capacities or price of raw materials. Thus it is possible to optimize the power plants production in order to have the best profit.

4.4 TYPE OF PRODUCTION

As said, the main generation type in Norway is hydro power. Water is a natural source of energy and consequently is free. However, water has a value called water value because it can be stocked. The water value is dependant of several parameters as the level of water in the reservoir, the quantity of snow in the mountain or the weather forecasts. By comparing this water value with the spot price, it is possible to optimize the production of a hydro power plant and consequently to derive the best benefit of this last one. For example, if two hydro power plants A and B are considered with a water value wva and wvb respectively and with a spot price sp, in the manner that wva>sp>wvb, the benefit will be maximum if the production is made by the plant B and if the water in the reservoir A is stored in order to use it when the spot price will be higher. However, for a hydro power plant with reservoir level at its maximum, if a water income is planned, then the water value become null and the production of the plant will be push to its maximum in order to increase its water value. This is the case with small hydro power plants which are numerous in Norway.

Wind is a free resource, but in the opposite of water, wind has no value because it can not be stocked and used when spot price is high. Wind is an “instantaneous” resource. A wind farm can produce power as long as the wind blows, and if a wind farm does not produce at its maximum, the resource is lost. Thus a wind farm will always have priority on the hydro power plant. One exception is when the reservoir is full then the hydro power plant will produce.

4.5 THE GRID CODE

The Norwegian power grid is divided in three parts, the main transmission grid, the regional grid and the local grid. Municipalities are often owner of the regional and local nets while Statnett the Norwegian TSO (Transmission System Operator), and thus the Norwegian state, owns the main transmission net. The Norwegian main transmission grid is composed of 9023km of lines divide in lines of 420kV (2431 km), 300kV (4512km) and a 132kV (2080 km). [38]

Norway and Statnett are part of Nordel which is the organization of the TSOs for the Nordic countries (Norway, Sweden, Finland, Eastern Denmark and Iceland). As the operations between the different TSOs have to be co-ordinated, Nordel is ruled by the “Nordel Grid Code”. This one consists on the planning code, the operational code, the connection code and the data exchange code. Operational and data exchange codes are biding agreements while planning and connection code are rules that should be observe in the grid. The Nordel Grid Code corresponds to the minimal requirements that must be observed by the participants. Each TSO has its own code which completes the Nordel code [39] [40].

For connected a generation plant in the grid, several rules have to be observed. These rules are technical requirements that a plant must satisfy in order to be connected to the transmission system and then to ensure the security of operation in the power system.

Today, wind farms have a significant impact on power systems due to their large size. Thus wind farms are subjected to specific rules. For the connections of a wind farm in the Norwegian grid, the requirements are given by Statnett. The main requirements include the following aspects [20] [41]:

- Operation at varying grid frequency (normal 49.0Hz-50.5Hz, limited 47.5Hz-52.0Hz).
- Normal operation at varying grid voltage (± 10% of the nominal voltage and *cos φ*= ±0.91).
- Active power control (Remote control of production-level, system for ramp-rate limitation and participation in frequency control).
- Reactive power. System able to operate in two modes: Active voltage control and set point *cos φ*.
- Operation in case of grid faults or abnormal grid voltages (fault ride-through for voltage down to 0.15pu at the grid connection point).

Frekvens [Hz]	Spenning [pu]	Varighet
45,0-47,5	0,90-1,05	>20s
47,5-49,0	0,90-1,05	>30 min
49,0-52,0	0,90-1,05	Kontinuerlig
52,0-53,0	0,90-1,05	>30 min
53,0-55,0	0,90-1,05	>20s
55,0-57,0	0,90-1,05	>10s

Table 4-2: Areas of functioning for generation plants. Frequency ranges are listed in the first column, voltage ranges are listed in the second column and the length are listed on the third column

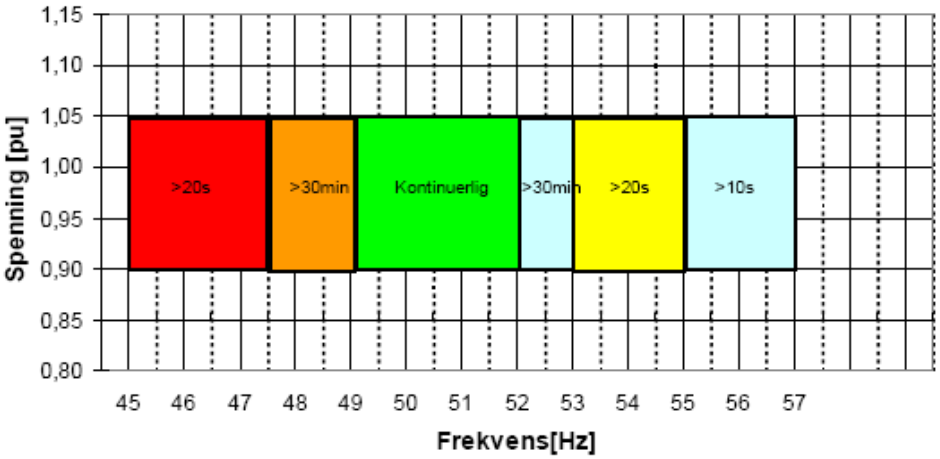

Figure 4-4: Areas of functioning for generation plants[4].[42] The horizontal axis represents the frequency and the vertical axis represents the voltage.

Statnett has also requirements concerning the power factor. For hydro or thermal generation, production units have to be able to work, at rated power, with a power factor superior to 0.91 inductive or capacitive. For the wind generation, the requirement is stricter and a wind farm has to be able to work with a power factor superior to 0.95 inductive or capacitive at rated power.

[4] *Wind plants can only operate in the frequency range of 47.5 to 52 Hz (orange and green zones) with corresponding voltage level and duration.*

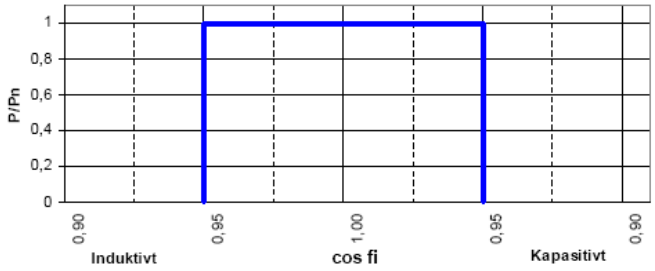

Figure 4-5: Reactive capacity for a wind farm.[42]

Other requirements are specific to wind power. Firstly, concerning the production, the wind has to be regulated down from the rated power to its stop in the maximum time of 30s. Secondly, the wind farm is also not suppose to limit its active power generation in case of low frequency and then should participate to the frequency regulation.

Concerning HVDC the Nordel requirements are [40]:

- HVDC link should be designed to have no negative effect on the grid (rapid voltage variations, harmonic voltage) and on the system operation (insufficient ability to tolerate of voltage dips, exaggerated input/output of reactive power).
- A bipolar cable should be designed to avoid the risk of losing both poles for the same reason
- For frequency between 49,5-49,9Hz, the HVDC interconnections should have a frequency-dependant regulation with droop.

As every generation plants, wind farms have also to respect some requirements in case of fault on the system. The production plants have to contribute to the short-circuit performance in order to avoid errors in the fault clearance and to ensure a satisfactory operation of the system after the disturbance. These requirements, also called low voltage fault ride through (LVRT), are given by Statnett. A power plant with nominal voltage superior to 200kV shall be able to operate and deliver power within the following voltages [42]:

- Voltage reduction to 0% voltage for up to 150 ms
- The voltage increases to 25%
- Linear increase in tension up to 90% within 750 ms.
- Constant grid voltage 90%

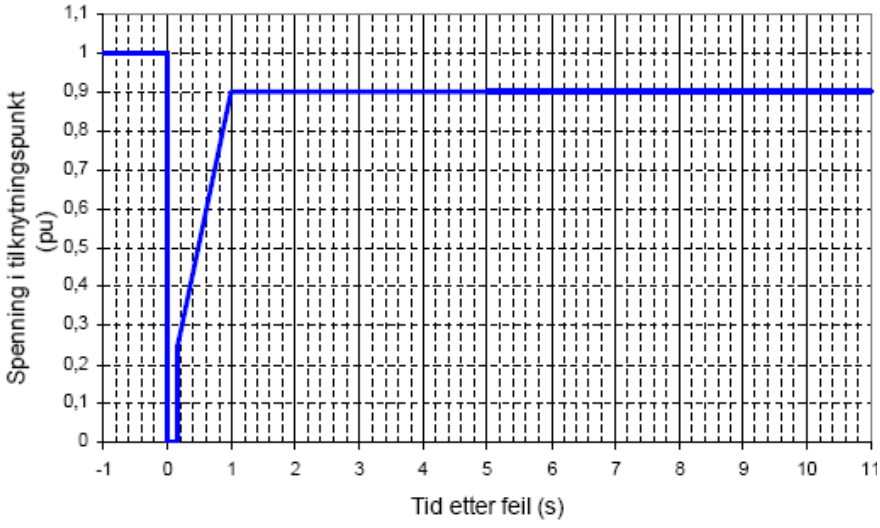

Figure 4-6: LVRT for power plants with a nominal voltage superior to 200kV.[42]

5 THE SIMULATION MODELS

5.1 PSS™E

Different programs are used by the industry to perform power systems performance in both steady-state and dynamic conditions. The three main programs available are SIMPOW from STRI, PowerFactory from Digsilent and PSS™E from Siemens. In a first time, the choice was made to use PowerFactory because of its easy use. However there were several problems with this software. Firstly, as the version available by NTNU was a demonstration version, the number of busses was limited to 50 which is very small. Secondly, the different models, like HVDC, wind farm or the Norwegian grid, were not available on this program. HVDC producer, ABB and Siemens, developed models of their products, respectively HVDC Light and HVDC PLUS on PSS™E and SINTEF has also available model of Norwegian grid on this software. Thus the choice of using PSS™E was taken.

All the stationary and dynamical simulations performed in this thesis were made by using PSS™E 31 from Siemens.

5.2 THE GRID MODEL

The grid model used in this thesis was given by SINTEF. It is a simplified model of the Nordel grid and it represents the grid in Scandinavia: Sweden, Norway, Finland, and East Denmark. The model consists in 37 busses from 22,5kV to 420 kV allocated in 13 geographical areas. Busses are divided as it follows in the Table 5-1. The 22,5kV bus corresponds to a SVC while the 150kV bus represents to a HVDC link between Sweden and Denmark. A comparison can be made in order to evaluate the simplification of the model: the model used by Statnett to perform analysis on the only Norwegian grid consists on 2200 busses.

Voltage level	*Number of Busses*
420 kV	23
300 kV	12
150 kV	1
22,5 kV	1

Table 5-1: Repartition of the model busses

In this simplified model, many busses of the real Nordic grid model are merged together with there generators and loads. For each area, the entire production and consumption are represented respectively by one or two generators and loads which lead to important production/consumption capacities compared to the reality. For example, some generator can produce more than 3000MW and some loads can absorb more than 1500MW.

In this model, Norway is more detailed than the other countries. Norway is represented by 23 busses allocated in 9 areas (12-420kV busses; 10-300kV busses; 1-22,5kV bus). The exchanges are also simplified. Norway is only linked to Sweden and the NorNed and Skagerrak connections are not represented. Figure 4-1 shows the production and the consumption in Norway the last 5 years. The average consumption is stable around 14000MW with an instantaneous maximum peak at 21915MW in 2006. For the production, the average value is around 15000MW with a tendency to increase the last few years. The maximum production was on 2005 with 24636MW. Due to the simplifications on

the model and the limited exchange possibilities, the choice was made for the simulations to use the average value of the consumption and production, respectively 14000MW and 16000MW.

Regarding the grid code exposed on part 4.5, the model complies with the requirements and the busses voltages are on the range 0.9-1.1 p.u. No branch is overloaded. However as the model is very simplified, the branches are not realistics and have a high rated power compare to real lines. Dynamics simulations have also been made in order to check the dynamic model and its behaviour. The system has been tested in normal operation and with a short-circuit on one bus. A test has also been made with the integration of a 1000MW machine representing the wind farm. In all the case the system remains stable. These tests and their results will be discussed in the part 8.

The simulation model is shown on the following figure:

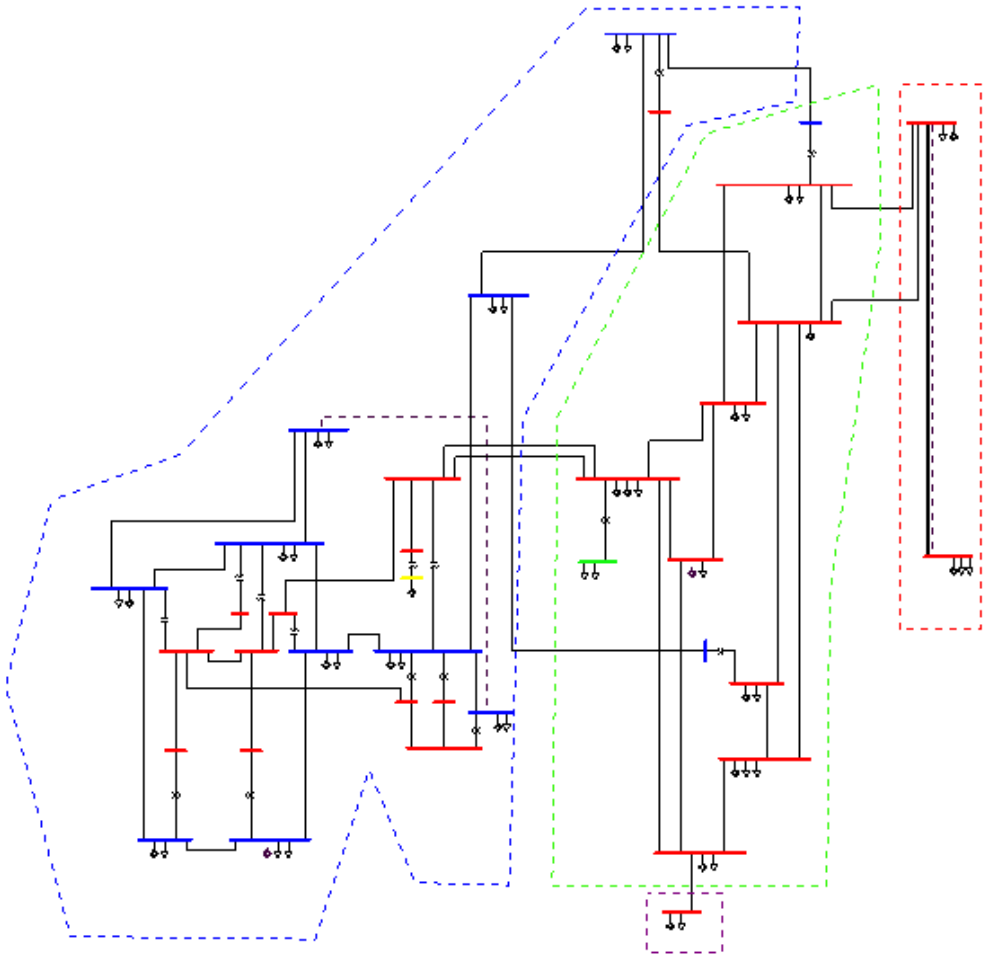

Figure 5-1: Nordic equivalent model

5.3 THE WIND FARM MODEL

As it has been said in the part 3.3.4, today the most common installed wind turbine concept is the variable speed concept, particularly the DFIG concept. In PSS™E a model of wind turbine with DFIG turbine, based on the G.E. 1.5MW wind turbine, is available. This model not only consists in an electrical model but also a mechanical model and a pitch control model. However as the object of this work was not to study the behaviour of the wind farm and as a 1000MW wind farm would have required 667 G.E. 1.5MW wind turbines, the choice was made to use only an induction machine to represent the 1000MW farm.

Commonly the models used to simulate induction wind generator in PSS™E are the standard models CIMTR1 and CIMTR3 [43]. These models represent single-cage or double-cage induction generator with rotor flux transients. The difference between the two is that the CIMTR3 model has an extra state which permits better results in case of large frequency variations. [44] A CIMTR3 model representing a Vestas V82 is given in the reference [43]. This model was used to represent the dynamic behaviour of the 1000MW wind farm. In this study, it is assumed that the wind farm is totally compensated at the offshore busbar. The voltage at the offshore busbar is 33kV and then is set up to 300kV by a transformer.

5.4 THE VSC-HVDC MODEL

The HVDC model used in this study is the VSC-HVDC model developed by PSS^{TM}E.
The model consists on two VSC converters and a bipolar transmission between them.

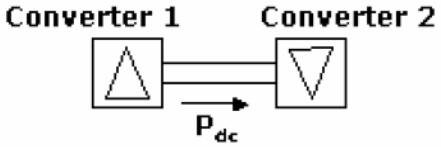

Figure 5-2: VSC-HVDC line in PSS^{TM}E.

In load flow, parameters as converter losses or line resistance have to be defined. Calculations of these parameters are based on the HVDC Light technology from ABB. However, due to different problem, the HVDC Light dynamic model from ABB has not been used for the dynamic simulations. A dynamic model of VSC-HVDC is available in the PSS^{TM}E user manual and after being adapted, this model has been used for the simulations. More detailed explanations on the VSC-HVDC model are given in the part 5.5.3.

5.5 THE DIFFERENT CONFIGURATIONS

5.5.1. INTRODUCTION

According to the wind farm size, to its distance from the shore or to the voltage of the wind farm, the type of connection will be different. In this study, four different connection configurations corresponding to four possible situations will be investigated.

5.5.2. CONFIGURATION 1

For distances until 75km HVAC is a simple and reliable solution and today all the offshore wind farms are equipped with this kind of systems. In the first configuration, a 1000MW wind farm situated at 50km from the shore is connected to the grid with a HVAC transmission system. The transmission system model used in the simulations is shown on Figure 5-3.

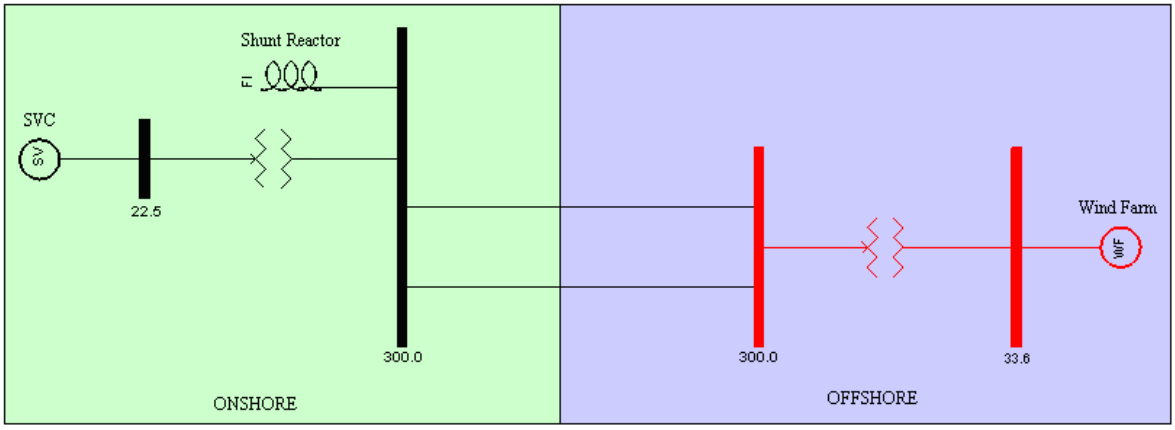

Figure 5-3: Configuration 1: Wind farm connected with HVAC

AC cable for a transmission of 1000MW at 300kV is not available on the market. In order to transmit this amount of power, two cables are used. The cables are cooper conductors with a cross section of 500mm^2. The per-phase resistance is 0.0604 Ω/km, per-phase inductance is 0.328mH/km and the shunt impedance is 0.13μF/km.

The length of both cables is 50km. These cables can be modelled as medium line, as follow:

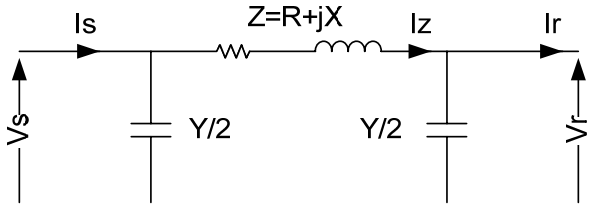

Figure 5-4: Π-model for medium line

Due to their capacitive properties, the AC cables produce a large amount of reactive power which has to be compensated at the receiving end of the cable. By using the ABCD transmission matrix, the losses and the reactive power production are calculated and then the compensation elements can be dimensioned. In this case and in normal operation, the received power is around 980MW and the production of reactive power is around 320MVar. A 320MVar shunt reactor is installed on the onshore side in order to absorb the reactive power produced by the cables.

As it has been explained in the part 4.5, the connection of a wind farm on the grid is ruled by the Statnett grid code. Concerning the power factor, the wind farm has to be able to work with a power factor *cosφ* superior to 0.95 inductive and capacitive. In order to respect this requirement, extra equipments have to be installed at the connection point. One SVC will ensure the operation of the wind in the power factor range of 0.95 inductive and capacitive. The dimensioning of the SVC is made in function of the received power and the limited power factor. It is given by the equation (5.1):

$$Q_{svc} = P_{rec} \times \tan(\cos^{-1}(\cos\varphi)) \tag{5.1}$$

with Q_{SVC} the reactive power of the SVC (MVar), P_{rec} the received power on the onshore bus, and *cosφ* the limited power factor. In this configuration, the received power is 980MW and the limited power factor is 0.95. Then the SVC should be dimensioned with a rated reactive 325MVar. The SVC voltage is set to 22.5kV for practical reasons with dynamics models.

5.5.3. CONFIGURATION 2

For distances from the shore superior to 150 km the need of compensation for an AC system become too important and too expensive. HVDC becomes the only feasible option, as well from the economical point of view as from the technological point of view. In the second configuration, a 1000MW wind farm situated 200km from the shore is connected to the grid via a HVDC transmission system. The transmission system model used in the simulations is shown on Figure 5-5.

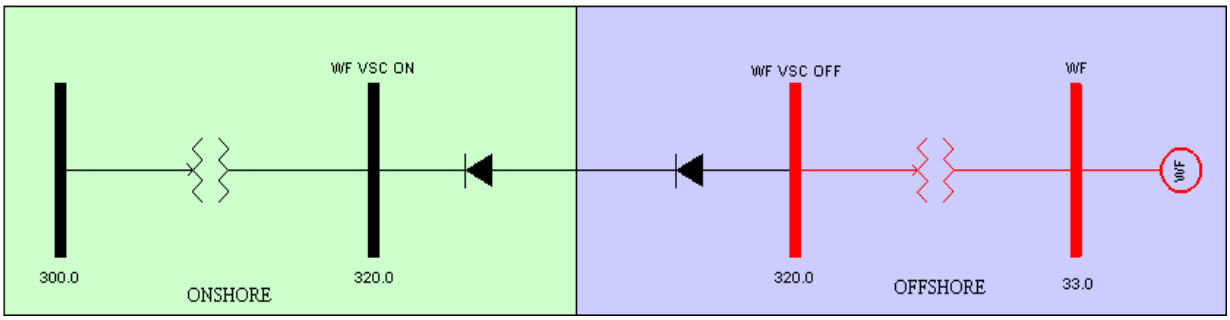

Figure 5-5: Configuration 2: Wind farm connected with HVDC

The parameters of the HVDC transmission link are based on the HVDC Light technology from ABB. HVDC Light technology is a modular concept. Several modules are available from power rating of 100MW to more than 1000MW.

HVDC Light® modules		Currents		
		580A (2 sub)	1140A (4 sub)	1740A (6 sub)
Voltages	± 80 kV	M1	M2	M3
	± 150 kV	M4	M5	M6
	± 320 kV	M7	M8	M9

Table 5-2: HVDC Light modules [45]

For this configuration, the module M9 was chosen. This module is a 320kV module with a base power of 1216 MVA. Due to that operation voltage, two transformers are used to step up the voltage from the wind farm to the offshore converter and to step down the voltage between the onshore converter and the grid. The typical values for this module are given in the following table.

Converter types		M7	M8	M9
Max. DC voltage (pole to ground)	kV	320	320	320
Base power	MVA	405	798	1216
DC current (I_{dN})	A	627	1233	1881

Table 5-3: Data for 320kV modules, typical values [45]

In the PSS^{TM}E model the losses of the VSC-HVDC transmission has to be define. The losses in HVDC are of two types, the converter losses and the cable losses. The following table gives the transfer capabilities of HVDC Light for the module M9.

Converter	DC voltage	DC current	DC Cable	Sending power	Receiving power (MW)					
types	kV	A	Cu in mm²	MW	Back-to-back	50 km	100 km	200 km	400 km	800 km
M7	320	627	300	408.1	396.4	391.4	388.8	382.9	370.6	
M8	320	1233	1200	802.2	775.7	772.8	770.1	764.2	752.5	729.0
M9	320	1881	2800	1224.4	1184.1	1180.8	1178.1	1172.2	1160.5	1137.0

Table 5-4: Transfer capabilities for different cable length, typical values [45]

The back-to-back configuration is used to calculate the converter losses. Indeed in this configuration the two converters are in the same place and are directly connected without cable. So for the module M9 the converter losses are:

$$P_{loss,conv} = P_S - P_R = 1224.4 - 1184.1 = 40.3\,MW \tag{5.2}$$

with P_S the sent power (MW) and P_R the received power (MW). The converter losses can be considered independent of the transmitted power since they are quasi integrally due to the commutation of the IGBTs. It is assumed that for a 1000MW sent power, the converter losses are the same.

The cable chosen for the system is a HVDC Light submarine cable with a set of two 1400mm^2 copper conductors. The resistance is 0, 0126 Ω/km for each conductor and the length of the system is 200km [45]. The DC current flowing in this cable is then:

$$I_{DC} = \frac{P_{DC}}{2 \times V_{DC}} \tag{5.3}$$

with P_{DC} the power flowing in the DC cable and V_{DC} the DC voltage. The power flowing in the DC cable is the sent power minus the losses in the inverter. Then the DC current is:

$$I_{DC} = \frac{1000 - \frac{40.3}{2}}{2 \times 320} \times 10^3 = 1531A \tag{5.4}$$

So the DC losses on the cable are:

$$P_{cable,loss} = R \times {I_{DC}}^2 = 2 \times 0.0126 \times 200 \times 1531^2 = 11.8\,MW \tag{5.5}$$

with R the resistance of the cable. The total losses of the system are 52.1MW and the received power in the grid is then:

$$P_{received} = P_{sending} - P_{losses} = 1000 - 52.1 = 947.9\,MW \tag{5.6}$$

The losses on the simulations are considered to be around 50MW which represents 5% of total losses.

The main advantage of using VSC-HVDC is that both converters can be controlled independently in active and reactive power. Furthermore, DC cables do not produce reactive power. There is no need of extra equipment to fulfil the connection requirements. The offshore converter can provide/absorb reactive power to/from the wind farm in order to ensure a power factor in the range of 0.95 inductive and capacitive. The onshore converter can be used like a SVC and contributes to the stability of the grid. However, production or absorption of reactive power by the converters have some limits. The limits of the converters should be set up by the user according to the P/Q diagram.

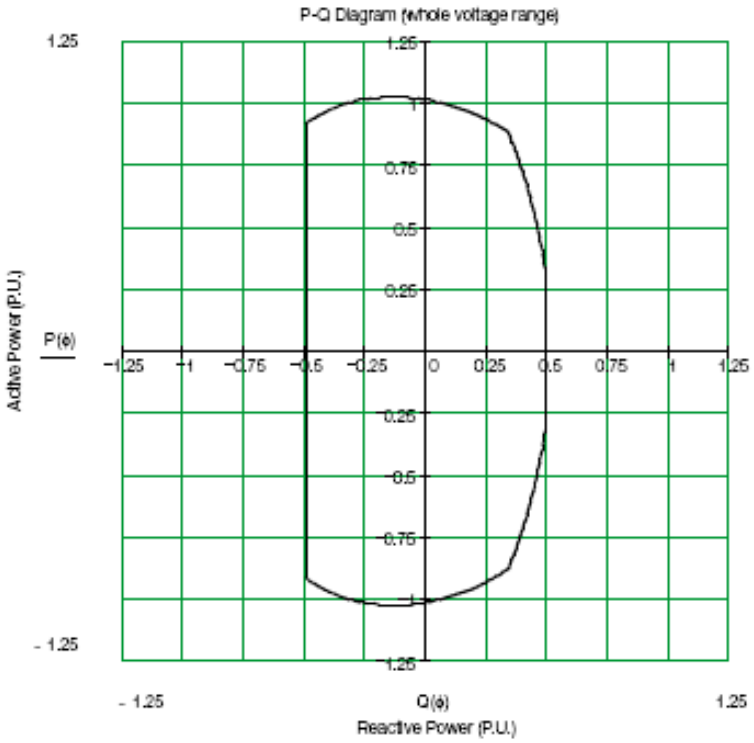

Figure 5-6: Typical P/Q diagram for HVDC converter

In the system, the module M9 has a base power of 1216MVA.The offshore rectifier have to transmit 1000MW which represents 0.82 p.u. With the 200km DC cable, the received power at the inverter will be 950MW i.e. 0.78 p.u. The reactive power limits of the converters can be calculated with the capabilities curve of the HVDC converters and are resumed in the

Table ***3-1***.

	Inverter		Rectifier	
	MVar	p.u.	MVar	p.u.
Qmax	413	0.34	389	0.32
Qmin	-608	-0.5	-608	-0.5

Table 5-5: Reactive power limits of the converters

The reactive power limits of the rectifier correspond to power factors between 0.85 inductive and 0.93 capacitive. Then the requirements of Statnett concerning the power factor can be assured by the inverter offshore without need of extra compensation equipments. The rectifier can also play a rule in the stability of the system and provide or absorb reactive power into its limits.

5.5.4. CONFIGURATION 3

The third configuration is a combination of the two previous systems. Two 500MW wind farms are connected to the grid at the same connection bus. The first farm is situated at 50km from the shore and is connected to the grid with a HVAC transmission system. The second wind farm is situated at 200 km from the shore and then is connected to the grid via a HVDC transmission system. In reality this configuration could be an evolution of the first configuration. The transmission system model used in the simulations is shown on Figure 5-7.

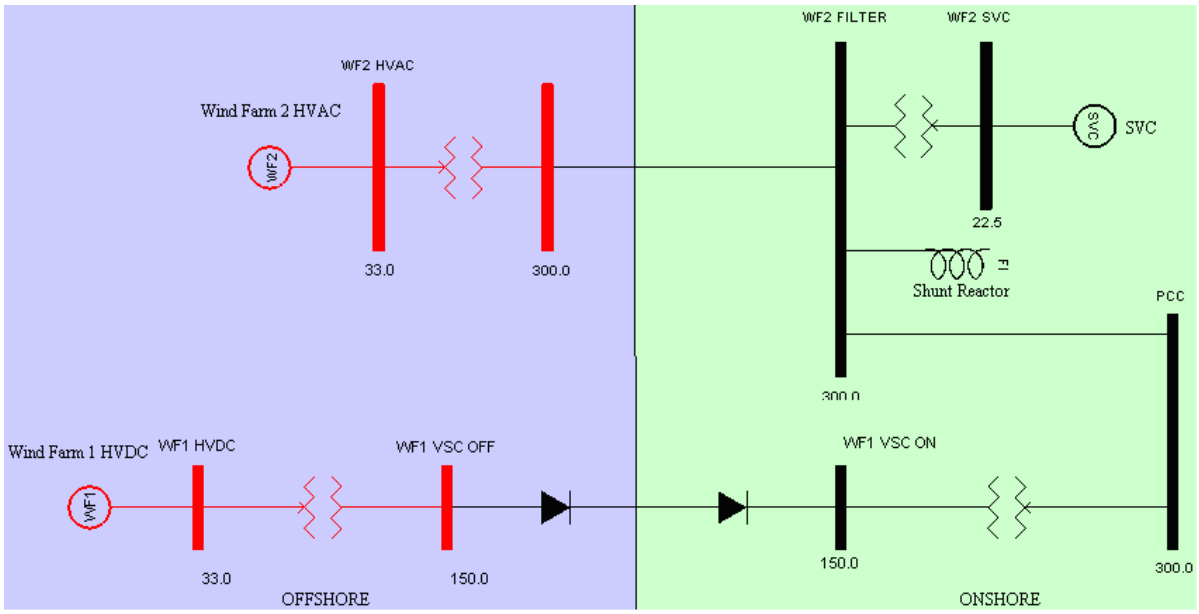

Figure 5-7: Configuration 3: two 500MW wind farms connected with HVDC and HVAC.

For the HVAC connection, only one cable is used. This one has the same characteristics than the one used in configuration 1 but the flowing power is reduced to 500MW. Consequently the compensation elements have to be re-dimensioned.

The active power losses and the reactive power production can be calculated by using the same approach than for the configuration 1. The received power for the HVAC connection is around 490MW and the reactive power created by the cable is around 160MVar. A 160MVar shunt reactor is then installed in order to compensate the reactive power production of the cable.

The grid code requirements have to be fulfilled and the installation of a SVC is necessary to ensure the operation of the wind farm in the power factor range of 0.95 inductive and capacitive. The received power is 490MW and then the SVC capacity corresponding to this power is 161MVar by using equation (5.1).

Concerning the HVDC link, as the transmitted power is lower than in the configuration 2, it is possible to use a different module in the converters. The chosen module is the M6 module. This module is a 150kV module with a base power of 570 MVA. Voltages on the offshore and onshore side are respectively step up and step down by transformers. The typical values for this module are given in the following table.

Converter types		**M4**	**M5**	**M6**
Max. DC voltage (pole to ground)	kV	150	150	150
Base power	MVA	190	373	570
DC current (I_{dcN})	A	627	1233	1881

Table 5-6: Data for150kV modules, typical values [45]

Losses of the HVDC transmission are calculated with the same approach as the configuration 3. However the transfer capabilities for a system with M6 modules are different than for a system with a M9 module. The typical transfer capabilities of a HVDC system with M6 modules are resumed in the following Table.

Converter	DC voltage	DC current	DC cable	Sending power	Receiving power (MW)					
types	kV	A	Cu in mm²	MW	Back-to-back	50 km	100 km	200 km	400 km	800 km
M4	150	627	300	191.3	185.0	182.0	179.0	174.0		
M5	150	1233	1200	376.0	363.7	361.0	358.0	353.0	342.0	
M6	150	1881	2800	573.9	555.1	552.0	549.5	544.0	533.0	

Table 5-7: Transfer capabilities for different cable length, typical values [45]

The converters losses with M6 modules are:

$$P_{loss,conv} = P_S - P_R = 573.9 - 555.1 = 18.8MW \tag{5.7}$$

The same assumptions than for configuration 2 are made concerning the converter losses. The DC cable is also different than the one used in the configuration 2. The cable is a HVDC Light submarine cable with a set of two 1200mm^2 copper conductors and a resistance of 0, 0151 Ω/km for each conductor and the length of the system is 200km [45]. The DC current flowing in this cable is then:

$$I_{DC} = \frac{500 - \frac{18.8}{2}}{2 \times 150} \times 10^3 = 1635.3A \tag{5.8}$$

So the DC losses on the cable are:

$$P_{cable,loss} = R \times {I_{DC}}^2 = 2 \times 0.0151 \times 200 \times 1635^2 = 16.15MW \tag{5.9}$$

with R the resistance of the cable. The total losses of the system are 35MW and the received power in the grid is then:

$$P_{received} = P_{sending} - P_{losses} = 500 - 35 = 465MW \tag{5.10}$$

The losses on the simulations are considered to be around 35MW which represents 7% of the total losses.

The base power of the module is 570 MVA. Then, the sent and received powers correspond respectively to 0.87 p.u and 0.81 p.u. Regarding the capability curve of the converters (Figure 5-6), the new reactive power limits of the converters are:

	Inverter		Rectifier	
	MVar	p.u.	MVar	p.u.
Qmax	183	0.32	160	0.28
Qmin	-285	-0.5	-285	-0.5

Table 5-8: Reactive power limits of the converters

The reactive power limits of the rectifier correspond to power factors between 0.87 inductive and 0.95 capacitive. Then the requirement of Statnett concerning the power factor can be assured by the rectifier offshore without need of extra compensation equipments.

5.5.5. CONFIGURATION 4

The last configuration is a combination of the first and second one. Two 500MW wind farms are connected to an offshore HVDC converter via HVAC transmission system. The HVDC transmission is then connected to the grid. This configuration permits to exploit several offshore sites in a limited area but far from the shore. The two wind farms are 50 km apart from the offshore HVDC converter which is situated 200km from the shore. The transmission system model used in the simulations is shown on Figure 5-8.

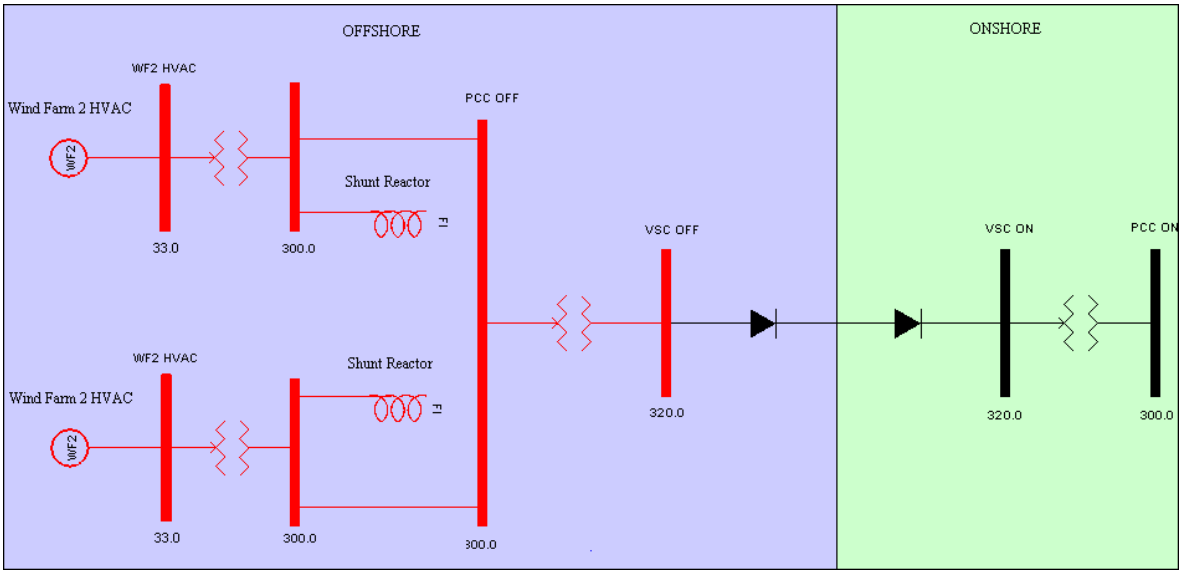

Figure 5-8: Configuration 4: two 500MW wind farms connected with HVAC and HVDC

The HVAC cables are the same as the one used in the configuration 3. Each cable produces 160MVar which are compensated by two shunt reactors. The need of reactive power of each HVAC system for fulfilling the Statnett requirements regarding the power factor is 160MVar. However, in this configuration, there is no need of extra compensation. The HVDC transmission link is dimensioned like in the configuration 3. By considering the reactive limits of the offshore converter (Qmax = +389MVar, Qmin=-608MVar), it is possible to use it as a SVC and then to have a power factor in the range of 0.95 inductive and capacitive.

6 POWER SYSTEM STABILITY

A definition of Power System Stability is given by IEEE in [46]:
"Power system stability is the ability of an electric power system, for a given initial operating condition, to regain a state of operating equilibrium after being subjected to a physical disturbance, with most system variables bounded so that practically the entire system remains intact."

Stability is the condition of equilibrium between opposite forces. In normal operation, electrical systems operate in such a way that these forces are equilibrated. However if a disturbance happens in the system the state of the forces regarding the equilibrium changes and the system have to react in order to regain the equilibrium. For example if a generator runs temporarily faster, the angular position of its rotor will change and then will influence its output power.

Power system stability can be classified according to its nature. There are there main categories of stabilities: rotor angle stability, frequency stability and voltage stability.

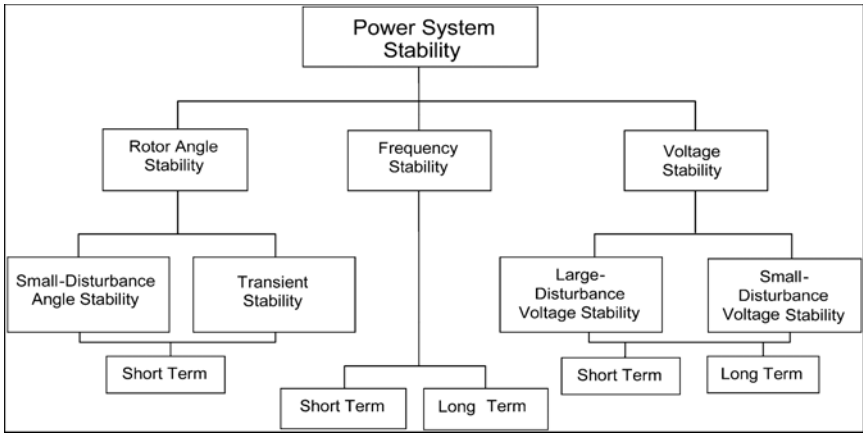

Figure 6-1: Classification of power system stability [46]

In this study, the choice was made to focus on the voltage stability and the frequency stability. The reason of this choice is because the model is a simplification of the reality. One generator in the model represents the whole production units in one area. It would have been incorrect to focus on the rotor angle stability because the results would have been unrealistic.

The voltage stability is defined like *"the ability of a power system to maintain steady voltages at all busses in the system after being subjected to a disturbance from a given initial operating condition."* and the frequency stability like *"the ability of a power system to maintain steady frequency following a severe system upset resulting in a significant imbalance between generation and load."[46]*

Voltage stability is divided in two categories, the small-disturbance stability and large-disturbance stability. The first one is the ability of the system to maintain equilibrium under small disturbance, like small changes in the load or in the generation. Small-signal stability is a problem which is largely influence by the lack of oscillation damping of the system. The second category of stability is the large-disturbance stability. This is the ability of the system to maintain equilibrium under and after transient disturbances like phase-to-ground, phase-to-phase or three-phase short-circuit. These events can occur in lines, transformers or busbar. The choice was made to studying large-disturbance stability because of the simplified model. A study on small-disturbance stability would have been more appropriate with a detailed model.

7 LOAD FLOW

7.1 INTRODUCTION

Before dynamics simulations are made, the initials operations conditions have to be set as the base-case. For steady state operations, voltages magnitudes and angles as well as active and reactive power flows, are calculated for every busses and branches in the system. All values can be found in Appendix B, C and D. The choice of the connection busses is presented on the following part.

7.2 CONNECTION POINTS

The connection of a 1000MW wind farm on a grid requires sufficient capabilities concerning busses and branches near the connection point. First of all the transfer capabilities of the connection bus has to be sufficient for the adding of an extra 1000MW. Secondly, the thermal limits of the lines linked to the connection bus have to be large enough. Finally the busbar should be strength enough regarding faults. The short-circuit power (SC_{MVA}) is a typical indicator of the strength of a busbar. The SC_{MVA} is defined by:

$$SC_{MVA} = \frac{V_{AC}^{\ 2}}{Z_{th}} \tag{7.1}$$

where V_{AC} is the bus nominal voltage and Z_{th} is the Thevenin impedance seen from the bus. However, due to the simplifications on the model, the capabilities of every bus are sufficient for the connection of a 1000MW wind farm. Then, the investigated busses have been chosen according to there geographical situations. The west and south coast of Norway are the areas where the integration of offshore wind power is the more probable. The chosen busses are shown on Figure 7-1.

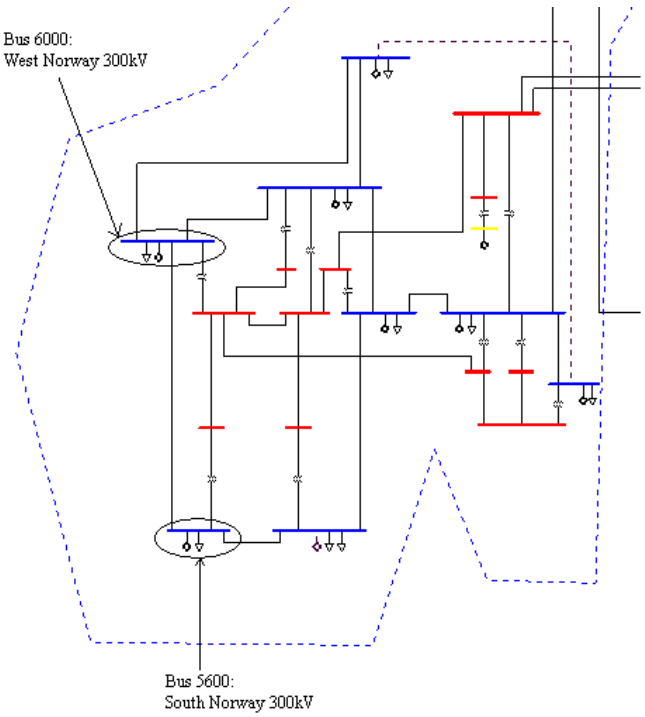

Figure 7-1: Investigated busbars

7.3 WEST NORWAY BUS 6000

The busbar 6000 represents the 300kV grid in the West Norway, in the Bergen region. In normal operation, without the wind farm, the load flow around this bus bas is given in the following figure.

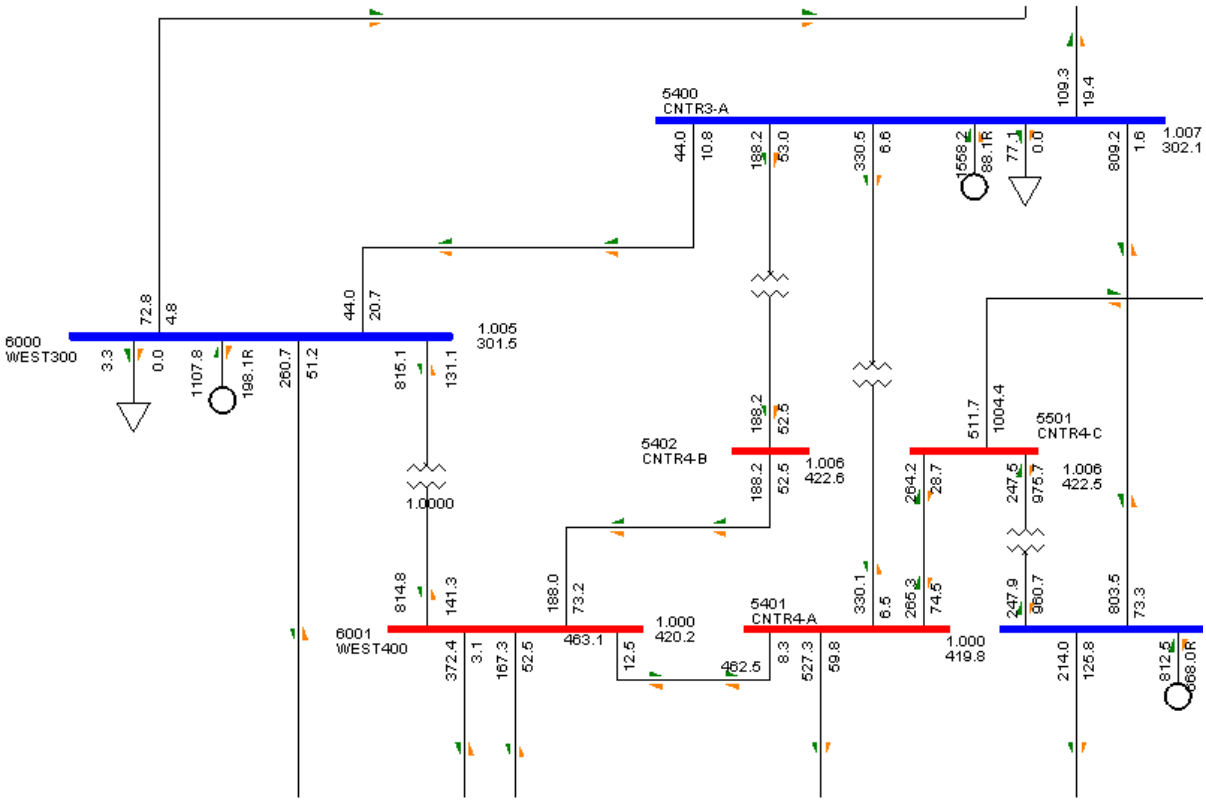

Figure 7-2: Load flow at the bus 6000, base-case

The blue busses are the busses with a voltage of 300kV and the red ones are the busses with a voltage of 420kV. The numbers on right of the busses are the voltages in p.u (superior) and in kV (inferior). The numbers left of the branches, loads and generators represent the active power whereas the numbers on the right represent the reactive power. The active and reactive power flows are represented be green arrows and orange arrows respectively.

A generator of 1000MW representing the wind farm is added on the bus 6000. This simulation permits to have an idea of the behaviour of the system with the connection of the wind farm. Figure 7-3 shows the new load flow.

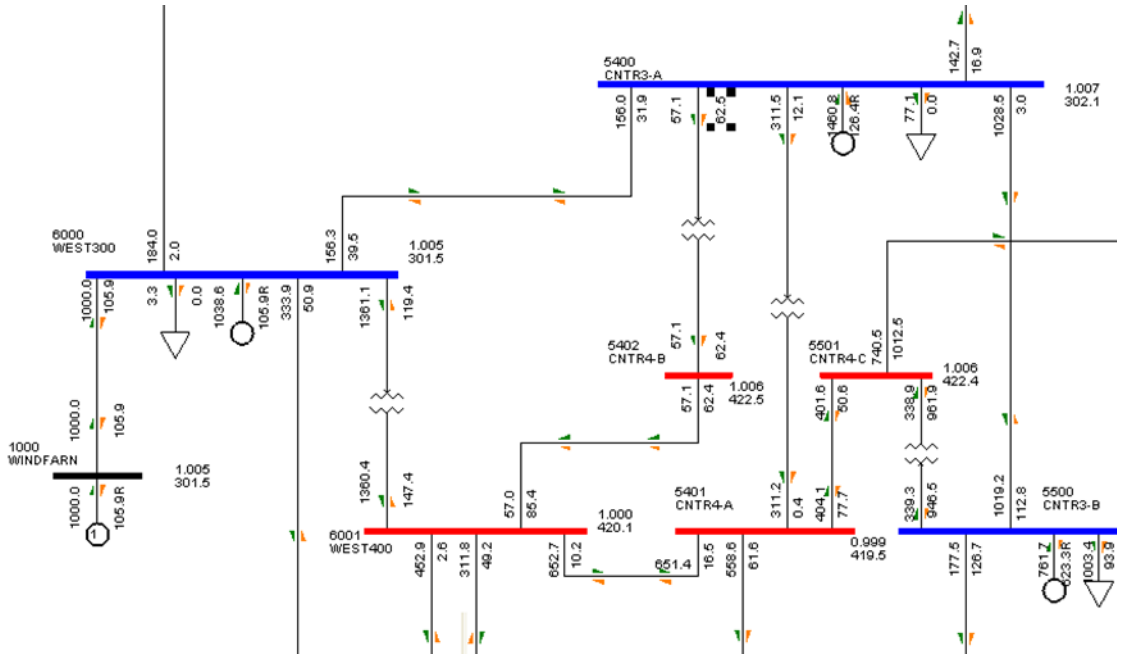

Figure 7-3: Load flow at the bus 6000, 1000MW wind farm connected at the bus 6000

In this situation, the wind farm produces 1000MW of active power and consumes 105.9MVar of reactive power. The wind farm operates at a power factor $cos\varphi$=0.99 inductive. With a 1000MW wind farm connected at the bus 6000, this last one becomes "exporter" of active power. In the base-case, the active power was flowing from the bus 5400 to the bus 6000 whereas with the wind farm, the bus 6000 supplies the bus 5400. It can also be noticed that the generator in bus 6000 produces less power than in the base-case. However, the decrease of generation is small compare to the added capacity. This can be explained by the fact that the swing bus of the whole system is situated in Sweden, far from the investigated zone. The swing bus is a bus with no active and reactive power limits and which regulates the voltage at a fixed reference angle. Then with the adding of 1000MW, the demand of active and reactive power from the swing bar in Norway is reduced because the total generation is increased. Bus 6000 plays the rule of "swing bar" in its neighbour area. All the data from these simulations can be found in Appendix B and C.

BUS 5400 CNTR3-A	MW	MVAR	MVA	LOSSES	
FROM GENERATION	1558.2	88.1	1560.7	MW	MVAR
TO LOAD-PQ	77.1	0	77.1		
TO 5401 CNTR4-A	330.5	6.6	330.5	0.35	13.09
TO 5402 CNTR4-B	188.2	53	195.5	0.02	0.57
TO 5500 CNTR3-B	809.2	-1.6	809.2	5.75	71.68
TO 6000 WEST300	44	10.8	45.3	0.02	0.22
TO 6100 NWEST3	109.3	19.4	111	0.25	2.48

BUS 5400 CNTR3-A	MW	MVAR	MVA	LOSSES	
				MW	MVAR
FROM GENERATION	1460.8	126.4	1466.3		
TO LOAD-PQ	77.1	0	77.1		
TO 5401 CNTR4-A	311.5	12.1	311.8	0.31	11.65
TO 5402 CNTR4-B	57.1	62.5	84.7	0	0.11
TO 5500 CNTR3-B	1028.5	3	1028.5	9.28	115.8
TO 6000 WEST300	-156	31.9	159.3	0.25	2.54
TO 6100 NWEST3	142.7	16.9	143.7	0.41	4.12

BUS 6000 WEST300	MW	MVAR	MVA	LOSSES	
				MW	MVAR
FROM GENERATION	1107.8	-198.1	1125.4		
TO LOAD-PQ	3.3	0	3.3		
TO 5400 CNTR3-A	-44	-20.7	48.6	0.02	0.22
TO 5600 SOUTH3A	260.7	-51.2	265.7	2.38	23.83
TO 6001 WEST400	815.1	-131.1	825.5	0.27	10.25
TO 6100 NWEST3	72.8	4.8	72.9	0.12	1.31

BUS 6000 WEST300	MW	MVAR	MVA	LOSSES	
				MW	MVAR
FROM GENERATION	1038.6	-105.9	1044		
TO LOAD-PQ	3.3	0	3.3		
TO 1000 WINDFARN	-1000	105.9	1005.6	0	0
TO 5400 CNTR3-A	156.3	-39.5	161.2	0.25	2.54
TO 5600 SOUTH3A	333.9	-50.9	337.7	3.89	38.91
TO 6001 WEST400	1361.1	-119.4	1366.3	0.75	28.07
TO 6100 NWEST3	184	-2	184	0.74	8.04

BUS 6001 WEST400	MW	MVAR	MVA	LOSSES	
				MW	MVAR
TO 5102 EAST4-B	167.3	-52.5	175.3	0.56	9.76
TO 5401 CNTR4-A	463.1	-12.5	463.3	0.64	10.71
TO 5402 CNTR4-B	-188	-73.2	201.7	0.2	2.93
TO 5601 SOUTH4A	372.4	-3.1	372.4	1.91	28.3
TO 6000 WEST300	-814.8	141.3	827	0.27	10.25

BUS 6001 WEST400	MW	MVAR	MVA	LOSSES	
				MW	MVAR
TO 5102 EAST4-B	311.8	-49.2	315.6	1.94	33.96
TO 5401 CNTR4-A	652.7	-10.2	652.8	1.28	21.28
TO 5402 CNTR4-B	-57	-85.4	102.7	0.04	0.65
TO 5601 SOUTH4A	452.9	-2.6	452.9	2.82	41.81
TO 6000 WEST300	-1360.4	147.4	1368.3	0.75	28.07

Table 7-1: Load flow for busses 5400, 6000 and 6001.
Left: Base-Case; Right: with 1000MW on bus 6000.

7.4 SOUTH NORWAY A BUS 5600

The busbar 5600 represents the 300kV grid in the South Norway, between Kristiansand and Stavanger. In normal operation, without the wind farm, the load flow around this bus bas is given in the following figure.

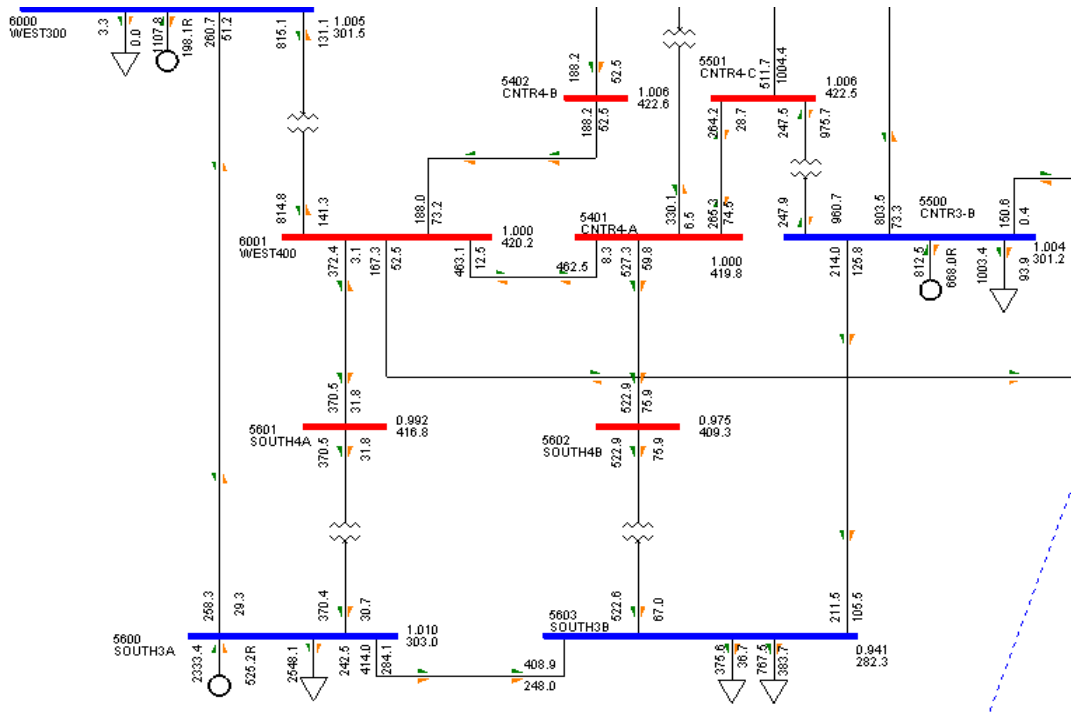

Figure 7-4: Load flow at the bus 5600, base-case

The signs, numbers and colours used are the same as in the previous case. As for the connection point on the bus 6000, a generator of 1000MW representing the wind farm is added on the bus 5600. This simulation permits to have an idea of the behaviour of the system with the connection of the wind farm. Figure 7-5 shows the new load flow.

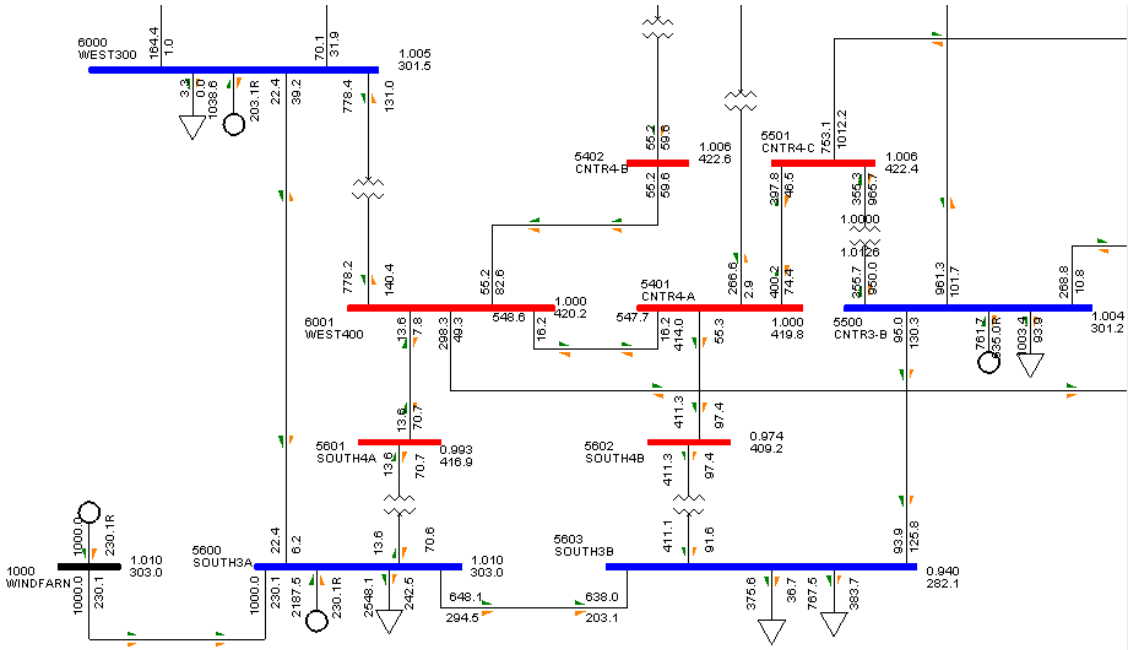

Figure 7-5: Load flow at the bus 5600, 1000MW wind farm connected at the bus 5600

The same comments as the previous case can be made. However, bus 5600 is only connected to busses without generation (except for bus 6000). The neighbour bus 5603 is one of these busses and its demand in active and reactive power is very important. In the base-case, this demand is supplied at 40% by the bus 5600. Furthermore, the load in the bus 5600 is also important, with 2548MW and 242MVar. The generator on bus 5600 can not supply both the load in the bus and the bus 5603. Then bus 5600 import a lot of power from busses 6000 and 6001 (via the bus 5601). With the addition of the wind farm, this situation evolved and except 22MW imported from the bus 6000, the bus 5600 becomes "exporter" whereas the generation on the bus decreases. The demand of bus 5603 is supplied at 55% of the bus 5600 and this last one also supplies power to the bus 6001.

The wind farm operates at a power factor $cos\varphi$=0.97 capacitive which in the limits of the Statnett requirements. The demand of power from the swing bus is also reduced. All the data from these simulations can be found in Appendix B and D.

BUS 5600 SOUTH3A	MW	MVAR	MVA	LOSSES	
				MW	MVAR
FROM GENERATION	2333.4	525.2R	2391.8		
TO LOAD-PQ	2548.1	242.5	2559.7		
TO 5601 SOUTH4A	-370.4	-30.7	371.7	0.03	1.07
TO 5603 SOUTH3B	414	284.1	502.1	5.09	55.98
TO 6000 WEST300	-258.3	29.3	260	2.38	23.83

BUS 5600 SOUTH3A	MW	MVAR	MVA	LOSSES	
				MW	MVAR
FROM GENERATION	2187.5	230.0R	2199.6		
TO LOAD-PQ	2548.1	242.5	2559.7		
TO 1000 WINDFARN	-1000	-230	1026.1	0	0
TO 5601 SOUTH4A	13.6	-70.6	71.9	0	0.04
TO 5603 SOUTH3B	648.1	294.4	711.9	10.11	111.22
TO 6000 WEST300	-22.4	-6.2	23.2	0.03	0.27

BUS 5603 SOUTH3B	MW	MVAR	MVA	LOSSES	
				MW	MVAR
TO LOAD-PQ	1143	420.5	1217.9		
TO 5500 CNTR3-B	-211.5	-105.5	236.4	2.5	28.07
TO 5600 SOUTH3A	-408.9	-248	478.2	5.09	55.98
TO 5602 SOUTH4B	-522.6	-67	526.9	0.24	8.96

BUS 5603 SOUTH3B	MW	MVAR	MVA	LOSSES	
				MW	MVAR
TO LOAD-PQ	1143	420.5	1217.9		
TO 5500 CNTR3-B	-93.9	-125.8	157	1.09	12.22
TO 5600 SOUTH3A	-638	-203.1	669.5	10.11	111.22
TO 5602 SOUTH4B	-411.1	-91.6	421.2	0.15	5.74

BUS 6001 WEST400	MW	MVAR	MVA	LOSSES	
				MW	MVAR
TO 5102 EAST4-B	167.3	-52.5	175.3	0.56	9.76
TO 5401 CNTR4-A	463.1	-12.5	463.3	0.64	10.71
TO 5402 CNTR4-B	-188	-73.2	201.7	0.2	2.93
TO 5601 SOUTH4A	372.4	-3.1	372.4	1.91	28.3
TO 6000 WEST300	-814.8	141.3	827	0.27	10.25

BUS 6001 WEST400	MW	MVAR	MVA	LOSSES	
				MW	MVAR
TO 5102 EAST4-B	298.3	-49.3	302.4	1.78	31.08
TO 5401 CNTR4-A	548.6	-16.2	548.8	0.9	15.03
TO 5402 CNTR4-B	-55.2	-82.6	99.4	0.04	0.61
TO 5601 SOUTH4A	-13.6	7.8	15.7	0.02	0.36
TO 6000 WEST300	-778.2	140.4	790.7	0.25	9.37

Table 7-2: Load flow for busses 5600, 5603 and 6001.
Left: Base-Case; Right: with 1000MW on bus 5600

8 DYNAMIC SIMULATIONS

8.1 DYNAMIC MODELS

8.1.1. THE GRID DYNAMIC MODEL

As said in part 5.2, the model was provided by SINTEF. The dynamic models of the generator are from two types, GENROU and GENSAL. These models are PSS^{TM}E models. GENROU represents a solid rotor machine whereas GENSAL represents a salient pole machine. The excitation of the entire generator on the model is ensured by the PSS^{TM}E model called SCRX. This last one represents a controlled rectifier excitation system. Governors of the generators are modelled by using the PSS^{TM}E model called HYGOV. This model represents a straightforward hydro electric plant governor, with a simple hydraulic representation and no surge tank. Finally, the SVCs are modelled by the PSS^{TM}E model CSVGN5. The SVC of the HVAC transmission are also modelled with CSVGN5.

Simulations have been made in order to validate the dynamic behaviour of the model for the future simulation. In normal operation, the system remains stable in voltage and frequency. All the voltages are in the range of 0.9-1.1 p.u imposed by Statnett. Disturbances have been applied on several busses of the grid during 150ms. These disturbances are three-phase faults with zero value impedance. The busses where the disturbances are applied are the busses, 5401, 5600 and 6000.

For all this situations, the behaviour of the system is the same. Only the results for the fault on the bus 5401 are presented, the other results can be found on Appendix E

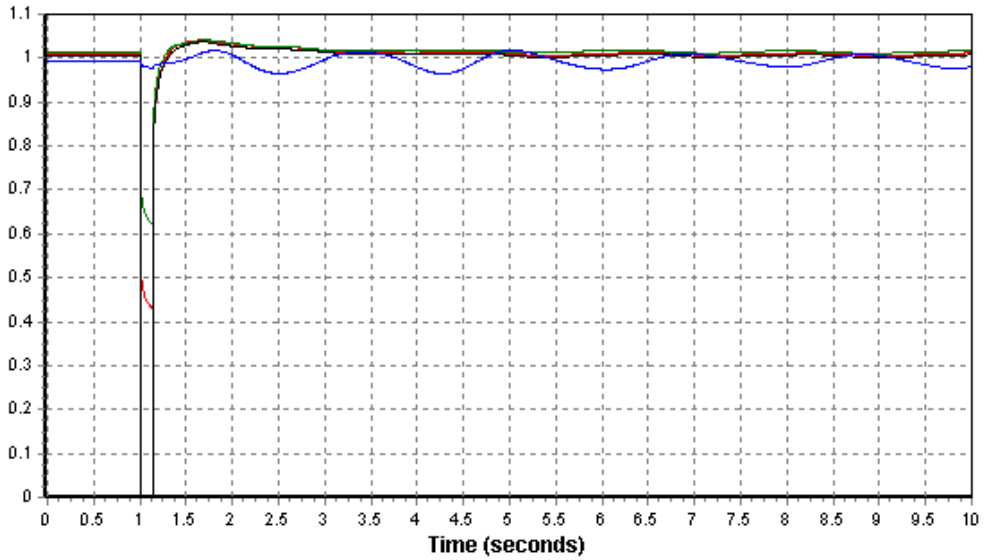

Figure 8-1 : Voltage at different busses after a three-phase fault on bus 5401[p.u].
Red: bus 6000(West Norway 300kV),
Green: bus 5600 (South Norway 300kV),
B lack: Bus 5401 (Central Norway420kV)
Blue: Bus 3300 (Swing bus Sweden 420kV)

The voltage at the bus 5401 is null during 150ms. After the fault clearance, the voltage recovers a value superior to 0.9 p.u in 50ms and recovers its initial value after 2.5 seconds. The fault-ride-through requirements are satisfied. The busses 6000 and 5600 react in the same way than the bus 5401. However, the voltages at these busses never fall to zero and have a minimum of 0.45 p.u for the bus 6000 which is connected to the bus 5401 and 0.65 p.u for the bus 5600 which is more far from the

fault bus. It can be noticed that on these three busses, the voltages do not recover a perfect stability after the fault. This is caused by the dynamic models of the generators. As said on part 5.2, generators have important generation capabilities. Furthermore in the dynamic models the inertia of the generators is relatively important. Then the system takes some time to be totally stabilized. However it can be seen on the voltages curves that the magnitude of the oscillations is very small.

The blue curve is the voltage magnitude on bus 3300 in Sweden. This bus is far from the fault bus, so the contribution of this bus is small and the voltage during the fault does not fall as for the other busses. However after the clearance of the fault, oscillations appear in the voltage. However the voltage magnitude remains in the 0.9-1.1 p.u limits and the oscillations damp. Bus 3300 is the swing bus of the whole system, and then it has to regulate the voltage magnitude with a certain angle. The oscillations are a consequence of the small instabilities on the different other busses.

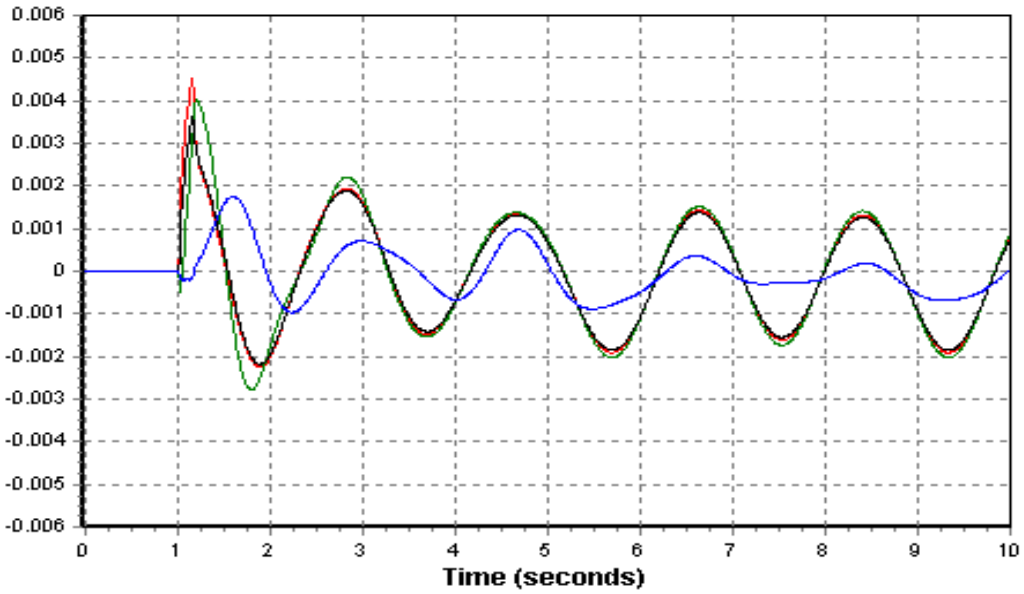

Figure 8-2: Frequency deviation for different busses after a three-phase fault on bus 5401[p.u].
Red: bus 6000(West Norway 300kV),
Green: bus 5600 (South Norway 300kV),
B lack: Bus 5401 (Central Norway420kV)
Blue: Bus 3300 (Swing bus Sweden 420kV)

During the fault, frequencies on bus 5401, 5600 and 6000 increase fast. The fault in the grid implies a reduction of the production. Then the speed of the machines increases which tends to rise up the frequency in the grid. After the clearance of the fault, oscillations on the frequency appear. It can be noticed that the oscillations on the bus 3300 are not regular. However the oscillations have a tendency to damp. Furthermore, frequency oscillates between ±0.002 p.u which represents ±0.1Hz. The requirements of Statnett about frequency in normal operation are respected.

After the fault, the system is not perfectly stable but the oscillations remain small and tend to damp. During the simulations, this behaviour will be considered as normal operation of the system. Nevertheless the magnitude of the oscillations will be considered.

8.1.2. THE HVDC DYNAMIC MODEL

The VSC-HVDC model included in PSS^{TM}E is a general performance model, developed in order to evaluate the interaction of a VSC-HVDC system with an AC system. This model represents the transient behaviour of the outer i.e. controls, because their actions have the most influence on the AC system. The control and response of the DC side of the HVDC system have not been specifically modelled and approximate DC characteristics are available. [44]

The model is composed of three modules, one represent the DC transmission line (DCLINE) and two represent the voltage source converters (VSCDYN). The model is a current injection model. The model can be schematically represented as follow:

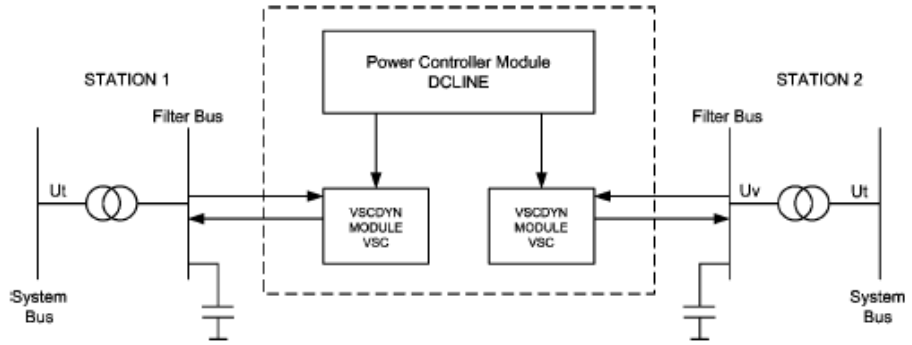

Figure 8-3: VSC-HVDC model. [44]

The VSCDYN model represents the control function of the VSC converter. With this model, the DC side of the converter can control the active power transfer or the DC voltage in the transmission line whereas the AC side can control the AC voltage or the power factor. In normal operation, the model imposes that one of the VSC has to control the DC voltage and the other one the active power. In the simulations, the power generated by the wind farm will not vary and the generation will be constantly 1000MW. Then it has been decided that the offshore converter i.e. the rectifier will control the active power flow whereas the onshore converter i.e. inverter will control the DC voltage. According to the VSC-HVDC control explained in part 2.6.5, both converters have been set to control the AC voltage. The reactive power production of the converters varies in order to regulate the voltage at the connection busses. The DC voltage set point is fixed to the rated power of the DC line (320kV or 150kV according to the configuration), the active power flow is set to 1000MW and the AC voltage is set to 1 p.u.

The DCLINE module has been developed in order to coordinate the power flow between the two converters. The module uses the load flow data to control the DC voltage and to maintain it at its reference value. During simulations, a difference in active power between the converters can occur. In the model, this difference creates an error in the DC voltage and a regulator is activated in order to eliminate the unbalanced powers. Losses in the line are also calculated according to the DC resistance of the transmission line. These losses are considered by the model during the simulations. [44]

During an onshore fault, the wind turbine does not stop its production. Nevertheless the onshore converter has to reduce the transfer of active power to the grid in order to avoid an augmentation of the DC voltage. To reduce the transfer of power in the DC line, the frequency offshore, and then the speed of the wind generator, will increase quickly. The power is used to accelerate the generator until the fault clearance. After that, the power transfer regains its rated value, and so the frequency and the speed of the generator offshore. The model is made to regulate automatically the active power transfer in case of onshore fault. [44]

8.2 SIMULATIONS

The dynamics simulations have been done for the four configurations presented on part 5 connected to the two different busbars presented on part 7. The connection busbars are the busses 6000 (West Norway, 300kV) and 5600 (South Norway A, 300kV). The wind farm busbar is the bus 1000 for the configurations 1 and 2. For configuration 3, the busbar of the wind farm connected via HVDC is the bus 1100 and the busbar of the wind farm connected via HVAC is the bus 1200. For the configuration 4, the wind farms busbars are the busses 1100 and 1200. Different events have been applied in order to investigate the dynamic behaviour of the system with integration of a 1000MW wind farm.

8.3 DISTURBANCES

In order to have a general overview of the behaviour of the system, four different disturbances have been applied to the system. All faults are three-phase short-circuit modelled by shunt impedances equal to zero. The faults are applied at t=1s and are cleared after 150ms according to the Statnett requirements. The faults are defined as follow:

- Fault 1: the first fault is applied directly on the connection busbar. This fault leads to a voltage equal to zero at the connection point which is the worst case regarding to the Statnett requirements.

- Fault 2: the second fault is applied in a neighbour bus of the connection bus. For the connection bus 6000 (West Norway, 300kV), the fault is applied on the bus 5400 (Central Norway, 300kV) and for the connection bus 5600 (South Norway A, 300kV) the fault is applied on bus 5603.

- Fault 3: the third fault is applied on line going from the connection bus to a neighbour bus. For the connection bus 6000, the fault is applied on the line between the bus 6000 and the bus 5400 and for the connection bus 5600 the fault is applied on the line between the bus 5600 and the bus 5603. After the clearance of the fault, the line is disconnected. The choice of the line has been made in regard of the lines which give the largest contribution to the connection point.

- Fault 4: the fourth fault is a short-circuit on the wind farm busbar. In configuration 3 and 4, three different cases have been differentiated. The two first one are the cases where a fault occurs on one of the 500MW wind farm busbar. The third one is the case where two simultaneous faults occur on the two 500MW wind farm. For the configuration 4, the two first cases are the same because of the nature of the configuration.

For the configuration 4, the fault 4 leads to the instability of the system and PSS^{TM}E can not execute the simulations. A solution to this problem is explained in part 8.13.

The different faults can be located on the following figures.

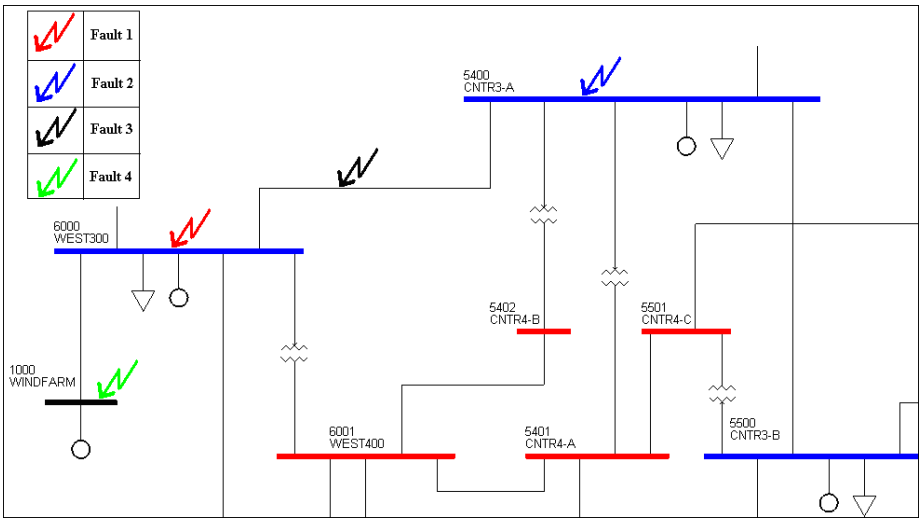

Figure 8-4: Faults locations, connection bus 6000

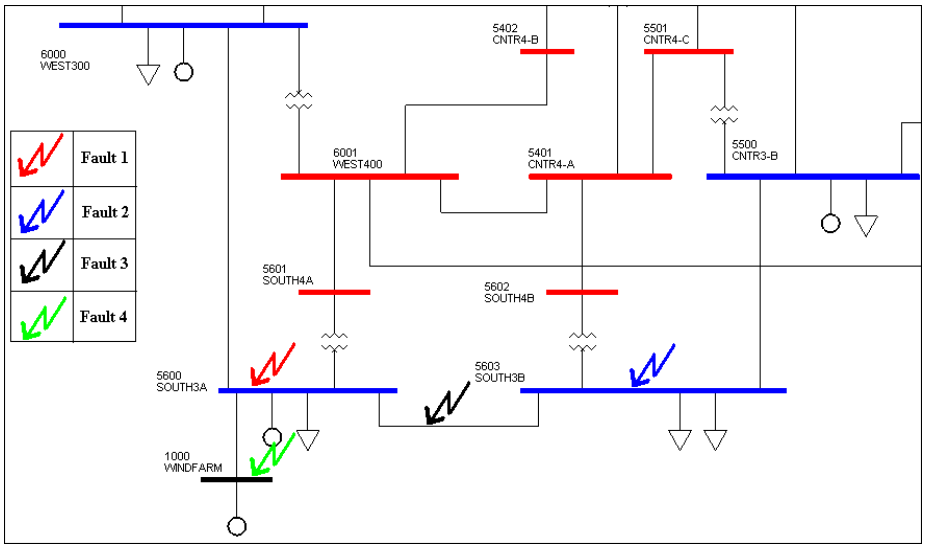

Figure 8-5: Faults locations, connection bus 6000

The short-circuit power and current contribution of the busses where the disturbances occur can be found in Appendix A.

8.4 PLOTS

This part presents the results of the simulations. The most significant results are presented on this part. However, all results and plots of these simulations can be found on Appendix F.

For simulations with the configuration 1, the plotted variables are:

- The voltages at the connection busbar and at the wind farm busbar [p.u]
- The frequency deviation at the connection busbar and at the wind farm busbar [p.u]
- The speed deviation of the wind turbine generator[p.u]
- The reactive power from the SVC [p.u]

For simulations with the configuration 2, the plotted variables are:

- The voltages at the connection busbar and at the wind farm busbar [p.u]
- The frequency deviation at the connection busbar and at the wind farm busbar [p.u]
- The speed deviation of the wind turbine generator[p.u]

- The reactive power from the onshore VSC-HVDC converter [MVar]
- The losses on the DC line [MW]

For simulations with the configuration 3, the plotted variables are:

- The voltages at the connection busbar and at the wind farm busbar [p.u]
- The frequency deviation at the connection busbar and at the wind farm busbar [p.u]
- The speed deviation of the wind turbine generator[p.u]
- The reactive power from the SVC [p.u]
- The reactive power from the onshore VSC-HVDC converter [MVar]
- The losses on the DC line [MW]

For simulations with the configuration 4, the plotted variables are:

- The voltages at the connection busbar and at the wind farm busbar [p.u]
- The frequency deviation at the connection busbar and at the wind farm busbar [p.u]
- The speed deviation of the wind turbine generator[p.u]
- The reactive power from the onshore VSC-HVDC converter [MVar]
- The losses on the DC line [MW]
- The reactive power from the offshore VSC-HVDC converter [MVar]

For the event 4 (three-phase fault at the wind farm busbar) and the configuration 2 and 3, the reactive power from the offshore VSC-HVDC converter is also plotted.

The base power of the system is 1000MVA.

8.5 CONFIGURATION 1, CONNECTION BUS 6000

In this case, the simulations are made with the configuration 1 connected to the grid on the bus 6000. The configuration 1 represents a 1000MW wind farm connected to the grid via a HVAC transmission system.

8.5.1. FAULT 1

A 150ms three-phase short-circuit is applied on the connection bus (bus 6000) at the time t=1s. The voltage at the connection busbar becomes null whereas the voltage of the wind farm falls to 0.04p.u. After the clearance of the fault at t=1.15ms, the voltages at both busses increase instantaneously to 0.75p.u and less than 500ms after the beginning of the fault, both voltages reach the value of 0.9 p.u. The voltages are stabilized at their reference values 2 seconds after the beginning of the fault. The fault-ride-through requirements concerning the voltage are respected.

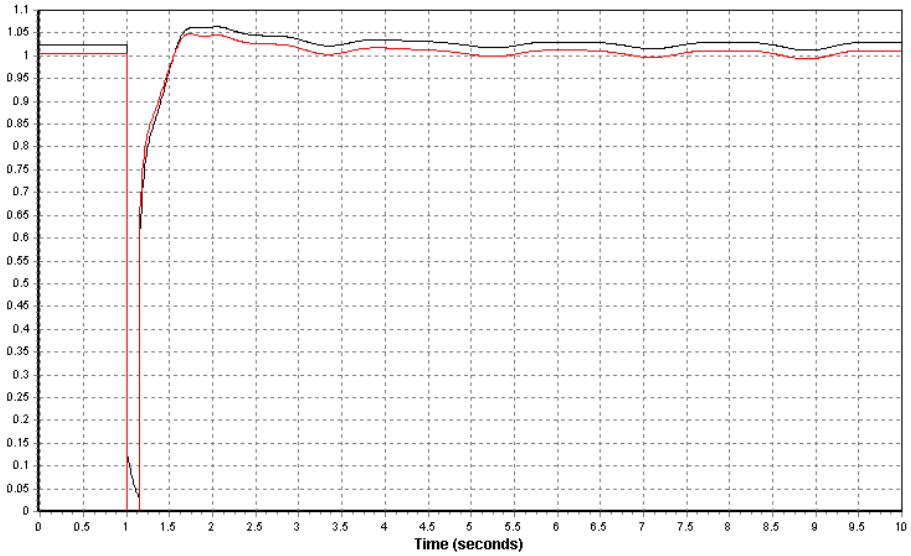

Figure 8-6: Voltage at offshore bus (black) and onshore bus (red) [p.u]

After the beginning of the fault, the frequency at the wind farm increases and reaches the value of 1.03p.u which corresponds to a frequency of 51.5Hz. The power transfer between the offshore wind farm and the connection point is reduced which implies that the electrical torque of the generator decreases. Then, the wind generator increases its speed and the frequency. After the fault, the frequency and the speed of the generator rapidly return to their reference values.

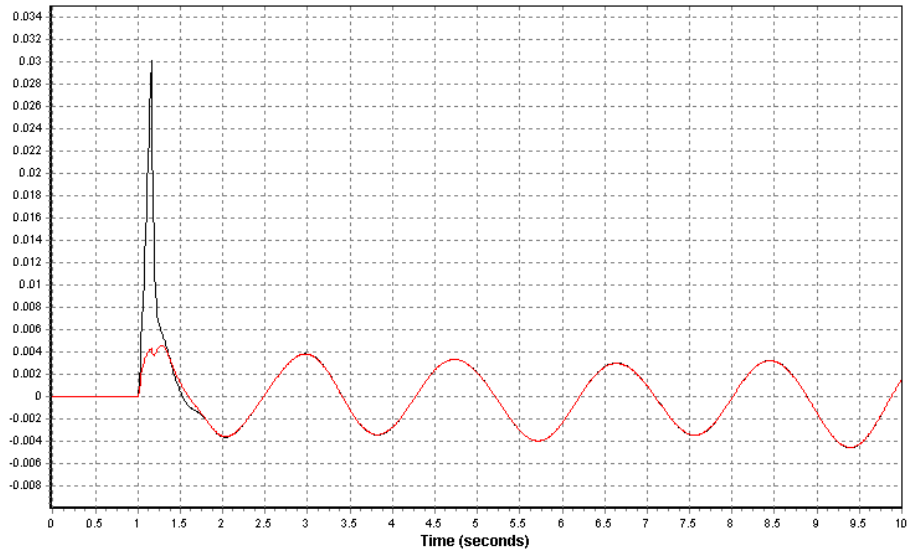

Figure 8-7: Frequency deviation at bus offshore (black) and onshore bus (red) [p.u]

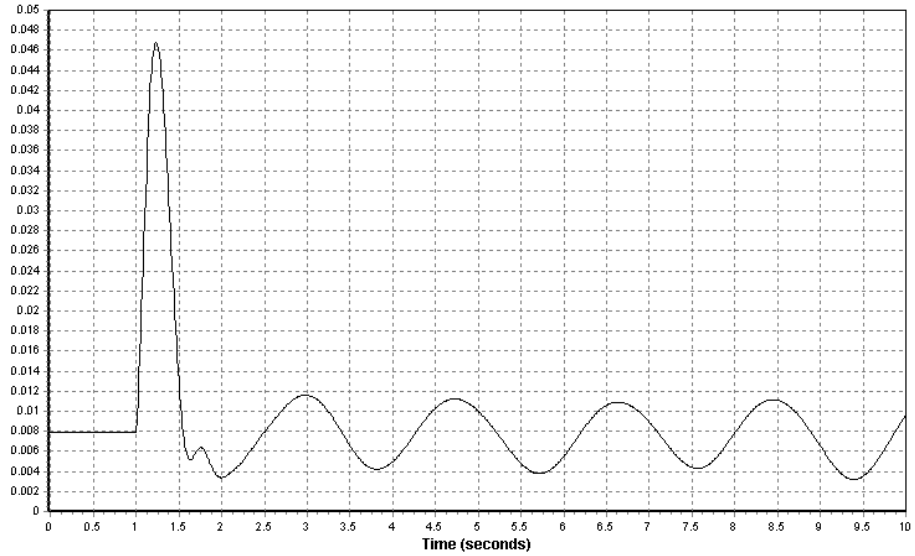

Figure 8-8: Speed deviation of the wind turbine generator [p.u]

After the fault clearance, the SVC will produce reactive power in order to stabilize the voltage. The maximum production, 350MVar at t=1.75s, corresponds to the maximum value of the voltage. After reaching its maximum, the reactive power is quickly reduced in order to maintain the voltage at its reference value. The oscillations after the fault clearance are caused by the oscillations on the voltages.

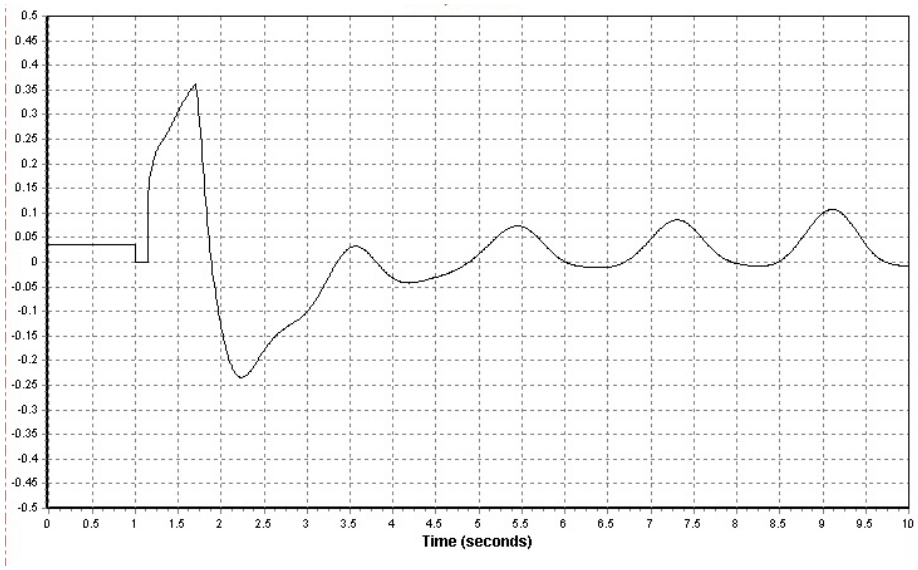

Figure 8-9: Reactive power from wind farm SVC [p.u]

8.5.2. FAULT 2

A 150ms three-phase short-circuit is applied on the bus 5400 at the time t=1s. This bus is a neighbour bus of the connection bus. The voltage of the wind farm falls to 0.35p.u whereas the voltage at the busbar becomes close to zero. But compared to the previous simulation, the voltages are less reduced. After the clearance of the fault the behaviour of the voltages is similar to the previous case.

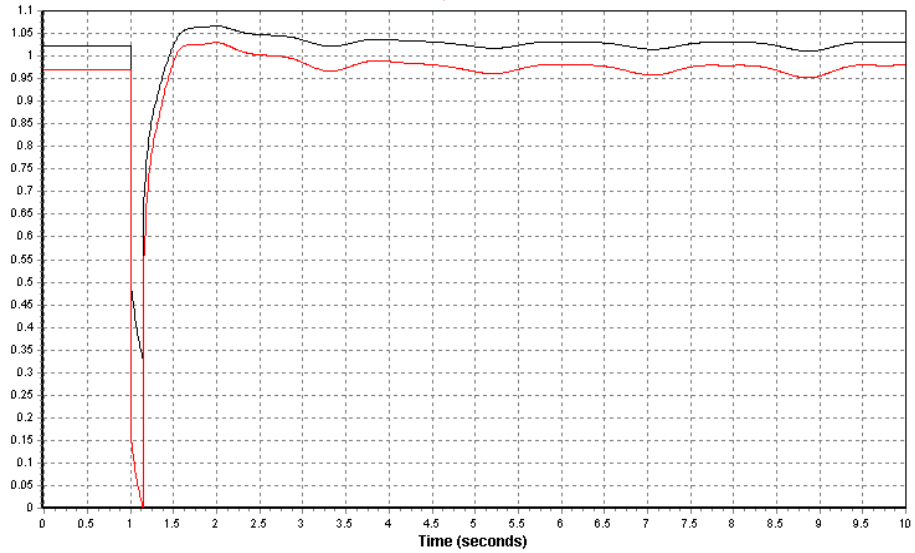

Figure 8-10: Voltage at offshore bus (black) and onshore bus (red) [p.u]

It can be noticed that the peak on the wind farm frequency is small and the frequency at the wind farm bus follows the behaviour of the frequency at the connection point. The deviation of the wind turbine generator speed is also small.

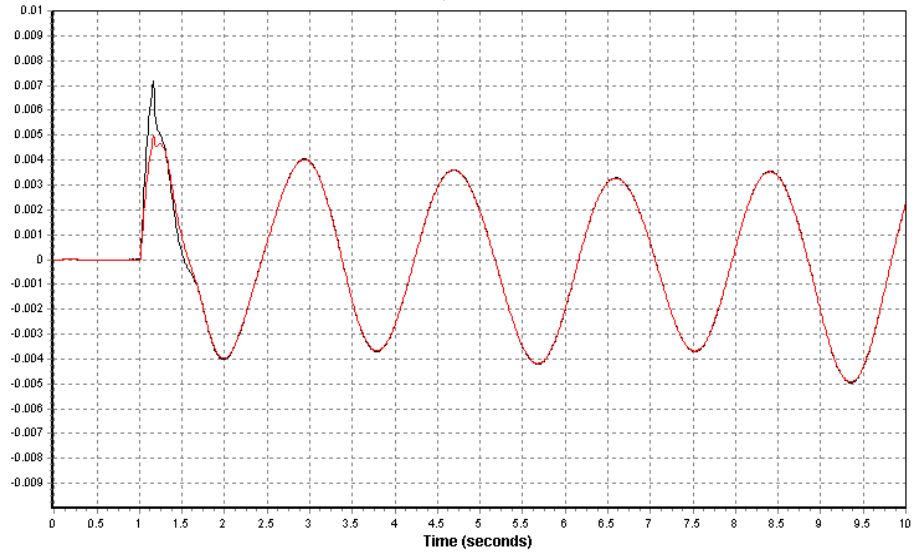

Figure 8-11: Frequency deviation at bus offshore (black) and onshore bus (red) [p.u]

The reactive power produced by the SVC is similar to the previous case. Nevertheless, the reactive power production after the fault is less important. This is explained by the fact that the voltage reduction is less important.

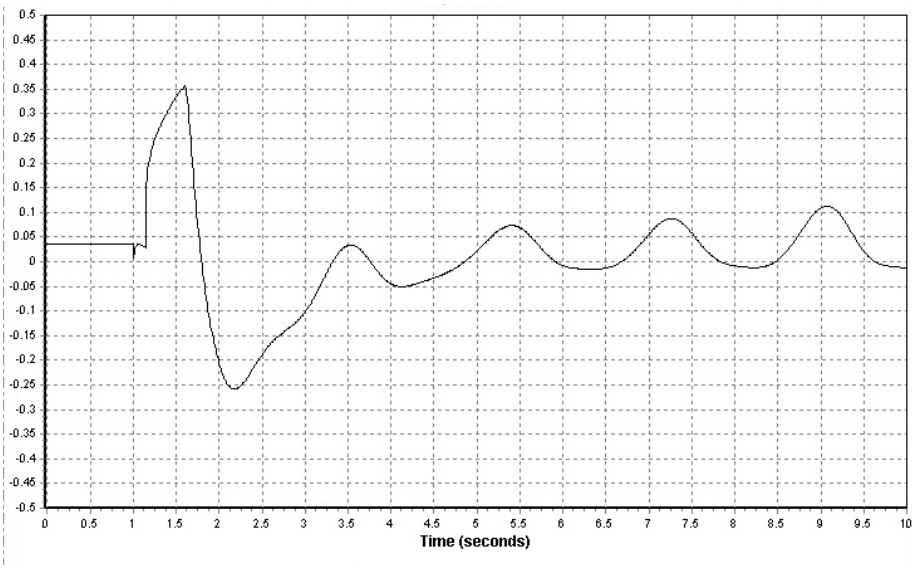

Figure 8-12: Reactive power from wind farm SVC [p.u]

The consequences of the short-circuit on the neighbour bus at the connection bus and at the offshore bus are generally less important. This is explained by the fact that the contribution of the busses on the short-circuit is "indirect" in the meaning that the fault does not occur directly on the connection bus.

8.5.3. FAULT 3

A 150ms three-phase short-circuit is applied on the line between the connection bus 6000 and its neighbour bus 5400 at the time t=1s. After the clearance of the fault the line is disconnected. The dynamic behaviour of the wind farm and the connection bus are the same as for the event 1. A short-circuit on a line implies that the voltages at the connected busses will drop to zero. Then as the voltage at the connection bus become null, the behaviour is the same as if the short-circuit happens on the connection bus.

8.5.4. FAULT 4

A 150ms three-phase short-circuit occurs on the wind farm busbar at the time t=1s. The voltage at the wind farm bus drops to zero and the voltage at the connection bus is reduced to 0.4p.u. After the fault clearance, the voltages increase quickly to 0.9 p.u and are stabilized to their reference values 2 seconds after the fault. It can be noticed that there is no oscillations on the voltages.

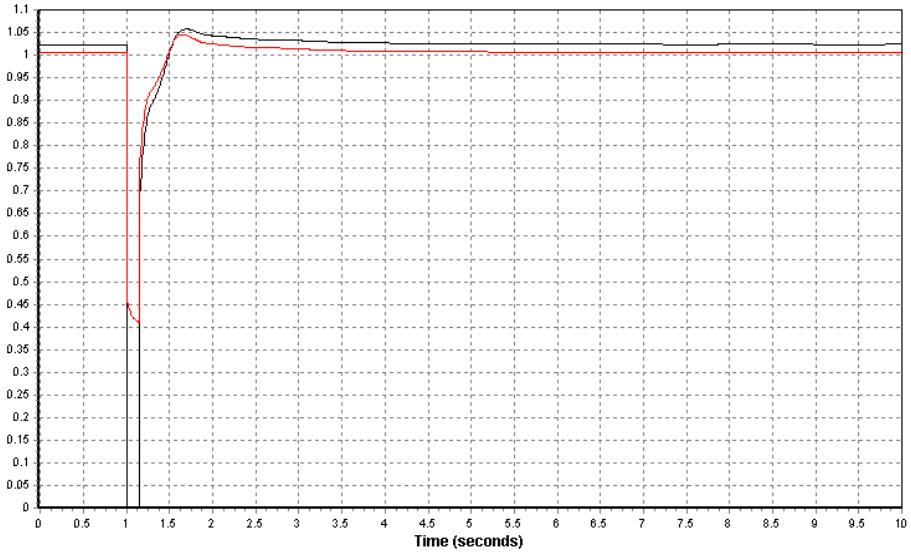

Figure 8-13: Voltage at offshore bus (black) and onshore bus (red) [p.u]

The wind farm bus frequency increases during the fault, and after the clearance, fast oscillation appears. However, the oscillations are quickly damped and their magnitudes are very small. The frequency on the busbar decreases during the fault. After the fault, the frequency is reduced and it returns to its reference value after 8 seconds. As the fault occurs on the wind farm, the connection bus is the only one to contribute to the short-circuit power. The production on the bus increases which leads to the reduction of the frequency.

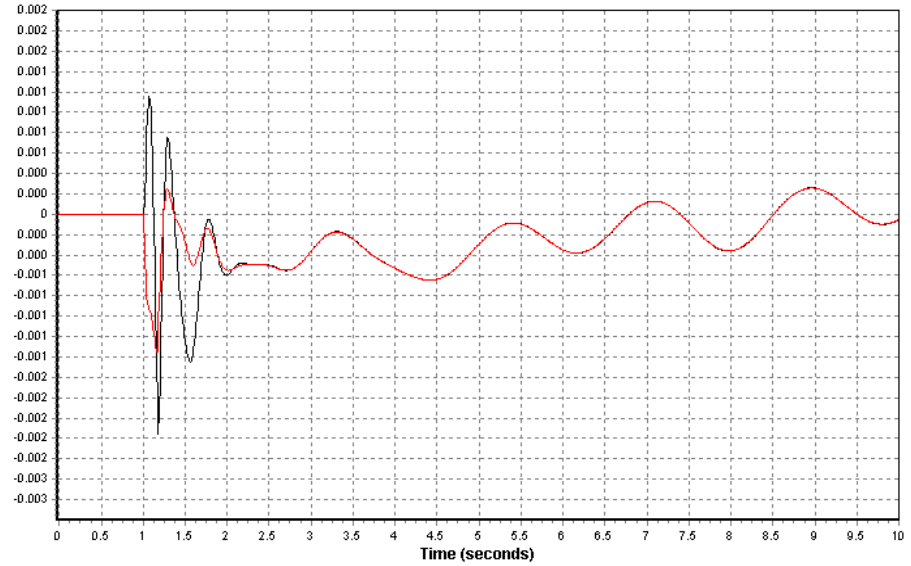

Figure 8-14: Frequency deviation at bus offshore (black) and onshore bus (red) [p.u]

The speed of the wind farm generator increases to reach the value of 1.05p.u during the fault and reduces quickly after the clearance. Small oscillations appear after the clearance. This can be linked to the oscillations in the wind farm bus frequency.

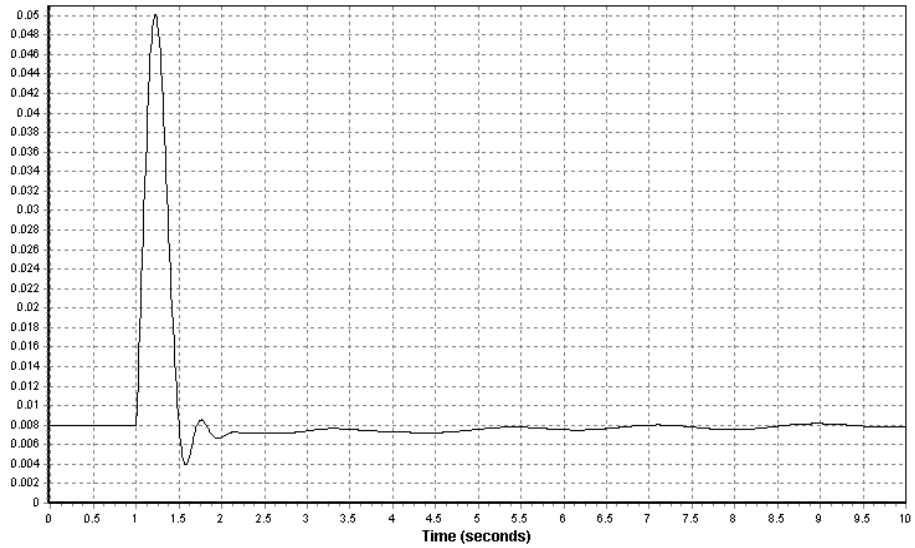

Figure 8-15: Speed deviation of the wind turbine generator [p.u]

The production of reactive power is similar to the other case. The SVC produces reactive power to regulate the voltage at the wind farm bus. But as there are no oscillations on the voltage, the oscillations on the reactive power disappear.

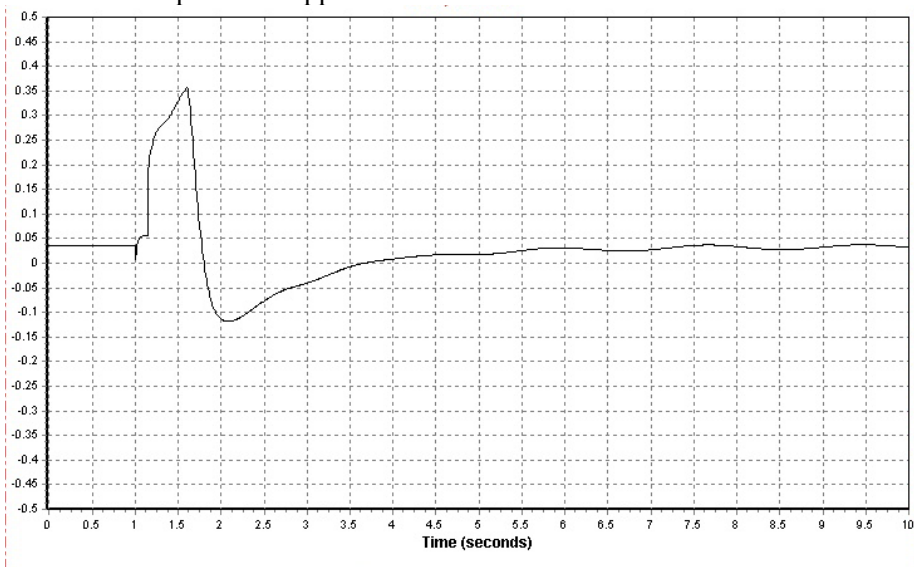

Figure 8-16: Reactive power from wind farm SVC [p.u]

8.6 CONFIGURATION 1, CONNECTION BUS 5600

The results of the simulations for the configuration 1 at the connection bus 5600 are similar to the results for the configuration 1 at the connection bus 6000. The comments made for the previous simulations can be applied to the following simulations.

8.6.1. FAULT 1

A 150ms three-phase short-circuit is applied on the connection bus (bus 5600) at the time t=1s. The voltage at the connection busbar becomes null whereas the voltage of the wind farm falls to 0.04p.u. However, after the clearance of the fault, the voltages recover more slowly and reach the value of 0.9p.u around 700ms after the beginning of the fault.

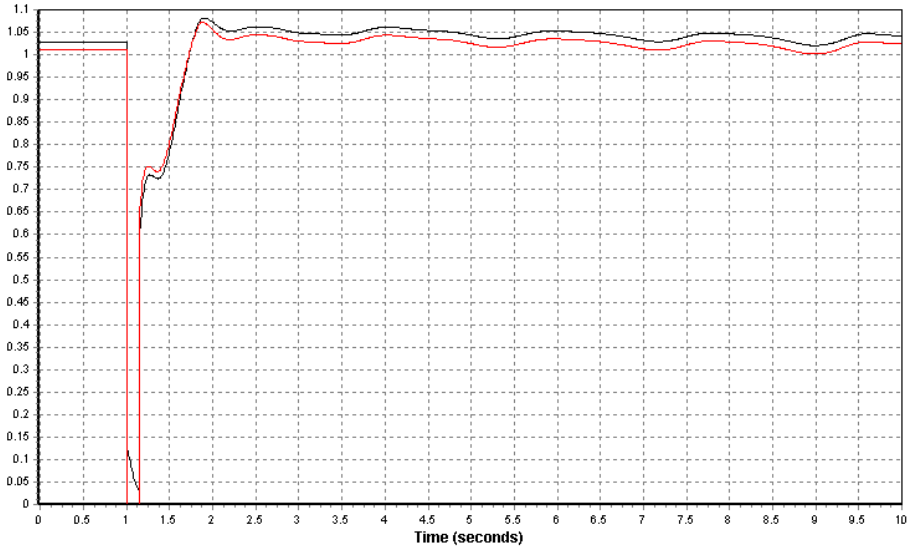

Figure 8-17: Voltage at offshore bus (black) and onshore bus (red) [pu]

8.6.2. FAULT 2

A 150ms three-phase short-circuit is applied on the bus 5603 at the time t=1s. This bus is a neighbour bus of the connection bus. The voltages at both busses are reduced to 0.8p.u during the fault and they recover quasi instantaneously after the fault. This means that the bus 5600 has a small contribution in the short-circuit power. Besides the short-circuit power of the bus 5603 is small due to the nature of the bus.

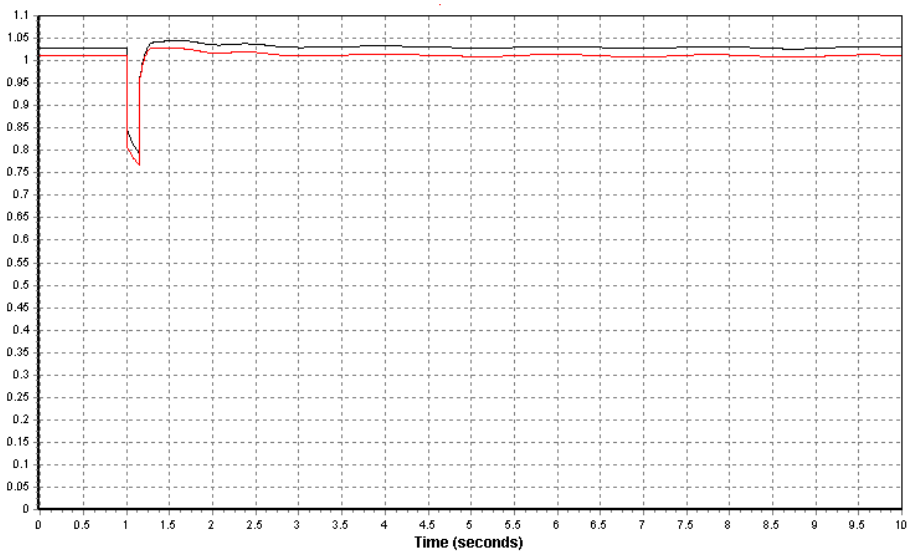

Figure 8-18: Voltage at offshore bus (black) and onshore bus (red) [p.u]

Due to the behaviour of the voltage, the production of reactive power is less important and the regulation of the voltage is faster.

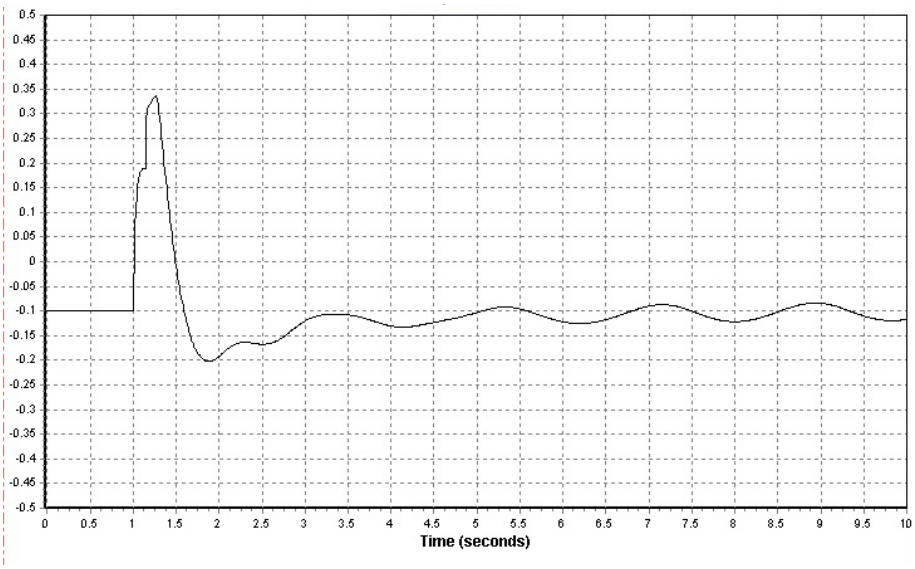

Figure 8-19 Reactive power from wind farm SVC [p.u]

8.6.3. FAULT 3

A 150ms three-phase short-circuit is applied on the line between the connection bus 5600 and its neighbour bus 5603 at the time t=1s. After the clearance of the fault the line is disconnected. The dynamic behaviour of the wind farm and the connection bus are the same as for the event 1, for the same reasons explained in the part 8.5.3.

8.6.4. FAULT 4

A 150ms three-phase short-circuit occurs on the wind farm busbar at the time t=1s. The voltage at the wind farm bus drops to zero and the voltage at the connection bus are reduced to 0.3p.u. After the fault clearance, the voltages increase quickly to 0.9 p.u and are stabilized to their reference values 2 seconds after the faults. As for the fault 4 in the previous case, there are no oscillations on the voltages. The other variables, the frequency, the generator speed and the SVC reactive power production have the same behaviour as for the fault 4 in the previous case.

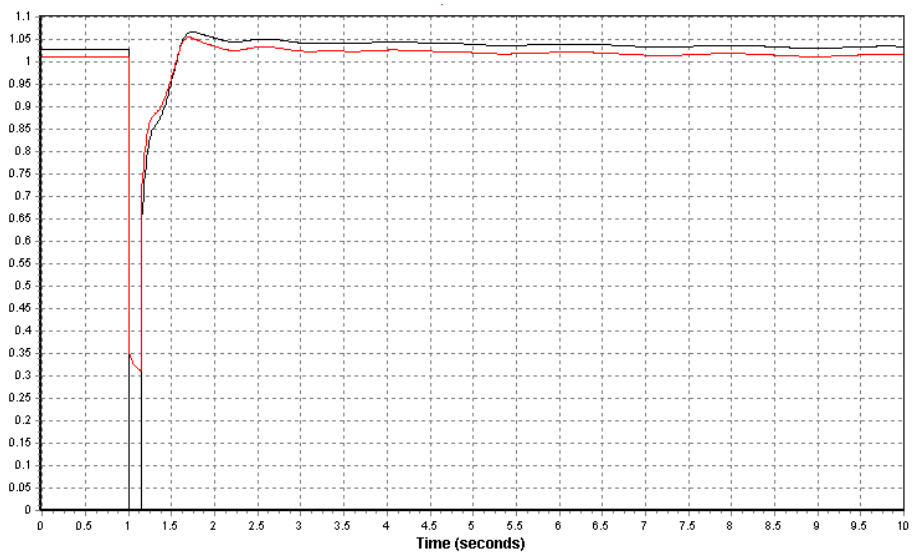

Figure 8-20: Voltage at offshore bus (black) and onshore bus (red) [p.u]

It can be noticed that with the configuration 1 and at the two possible connection busses, the grid code requirements from Statnett are respected.

8.7 CONFIGURATION 2, CONNECTION BUS 6000

In this case, the simulations are made with the configuration 2 connected to the grid in connection bus 6000. The configuration 2 represents a 1000MW wind farm connected to the grid via a HVDC transmission system.

8.7.1. FAULT 1

A 150ms three-phase short-circuit is applied on the connection bus (bus 6000) at the time t=1s. The voltage at the connection busbar becomes null. The voltage of the wind farm is quasi-constant during the fault. After the clearance of the fault at t=1.15ms, the voltage at connection bus increases quasi-instantaneously to 0.9 p.u and stabilizes at its reference value 1.5 seconds after the beginning of the fault. During the fault, the onshore and offshore systems operate independently and the fault does not affect the voltage offshore.

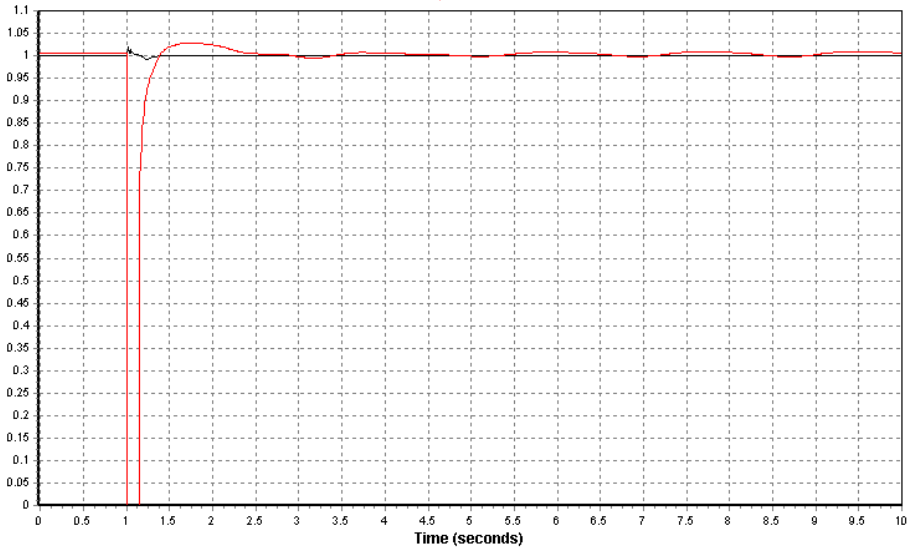

Figure 8-21: Voltage at offshore bus (black) and onshore bus (red) [p.u]

The onshore frequency has the same behaviour as if there was no wind farm connected. The offshore frequency and the generator speed increase quickly during the fault. As explained previously, the wind generator accelerates in order to limit the transfered power to the grid and the energy produced during the fault is stored as kinetic energy in the wind turbine. After the fault clearance, the frequency and the speed decrease slowly. Then, the energy stored is transform in electrical energy and is transferred to the grid.

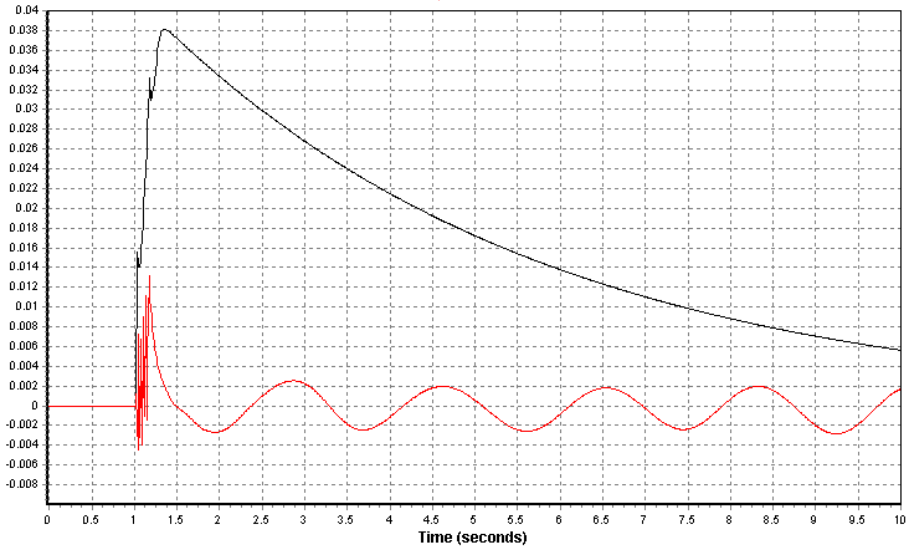

Figure 8-22: Frequency deviation at bus offshore (black) and onshore bus (red) [p.u]

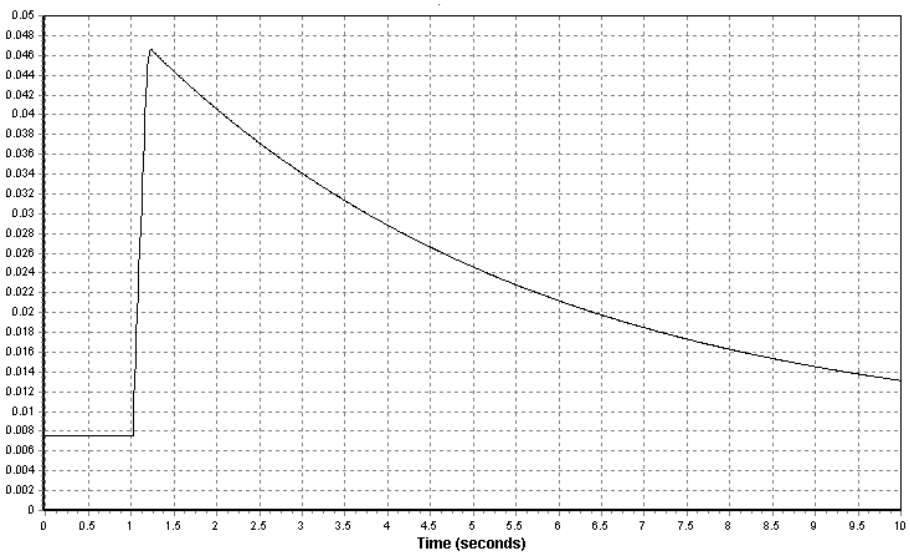

Figure 8-23: Speed deviation of the wind turbine generator [p.u]

The onshore converter produces a large amount of reactive power during the fault which means that it contribute to the short-circuit power during the fault. Then the voltage at the connection bus recovers its reference value quickly. However, the production of reactive power is limited and the converter can only operate in the limit of its P/Q diagram.

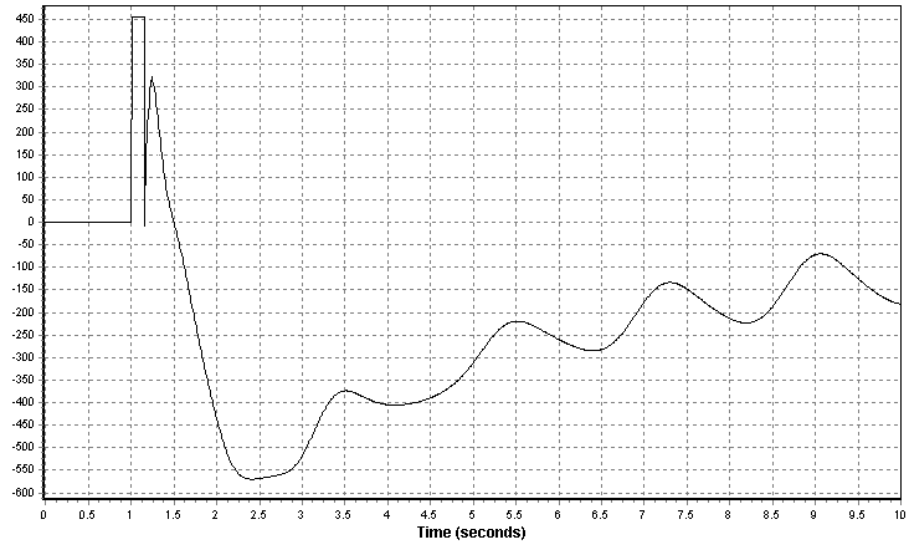

Figure 8-24 : Reactive power from the onshore converter [MVar]

The losses on the DC line drops to 25MW during the fault. This value represents the fixed losses of the converters. So it can be concluded that no active power flows in the DC line during the fault.

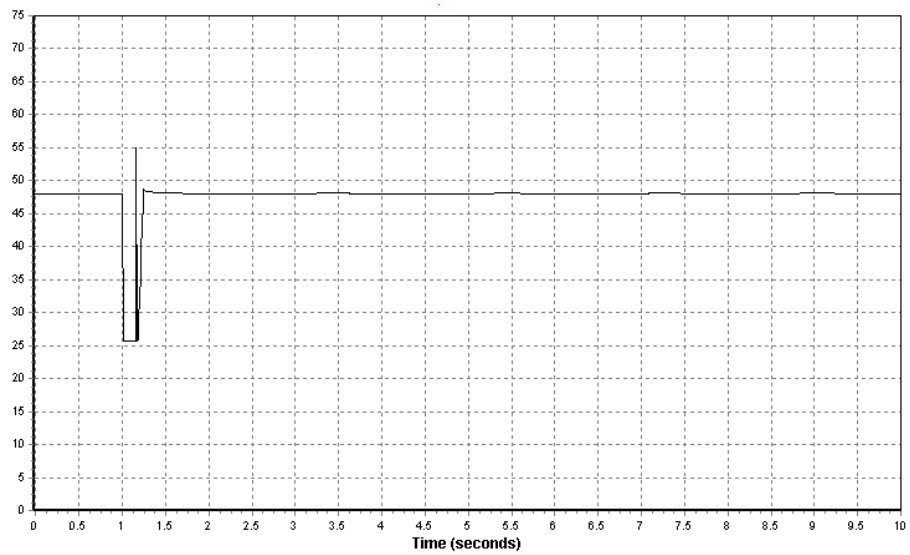

Figure 8-25: Losses on the DC line [MW]

8.7.2. FAULT 2

A 150ms three-phase short-circuit is applied on the bus 5400 at the time t=1s. This bus is a neighbour bus of the connection bus. The voltage on the connection bus drops to 0.3 p.u during the fault and reaches 0.9p.u instantaneously when the fault is cleared. It is stabilized after 2 seconds. The fault has no effect on the offshore voltage. The voltage drop is smaller than with the configuration 1, which means that the contribution of the bus 6000 in the short –circuit power is smaller.

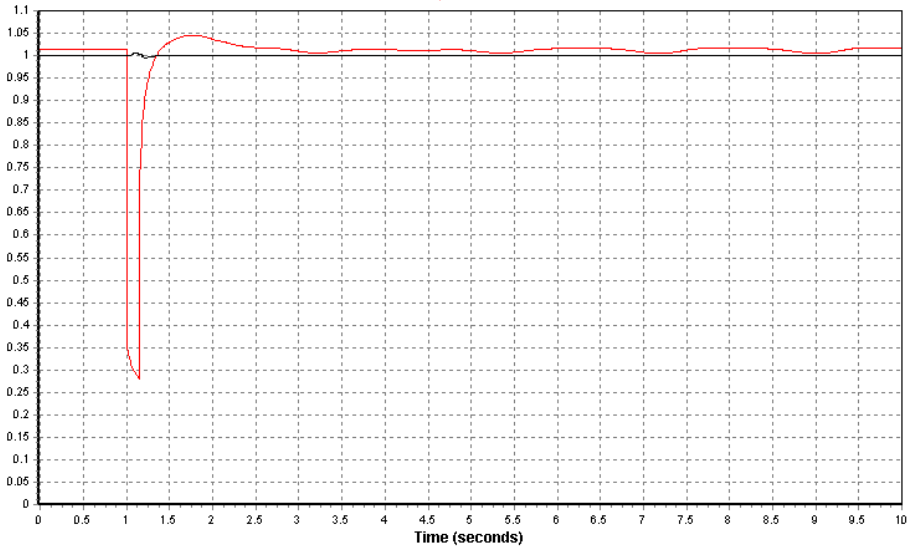

Figure 8-26: Voltage at offshore bus (black) and onshore bus (red) [p.u]

The losses on the DC line show that the flow of power in the transmission is not to totally stopped during the fault. Indeed, the minimal value of the losses is around 30MW whereas the fixed losses of the converters are around 25MW. Then there are losses created in the DC line by a flow of current. The wind farm contributes to the short-circuit power which leads to the reduction of the bus 6000 contribution, and to the reduction in its voltage drop.

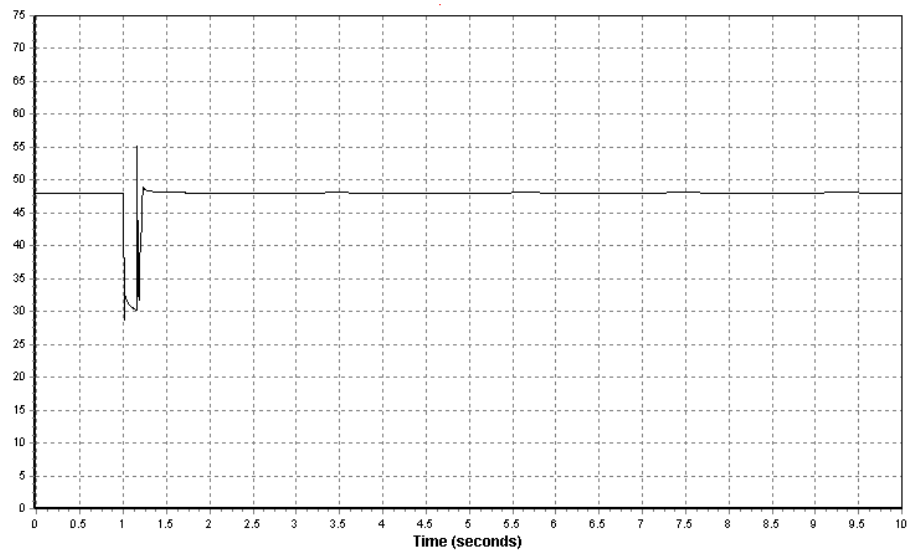

Figure 8-27: Losses on the DC line [MW]

The dynamic behaviour of the other variables is the same as for the fault 1 but with smaller the values.

8.7.3. FAULT 3

A 150ms three-phase short-circuit is applied on the line between the connection bus 6000 and its neighbour bus 5400 at the time t=1s. After the clearance of the fault the line is disconnected. The dynamic behaviour of the wind farm bus and the connection bus are the same as for the event 1, for the same reasons explained in the part 8.5.3.

8.7.4. FAULT 4

A 150ms three-phase short-circuit occurs on the wind farm busbar at the time t=1s. The voltage at the wind farm bus drops to zero during the fault. After the clearance, the voltage increases instantaneously to 0.55 p.u. and reaches 0.9 p.u at t=2s. The voltage is stabilized 1.5 second after the clearance of the fault. According to the grid code requirements, the voltage at the offshore bus is too slow to reach the value of 0.9p.u. However, with the HVDC transmission, the fault offshore does not affect the onshore grid. The voltage at the connection bar does not change during and after the fault. As the voltage does not change, no reactive power is produced by the onshore converter.

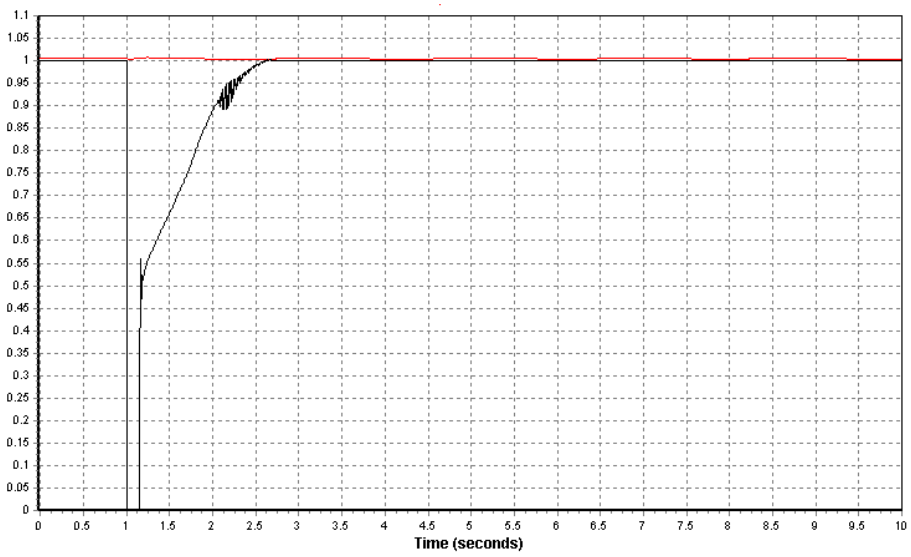

Figure 8-28: Voltage at offshore bus (black) and onshore bus (red) [p.u]

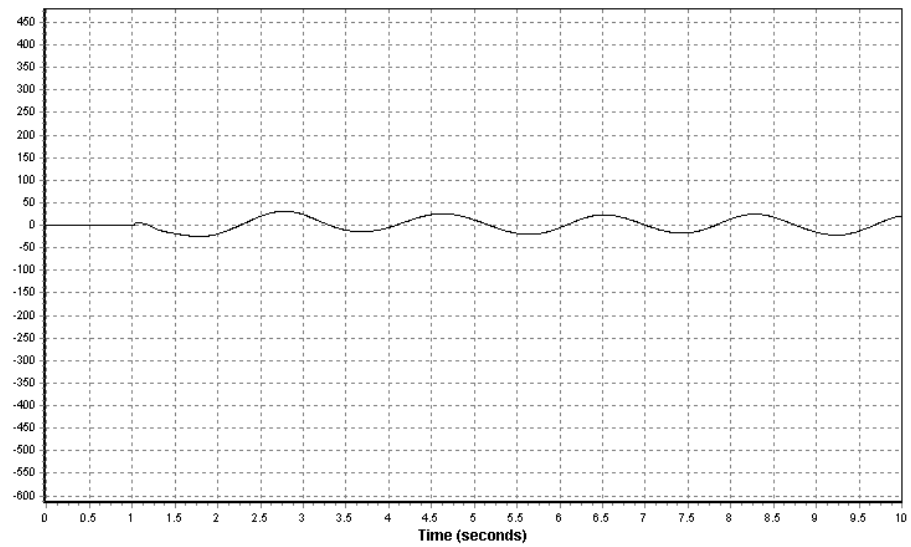

Figure 8-29: Reactive power from the onshore converter [MVar]

As for the voltage, the frequency onshore is not affected by the fault and it remains at its reference value. During the fault, important oscillations with a peak value at 57 Hz appear in the offshore frequency. At the clearance of the fault, the frequency continues to increase until the voltage is stabilized and reaches the value of 53 Hz. Then, the frequency decreases. These frequencies deviations do not respect the Statnett requirement.

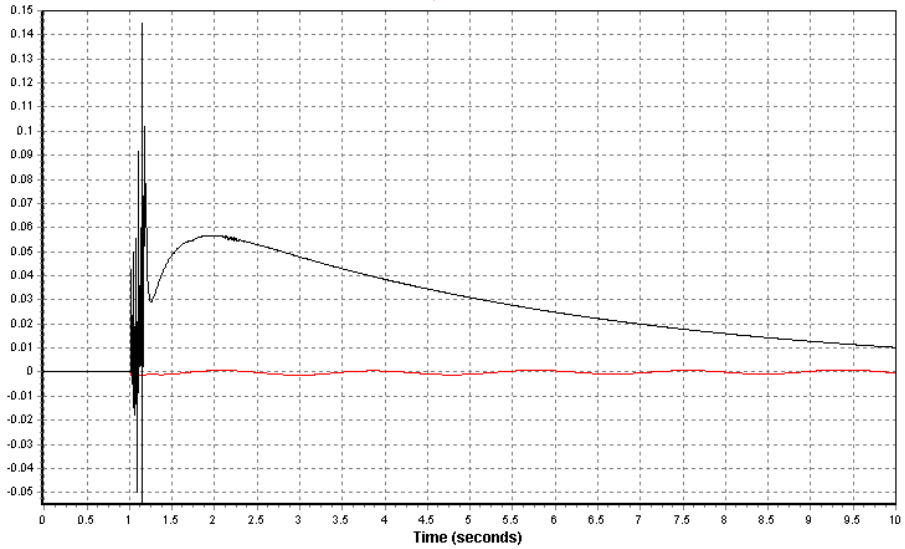

Figure 8-30: Frequency deviation at bus offshore (black) and onshore bus (red) [p.u]

The losses on the DC line show that the power on the DC line is null during the fault. Then the power transfer is restored progressively. This explains that the speed and the frequency continue to increase even after the fault clearance but with a decreasing slope.

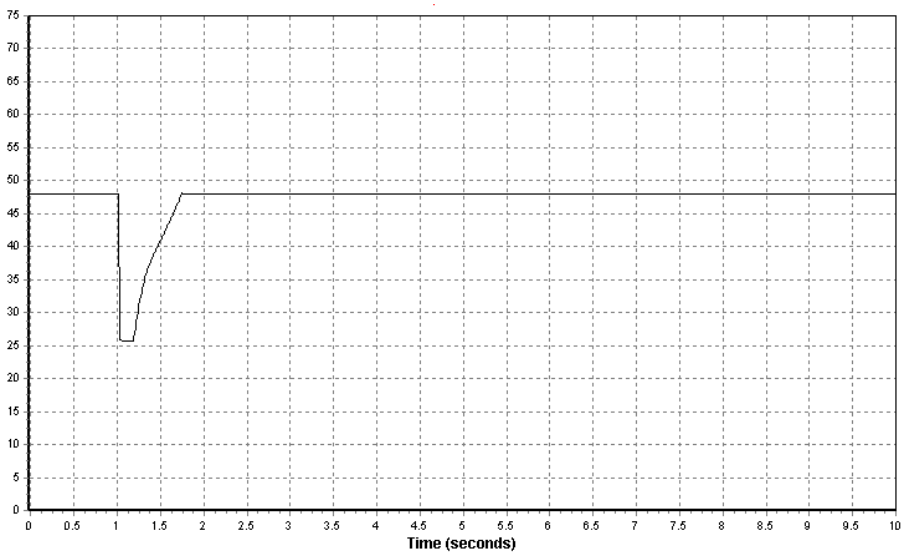

Figure 8-31: Losses on the DC line [MW]

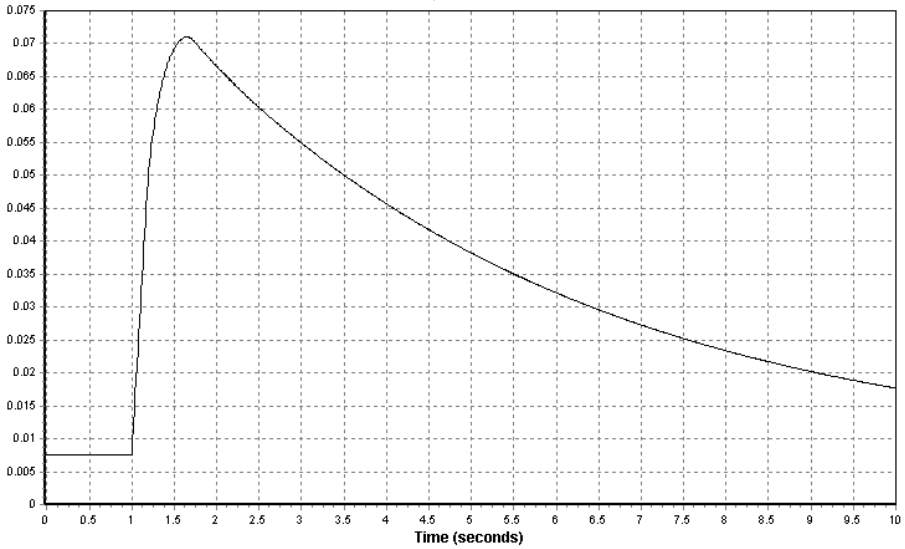

Figure 8-32: Speed deviation of the wind turbine generator [p.u]

The reactive power produce by the converter is maximal until the voltage is stabilized. At t=2s, important oscillations appears. These oscillations are caused by the oscillations that can be seen on the voltage.

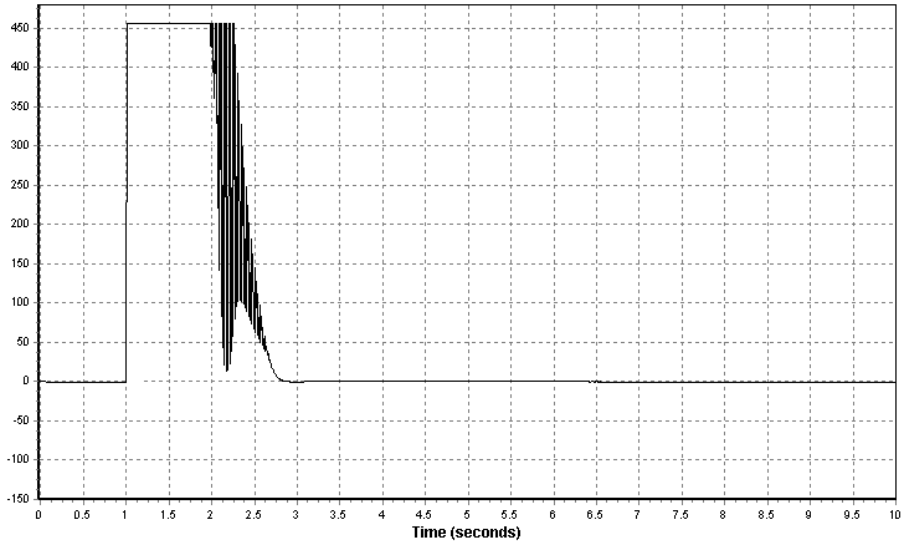

Figure 8-33: Reactive power from the offshore converter [MVar]

The offshore behaviour is not normal when a fault occurs on the wind farm. It is explained by the fact that the VSC-HVDC model and its variables, as the different gains and time constants, are not optimized for the application. However, the behaviour of the onshore grid is realistic, and the HVDC link permits to create two independent systems. If a fault occurs at the offshore side, there are no repercussions on the onshore side and vice-versa.

8.8 CONFIGURATION 2, CONNECTION BUS 5600

8.8.1. FAULT 1

A 150ms three-phase short-circuit is applied on the connection bus (bus 5600) at the time t=1s. The voltage at the connection busbar becomes null. The voltage of the wind farm is quasi-constant during the fault. After the clearance of the fault at t=1.15ms, the voltage at connection bus increases quasi-instantaneously to 0.8 p.u. However after 2 seconds, the voltage at the connection bus begins to oscillate. The amplitude of these oscillations is around 1 p.u which is very important compared to the oscillation on the normal system (see part 8.1.1).

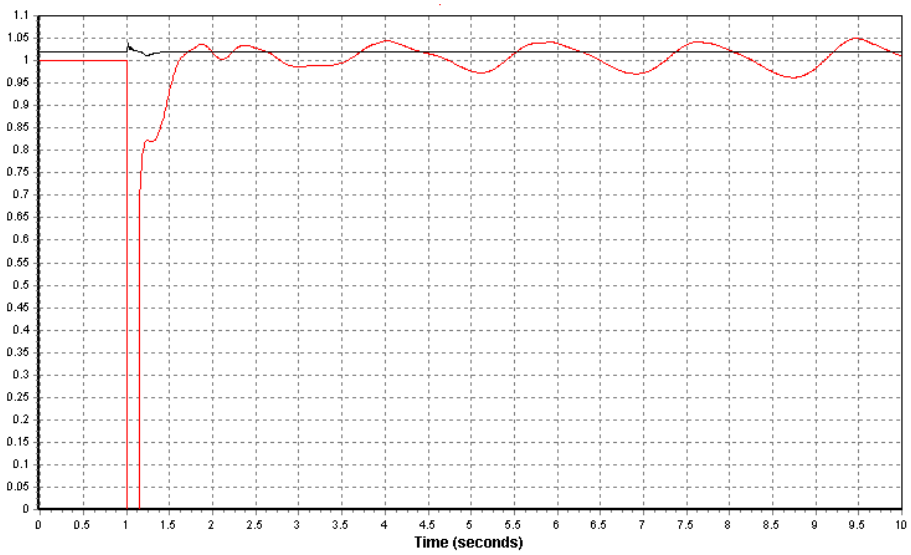

Figure 8-34: Voltage at offshore bus (black) and onshore bus (red) [p.u]

Oscillations appear also on the frequency at the connection busbar. Furthermore, they tend to grow.

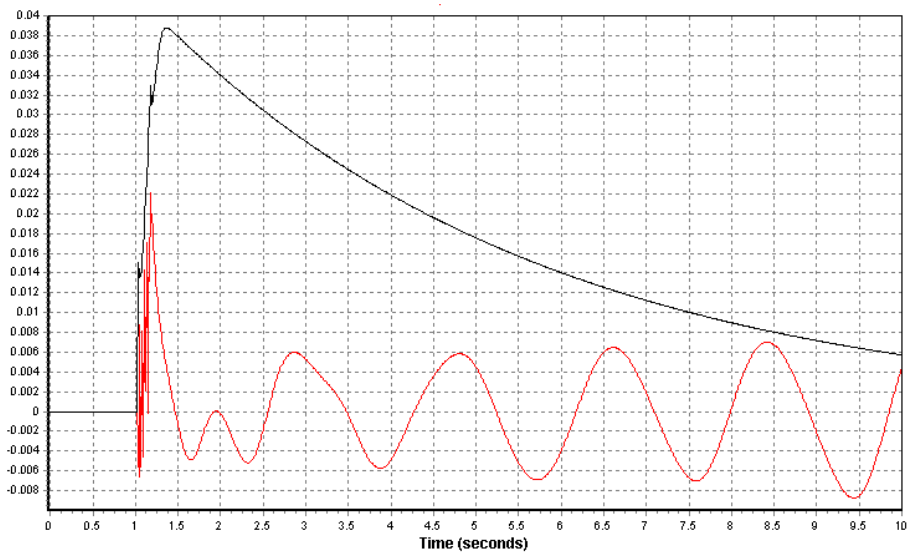

Figure 8-35: Frequency deviation at bus offshore (black) and onshore bus (red) [p.u]

The configuration 2 connected on the bus 5600 leads to instability in the system after the fault 1. As explain in the part 7.4, the bus 5600 is in a situation where it has to supply other busses. Moreover the contributions of its neighbours represent 40% of the short-circuit current whereas the bus generator contributes at 60% to the short-circuit current. The demand from its neighbours, particularly the bus 5603, is too important and when a fault occurs, the bus does not manage to recover equilibrium. Furthermore, the onshore converter can not meet the demand of reactive power of the bus because it is limited in the P/Q diagram.

8.8.2. FAULT 2

A 150ms three-phase short-circuit is applied on the bus 5603 at the time t=1s. This bus is a neighbour bus of the connection bus. The voltage on the connection bus drops to 0.75 p.u during the fault and reaches 0.95p.u instantaneously when the fault is cleared. It is stabilized after 2 seconds. The contribution of the connection bus to the short-circuit power is small. Besides, as bus 5603 is only a load bus, its short-circuit power is not important. The fault has no effect on the offshore voltage. The onshore converter produces reactive power in order to regulate the voltage at the bus 5600.

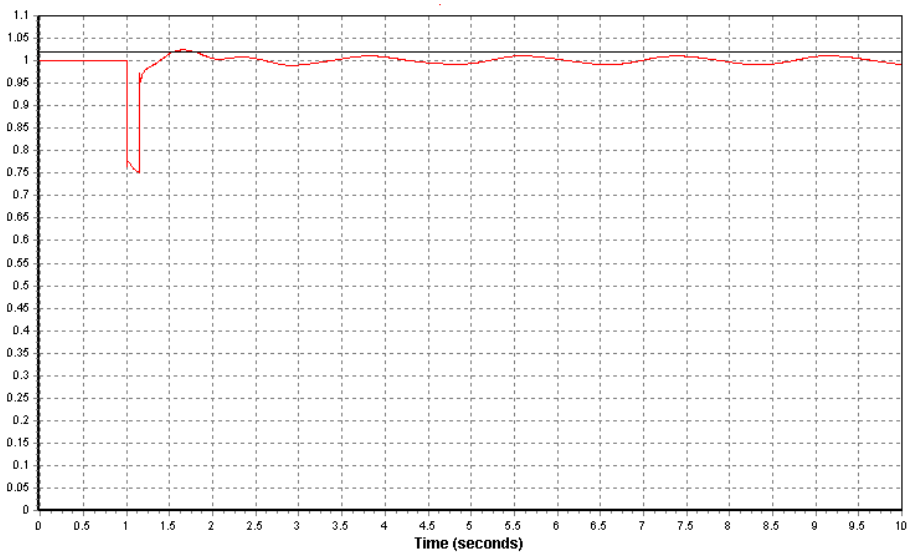

Figure 8-36: Voltage at offshore bus (black) and onshore bus (red) [p.u]

The consequences of the fault on the frequency are also limited. The frequency onshore increases a little bit during the fault but is stabilized quickly. The fault has no effect on the frequency offshore and then the speed of the wind generator remains constant during and after the fault.

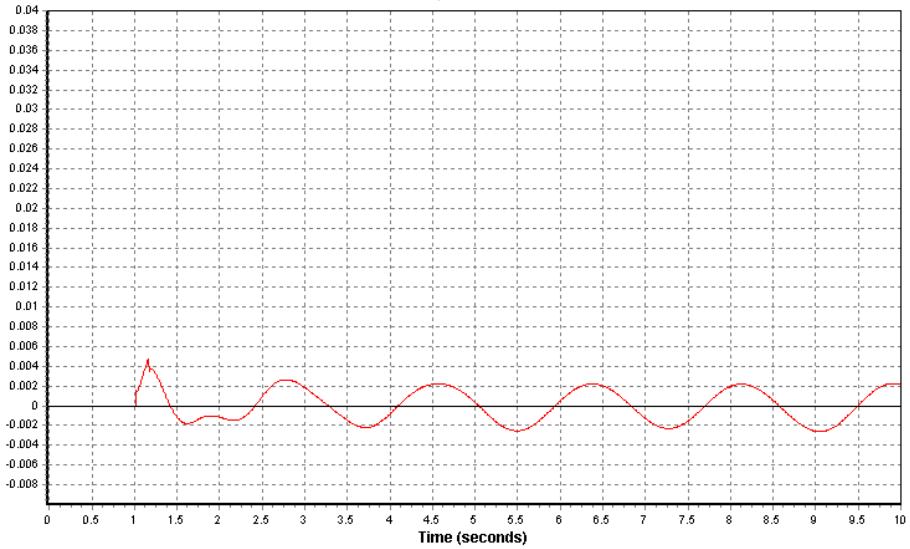

Figure 8-37: Frequency deviation at bus offshore (black) and onshore bus (red) [p.u]

It can be seen from the losses of the DC line that the transfer of power from the wind farm to the grid is never reduced or stopped. It explains the constancy in the voltage and the frequency at the offshore busbar.

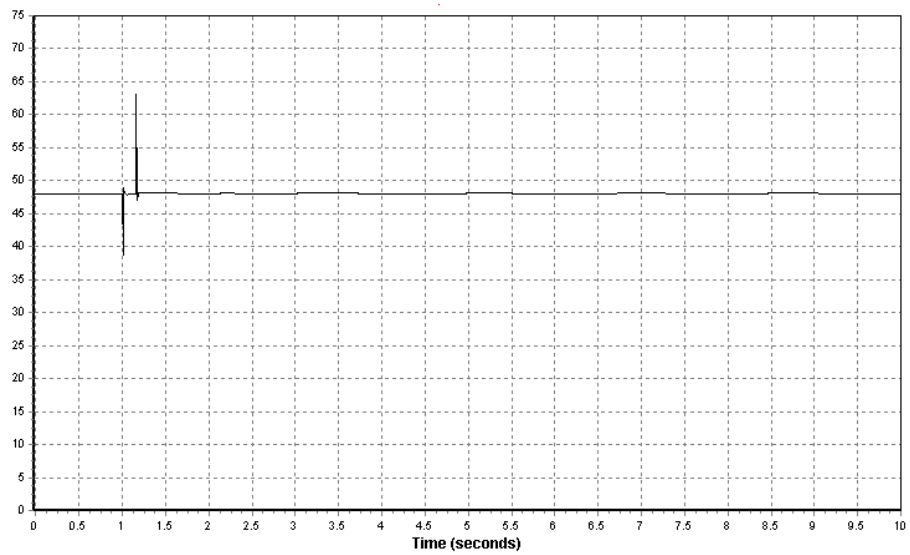

Figure 8-38: Losses on the DC line [MW]

8.8.3. FAULT 3

A 150ms three-phase short-circuit is applied on the line between the connection bus 5600 and its neighbour bus 5603 at the time t=1s. After the clearance of the fault the line is disconnected. The conclusions for this fault are the same as for the fault 1. The system is unstable for this fault. The fact that the voltage at the bus 5600 drops to zero, creates the instability, and the system is not able to recover its initial state.

8.8.4. FAULT 4

When a fault is applied at the offshore busbar, the system has the same dynamic behaviour for the connection of the configuration 2 at the connection bus 6000. The grid is unaffected by the offshore fault and the offshore variables react in the same way as the one presented on part 8.7.4

8.9 CONFIGURATION 3, CONNECTION BUS 6000

In this case, the simulations are made with the configuration 3 connected to the grid on the bus 6000. The configuration 3 represents two 500MW wind farms connected to the grid. One of them is connected with a HVDC transmission system whereas the other one is connected with a HVAC transmission system. The first farm will be called "HVDC wind farm" and the second one "HVAC wind farm" in these simulations. The results for each farm are similar to the results for configurations 1 and 2.

8.9.1. FAULT 1

A 150ms three-phase short-circuit is applied on the connection bus (bus 6000) at the time t=1s. The voltage at the connection busbar becomes null. The voltage at the HVAC wind farm evolves as in the case with the configuration 1. It drops to 0.04p.u during the fault and recovers the value of 0.9 p.u 100ms after the fault clearance. However, the stabilization of the voltages is quicker than with the configuration 1 and happens after 1.5 seconds. For its part, the voltage of the wind farm is quasi-constant during the fault which is the same as in the case with the configuration 2. During the fault, the onshore and HVDC offshore systems operate independently and the fault does not affect the voltage of the HVDC offshore busbar. The frequencies and the generator speeds behaviour are the same as with configuration 1 and 2.

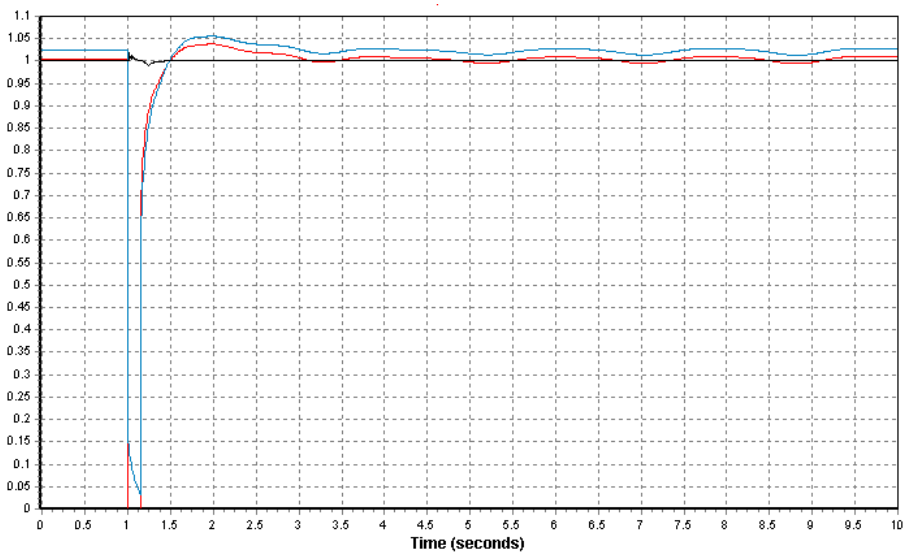

Figure 8-39: Voltage at offshore HVDC bus (black), offshore HVAC bus (blue) and onshore bus (red) [p.u]

Concerning the reactive power, the SVC still produces reactive power in order to regulate the voltage. But the peak of production is quicker and less important than for the configuration 1. That is explained by the fact that the onshore converter of the HVDC transmission system plays a rule of SVC during the fault, and it also contributes to the voltage stability.

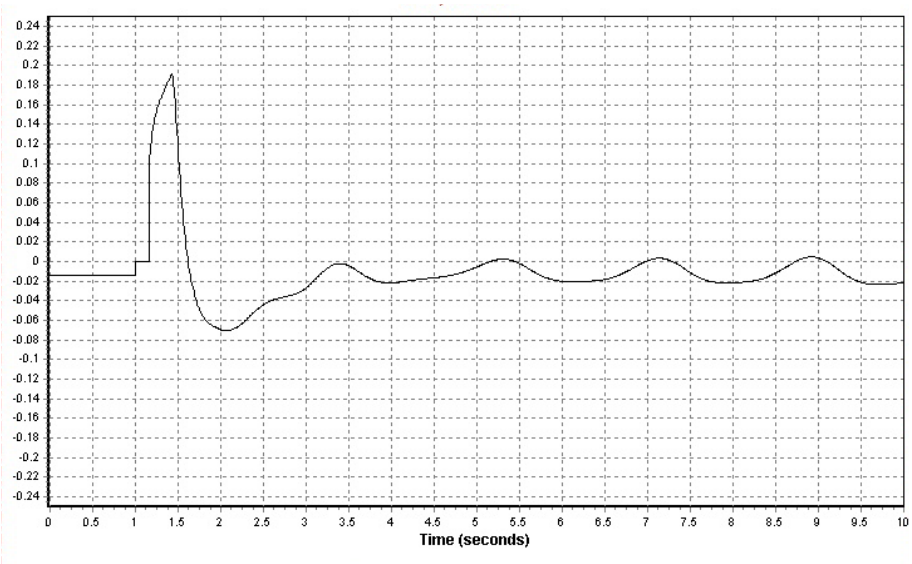

Figure 8-40: Reactive power from wind farm SVC [p.u]

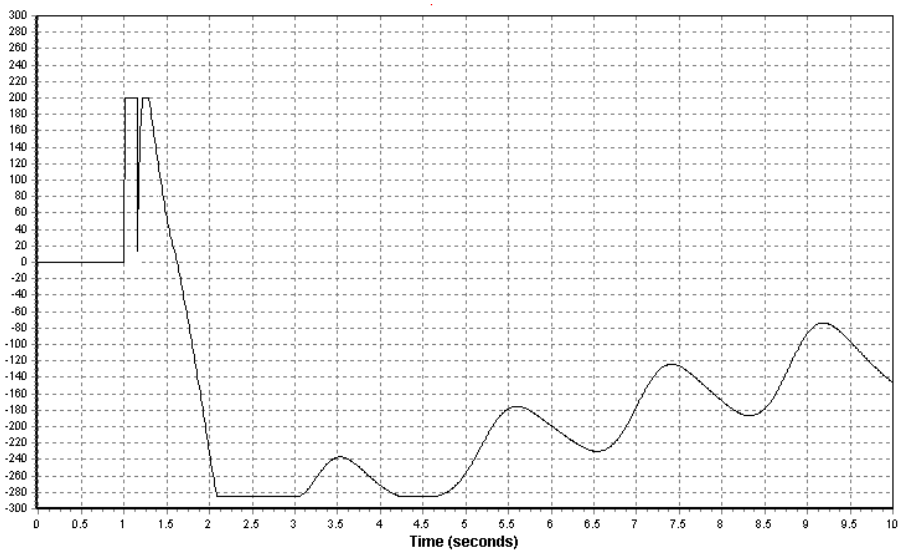

Figure 8-41: Reactive power from the onshore converter [MVar]

From the DC losses it can be seen that the transfer of power in the DC line is stopped during the fault as with the configuration 2.

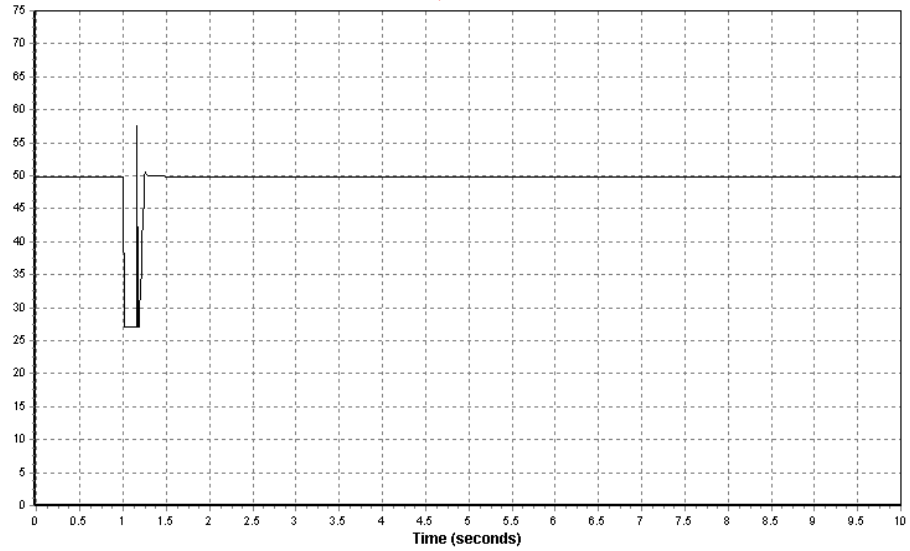

Figure 8-42: Losses on the DC line [MW]

8.9.2. FAULT 2

A 150ms three-phase short-circuit is applied on the bus 5400 at the time t=1s. This bus is a neighbour bus of the connection bus. During the fault, the voltage at the connection bus drops to 0.3p.u and voltage at the HVAC wind farm drops to 0.35 p.u. The voltage at the HVDC wind farm still remains unchanged during the fault. The drop in the connection bus voltage is less important than in the case with only one HVAC wind farm. This means that the contribution of the bus is less important in the short-circuit power.

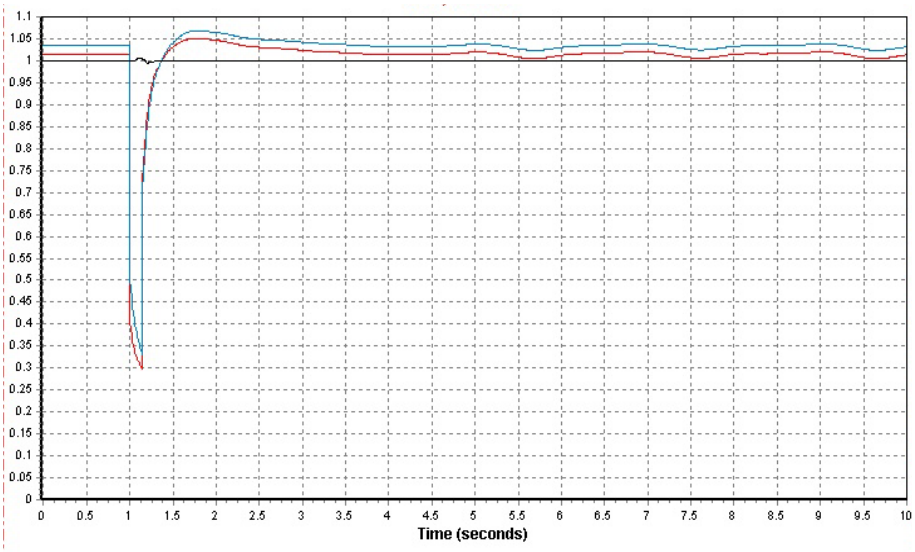

Figure 8-43: Voltage at offshore HVDC bus (black), offshore HVAC bus (blue) and onshore bus (red) [p.u]

The following plot shows that the transfer power is not totally stop in the DC line, as with configuration 2. The contribution of the bus 6000 in the short-circuit power is reduced and so the voltage drop is less important.

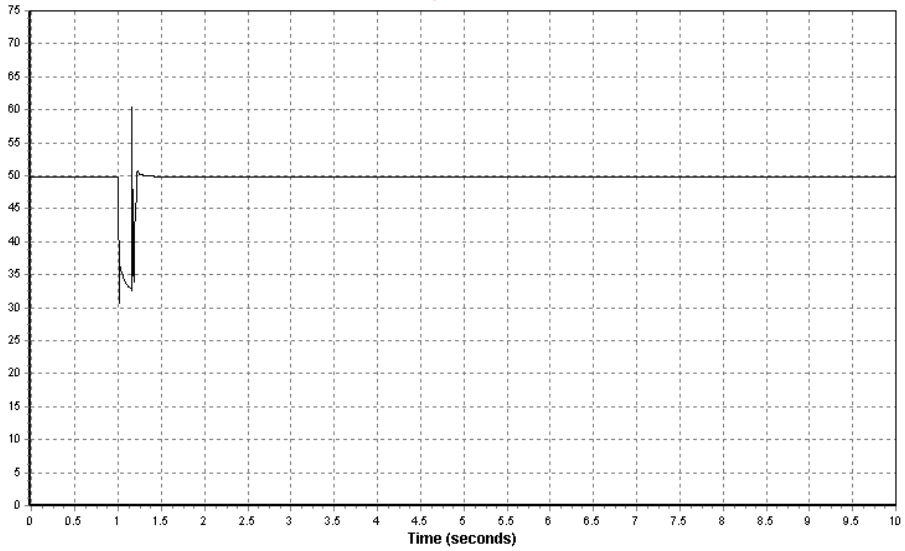

Figure 8-44: Losses on the DC line [MW]

8.9.3. FAULT 3

A 150ms three-phase short-circuit is applied on the line between the connection bus 6000 and its neighbour bus 5400 at the time t=1s. After the clearance of the fault, the line is disconnected. The dynamic behaviour of the wind farm and the connection bus are the same as for the event 1, for the same reasons explained in the part 8.5.3.

8.9.4. FAULT 4

8.9.4.1 *TYPE A*

A 150ms three-phase short-circuit is applied at the time t=1s on the bus 1100 which is the HVDC wind farm busbar. The HVDC wind farm, because of the nature of its transmission system is totally independent of the rest of the system. So the fault does not affect the HVAC wind farm voltage and the voltage at the connection bus. For its part, the HVDC wind farm voltage drops to zero during the fault. After the clearance of the fault, the voltage increases instantaneously to 0.5 p.u and begins to oscillate during 1.5 seconds. At t=2s the voltage increases quickly to 0.9 p.u. and recovers its initial value 500 ms after.

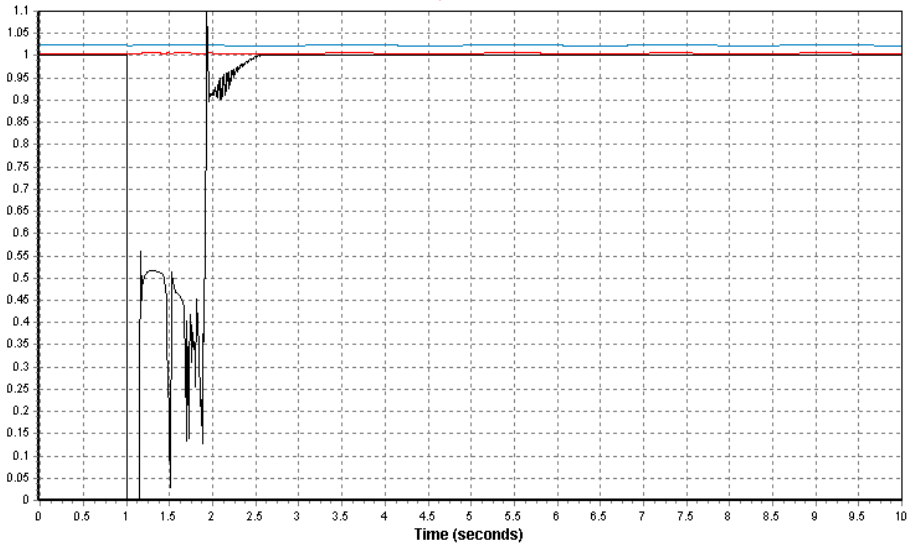

Figure 8-45: Voltage at offshore HVDC bus (black), offshore HVAC bus (blue) and onshore bus (red) [p.u]

The frequency during and 2 seconds after the fault, behaves like the voltage. Furthermore, at t=2s, the frequency begins to decrease from its peak value at 1.12pu, which represents 56 Hz. This value is too important regarding the grid code requirements.

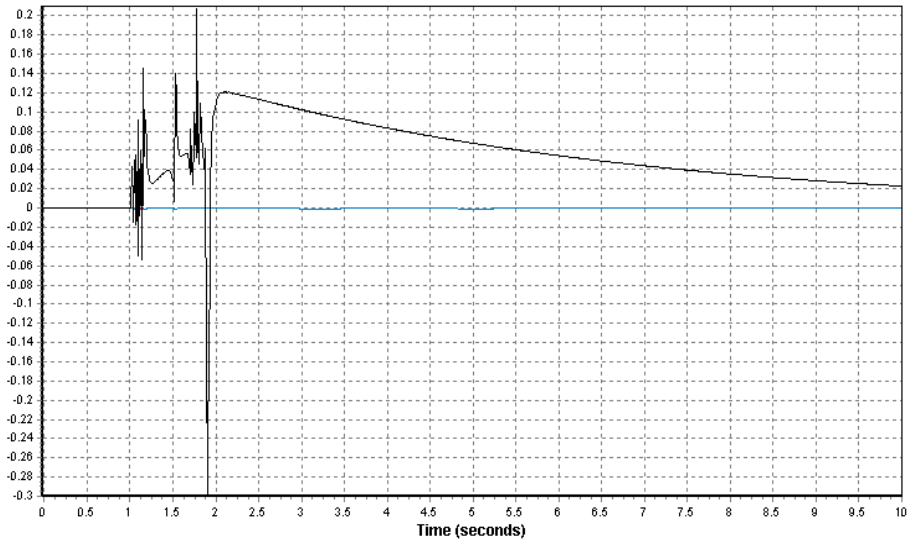

Figure 8-46: Frequency deviation at offshore HVDC bus (black), offshore HVAC bus (blue) and onshore bus (red)) [p.u]

During the fault, the HVDC wind farm busbar is the only one to contribute to the short-circuit fault. After the clearance of the fault the offshore system is not able to recover its initial conditions quickly.

8.9.4.2 *TYPE B*

A 150ms three-phase short-circuit is applied at the time t=1s on the bus 1200 which is the HVAC wind farm busbar. The voltage at the HVAC wind farm busbar drops to zero and the voltage at the connection busbar is reduced to 0.6p.u. The HVDC wind farm voltage is not affected by the fault.

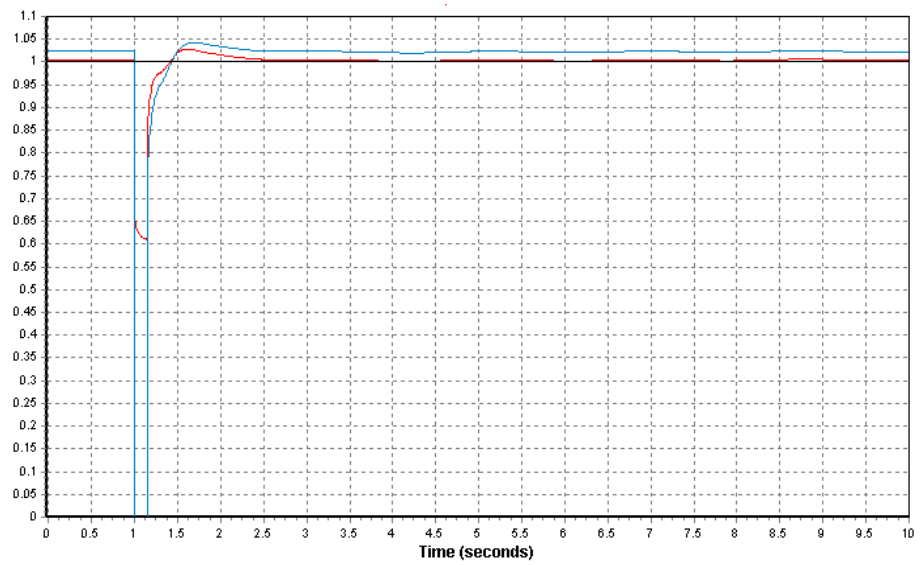

Figure 8-47: Voltage at offshore HVDC bus (black), offshore HVAC bus (blue) and onshore bus (red) [p.u]

The contribution of the connection busbar is less important than if the HVAC was alone as in configuration 1. The HVDC wind farm contribute to the short-circuit power which reduces the contribution of the connection bus.

Both the SVC and the onshore converter produce reactive power in order to regulate the voltage. However, their productions are faster than with the configuration 1 or 2.

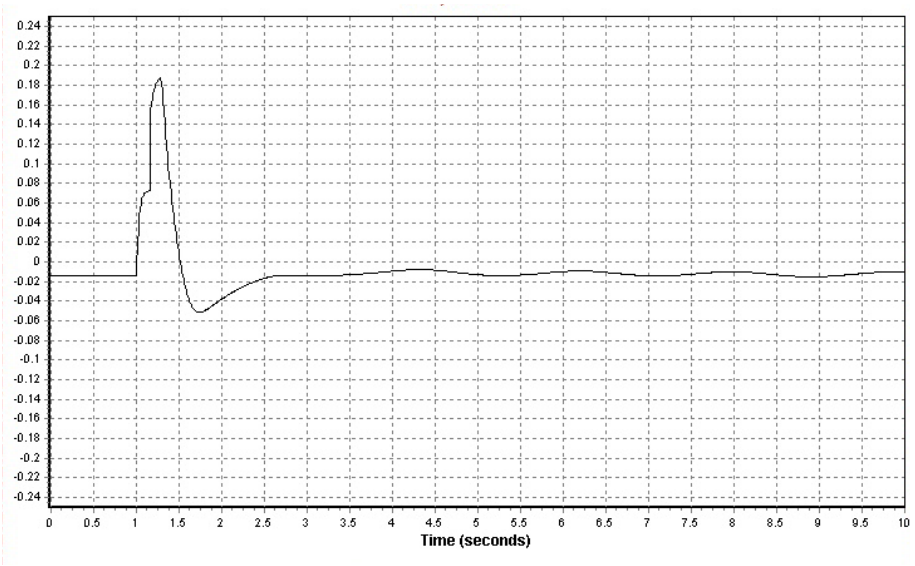

Figure 8-48: Reactive power from wind farm SVC [p.u]

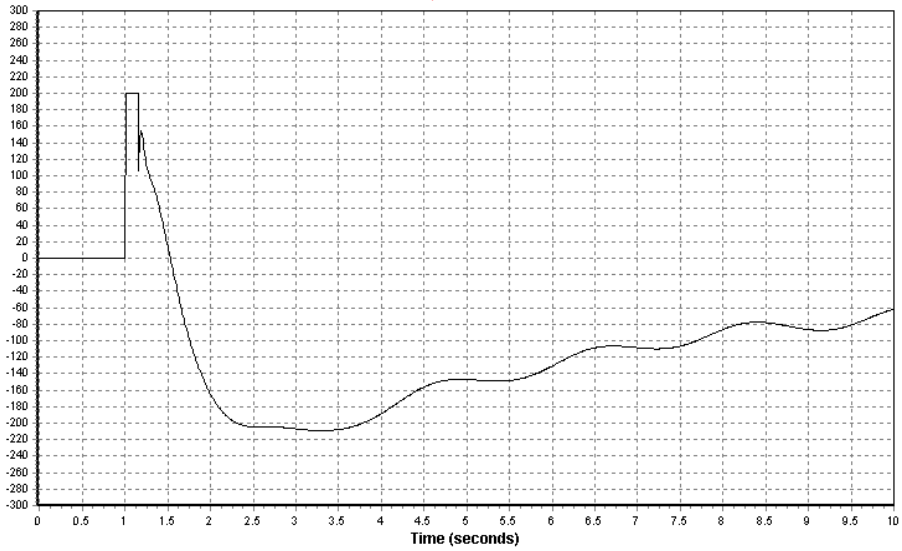

Figure 8-49: Reactive power from the onshore converter [MVar]

8.9.4.3 *TYPE C*

At the time t=1s, two 150ms three-phases short-circuits occurs on both wind farms at the same time. This kind of fault is not realistic, but it illustrates the loss of production from both wind farms. The results of this simulation are the addition of the results showed for the fault 4 type A and for the fault 4 type B. The dynamic behaviour is similar for both wind farm and the grid.

8.10 CONFIGURATION 3, CONNECTION BUS 5600

The results of the simulations for the configuration 3 at the connection bus 5600 are similar to the results for the configuration 3 at the connection bus 6000. The comments made for the previous simulations can be applied to the following simulations.

8.10.1. FAULT 1

A 150ms three-phase short-circuit is applied on the connection bus (bus 5600) at the time t=1s. The voltage at the connection busbar becomes null and the voltage at the HVAC wind farm falls to 0.05p.u. The voltage of the wind farm is quasi-constant during the fault. After the clearance of the fault at t=1.15ms, the voltages at connection bus and at the HVAC wind farm increase quasi-instantaneously to 0.8 p.u. The voltages stabilize after 2 seconds.

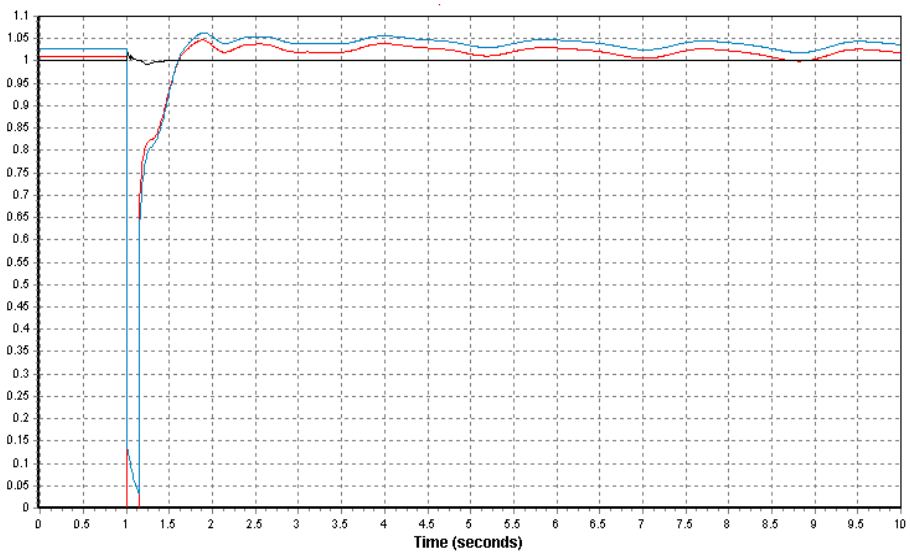

Figure 8-50: Voltage at offshore HVDC bus (black), offshore HVAC bus (blue) and onshore bus (red) [p.u]

The frequencies at the connection busbar and at the HVAC wind farm behave like with configuration 1. There is a peak in the frequencies during the fault. After clearance of the fault, they stabilize at their reference values. The HVDC wind farm frequency behaves as with the configuration 2. The power transmission in the DC line is stopped during the fault as it can be seen on the plot of the DC losses.

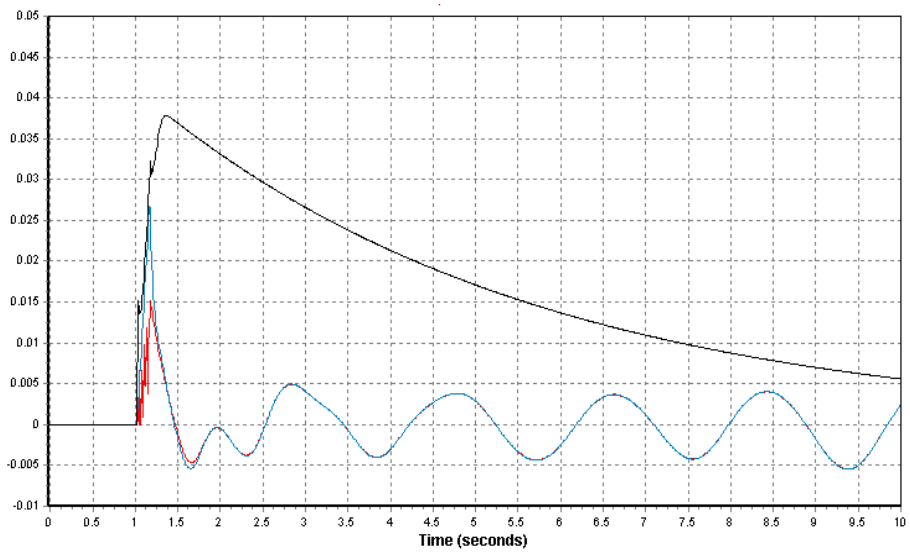

Figure 8-51: Frequency deviation at offshore HVDC bus (black), offshore HVAC bus (blue) and onshore bus (red)) [p.u]

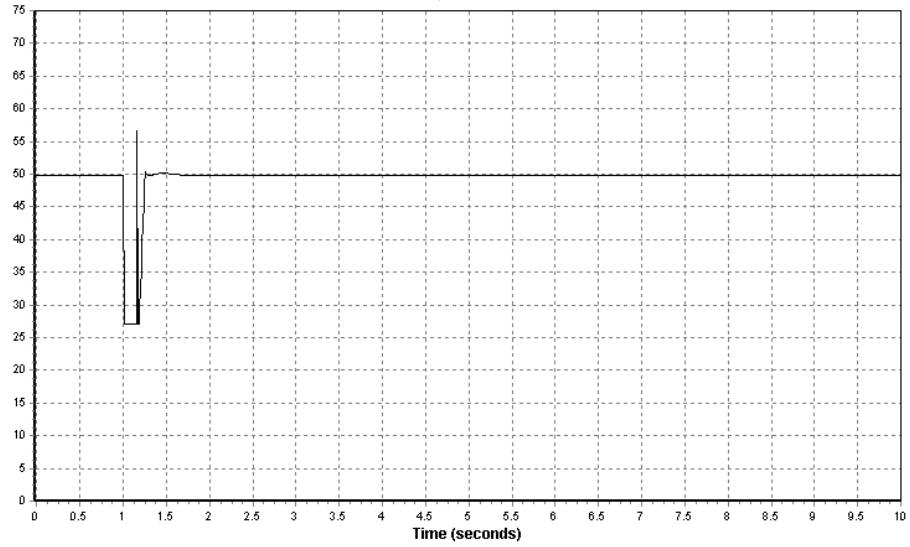

Figure 8-52: Losses on the DC line [MW]

Contrarily to the case with only a HVDC transmission system, the system remains stable after the fault. Indeed, the HVAC wind farm contributes to the short-circuit power. Then the contribution of the bus 5600 is less important which permits to this last one to regain equilibrium after the fault clearance.

8.10.2. FAULT 2

A 150ms three-phase short-circuit is applied on the bus 5603 at the time t=1s. This bus is a neighbour bus of the connection bus. The voltages and frequencies behave like with the configuration 1 and 2. The conclusions and comments made in part 8.6.2 and in part 8.8.2, are the same for this simulation.

8.10.3. FAULT 3

A 150ms three-phase short-circuit is applied on the line between the connection bus 5600 and its neighbour bus 5603 at the time t=1s. After the clearance of the fault the line is disconnected. The dynamic behaviour of the system is the same as for the fault 1. The conclusions and comments made in part 8.10.1, can be applied to this simulation. Contrarily to the case with only a HVDC transmission, the system regains its stability after the fault.

8.10.4. FAULT 4

8.10.4.1 *TYPE A*

The HVDC wind farm and the rest of the system are independent. When a fault occurs on the HVDC wind farm busbar, there are no consequences on the rest of the system. The consequences of this fault are only on the HVDC wind farm independently of the connection point. Then the conclusions made on part 8.9.4.1 can be applied to this simulation.

8.10.4.2 *TYPE B*

A 150ms three-phase short-circuit is applied at the time t=1s on the bus 1200 which is the HVAC wind farm busbar. The voltage at the HVAC wind farm busbar drops to zero and the voltage at the connection busbar is reduced to 0.5p.u. The HVDC wind farm voltage is not affected by the fault.

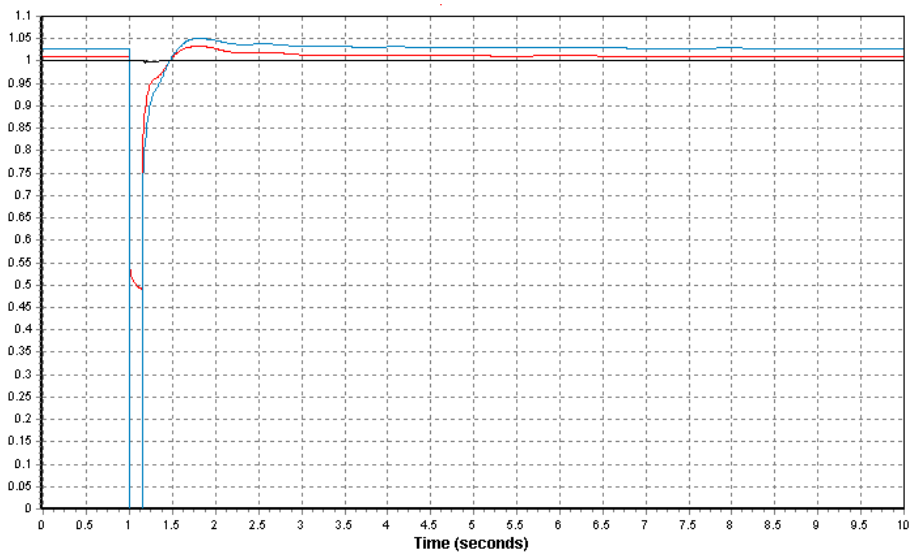

Figure 8-53: Voltage at offshore HVDC bus (black), offshore HVAC bus (blue) and onshore bus (red) [p.u]

The contribution of the connection busbar is less important than if the HVAC was alone as in configuration 1. The HVDC wind farm contributes to the short-circuit power which reduces the contribution of the connection bus. As it can be seen on the DC losses plot, the power transmission in the DC line is reduced but not stopped during the fault.

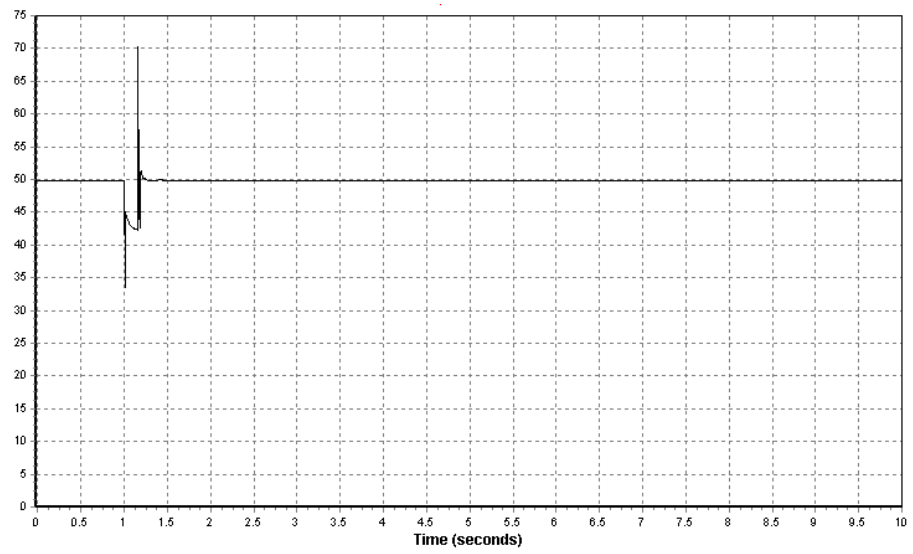

Figure 8-54: Losses on the DC line [MW]

8.10.4.3 *TYPE C*

At the time t=1s, two 150ms three-phases short-circuits occurs on both wind farms at the same time. The results of this simulation are the addition of the results showed for the fault 4 type A and for the fault 4 type B. The same comments and conclusions as in part 8.9.4.3, can be made.

8.11 CONFIGURATION 4, CONNECTION BUS 6000

In this case, the simulations are made with the configuration 4 connected to the grid at the bus 6000. The configuration 4 represents two 500MW wind farms connected to the offshore converter of a HVDC transmission via HVAC transmission. The onshore converter is connected to the grid. The two farms will be called "wind farm 1" and "wind farm 2". The results are similar to the results with configuration 2, so the same conclusion can be made. The main differences are on the offshore side.

8.11.1. FAULT 1

A 150ms three-phase short-circuit is applied on the connection bus (bus 6000) at the time t=1s. The voltage at the connection busbar becomes null during the fault. After the clearance the voltage drops instantaneously to 0.75 p.u and recovers its stability after 1.5 seconds. The offshore voltage is almost not affected by the fault onshore. This is explained by the independence between the offshore and the onshore.

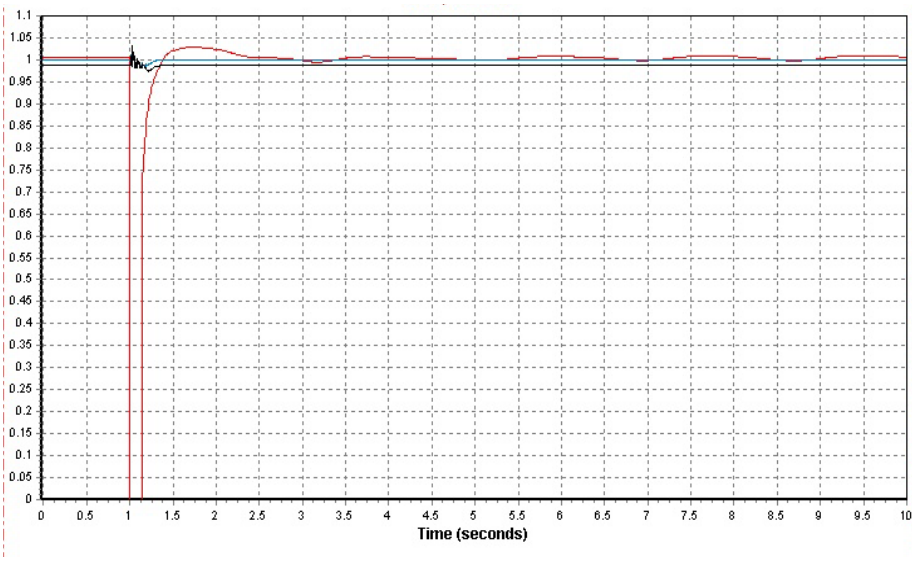

Figure 8-55: Voltage at offshore HVDC bus (black), at one of offshore wind farm bus (blue) and at the connection bus (red) [p.u]

As it can be seen on the DC losses plot, during the fault the transmitted power become null which leads to the increase of the offshore frequency for the same reasons explained in part 8.7.1.

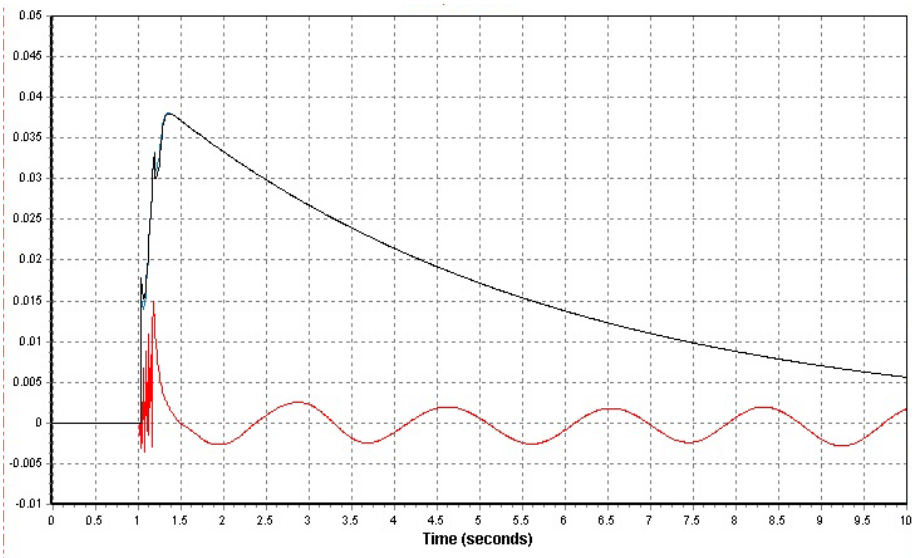

Figure 8-56: Frequency deviation at offshore HVDC bus (black), at one of offshore wind farm bus (blue) and at the connection bus (red) [p.u]

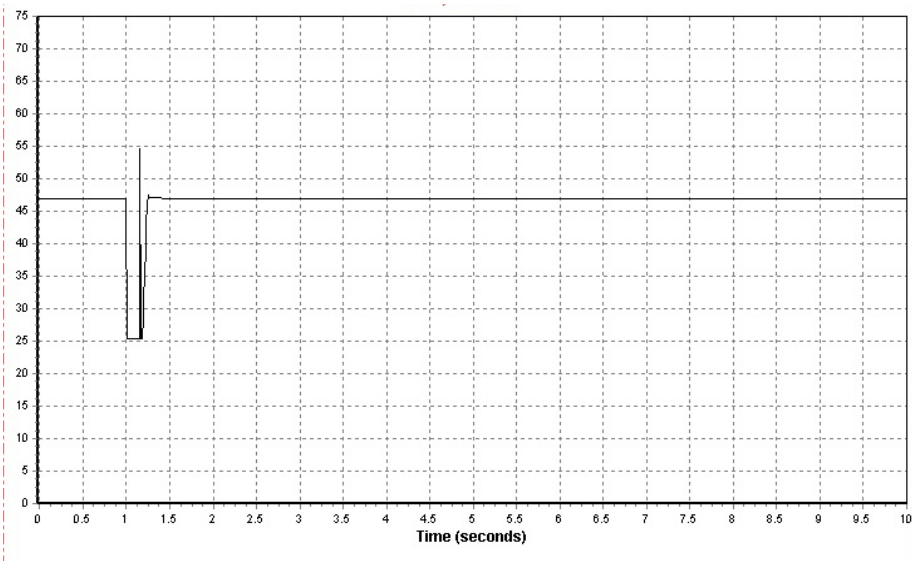

Figure 8-57: Losses on the DC line [MW]

The offshore converter plays the rule of SVC during the fault and produces reactive power in order to regulate the offshore voltage.

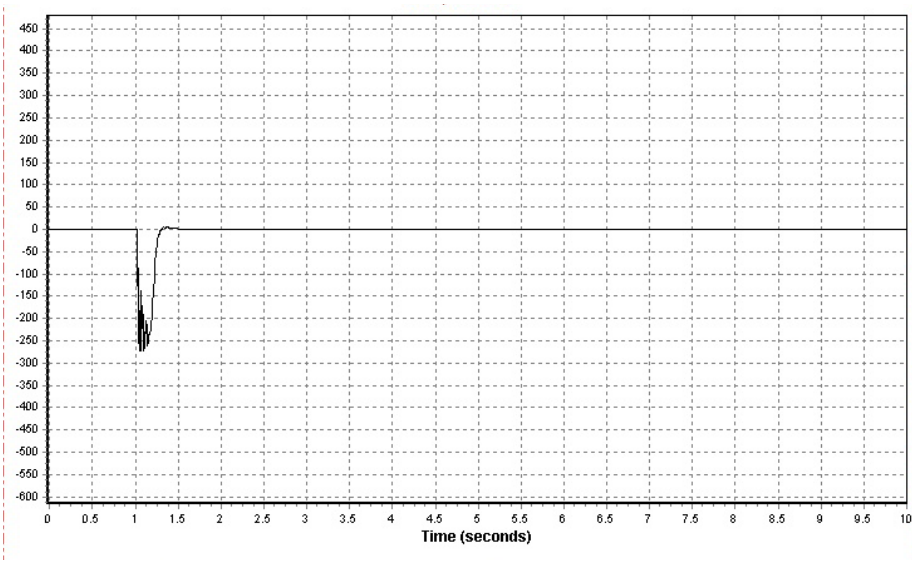

Figure 8-58: Reactive power from the offshore converter [MVar]

8.11.2. FAULT 2

A 150ms three-phase short-circuit is applied on the bus 5400 at the time t=1s. This bus is a neighbour bus of the connection bus. During the fault, the voltage at the connection bus drops to 0.3 p.u. The voltage at the HVDC wind farm still remains unchanged during the fault. The behaviour of the system is the same as described in the 8.7.2.

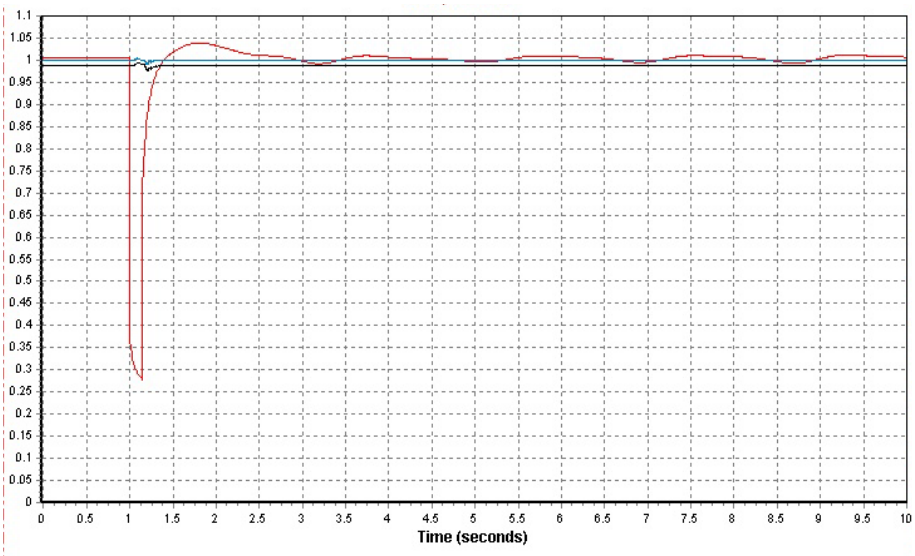

Figure 8-59: Voltage at offshore HVDC bus (black), at one of offshore wind farm bus (blue) and at the connection bus (red) [p.u]

8.11.3. FAULT 3

A 150ms three-phase short-circuit is applied on the line between the connection bus 6000 and its neighbour bus 5400 at the time t=1s. After the clearance of the fault the line is disconnected. The dynamic behaviour of the system is the same as for the fault 1. The conclusions and comments made in part 8.11.1 can be applied to this simulation.

8.12 CONFIGURATION 4, CONNECTION BUS 5600

8.12.1. FAULT 1

A 150ms three-phase short-circuit is applied on the connection bus (bus 5600) at the time t=1s. The voltage at the connection busbar becomes null during the fault. After the clearance the voltage drops instantaneously to 0.85 p.u and recovers its stability after 1.5 seconds. The offshore voltage is almost not affected by the fault onshore. This is explained by the independence between the offshore and the onshore. However, the small disturbance on the voltage is more important than for the case with the connection bus 6000. The general dynamic behaviour is the same as for the connection point at the bus 6000. Contrarily to configuration 2, configuration 4 is stable after the fault.

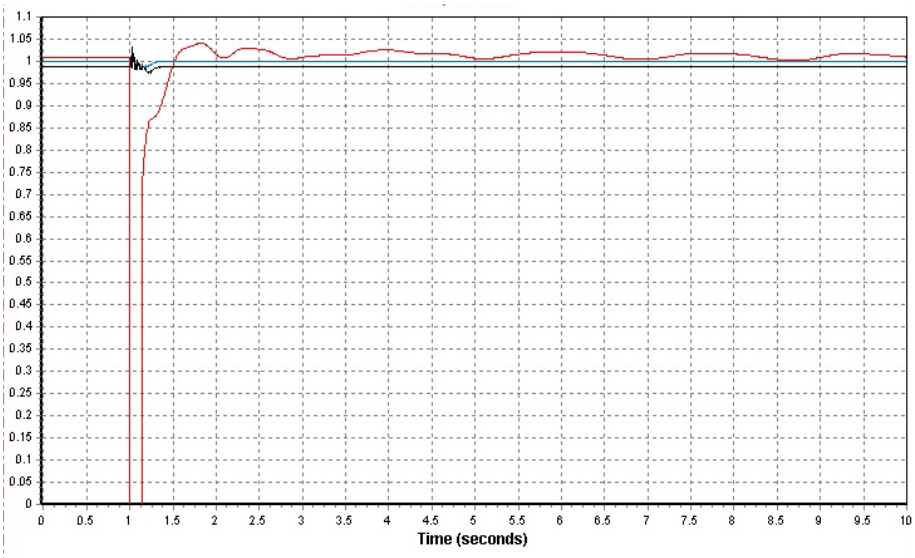

Figure 8-60: Voltage at offshore HVDC bus (black), at one of offshore wind farm bus (blue) and at the connection bus (red) [p.u]

One difference can be noticed in the production of reactive power of the onshore converter. The bus 5600 is "weaker" and more isolated than the bus 6000. Then, in order to regulate the voltage, its demand of reactive power from the converter is more important. The converter reaches its limits of production.

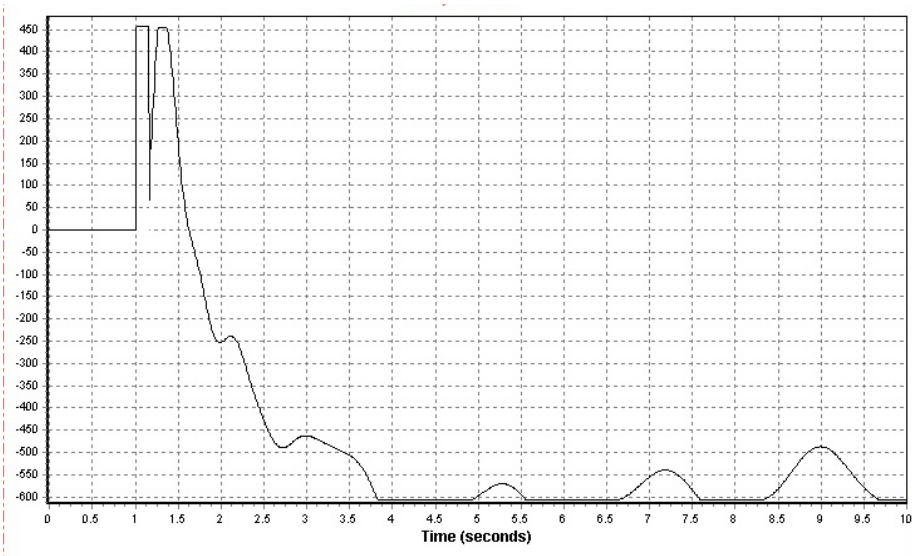

Figure 8-61: Reactive power from the onshore converter [MVar]

8.12.2. FAULT 2

A 150ms three-phase short-circuit is applied on the bus 5400 at the time t=1s. This bus is a neighbour bus of the connection bus. The dynamic behaviour is very similar to the case with the configuration 2 presented in part 8.8.2.

8.12.3. FAULT 3

A 150ms three-phase short-circuit is applied on the line between the connection bus 5600 and its neighbour bus 5603 at the time t=1s. After the clearance of the fault the line is disconnected. The dynamic behaviour of the system is the same as for the fault 1. The conclusions and comments made in part 8.11.1 can be applied to this simulation.

8.13 CONFIGURATION 4, FAULT 4

As said before, when a fault is applied on the offshore side, the system becomes instable and PSS^{TM}E can not do the simulations. In this configuration, the contribution to short-circuit power comes only from the wind generators. Furthermore, the only source of reactive power in the offshore system is the HVDC converter. When a short-circuit happens, the voltage offshore falls and the converter will produce reactive power in order to regulate this voltage. The problem is that the production of the converter is limited, and then the voltage can not regain its reference value, which causes the collapse of the offshore system. A solution of this problem is to install a SVC at the offshore station in order to produce the necessary reactive power offshore. The following simulations have been made with the configuration 4 and a 400MVar SVC installed at the offshore station.

As explained before, the onshore and the offshore sides of the system are independent and the onshore system is not affected by the offshore fault. Then, the results are the same for the connection bus 6000 and 5600. Only the results for the bus 6000 are presented. The plots for the bus 5600 can be found on Appendix F.

8.13.1. TYPE A

A 150ms three-phase short-circuit is applied at the time t=1s on the wind farm bus 1100. During the fault, the voltage at the wind farm 1 becomes null. The voltages at the wind farm and at the offshore converter fall to 0.15p.u and 0.1p.u respectively. After the clearance of the fault, the three voltages offshore behave in the same way. The voltages increase instantaneously to 0.65p.u. Then the voltages reach the value of 0.9p.u in 350ms. Then, oscillations appear on the signals. At t=2s, the voltages stabilize at their reference values. The voltage onshore is not affected by the fault and stays constant. The behaviour of this configuration during the fault is very similar to the behaviour of the configuration 2 presented in the part 8.7.4 and the same comments can be made. The main difference is that the stabilization of the system is quicker.

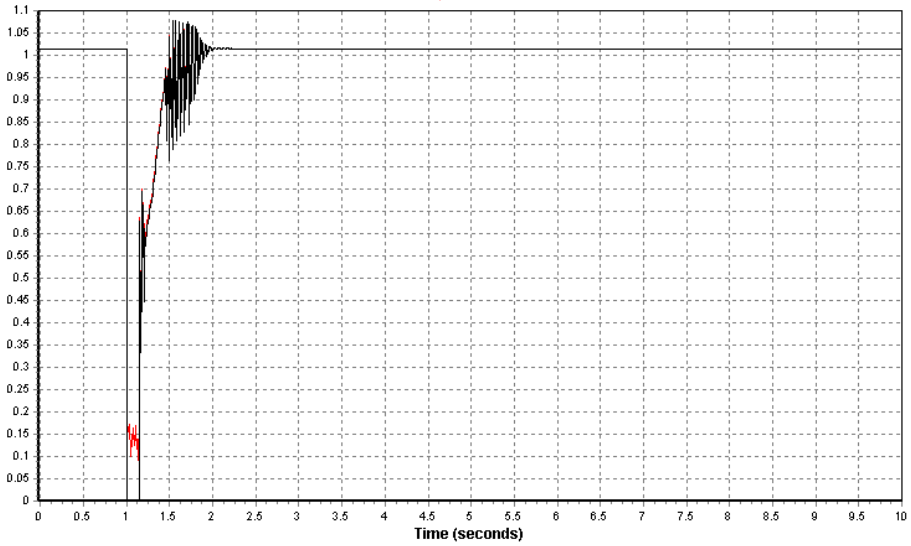

Figure 8-62: Voltage at the bus of the wind farm 1 (black) and at bus of the wind farm 2 (red) [p.u]

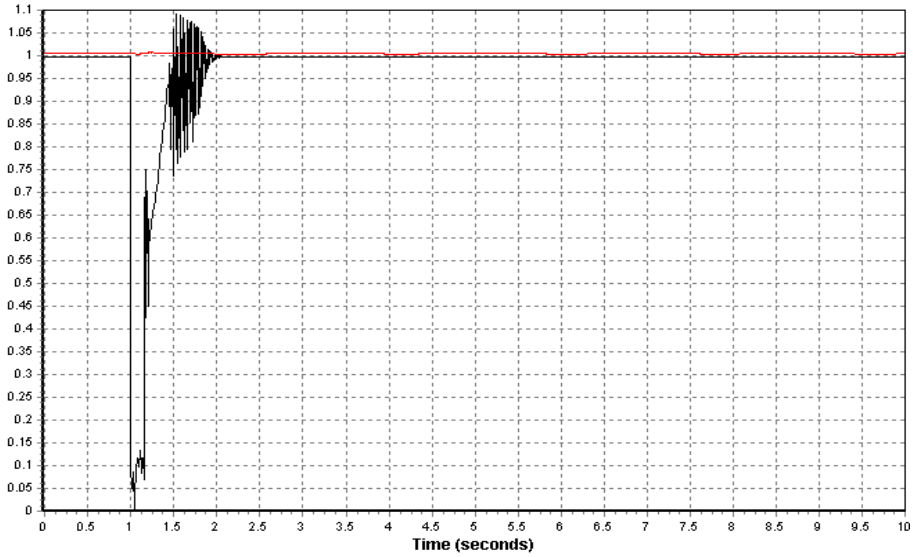

Figure 8-63: Voltage at the offshore converter (black) and at the connection point (red) [p.u]

During the fault, the offshore frequencies reach a peak at 62 Hz. At the clearance of the fault, the frequencies decrease to the value 52Hz and then to their reference value. The onshore frequency is not affected by the fault.

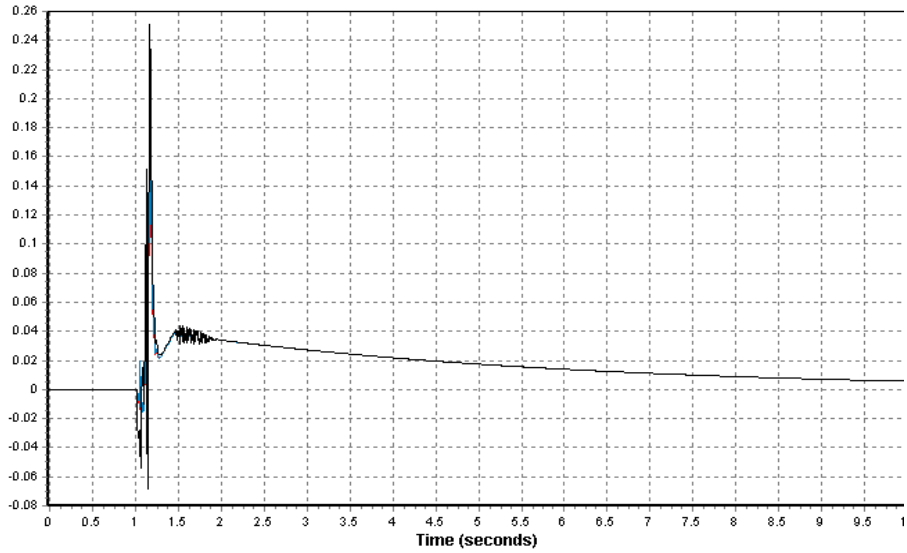

Figure 8-64: Frequency deviation at the wind farm 1 (blue), at the wind farm 2 (red) and at the offshore converter (black) [p.u]

The SVC produces large amount of reactive power after the clearance of the fault in order to regulate the voltage on the offshore side of the system.

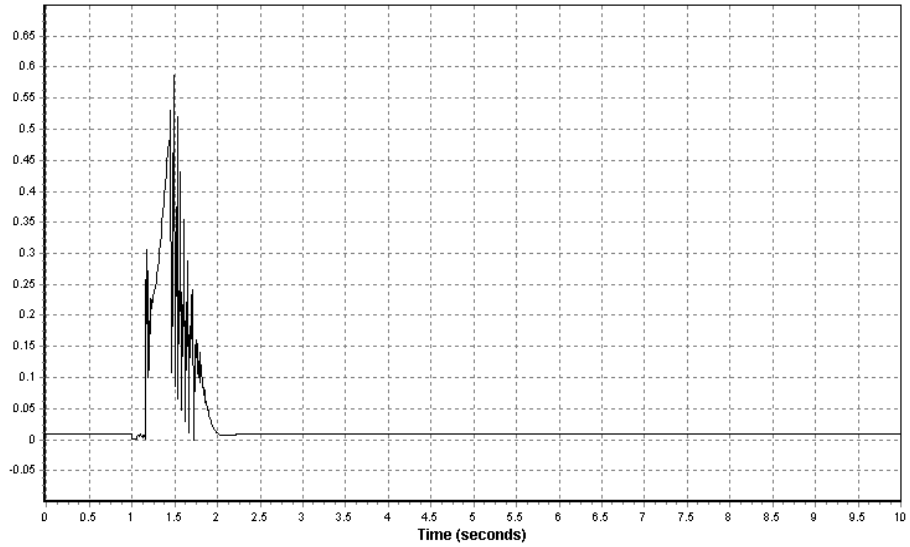

Figure 8-65: Reactive power from the SVC [p.u]

The system is quicker than with the configuration 2. This is explained by the large amount of reactive power that the SVC produces.

8.13.2. TYPE B

At the time t=1s, two 150ms three-phases short-circuits occurs on both wind farms at the same time. This kind of fault is not realistic, but it illustrates the loss of production from the wind farms. The results are the same as the previous case. The difference is that faults occur on both wind farms busses. Then, the behaviour of the two wind generator is the same.

9 DISCUSSION

Different transmission systems and configurations for the integration of large wind farm have been investigated on the previous chapter. However the simulation results made with the equivalent grid model can not be used directly to the reality. Indeed both grid, wind farm and transmission systems are strongly simplified. Nevertheless, the simulations results can be used as a first approach for the integration of a large wind farm and to have an idea of the probable behaviour of the Norwegian power system.

The first case used a HVAC transmission link to connect the wind farm to the grid. The simulations show that the grid code is respected and both the voltage and the frequency behave as required. The stability of the system is affected by the different disturbances as excepted. It can be noticed that the system is faster to recover its stability when the wind farm is connected in the bus 6000. The bus 5600 is less strong than the bus 6000 which can cause problems with the power factor and the compensation equipments.

The second case used a HVDC transmission link to connect the wind farm to the grid. When the wind farm is connected to the bus 6000, the system behaves as expected, and the requirements of the grid code are respected. HVDC onshore converter contributes to the onshore voltage recovery. The HVDC transmission creates independency between the grid and the wind farm which ensures a faster and cleaner behaviour in case of disturbance. In the opposite, due to the weakness and the isolate location of the bus 5600, the system becomes instable when the wind farm is connected to this bus. More studies and a more detailed model could permit to find a solution to this problem.

The third configuration is a combination of a HVDC and HVAC transmission link. In the case of an offshore wind farm near the coast, this configuration can be used if a second offshore wind farm further from the shore is installed in the same area. By the adding of the HVDC system, the behaviours of the “HVAC” wind farm and the grid are quicker and cleaner for the different connection busbars. However in the case of a short-circuit in the “HVDC” wind farm side, the requirements of the grid code are not respected. This point can be more investigated with a more accurate HVDC transmission link model.

The last configuration is a hybrid system. It is composed of two offshore HVAC transmission systems connected to two wind farms and the offshore converter of a HVDC transmission system. Due to the size of the different equipments, the development of the different offshore substations is not feasible today. However in the future, an oil platform can be used to install the different offshore equipments and to create an offshore wind farms network.

As for the second configuration, the fourth configuration permits to create an independency of the offshore and onshore side. The behaviour of the power system is faster and cleaner regarding the different disturbance. However in the case of an offshore fault, the need of reactive power is too important for the only HVDC converter which causes the collapse of the system. With the adding of an offshore SVC, the behaviour is better, but more studies will permit to solve this problem.

10 CONCLUSION AND FURTHER WORK

The Norwegian demand in electrical power increases in the last years and so, more power have to be generated for fulfilling this demand. But, in order to achieve its goal of no CO2 emissions in 2050, Norway has to consider new types of generation. Wind power generation seems to be one of the best alternatives. However, a large and efficient penetration of wind power in the Norwegian production system is possible only through the integration of a large capacity of offshore wind generation.

An advantage of Norway for offshore wind power is its long coasts on the North Sea where winds are powerful and stable. It gives to Norway a great offshore wind potential. Nevertheless, the depth of the sea is very deep near the Norwegian coast and it is very difficult to exploit this potential with the current technologies. Floating windmills are the most indicated solution for this situation. Several promising concepts are under development and should be operational by 2015.

With floating windmills it is also possible to install the offshore wind farms further from the coast, where the wind conditions are better. This leads to another challenge for offshore wind power, the connection to the grid. Today, the main type of connection for offshore wind power is HVAC transmission which is a well-known and cost efficient technology. However, this type of transmission shows its limits with distances superior to 75km. HVAC cables create reactive power and longer are the cables, larger is the created reactive power. The use of HVDC and particularly VSC-HVDC is the solution to this problem. The current technology permits the transmission of large power, up to 1000MW.

In this thesis, the integration of the integration of a 1000MW offshore wind farm in the Norwegian power system has been studied. Four different configurations of transmission systems have been investigated: one 50km HVAC transmission system, one 200km HVDC transmission system and two hybrid transmission configurations combining HVAC and HVDC. Regarding to the probable areas where offshore wind farms will be connected in the future, two connection points have been selected. One is situated in the region of Bergen, in the West of Norway and the other one is situated in the South of Norway, between Stavanger and Kristiansand.

Dynamics simulations have been made for the four configurations connected at the two different busses. Disturbances have been applied to the system in order to look at the impact of the offshore wind power integration on the dynamic behaviour of the system. Two disturbances have been applied in the neighbourhood of the connection bus, one has been applied to the connection but itself, and one has been applied to the offshore bus.

Firstly, the results of these simulations show that the connection of an offshore wind farms near the west coast and the south coast of Norway is possible with HVAC. The requirements of the Statnett are completely fulfilled for both connection points and the dynamic behaviour of the system is not changed with the integration of the wind farm. However, it has to be emphasized that the need of compensation equipments for reactive power is very important with HVAC.

Then, simulations with the HVDC transmission system at the west coast connection point show that the integration of an offshore wind farm with this kind of transmission is possible regarding the requirements of Statnett. The HVDC link creates an independency of the offshore and the onshore side. This means that in case of disturbance on one side, the other side is not affected. Furthermore, in case of onshore disturbance, the onshore HVDC converter contributes to the voltage stability of the grid, and the recovery of the system is quicker than for the HVAC case.

In the case of the south coast connection point and the HVDC transmission system, the conclusions are different. The dynamic behaviour of the system during and after the fault meets

expectations. But after 3 seconds, oscillations appear in the frequency and in the voltage. The oscillations are not damped which leads to the instability in the system. However this instability can be explained by the grid model used during the simulations and the isolation of the connection bus.

The third configuration is a combination of a HVAC transmission system and a HVDC transmission system connected to the same point. The results of the simulations with this configuration connected to the west coast and to the south coast show that the requirements of Statnett are fulfilled. The system is more stable than in the first case due to the introduction of the HVDC link. In addition to the SVC, the onshore HVDC converter contributes to the voltage stability when a fault occurs on the onshore. It gives to the system a quicker recovery than with only a HVAC transmission link. Furthermore, when a fault occurs on the wind farm connected to the HVDC link, the other wind farm and the grid are not affected by the fault because of the independency of the two sides created by the HVDC link. However, the recovery of the wind farm connected to the HVDC transmission system is long and the grid code requirements are not respected.

The last configuration represents two offshore wind farm connected to an offshore HVDC converter with two 50km HVAC transmission systems. The 200km HVDC transmission is then connected to the grid. The results, for each connection point, are the same as for the configuration 2 except for a fault on the offshore side because of the limited reactive power production capacities of the HVDC converter. This problem has been solved by the installation of compensation equipment offshore. This configuration could be used for the creation of an offshore wind farm network where the offshore station could be installed on a oil platform for example.

The results of the different simulations lead to the conclusion that the integration of a large offshore wind farm in the Norwegian power grid is possible and respect the requirement of Statnett. Compare to the south coast, the west coast of Norway is a better place for the connection of the wind farm. Furthermore the HVDC solution for the transmission system is preferable because of its better performances.

It should be emphasized that the models used in these simulations are strongly simplified, so the results of this study reflect the general behaviour of the system. Further work can be done in the continuity of this thesis. By using more developed models for the grid, the wind farm and the transmission system, more accurate results could be found. It also could be interesting to investigate a configuration with a multiterminal HVDC. With this technology, a large offshore wind farm network could be created. A comparison between the different HVDC available on the market (HVDC Light and HVDC PLUS) can also be interesting.

REFERENCES

[1] D. McAllister,*Electrical Cables handbook* , D.C. Cables, Chapter 40, page 546, 1984.
[2] ABB website: http://www.abb.com/industries/us/9AAC30100013.aspx
[3] D. McAllister,*Electrical Cables handbook* , Self-contained Oil-filled Cables, Chapter 32, page 444, 1984.
[4] R. L. Hendriks, J. H. Den Boon, G. C. Paap, and W. L. Kling, *"Connecting Offshore Wind Farms to (VSC-) HVDC Interconnectors",* Nordic Wind Power Conference, Espoo, Finland, May 2006.
[5] M. P. Bahrman, *"HVDC Transmission Overview"*, 21-24 April 2008.
[6] *"High Voltage Direct Current Transmission – Proven Technology for Power Exchange"* Siemens Document.
[7] S. Pittet, *"Modélisation physique d'un transistor de puissance IGBT—traînée en tension à l'enclenchement"* Ph.D. dissertation, Swiss Federal Inst. Technol., Lausanne, 2005.
[8] M. Ikonen, O. Laakkonnen, M. Kettunen, "*Two-level and Three-level converter comparison in Wind Power application"*, Lappeenranta, Finland, 2005.
[9] Siemens Website: https://www.energy-portal.siemens.com
[10] M. Haeusler, H. Koelsh. V. Ramaswami, *"Design aspects of UHVDC Equipment"*, Siemens, Erlangen, Germany.
[11]R. Rudervall, J.P. Charpentier, R. Sharma, *"High Voltage Direct Current (HVDC) Transmission Systems Technology Review Paper"*.
[12]Mohan N., Undeland T. M., Robbins W.P., *"Power electronics-Converters, Applications, and Design",*2003, John Wiley &Sons Icn.
[13] X.I. Koutiva, T.D. Vrionis, N.A. Vovos, G.B. Giannakopoulos, "*Optimal Integration of an Offshore Wind Farm to a Weak AC Grid",* April 2006.
[14] R. C. Dorf, *"The electrical Engineering Handbook"*, Energy, Section VI - Transmission, Chapter 58 – page 1242 – 1993.
[15] Nordel annual report 2007, www.nordel.org
[16] NVE 2005, "*Kraftbalansen i Norge mot 2020 – oppdaterte anslag per juni 2005",* www.nve.no
[17] Danish Wind Insustry Association, www.windpower.org
[18] J.O. Tande, "*Offshore Wind Energy – Some Thoughts for the Future",* Sintef, April 2008
[19] NVE, "*Norwegian Wind Atlas",* www.nve.no/vindatlas.
[20] J.O. Tande, "*Impacts of integration wind power in the Norwegian"*, SINTEF Energy Research, April 2006.
[21] J.O. Tande, K.O. Vogstad, "*Operational implications of Wind Power in a hydro based power system",* EWEC'99, March 1999, Nice, France.
[22] EWEA (European Wind Energy Association), "*Wind Power- the Facts"*, www.ewea.org.
[23] WWEA (World Wind Energy Association), www.wwindea.org.
[24] E.L. Peterson, N.G. Mortensen, L. Landberg, J. Høsjtrup, H.P. Franck, "*Wind Power Meteorology",* Risøe National Laboratory, Denmark, December 1997.
[25]M.R. Patel, *"Wind and Solar Wind Power- Design, Analysis, and Operation – Second Edition",* Taylor & Francis Group.
[26] Danish Wind Power Association, www.windpower.org/en/tour.htm
[27] EWEA, *"Large scale integration of wind energy into the European power supply: analysis, issues and recommendation"s*, December 2005, www.ewea.org.
[28]EWEA, "*Delivering Offshore Wind Power in Europe"*, 2007, www.ewea.org
[29] www.offshorewindenergy.org
[30]Global Wind Energy Council, www.gwec.net
[31] DENA, Deutsch Energie-agentur. www.offshore-wind.de
[32] Hersleth P., "*1000MW i 2012"*, Oslo, June 2007.
[33] NVE, www.nve.no
[34] B.W. Byrne, G.T. Houlsby, "*Assessing Novel Foundation Options for Offshore Wind Turbines",* Oxford University, UK.

[35] P. Sclavounos, S. Butterfield, W. Musial, and J. Jonkman "*Engineering Challenges for Floating Offshore Wind Turbines",* Copenhagen, Denmark, October 2005
[36] StatoilHydro website, www.statoilhydro.com
[37] National Renewable Energy Laboratory, www.nrel.gov
[38] Annual statistics 2007, www.nordel.org.
[39]Nordel Website, www.nordel.org
[40] Nordic grid code 2007, www.nordel.org
[41] R. K. Mork, T. Langeland, "*The Norwegian TSO Statnett, Information and Views"*, Statnett, October 2008.
[42] Statnett, *FIKS* – "*Funksjonskrav i kraftsystemet",* www.statnett.no.
[43] Midwest Reliability Organisation, "*Model Building Manuel - Addendum – Wind Generator"*, October 2007, Roseville, USA.
[44]PSS^{TM}E user manuel
[45]ABB, "*It's Time to Connect"*, www.abb.com
[46]IEEE/CIGRE Work Group on Stability Terms and Definitions, "*Definition and Classification of Power System Stability",* May 2004.

APPENDIX A: SHORT-CIRCUIT POWER

SHORT-CIRCUIT POWER FOR BUS 6000:

```
                                  <-SCMVA-> <-Sym I''k rms--> <-ip(B)-> <-ip(C)-> <-DC Ib-> <Sym Ib-> <Asym Ib>
                                              /I/    AN(I)      /I/       /I/       /I/       /I/       /I/
X---------- BUS ----------X          P.U.       P.U.     DEG       P.U.      P.U.      P.U.      P.U.      P.U.
  6000 [WEST300     300.00] 3PH      26.82   26.8212   -87.72   71.6820   71.7209    9.8282  218.4014  218.3041

THEVENIN IMPEDANCE (PU), X/R
Z+: 0.001629+j0.040980, 25.149437

-------------------------------------------------------------------------------------------------------------------|
      *** FAULTED BUS IS:   6000 [WEST300     300.00] ***   0 LEVELS AWAY ***
AT BUS   6000 [WEST300     300.00] AREA   60
    (PU) VA:   0.0000+J 0.0000     VB:   0.0000+J 0.0000     VC:   0.0000+J 0.0000

                                          X-------------------------THREE PHASE FAULT-------------------------X
X--------- FROM ----------X AREA CKT    I     RE(IA)   IM(IA)   RE(IB)   IM(IB)   RE(IC)   IM(IC)
MACHINE 1                               PU    3.3401  -3.6561  -4.8364  -1.0645   1.4963   4.7207
  5400 [CNTR3-A     300.00]   54 1      PU    0.3873  -5.1315  -4.6377   2.2303   4.2504   2.9012
  5600 [SOUTH3A     300.00]   56 1      PU    0.1294  -1.8210  -1.6418   0.7984   1.5123   1.0226
  6001 [WEST400     420.00]   60 1      PU    0.3476 -12.0207 -10.5840   5.7093  10.2364   6.3114
  6100 [NWEST3      300.00]   61 1      PU    0.2129  -3.2636  -2.9328   1.4474   2.7199   1.8162
INITIAL SYM. S.C. CURRENT(I''k)(RMS)   P.U.   1.0656 -26.8000 -23.7423  12.4772  22.6767  14.3229
                     I''k (MAG/ANG)    P.U.  26.8212   -87.72  26.8212   152.28  26.8212    32.28

-------------------------------------------------------------------------------------------------------------------
```

SHORT-CIRCUIT POWER FOR BUS 5600:

```
                                  <-SCMVA-> <-Sym I''k rms--> <-ip(B)-> <-ip(C)-> <-DC Ib-> <Sym Ib-> <Asym Ib>
                                              /I/    AN(I)      /I/       /I/       /I/       /I/       /I/
X---------- BUS ----------X          P.U.       P.U.     DEG       P.U.      P.U.      P.U.      P.U.      P.U.
  5600 [SOUTH3A     300.00] 3PH      18.15   18.1490   -88.28   49.1618   49.2011   12.6136  213.8027  213.6021

THEVENIN IMPEDANCE (PU), X/R
Z+: 0.001823+j0.060582, 33.228485

-------------------------------------------------------------------------------------------------------------------
      *** FAULTED BUS IS:   5600 [SOUTH3A     300.00] ***   0 LEVELS AWAY ***
AT BUS   5600 [SOUTH3A     300.00] AREA   56
    (PU) VA:   0.0000+J 0.0000     VB:   0.0000+J 0.0000     VC:   0.0000+J 0.0000

                                          X-------------------------THREE PHASE FAULT-------------------------X
X--------- FROM ----------X AREA CKT    I     RE(IA)   IM(IA)   RE(IB)   IM(IB)   RE(IC)   IM(IC)
MACHINE 1                               PU    6.5561  -8.8883 -10.9756  -1.2336   4.4195  10.1219
  5601 [SOUTH4A     420.00]   56 1      PU    0.2505  -5.9255  -5.2568   2.7458   5.0064   3.1796
  5603 [SOUTH3B     300.00]   56 1      PU    0.1626  -2.2223  -2.0059   0.9704   1.8433   1.2520
  6000 [WEST300     300.00]   60 1      PU    0.1966  -2.2372  -2.0358   0.9483   1.8392   1.2889
INITIAL SYM. S.C. CURRENT(I''k)(RMS)   P.U.   0.5459 -18.1408 -15.9834   8.5976  15.4374   9.5432
                     I''k (MAG/ANG)    P.U.  18.1490   -88.28  18.1490   151.72  18.1490    31.72

-------------------------------------------------------------------------------------------------------------------
```

SHORT-CIRCUIT POWER FOR BUS 5400:

```
                                  <-SCMVA-> <-Sym I''k rms--> <-ip(B)-> <-ip(C)-> <-DC Ib-> <Sym Ib-> <Asym Ib>
                                              /I/    AN(I)      /I/       /I/       /I/       /I/       /I/
X---------- BUS ----------X          P.U.       P.U.     DEG       P.U.      P.U.      P.U.      P.U.      P.U.
  5400 [CNTR3-A     300.00] 3PH      32.24   32.2449   -88.04   86.8405   86.8932   16.7560  215.6259  215.3585

THEVENIN IMPEDANCE (PU), X/R
Z+: 0.001167+j0.034094, 29.211594

-------------------------------------------------------------------------------------------------------------------
      *** FAULTED BUS IS:   5400 [CNTR3-A     300.00] ***   0 LEVELS AWAY ***
AT BUS   5400 [CNTR3-A     300.00] AREA   54
    (PU) VA:   0.0000+J 0.0000     VB:   0.0000+J 0.0000     VC:   0.0000+J 0.0000

                                          X-------------------------THREE PHASE FAULT-------------------------X
X--------- FROM ----------X AREA CKT    I     RE(IA)   IM(IA)   RE(IB)   IM(IB)   RE(IC)   IM(IC)
MACHINE 1                               PU    7.3278  -9.6848 -12.0512  -1.5037   4.7233  11.1885
  5401 [CNTR4-A     420.00]   54 1      PU    0.0476  -2.9581  -2.5856   1.4379   2.5380   1.5203
  5402 [CNTR4-B     420.00]   54 1      PU    0.1499  -4.1612  -3.6787   1.9508   3.5288   2.2104
  5500 [CNTR3-B     300.00]   55 1      PU    0.3681  -5.6156  -5.0473   2.4891   4.6793   3.1266
  6000 [WEST300     300.00]   60 1      PU    0.2837  -3.9623  -3.5733   1.7355   3.2896   2.2268
  6100 [NWEST3      300.00]   61 1      PU    0.2555  -3.7126  -3.3430   1.6350   3.0874   2.0776
INITIAL SYM. S.C. CURRENT(I''k)(RMS)   P.U.   1.1032 -32.2260 -28.4601  15.1576  27.3569  17.0684
                     I''k (MAG/ANG)    P.U.  32.2449   -88.04  32.2449   151.96  32.2449    31.96

-------------------------------------------------------------------------------------------------------------------
```

SHORT-CIRCUIT POWER FOR BUS 5603:

	<-SCMVA->	<-Sym I''k rms--> /I/	AN(I)	<-ip(B)-> /I/	<-ip(C)-> /I/	<-DC Ib-> /I/	<Sym Ib-> /I/	<Asym Ib> /I/
X---------- BUS ----------X	P.U.	P.U.	DEG	P.U.	P.U.	P.U.	P.U.	P.U.
5603 [SOUTH3B 300.00] 3PH	8.98	8.9786	-86.20	23.1448	23.1519	0.7316	216.8946	216.8939

THEVENIN IMPEDANCE (PU), X/R
Z+: 0.008129+j0.122243, 15.037429

*** FAULTED BUS IS: 5603 [SOUTH3B 300.00] *** 0 LEVELS AWAY ***
AT BUS 5603 [SOUTH3B 300.00] AREA 56
(PU) VA: 0.0000+J 0.0000 VB: 0.0000+J 0.0000 VC: 0.0000+J 0.0000

				X----------THREE PHASE FAULT----------X					
X--------- FROM ----------X	AREA	CKT	I	RE(IA)	IM(IA)	RE(IB)	IM(IB)	RE(IC)	IM(IC)
5500 [CNTR3-B 300.00]	55	1	PU	0.1699	-2.0725	-1.8798	0.8891	1.7098	1.1834
5600 [SOUTH3A 300.00]	56	1	PU	0.2585	-3.5987	-3.2458	1.5755	2.9873	2.0232
5602 [SOUTH4B 420.00]	56	1	PU	0.1362	-2.0983	-1.8852	0.9312	1.7491	1.1671
INITIAL SYM. S.C. CURRENT(I''k)(RMS)			P.U.	0.5958	-8.9588	-8.0565	3.9635	7.4607	4.9954
I''k (MAG/ANG)			P.U.	8.9786	-86.20	8.9786	153.80	8.9786	33.80

APPENDIX B: ORIGINAL CASE

BUS DATA

```
    PTI INTERACTIVE POWER SYSTEM SIMULATOR--PSS(tm)E    THU, DEC 11 2008  14:04
REDUCED NORDEL POWER SYSTEM MODEL                                      BUS DATA
V 3.2, 12.08.97
                                    S H U N T S
  BUS# X-- NAME --X BASKV CODE LOADS FIXED SWITCHED  VOLT   ANGLE AREA
  3000 STCKH       420.00   2    2     0       0    1.00000   36.5   40
  3100 STRFN       420.00   2    1     0       0    0.97000   45.1   40
  3115 SV-N1       420.00   2    0     0       0    1.00000   72.5   40
  3200 KRLSK       420.00   1    1     0       0    0.94555    8.3   40
  3244 SV-M2       300.00   1    0     0       0    1.00079   34.1   40
  3245 SV-M1       420.00   2    1     0       0    1.00000   33.6   40
  3249 SV-N2       420.00   2    1     0       0    1.00000   71.1   40
  3300 SV-SW       420.00   3    1     0       0    1.00000    0.0   40
  3359 SV-W        420.00   2    1     0       0    1.00000   16.9   40
  3360 KONT_135    135.00   1    2     0       0    0.99475   16.5   40
  3701 SV-N2B      300.00   1    0     0       0    1.00605   73.9   40
  5100 EAST3       300.00   2    1     0       0    1.00000   23.4   51
  5101 EAST4-A     420.00   1    0     0       0    0.99390   22.5   51
  5102 EAST4-B     420.00   1    0     0       0    0.99973   25.5   51
  5103 EAST4-C     420.00   1    0     0       0    0.99785   26.0   51
  5111 SVCTERM      22.500  2    0     0       0    1.00000   22.5   51
  5112 SVCHIGH     420.00   1    0     0       0    0.99390   22.5   51
  5300 HDAL3       300.00   2    1     0       0    1.00000   37.0   53
  5301 HDAL4       420.00   1    0     0       0    1.00059   31.9   53
  5400 CNTR3-A     300.00   2    1     0       0    1.00700   29.8   54
  5401 CNTR4-A     420.00   1    0     0       0    0.99958   27.5   54
  5402 CNTR4-B     420.00   1    0     0       0    1.00614   29.6   54
  5500 CNTR3-B     300.00   2    1     0       0    1.00400   24.7   55
  5501 CNTR4-C     420.00   1    0     0       0    1.00595   24.5   55
  5600 SOUTH3A     300.00   2    1     0       0    1.01000   24.3   56
  5601 SOUTH4A     420.00   1    0     0       0    0.99240   24.5   56
  5602 SOUTH4B     420.00   1    0     0       0    0.97459   20.1   56
  5603 SOUTH3B     300.00  -2    2     0       0    0.94106   19.2   56
  6000 WEST300     300.00   2    1     0       0    1.00500   29.6   60
  6001 WEST400     420.00   1    0     0       0    1.00048   28.8   60
  6100 NWEST3      300.00   2    1     0       0    1.00000   28.6   61
  6500 MID300      300.00   2    1     0       0    1.00000   35.3   65
  6700 NOR300      300.00   2    1     0       0    1.02000   79.5   67
  6701 NOR400      420.00   1    0     0       0    1.00615   79.1   67
  7000 SO-FIN      420.00   2    2     0       0    1.00000   28.9   70
  7100 NO-FIN      420.00   2    1     0       0    1.00000   37.8   71
  8500 SJOLLAND    420.00   2    1     0       0    1.02000   -0.3   90
```

LOAD FLOW

```
    PTI INTERACTIVE POWER SYSTEM SIMULATOR--PSS(tm)E    THU, DEC 11 2008  14:03
REDUCED NORDEL POWER SYSTEM MODEL
V 3.2, 12.08.97

BUS    3000 STCKH          MW     MVAR     MVA   X--- LOSSES ---X X---- AREA -----X
 FROM GENERATION        5300.0  1649.2R 5550.7         MW     MVAR    40 SWEDEN
 TO LOAD-PQ             2000.0   750.0  2136.0
 TO    3115 SV-N1       -550.8   118.6   563.5      52.58  375.55    40 SWEDEN
 TO    3245 SV-M1        293.0   -77.9   303.2       1.08   14.64    40 SWEDEN
 TO    3300 SV-SW       3557.8   858.6  3659.9     152.53 2296.10    40 SWEDEN

BUS    3100 STRFN          MW     MVAR     MVA   X--- LOSSES ---X X---- AREA -----X
 FROM GENERATION        1500.0  1539.4R 2149.4         MW     MVAR    40 SWEDEN
 TO LOAD-PQ              500.0   100.0   509.9
 TO    3115 SV-N1      -1061.5   234.7  1087.2      38.40  527.91    40 SWEDEN
 TO    3200 KRLSK       1008.2   163.4  1021.4      78.46  641.90    40 SWEDEN
 TO    3249 SV-N2      -2832.6   625.2  2900.8      97.32 1328.28    40 SWEDEN
 TO    3359 SV-W        3885.9   416.1  3908.1     147.80 1932.78    40 SWEDEN

BUS    3115 SV-N1          MW     MVAR     MVA   X--- LOSSES ---X X---- AREA -----X
 FROM GENERATION        3570.0  580.7R 3616.9         MW     MVAR    40 SWEDEN
 TO    3000 STCKH        603.4   -43.0   604.9      52.58  375.55    40 SWEDEN
 TO    3100 STRFN       1099.9   218.0  1121.3      38.40  527.91    40 SWEDEN
 TO    3245 SV-M1       1278.3   322.1  1318.3      53.07  884.43    40 SWEDEN
 TO    3249 SV-N2        129.9   -28.0   132.9       0.25    3.39    40 SWEDEN
 TO    6701 NOR400      -374.8    26.2   375.7       5.72   42.93    67 NOR-NORT
 TO    7100 NO-FIN       833.3    85.5   837.6      71.27  498.88    71 FIN-NORT

BUS    3200 KRLSK          MW     MVAR     MVA   X--- LOSSES ---X X---- AREA -----X
                                                       MW     MVAR    40 SWEDEN
 TO LOAD-PQ              500.0   100.0   509.9
 TO    3100 STRFN       -929.8   320.9   983.6      78.46  641.90    40 SWEDEN
 TO    3300 SV-SW        780.7  -316.6   842.5       9.80  133.29    40 SWEDEN
 TO    3359 SV-W        -351.0  -104.3   366.1       5.11   58.45    40 SWEDEN

BUS    3244 SV-M2          MW     MVAR     MVA   X--- LOSSES ---X X---- AREA -----X
                                                       MW     MVAR    40 SWEDEN
 TO    3245 SV-M1        403.6   -59.8   408.0       0.83    3.32    40 SWEDEN
 TO    6500 MID300      -403.6    59.8   408.0       0.83    8.31    65 NOR-MID

BUS    3245 SV-M1          MW     MVAR     MVA   X--- LOSSES ---X X---- AREA -----X
 FROM GENERATION         780.0 1000.5R 1268.6         MW     MVAR    40 SWEDEN
 TO LOAD-PQ             2700.0   500.0  2745.9
 TO    3000 STCKH       -291.9   -34.9   294.0       1.08   14.64    40 SWEDEN
 TO    3115 SV-N1      -1225.3   472.3  1313.1      53.07  884.43    40 SWEDEN
 TO    3244 SV-M2       -402.8    63.1   407.7       0.83    3.32    40 SWEDEN

BUS    3249 SV-N2          MW     MVAR     MVA   X--- LOSSES ---X X---- AREA -----X
 FROM GENERATION        4750.0  956.1R 4845.3         MW     MVAR    40 SWEDEN
 TO LOAD-PQ             1250.0   300.0  1285.5
 TO    3100 STRFN       2929.9   600.9  2990.9      97.32 1328.28    40 SWEDEN
 TO    3115 SV-N1       -129.6    -8.6   129.9       0.25    3.39    40 SWEDEN
 TO    3701 SV-N2B      -100.3    -5.6   100.5       0.20    5.05    40 SWEDEN
```

```
BUS   3300 SV-SW        MW     MVAR     MVA   X--- LOSSES ---X X---- AREA -----X
 FROM GENERATION      2215.9  3690.0R 4304.2       MW     MVAR   40 SWEDEN
 TO LOAD-PQ           9350.0  1500.0  9469.6
 TO   3000 STCKH     -3405.3  1321.1  3652.6    152.53 2296.10   40 SWEDEN
 TO   3200 KRLSK      -770.9   418.4   877.2      9.80  133.29   40 SWEDEN
 TO   3359 SV-W      -2958.2   665.0  3032.0     68.11  887.29   40 SWEDEN
 TO   8500 SJOLLAND      0.3  -214.6   214.6      0.33    1.29   90 SJELLAND

BUS   3359 SV-W         MW     MVAR     MVA   X--- LOSSES ---X X---- AREA -----X
 FROM GENERATION      3500.0  2828.3R 4499.9       MW     MVAR   40 SWEDEN
 TO LOAD-PQ           4500.0   700.0  4554.1
 TO   3100 STRFN     -3738.1  1495.1  4026.0    147.80 1932.78   40 SWEDEN
 TO   3200 KRLSK       356.1    89.3   367.1      5.11   58.45   40 SWEDEN
 TO   3300 SV-SW      3026.3   205.6  3033.3     68.11  887.29   40 SWEDEN
 TO   3360 KONT_135    360.8   183.3   404.7      0.82    3.27   40 SWEDEN
 TO   5101 EAST4-A    -502.6    77.5   508.5      3.87   50.45   51 NOR-EAST
 TO   5101 EAST4-A    -502.6    77.5   508.5      3.87   50.45   51 NOR-EAST

BUS   3360 KONT_135     MW     MVAR     MVA   X--- LOSSES ---X X---- AREA -----X
                                                  MW     MVAR   40 SWEDEN
 TO LOAD-PQ            360.0   180.0   402.5
 TO   3359 SV-W       -360.0  -180.0   402.5      0.82    3.27   40 SWEDEN

BUS   3701 SV-N2B       MW     MVAR     MVA   X--- LOSSES ---X X---- AREA -----X
                                                  MW     MVAR   40 SWEDEN
 TO   3249 SV-N2       100.5    10.6   101.1      0.20    5.05   40 SWEDEN
 TO   6700 NOR300     -100.5   -10.6   101.1      0.10   10.05   67 NOR-NORT

BUS   5100 EAST3        MW     MVAR     MVA   X--- LOSSES ---X X---- AREA -----X
 FROM GENERATION      1452.2  1177.4R 1869.6       MW     MVAR   51 NOR-EAST
 TO LOAD-PQ           3437.3   565.0  3483.4
 TO   5101 EAST4-A     503.5   396.1   640.6      0.33   12.52   51 NOR-EAST
 TO   5102 EAST4-B   -1186.8    61.5  1188.4      1.13   43.08   51 NOR-EAST
 TO   5103 EAST4-C    -441.1    42.3   443.1      0.49   19.64   51 NOR-EAST
 TO   5300 HDAL3      -576.1   103.0   585.3     13.93  139.32   53 NOR-HDAL
 TO   5500 CNTR3-B    -150.2   -17.6   151.2      0.41    3.39   55 NOR-C-B
 TO   6500 MID300      -134.3    27.2   137.1      2.82   28.22   65 NOR-MID

BUS   5101 EAST4-A      MW     MVAR     MVA   X--- LOSSES ---X X---- AREA -----X
                                                  MW     MVAR   51 NOR-EAST
 TO   3359 SV-W        506.4   -62.8   510.3      3.87   50.45   40 SWEDEN
 TO   3359 SV-W        506.4   -62.8   510.3      3.87   50.45   40 SWEDEN
 TO   5100 EAST3      -503.2  -383.6   632.7      0.33   12.52   51 NOR-EAST
 TO   5112 SVCHIGH       0.0  -165.3   165.3      0.00    0.00   51 NOR-EAST
 TO   5501 CNTR4-C     -509.7   674.5   845.4      1.85   19.45   55 NOR-C-B

BUS   5102 EAST4-B      MW     MVAR     MVA   X--- LOSSES ---X X---- AREA -----X
                                                  MW     MVAR   51 NOR-EAST
 TO   5100 EAST3      1188.0   -18.4  1188.1      1.13   43.08   51 NOR-EAST
 TO   5301 HDAL4     -1021.7    56.2  1023.2      7.94  114.25   53 NOR-HDAL
 TO   6001 WEST400     -166.3   -37.8   170.5      0.56    9.76   60 NOR-S-W

BUS   5103 EAST4-C      MW     MVAR     MVA   X--- LOSSES ---X X---- AREA -----X
                                                  MW     MVAR   51 NOR-EAST
 TO   5100 EAST3       441.6   -22.7   442.2      0.49   19.64   51 NOR-EAST
 TO   5301 HDAL4      -441.6    22.7   442.2      3.37   45.80   53 NOR-HDAL

BUS   5111 SVCTERM      MW     MVAR     MVA   X--- LOSSES ---X X---- AREA -----X
 FROM GENERATION         0.0  166.3R  166.3       MW     MVAR   51 NOR-EAST
 TO   5112 SVCHIGH       0.0   166.3   166.3      0.00    1.01   51 NOR-EAST

BUS   5112 SVCHIGH      MW     MVAR     MVA   X--- LOSSES ---X X---- AREA -----X
                                                  MW     MVAR   51 NOR-EAST
 TO   5101 EAST4-A       0.0   165.3   165.3      0.00    0.00   51 NOR-EAST
 TO   5111 SVCTERM       0.0  -165.3   165.3      0.00    1.01   51 NOR-EAST

BUS   5300 HDAL3        MW     MVAR     MVA   X--- LOSSES ---X X---- AREA -----X
 FROM GENERATION      2232.3   13.9R 2232.4       MW     MVAR   53 NOR-HDAL
 TO LOAD-PQ            164.1    9.2   164.4
 TO   5100 EAST3       590.1  -13.6   590.2     13.93  139.32   51 NOR-EAST
 TO   5301 HDAL4      1478.1   18.3  1478.3      3.50  133.30   53 NOR-HDAL

BUS   5301 HDAL4        MW     MVAR     MVA   X--- LOSSES ---X X---- AREA -----X
                                                  MW     MVAR   53 NOR-HDAL
 TO   5102 EAST4-B    1029.6   -70.6  1032.0      7.94  114.25   51 NOR-EAST
 TO   5103 EAST4-C     445.1   -44.4   447.3      3.37   45.80   51 NOR-EAST
 TO   5300 HDAL3     -1474.6   115.0  1479.1      3.50  133.30   53 NOR-HDAL

BUS   5400 CNTR3-A      MW     MVAR     MVA   X--- LOSSES ---X X---- AREA -----X
 FROM GENERATION      1558.2   88.1R 1560.7       MW     MVAR   54 NOR-C-A
 TO LOAD-PQ             77.1    0.0    77.1
 TO   5401 CNTR4-A     330.5    6.6   330.5      0.35   13.09   54 NOR-C-A
 TO   5402 CNTR4-B     188.2   53.0   195.5      0.02    0.57   54 NOR-C-A
 TO   5500 CNTR3-B     809.2   -1.6   809.2      5.75   71.68   55 NOR-C-B
 TO   6000 WEST300      44.0   10.8    45.3      0.02    0.22   60 NOR-S-W
 TO   6100 NWEST3      109.3   19.4   111.0      0.25    2.48   61 NOR-WEST

BUS   5401 CNTR4-A      MW     MVAR     MVA   X--- LOSSES ---X X---- AREA -----X
                                                  MW     MVAR   54 NOR-C-A
 TO   5400 CNTR3-A    -330.1     6.5   330.2      0.35   13.09   54 NOR-C-A
 TO   5501 CNTR4-C     265.3   -74.5   275.5      1.09   14.48   55 NOR-C-B
 TO   5602 SOUTH4B     527.3    59.8   530.7      4.45   69.55   56 NOR-SOUT
 TO   6001 WEST400     -462.5     8.3   462.5      0.64   10.71   60 NOR-S-W

BUS   5402 CNTR4-B      MW     MVAR     MVA   X--- LOSSES ---X X---- AREA -----X
                                                  MW     MVAR   54 NOR-C-A
 TO   5400 CNTR3-A    -188.2   -52.5   195.3      0.02    0.57   54 NOR-C-A
 TO   6001 WEST400     188.2    52.5   195.3      0.20    2.93   60 NOR-S-W
```

BUS 5500 CNTR3-B	MW	MVAR	MVA	X--- LOSSES ---X	X---- AREA -----X
FROM GENERATION	812.5	-668.0R	1051.8	MW MVAR	55 NOR-C-B
TO LOAD-PQ	1003.4	93.9	1007.8		
TO 5100 EAST3	150.6	-0.4	150.6	0.41 3.39	51 NOR-EAST
TO 5400 CNTR3-A	-803.5	73.3	806.8	5.75 71.68	54 NOR-C-A
TO 5501 CNTR4-C	247.9	-960.7	992.2	0.40 15.02	55 NOR-C-B
TO 5603 SOUTH3B	214.0	125.8	248.3	2.50 28.07	56 NOR-SOUT

BUS 5501 CNTR4-C	MW	MVAR	MVA	X--- LOSSES ---X	X---- AREA -----X
				MW MVAR	55 NOR-C-B
TO 5101 EAST4-A	511.7	-1004.4	1127.2	1.85 19.45	51 NOR-EAST
TO 5401 CNTR4-A	-264.2	28.7	265.7	1.09 14.48	54 NOR-C-A
TO 5500 CNTR3-B	-247.5	975.7	1006.6	0.40 15.02	55 NOR-C-B

BUS 5600 SOUTH3A	MW	MVAR	MVA	X--- LOSSES ---X	X---- AREA -----X
FROM GENERATION	2333.4	525.2R	2391.8	MW MVAR	56 NOR-SOUT
TO LOAD-PQ	2548.1	242.5	2559.7		
TO 5601 SOUTH4A	-370.4	-30.7	371.7	0.03 1.07	56 NOR-SOUT
TO 5603 SOUTH3B	414.0	284.1	502.1	5.09 55.98	56 NOR-SOUT
TO 6000 WEST300	-258.3	29.3	260.0	2.38 23.83	60 NOR-S-W

BUS 5601 SOUTH4A	MW	MVAR	MVA	X--- LOSSES ---X	X---- AREA -----X
				MW MVAR	56 NOR-SOUT
TO 5600 SOUTH3A	370.5	31.8	371.8	0.03 1.07	56 NOR-SOUT
TO 6001 WEST400	-370.5	-31.8	371.8	1.91 28.30	60 NOR-S-W

BUS 5602 SOUTH4B	MW	MVAR	MVA	X--- LOSSES ---X	X---- AREA -----X
				MW MVAR	56 NOR-SOUT
TO 5401 CNTR4-A	-522.9	-75.9	528.4	4.45 69.55	54 NOR-C-A
TO 5603 SOUTH3B	522.9	75.9	528.4	0.24 8.96	56 NOR-SOUT

BUS 5603 SOUTH3B	MW	MVAR	MVA	X--- LOSSES ---X	X---- AREA -----X
				MW MVAR	56 NOR-SOUT
TO LOAD-PQ	1143.0	420.5	1217.9		
TO 5500 CNTR3-B	-211.5	-105.5	236.4	2.50 28.07	55 NOR-C-B
TO 5600 SOUTH3A	-408.9	-248.0	478.2	5.09 55.98	56 NOR-SOUT
TO 5602 SOUTH4B	-522.6	-67.0	526.9	0.24 8.96	56 NOR-SOUT

BUS 6000 WEST300	MW	MVAR	MVA	X--- LOSSES ---X	X---- AREA -----X
FROM GENERATION	1107.8	-198.1R	1125.4	MW MVAR	60 NOR-S-W
TO LOAD-PQ	3.3	0.0	3.3		
TO 5400 CNTR3-A	-44.0	-20.7	48.6	0.02 0.22	54 NOR-C-A
TO 5600 SOUTH3A	260.7	-51.2	265.7	2.38 23.83	56 NOR-SOUT
TO 6001 WEST400	815.1	-131.1	825.5	0.27 10.25	60 NOR-S-W
TO 6100 NWEST3	72.8	4.8	72.9	0.12 1.31	61 NOR-WEST

BUS 6001 WEST400	MW	MVAR	MVA	X--- LOSSES ---X	X---- AREA -----X
				MW MVAR	60 NOR-S-W
TO 5102 EAST4-B	167.3	-52.5	175.3	0.56 9.76	51 NOR-EAST
TO 5401 CNTR4-A	463.1	-12.5	463.3	0.64 10.71	54 NOR-C-A
TO 5402 CNTR4-B	-188.0	-73.2	201.7	0.20 2.93	54 NOR-C-A
TO 5601 SOUTH4A	372.4	-3.1	372.4	1.91 28.30	56 NOR-SOUT
TO 6000 WEST300	-814.8	141.3	827.0	0.27 10.25	60 NOR-S-W

BUS 6100 NWEST3	MW	MVAR	MVA	X--- LOSSES ---X	X---- AREA -----X
FROM GENERATION	2302.0	747.6R	2420.3	MW MVAR	61 NOR-WEST
TO LOAD-PQ	2483.6	800.1	2609.3		
TO 5400 CNTR3-A	-109.0	-29.0	112.8	0.25 2.48	54 NOR-C-A
TO 6000 WEST300	-72.6	-23.6	76.4	0.12 1.31	60 NOR-S-W

BUS 6500 MID300	MW	MVAR	MVA	X--- LOSSES ---X	X---- AREA -----X
FROM GENERATION	1482.6	460.6R	1552.5	MW MVAR	65 NOR-MID
TO LOAD-PQ	1566.8	227.8	1583.2		
TO 3244 SV-M2	404.5	-52.5	407.9	0.83 8.31	40 SWEDEN
TO 5100 EAST3	137.2	0.0	137.2	2.82 28.22	51 NOR-EAST
TO 6700 NOR300	-625.8	285.2	687.7	38.06 523.39	67 NOR-NORT

BUS 6700 NOR300	MW	MVAR	MVA	X--- LOSSES ---X	X---- AREA -----X
FROM GENERATION	2719.0	576.9R	2779.5	MW MVAR	67 NOR-NORT
TO LOAD-PQ	1573.3	364.1	1614.9		
TO 3701 SV-N2B	100.6	15.6	101.8	0.10 10.05	40 SWEDEN
TO 6500 MID300	663.8	228.0	701.9	38.06 523.39	65 NOR-MID
TO 6701 NOR400	381.2	-30.7	382.5	0.72 2.88	67 NOR-NORT

BUS 6701 NOR400	MW	MVAR	MVA	X--- LOSSES ---X	X---- AREA -----X
				MW MVAR	67 NOR-NORT
TO 3115 SV-N1	380.5	-33.6	382.0	5.72 42.93	40 SWEDEN
TO 6700 NOR300	-380.5	33.6	382.0	0.72 2.88	67 NOR-NORT

BUS 7000 SO-FIN	MW	MVAR	MVA	X--- LOSSES ---X	X---- AREA -----X
FROM GENERATION	5300.0	1016.1R	5396.5	MW MVAR	70 FIN-SOUT
TO LOAD-PQ	5600.0	1250.0	5737.8		
TO 7100 NO-FIN	-150.0	-117.0	190.2	3.30 23.59	71 FIN-NORT
TO 7100 NO-FIN	-150.0	-117.0	190.2	3.30 23.59	71 FIN-NORT

BUS 7100 NO-FIN	MW	MVAR	MVA	X--- LOSSES ---X	X---- AREA -----X
FROM GENERATION	1310.0	683.1R	1477.4	MW MVAR	71 FIN-NORT
TO LOAD-PQ	2500.0	400.0	2531.8		
TO 3115 SV-N1	-762.0	313.4	823.9	71.27 498.88	40 SWEDEN
TO 3249 SV-N2	-734.6	288.6	789.3	65.43 458.03	40 SWEDEN
TO 7000 SO-FIN	153.3	-159.4	221.2	3.30 23.59	70 FIN-SOUT
TO 7000 SO-FIN	153.3	-159.4	221.2	3.30 23.59	70 FIN-SOUT

BUS 8500 SJOLLAND	MW	MVAR	MVA	X--- LOSSES ---X	X---- AREA -----X
FROM GENERATION	1000.0	909.8R	1351.9	MW MVAR	90 SJELLAND
TO LOAD-PQ	1000.0	1000.0	1414.2		
TO 3300 SV-SW	0.0	-90.2	90.2	0.33 1.29	40 SWEDEN

APPENDIX C: CASE WITH A 1000MW WIND FARM ON THE BUS 6000

BUS DATA

```
    PTI INTERACTIVE POWER SYSTEM SIMULATOR--PSS(tm)E    THU, DEC 11 2008  16:22
REDUCED NORDEL POWER SYSTEM MODEL                                     BUS DATA
V 3.2, 12.08.97
                                        S H U N T S
  BUS# X-- NAME --X BASKV CODE LOADS FIXED SWITCHED  VOLT   ANGLE AREA
  1000 WINDFARN    300.00    2     0     0       0    1.00500   34.7   10
  3000 STCKH       420.00    2     2     0       0    1.00000   35.6   40
  3100 STRFN       420.00    2     1     0       0    0.97000   44.7   40
  3115 SV-N1       420.00    2     0     0       0    1.00000   70.9   40
  3200 KRLSK       420.00    1     1     0       0    0.94597    8.4   40
  3244 SV-M2       300.00    1     0     0       0    1.00066   32.4   40
  3245 SV-M1       420.00    2     1     0       0    1.00000   32.0   40
  3249 SV-N2       420.00    2     1     0       0    1.00000   69.9   40
  3300 SV-SW       420.00    3     1     0       0    1.00000    0.0   40
  3359 SV-W        420.00    2     1     0       0    1.00000   17.4   40
  3360 KONT_135    135.00    1     2     0       0    0.99475   17.0   40
  3701 SV-N2B      300.00    1     0     0       0    1.00703   71.9   40
  5100 EAST3       300.00    2     1     0       0    1.00000   25.1   51
  5101 EAST4-A     420.00    1     0     0       0    0.99342   24.2   51
  5102 EAST4-B     420.00    1     0     0       0    0.99970   27.3   51
  5103 EAST4-C     420.00    1     0     0       0    0.99832   27.5   51
  5111 SVCTERM     22.500    2     0     0       0    1.00000   24.2   51
  5112 SVCHIGH     420.00    1     0     0       0    0.99342   24.2   51
  5300 HDAL3       300.00    2     1     0       0    1.00000   37.9   53
  5301 HDAL4       420.00    1     0     0       0    1.00117   33.1   53
  5400 CNTR3-A     300.00    2     1     0       0    1.00700   33.8   54
  5401 CNTR4-A     420.00    1     0     0       0    0.99890   31.7   54
  5402 CNTR4-B     420.00    1     0     0       0    1.00605   33.8   54
  5500 CNTR3-B     300.00    2     1     0       0    1.00400   27.3   55
  5501 CNTR4-C     420.00    1     0     0       0    1.00570   27.0   55
  5600 SOUTH3A     300.00    2     1     0       0    1.01000   28.0   56
  5601 SOUTH4A     420.00    1     0     0       0    0.99231   28.2   56
  5602 SOUTH4B     420.00    1     0     0       0    0.97399   23.8   56
  5603 SOUTH3B     300.00   -2     2     0       0    0.94068   22.8   56
  6000 WEST300     300.00    2     1     0       0    1.00500   34.7   60
  6001 WEST400     420.00    1     0     0       0    1.00022   33.5   60
  6100 NWEST3      300.00    2     1     0       0    1.00000   32.2   61
  6500 MID300      300.00    2     1     0       0    1.00000   33.4   65
  6700 NOR300      300.00    2     1     0       0    1.02000   75.7   67
  6701 NOR400      420.00    1     0     0       0    1.00663   75.4   67
  7000 SO-FIN      420.00    2     2     0       0    1.00000   27.5   70
  7100 NO-FIN      420.00    2     1     0       0    1.00000   36.4   71
  8500 SJOLLAND    420.00    2     1     0       0    1.02000   -0.3   90
```

LOAD FLOW

```
    PTI INTERACTIVE POWER SYSTEM SIMULATOR--PSS(tm)E    THU, DEC 11 2008  16:22
REDUCED NORDEL POWER SYSTEM MODEL                                     RATING
V 3.2, 12.08.97                                                        SET A

BUS    1000 WINDFARN       MW     MVAR     MVA   X--- LOSSES ---X X---- AREA -----X
 FROM GENERATION        1000.0  -105.9R 1005.6       MW     MVAR   10 WINDFARM
 TO    6000 WEST300     1000.0  -105.9  1005.6     0.00     0.00   60 NOR-S-W

BUS    3000 STCKH          MW     MVAR     MVA   X--- LOSSES ---X X---- AREA -----X
 FROM GENERATION        5300.0  1588.3R 5532.9       MW     MVAR   40 SWEDEN
 TO LOAD-PQ             2000.0   750.0  2136.0
 TO    3115 SV-N1        -541.8   110.0   552.8    50.56  361.12   40 SWEDEN
 TO    3245 SV-M1         364.9   -79.1   373.4     1.67   22.69   40 SWEDEN
 TO    3300 SV-SW        3476.9   807.5  3569.4   145.07 2183.76   40 SWEDEN

BUS    3100 STRFN          MW     MVAR     MVA   X--- LOSSES ---X X---- AREA -----X
 FROM GENERATION        1500.0  1412.9R 2060.7       MW     MVAR   40 SWEDEN
 TO LOAD-PQ              500.0   100.0   509.9
 TO    3115 SV-N1       -1016.1   207.4  1037.0    34.93  480.18   40 SWEDEN
 TO    3200 KRLSK         997.9   156.7  1010.1    76.71  627.55   40 SWEDEN
 TO    3249 SV-N2       -2755.7   581.2  2816.3    91.73 1251.93   40 SWEDEN
 TO    3359 SV-W         3773.8   367.6  3791.7   139.12 1819.31   40 SWEDEN

BUS    3115 SV-N1          MW     MVAR     MVA   X--- LOSSES ---X X---- AREA -----X
 FROM GENERATION        3570.0   525.8R 3608.5       MW     MVAR   40 SWEDEN
 TO    3000 STCKH         592.4   -48.8   594.4    50.56  361.12   40 SWEDEN
 TO    3100 STRFN        1051.0   197.5  1069.4    34.93  480.18   40 SWEDEN
 TO    3245 SV-M1        1277.8   321.7  1317.6    53.01  883.57   40 SWEDEN
 TO    3249 SV-N2          84.2   -25.6    88.0     0.11    1.42   40 SWEDEN
 TO    6701 NOR400       -262.6    -1.5   262.6     2.78   20.86   67 NOR-NORT
 TO    7100 NO-FIN        827.4    82.6   831.5    70.22  491.51   71 FIN-NORT

BUS    3200 KRLSK          MW     MVAR     MVA   X--- LOSSES ---X X---- AREA -----X
                                                      MW     MVAR   40 SWEDEN
 TO LOAD-PQ              500.0   100.0   509.9
 TO    3100 STRFN       -921.2   313.2   972.9    76.71  627.55   40 SWEDEN
 TO    3300 SV-SW        788.8  -313.9   849.0     9.94  135.27   40 SWEDEN
 TO    3359 SV-W        -367.7   -99.3   380.8     5.56   63.56   40 SWEDEN

BUS    3244 SV-M2          MW     MVAR     MVA   X--- LOSSES ---X X---- AREA -----X
                                                      MW     MVAR   40 SWEDEN
 TO    3245 SV-M1         332.6   -48.8   336.1     0.56    2.26   40 SWEDEN
 TO    6500 MID300       -332.6    48.8   336.1     0.56    5.64   65 NOR-MID

BUS    3245 SV-M1          MW     MVAR     MVA   X--- LOSSES ---X X---- AREA -----X
 FROM GENERATION         780.0   997.3R 1266.1       MW     MVAR   40 SWEDEN
 TO LOAD-PQ             2700.0   500.0  2745.9
 TO    3000 STCKH        -363.3   -25.6   364.2     1.67   22.69   40 SWEDEN
 TO    3115 SV-N1       -1224.7   471.9  1312.5    53.01  883.57   40 SWEDEN
 TO    3244 SV-M2        -332.0    51.1   335.9     0.56    2.26   40 SWEDEN
```

BUS	3249 SV-N2	MW	MVAR	MVA	X--- LOSSES ---X		X---- AREA -----X	
FROM GENERATION		4750.0	917.6R	4837.8	MW	MVAR	40	SWEDEN
TO LOAD-PQ		1250.0	300.0	1285.5				
TO	3100 STRFN	2847.4	568.5	2903.6	91.73	1251.93	40	SWEDEN
TO	3115 SV-N1	-84.0	-13.0	85.0	0.11	1.42	40	SWEDEN
TO	3701 SV-N2B	-69.2	-10.1	69.9	0.10	2.45	40	SWEDEN
TO	7100 NO-FIN	805.9	72.1	809.1	66.43	465.03	71	FIN-NORT

BUS	3300 SV-SW	MW	MVAR	MVA	X--- LOSSES ---X		X---- AREA -----X	
FROM GENERATION		2196.9	3661.3R	4269.8	MW	MVAR	40	SWEDEN
TO LOAD-PQ		9350.0	1500.0	9469.6				
TO	3000 STCKH	-3331.8	1259.8	3562.0	145.07	2183.76	40	SWEDEN
TO	3200 KRLSK	-778.9	417.6	883.8	9.94	135.27	40	SWEDEN
TO	3359 SV-W	-3042.7	698.3	3121.8	72.21	940.62	40	SWEDEN
TO	8500 SJOLLAND	0.3	-214.6	214.6	0.33	1.29	90	SJELLAND

BUS	3359 SV-W	MW	MVAR	MVA	X--- LOSSES ---X		X---- AREA -----X	
FROM GENERATION		3500.0	2827.8R	4499.6	MW	MVAR	40	SWEDEN
TO LOAD-PQ		4500.0	700.0	4554.1				
TO	3100 STRFN	-3634.7	1430.2	3906.0	139.12	1819.31	40	SWEDEN
TO	3200 KRLSK	373.2	89.4	383.8	5.56	63.56	40	SWEDEN
TO	3300 SV-SW	3114.9	225.7	3123.1	72.21	940.62	40	SWEDEN
TO	3360 KONT_135	360.8	183.3	404.7	0.82	3.27	40	SWEDEN
TO	5101 EAST4-A	-607.1	99.7	615.3	5.66	73.74	51	NOR-EAST
TO	5101 EAST4-A	-607.1	99.7	615.3	5.66	73.74	51	NOR-EAST

BUS	3360 KONT_135	MW	MVAR	MVA	X--- LOSSES ---X		X---- AREA -----X	
					MW	MVAR	40	SWEDEN
TO LOAD-PQ		360.0	180.0	402.5				
TO	3359 SV-W	-360.0	-180.0	402.5	0.82	3.27	40	SWEDEN

BUS	3701 SV-N2B	MW	MVAR	MVA	X--- LOSSES ---X		X---- AREA -----X	
					MW	MVAR	40	SWEDEN
TO	3249 SV-N2	69.3	12.6	70.4	0.10	2.45	40	SWEDEN
TO	6700 NOR300	-69.3	-12.6	70.4	0.05	4.83	67	NOR-NORT

BUS	5100 EAST3	MW	MVAR	MVA	X--- LOSSES ---X		X---- AREA -----X	
FROM GENERATION		1361.5	1186.2R	1805.7	MW	MVAR	51	NOR-EAST
TO LOAD-PQ		3437.3	565.0	3483.4				
TO	5101 EAST4-A	489.1	411.9	639.5	0.33	12.47	51	NOR-EAST
TO	5102 EAST4-B	-1247.5	66.5	1249.3	1.25	47.60	51	NOR-EAST
TO	5103 EAST4-C	-419.9	36.2	421.5	0.44	17.76	51	NOR-EAST
TO	5300 HDAL3	-543.7	91.9	551.4	12.37	123.73	53	NOR-HDAL
TO	5500 CNTR3-B	-259.5	-1.1	259.5	1.21	10.11	55	NOR-C-B
TO	6500 MID300	-94.3	15.9	95.6	1.37	13.73	65	NOR-MID

BUS	5101 EAST4-A	MW	MVAR	MVA	X--- LOSSES ---X		X---- AREA -----X	
					MW	MVAR	51	NOR-EAST
TO	3359 SV-W	612.8	-61.7	615.9	5.66	73.74	40	SWEDEN
TO	3359 SV-W	612.8	-61.7	615.9	5.66	73.74	40	SWEDEN
TO	5100 EAST3	-488.8	-399.4	631.3	0.33	12.47	51	NOR-EAST
TO	5112 SVCHIGH	0.0	-178.2	178.2	0.00	0.00	51	NOR-EAST
TO	5501 CNTR4-C	-736.8	701.1	1017.0	3.62	38.16	55	NOR-C-B

BUS	5102 EAST4-B	MW	MVAR	MVA	X--- LOSSES ---X		X---- AREA -----X	
					MW	MVAR	51	NOR-EAST
TO	5100 EAST3	1248.8	-18.9	1248.9	1.25	47.60	51	NOR-EAST
TO	5301 HDAL4	-939.4	35.7	940.0	6.70	96.35	53	NOR-HDAL
TO	6001 WEST400	-309.4	-16.8	309.9	1.94	33.96	60	NOR-S-W

BUS	5103 EAST4-C	MW	MVAR	MVA	X--- LOSSES ---X		X---- AREA -----X	
					MW	MVAR	51	NOR-EAST
TO	5100 EAST3	420.4	-18.4	420.8	0.44	17.76	51	NOR-EAST
TO	5301 HDAL4	-420.4	18.4	420.8	3.05	41.43	53	NOR-HDAL

BUS	5111 SVCTERM	MW	MVAR	MVA	X--- LOSSES ---X		X---- AREA -----X	
FROM GENERATION		0.0	179.4R	179.4	MW	MVAR	51	NOR-EAST
TO	5112 SVCHIGH	0.0	179.4	179.4	0.00	1.18	51	NOR-EAST

BUS	5112 SVCHIGH	MW	MVAR	MVA	X--- LOSSES ---X		X---- AREA -----X	
					MW	MVAR	51	NOR-EAST
TO	5101 EAST4-A	0.0	178.2	178.2	0.00	0.00	51	NOR-EAST
TO	5111 SVCTERM	0.0	-178.2	178.2	0.00	1.18	51	NOR-EAST

BUS	5300 HDAL3	MW	MVAR	MVA	X--- LOSSES ---X		X---- AREA -----X	
FROM GENERATION		2092.8	-6.7R	2092.8	MW	MVAR	53	NOR-HDAL
TO LOAD-PQ		164.1	9.2	164.4				
TO	5100 EAST3	556.1	-18.1	556.4	12.37	123.73	51	NOR-EAST
TO	5301 HDAL4	1372.6	2.2	1372.6	3.01	114.92	53	NOR-HDAL

BUS	5301 HDAL4	MW	MVAR	MVA	X--- LOSSES ---X		X---- AREA -----X	
					MW	MVAR	53	NOR-HDAL
TO	5102 EAST4-B	946.1	-68.1	948.5	6.70	96.35	51	NOR-EAST
TO	5103 EAST4-C	423.5	-44.6	425.8	3.05	41.43	51	NOR-EAST
TO	5300 HDAL3	-1369.5	112.7	1374.2	3.01	114.92	53	NOR-HDAL

BUS	5400 CNTR3-A	MW	MVAR	MVA	X--- LOSSES ---X		X---- AREA -----X	
FROM GENERATION		1460.8	126.4R	1466.3	MW	MVAR	54	NOR-C-A
TO LOAD-PQ		77.1	0.0	77.1				
TO	5401 CNTR4-A	311.5	12.1	311.8	0.31	11.65	54	NOR-C-A
TO	5402 CNTR4-B	57.1	62.5	84.7	0.00	0.11	54	NOR-C-A
TO	5500 CNTR3-B	1028.5	3.0	1028.5	9.28	115.80	55	NOR-C-B
TO	6000 WEST300	-156.0	31.9	159.3	0.25	2.54	60	NOR-S-W
TO	6100 NWEST3	142.7	16.9	143.7	0.41	4.12	61	NOR-WEST

BUS	5401 CNTR4-A	MW	MVAR	MVA	X--- LOSSES ---X		X---- AREA -----X	
					MW	MVAR	54	NOR-C-A
TO	5400 CNTR3-A	-311.2	-0.4	311.2	0.31	11.65	54	NOR-C-A
TO	5501 CNTR4-C	404.1	-77.7	411.5	2.49	33.19	55	NOR-C-B
TO	5602 SOUTH4B	558.6	61.6	561.9	4.99	77.91	56	NOR-SOUT
TO	6001 WEST400	-651.4	16.5	651.7	1.28	21.28	60	NOR-S-W

BUS	5402 CNTR4-B	MW	MVAR	MVA	X--- LOSSES ---X		X---- AREA -----X
					MW	MVAR	54 NOR-C-A
TO	5400 CNTR3-A	-57.1	-62.4	84.6	0.00	0.11	54 NOR-C-A
TO	6001 WEST400	57.1	62.4	84.6	0.04	0.65	60 NOR-S-W

BUS	5500 CNTR3-B	MW	MVAR	MVA	X--- LOSSES ---X		X---- AREA -----X
FROM	GENERATION	761.7	-623.3R	984.2	MW	MVAR	55 NOR-C-B
TO	LOAD-PQ	1003.4	93.9	1007.8			
TO	5100 EAST3	260.7	-10.2	260.9	1.21	10.11	51 NOR-EAST
TO	5400 CNTR3-A	-1019.2	112.8	1025.5	9.28	115.80	54 NOR-C-A
TO	5501 CNTR4-C	339.3	-946.5	1005.5	0.41	15.43	55 NOR-C-B
TO	5603 SOUTH3B	177.5	126.7	218.1	1.94	21.80	56 NOR-SOUT

BUS	5501 CNTR4-C	MW	MVAR	MVA	X--- LOSSES ---X		X---- AREA -----X
					MW	MVAR	55 NOR-C-B
TO	5101 EAST4-A	740.5	-1012.5	1254.4	3.62	38.16	51 NOR-EAST
TO	5401 CNTR4-A	-401.6	50.6	404.8	2.49	33.19	54 NOR-C-A
TO	5500 CNTR3-B	-338.9	961.9	1019.9	0.41	15.43	55 NOR-C-B

BUS	5600 SOUTH3A	MW	MVAR	MVA	X--- LOSSES ---X		X---- AREA -----X
FROM	GENERATION	2187.5	555.3R	2256.9	MW	MVAR	56 NOR-SOUT
TO	LOAD-PQ	2548.1	242.5	2559.7			
TO	5601 SOUTH4A	-450.0	-17.2	450.4	0.04	1.57	56 NOR-SOUT
TO	5603 SOUTH3B	419.4	285.9	507.6	5.20	57.18	56 NOR-SOUT
TO	6000 WEST300	-330.0	44.1	332.9	3.89	38.91	60 NOR-S-W

BUS	5601 SOUTH4A	MW	MVAR	MVA	X--- LOSSES ---X		X---- AREA -----X
					MW	MVAR	56 NOR-SOUT
TO	5600 SOUTH3A	450.1	18.7	450.5	0.04	1.57	56 NOR-SOUT
TO	6001 WEST400	-450.1	-18.7	450.5	2.82	41.81	60 NOR-S-W

BUS	5602 SOUTH4B	MW	MVAR	MVA	X--- LOSSES ---X		X---- AREA -----X
					MW	MVAR	56 NOR-SOUT
TO	5401 CNTR4-A	-553.6	-69.3	557.9	4.99	77.91	54 NOR-C-A
TO	5603 SOUTH3B	553.6	69.3	557.9	0.26	10.01	56 NOR-SOUT

BUS	5603 SOUTH3B	MW	MVAR	MVA	X--- LOSSES ---X		X---- AREA -----X
					MW	MVAR	56 NOR-SOUT
TO	LOAD-PQ	1143.0	420.5	1217.9			
TO	5500 CNTR3-B	-175.5	-112.7	208.5	1.94	21.80	55 NOR-C-B
TO	5600 SOUTH3A	-414.2	-248.5	483.1	5.20	57.18	56 NOR-SOUT
TO	5602 SOUTH4B	-553.3	-59.3	556.5	0.26	10.01	56 NOR-SOUT

BUS	6000 WEST300	MW	MVAR	MVA	X--- LOSSES ---X		X---- AREA -----X
FROM	GENERATION	1038.6	-105.9R	1044.0	MW	MVAR	60 NOR-S-W
TO	LOAD-PQ	3.3	0.0	3.3			
TO	1000 WINDFARN	-1000.0	105.9	1005.6	0.00	0.00	10 WINDFARM
TO	5400 CNTR3-A	156.3	-39.5	161.2	0.25	2.54	54 NOR-C-A
TO	5600 SOUTH3A	333.9	-50.9	337.7	3.89	38.91	56 NOR-SOUT
TO	6001 WEST400	1361.1	-119.4	1366.3	0.75	28.07	60 NOR-S-W
TO	6100 NWEST3	184.0	-2.0	184.0	0.74	8.04	61 NOR-WEST

BUS	6001 WEST400	MW	MVAR	MVA	X--- LOSSES ---X		X---- AREA -----X
					MW	MVAR	60 NOR-S-W
TO	5102 EAST4-B	311.8	-49.2	315.6	1.94	33.96	51 NOR-EAST
TO	5401 CNTR4-A	652.7	-10.2	652.8	1.28	21.28	54 NOR-C-A
TO	5402 CNTR4-B	-57.0	-85.4	102.7	0.04	0.65	54 NOR-C-A
TO	5601 SOUTH4A	452.9	-2.6	452.9	2.82	41.81	56 NOR-SOUT
TO	6000 WEST300	-1360.4	147.4	1368.3	0.75	28.07	60 NOR-S-W

BUS	6100 NWEST3	MW	MVAR	MVA	X--- LOSSES ---X		X---- AREA -----X
FROM	GENERATION	2158.1	765.3R	2289.8	MW	MVAR	61 NOR-WEST
TO	LOAD-PQ	2483.6	800.1	2609.3			
TO	5400 CNTR3-A	-142.3	-24.8	144.4	0.41	4.12	54 NOR-C-A
TO	6000 WEST300	-183.3	-10.0	183.5	0.74	8.04	60 NOR-S-W

BUS	6500 MID300	MW	MVAR	MVA	X--- LOSSES ---X		X---- AREA -----X
FROM	GENERATION	1390.0	443.7R	1459.1	MW	MVAR	65 NOR-MID
TO	LOAD-PQ	1566.8	227.8	1583.2			
TO	3244 SV-M2	333.1	-44.2	336.0	0.56	5.64	40 SWEDEN
TO	5100 EAST3	95.6	-3.1	95.7	1.37	13.73	51 NOR-EAST
TO	6700 NOR300	-605.6	263.2	660.3	35.09	482.49	67 NOR-NORT

BUS	6700 NOR300	MW	MVAR	MVA	X--- LOSSES ---X		X---- AREA -----X
FROM	GENERATION	2549.1	559.0R	2609.6	MW	MVAR	67 NOR-NORT
TO	LOAD-PQ	1573.3	364.1	1614.9			
TO	3701 SV-N2B	69.3	12.3	70.4	0.05	4.83	40 SWEDEN
TO	6500 MID300	640.6	209.1	673.9	35.09	482.49	65 NOR-MID
TO	6701 NOR400	265.8	-26.5	267.1	0.35	1.41	67 NOR-NORT

BUS	6701 NOR400	MW	MVAR	MVA	X--- LOSSES ---X		X---- AREA -----X
					MW	MVAR	67 NOR-NORT
TO	3115 SV-N1	265.4	-27.9	266.9	2.78	20.86	40 SWEDEN
TO	6700 NOR300	-265.4	27.9	266.9	0.35	1.41	67 NOR-NORT

BUS	7000 SO-FIN	MW	MVAR	MVA	X--- LOSSES ---X		X---- AREA -----X
FROM	GENERATION	5300.0	1016.1R	5396.5	MW	MVAR	70 FIN-SOUT
TO	LOAD-PQ	5600.0	1250.0	5737.8			
TO	7100 NO-FIN	-150.0	-117.0	190.2	3.30	23.59	71 FIN-NORT
TO	7100 NO-FIN	-150.0	-117.0	190.2	3.30	23.59	71 FIN-NORT

BUS	7100 NO-FIN	MW	MVAR	MVA	X--- LOSSES ---X		X---- AREA -----X
FROM	GENERATION	1310.0	683.0R	1477.3	MW	MVAR	71 FIN-NORT
TO	LOAD-PQ	2500.0	400.0	2531.8			
TO	3115 SV-N1	-757.2	308.9	817.8	70.22	491.51	40 SWEDEN
TO	3249 SV-N2	-739.4	292.9	795.3	66.43	465.03	40 SWEDEN
TO	7000 SO-FIN	153.3	-159.4	221.2	3.30	23.59	70 FIN-SOUT
TO	7000 SO-FIN	153.3	-159.4	221.2	3.30	23.59	70 FIN-SOUT

BUS	8500 SJOLLAND	MW	MVAR	MVA	X--- LOSSES ---X		X---- AREA -----X
FROM	GENERATION	1000.0	909.8R	1351.9	MW	MVAR	90 SJELLAND
TO	LOAD-PQ	1000.0	1000.0	1414.2			
TO	3300 SV-SW	0.0	-90.2	90.2	0.33	1.29	40 SWEDEN

APPENDIX D: CASE WITH A 1000MW WIND FARM ON THE BUS 5600

BUS DATA

```
    PTI INTERACTIVE POWER SYSTEM SIMULATOR--PSS(tm)E    THU, DEC 11 2008  16:31
REDUCED NORDEL POWER SYSTEM MODEL                                     BUS DATA
V 3.2, 12.08.97
                                        S H U N T S
  BUS# X-- NAME --X BASKV CODE LOADS FIXED SWITCHED  VOLT   ANGLE AREA
  1000 WINDFARN    300.00    2    0     0       0    1.01000   33.5   10
  3000 STCKH       420.00    2    2     0       0    1.00000   35.6   40
  3100 STRFN       420.00    2    1     0       0    0.97000   44.7   40
  3115 SV-N1       420.00    2    0     0       0    1.00000   70.9   40
  3200 KRLSK       420.00    1    1     0       0    0.94592    8.4   40
  3244 SV-M2       300.00    1    0     0       0    1.00066   32.4   40
  3245 SV-M1       420.00    2    1     0       0    1.00000   32.0   40
  3249 SV-N2       420.00    2    1     0       0    1.00000   69.9   40
  3300 SV-SW       420.00    3    1     0       0    1.00000    0.0   40
  3359 SV-W        420.00    2    1     0       0    1.00000   17.4   40
  3360 KONT_135    135.00    1    2     0       0    0.99475   17.0   40
  3701 SV-N2B      300.00    1    0     0       0    1.00703   71.9   40
  5100 EAST3       300.00    2    1     0       0    1.00000   25.1   51
  5101 EAST4-A     420.00    1    0     0       0    0.99341   24.3   51
  5102 EAST4-B     420.00    1    0     0       0    0.99977   27.3   51
  5103 EAST4-C     420.00    1    0     0       0    0.99834   27.6   51
  5111 SVCTERM     22.500    2    0     0       0    1.00000   24.3   51
  5112 SVCHIGH     420.00    1    0     0       0    0.99341   24.3   51
  5300 HDAL3       300.00    2    1     0       0    1.00000   38.0   53
  5301 HDAL4       420.00    1    0     0       0    1.00120   33.2   53
  5400 CNTR3-A     300.00    2    1     0       0    1.00700   33.6   54
  5401 CNTR4-A     420.00    1    0     0       0    0.99962   31.7   54
  5402 CNTR4-B     420.00    1    0     0       0    1.00609   33.5   54
  5500 CNTR3-B     300.00    2    1     0       0    1.00400   27.4   55
  5501 CNTR4-C     420.00    1    0     0       0    1.00575   27.1   55
  5600 SOUTH3A     300.00    2    1     0       0    1.01000   33.5   56
  5601 SOUTH4A     420.00    1    0     0       0    0.99262   33.5   56
  5602 SOUTH4B     420.00    1    0     0       0    0.97431   25.9   56
  5603 SOUTH3B     300.00   -2    2     0       0    0.94018   25.2   56
  6000 WEST300     300.00    2    1     0       0    1.00500   34.0   60
  6001 WEST400     420.00    1    0     0       0    1.00048   33.3   60
  6100 NWEST3      300.00    2    1     0       0    1.00000   31.7   61
  6500 MID300      300.00    2    1     0       0    1.00000   33.4   65
  6700 NOR300      300.00    2    1     0       0    1.02000   75.8   67
  6701 NOR400      420.00    1    0     0       0    1.00663   75.5   67
  7000 SO-FIN      420.00    2    2     0       0    1.00000   27.6   70
  7100 NO-FIN      420.00    2    1     0       0    1.00000   36.4   71
  8500 SJOLLAND    420.00    2    1     0       0    1.02000   -0.3   90
```

LOAD FLOW

```
    PTI INTERACTIVE POWER SYSTEM SIMULATOR--PSS(tm)E    THU, DEC 11 2008  16:31
REDUCED NORDEL POWER SYSTEM MODEL                                     RATING
V 3.2, 12.08.97                                                        SET A

BUS    1000 WINDFARN      MW     MVAR     MVA   X--- LOSSES ---X X---- AREA -----X
 FROM GENERATION       1000.0   230.0R 1026.1       MW     MVAR   10 WINDFARM
 TO    5600 SOUTH3A    1000.0   230.0  1026.1      0.00    0.00   56 NOR-SOUT

BUS    3000 STCKH         MW     MVAR     MVA   X--- LOSSES ---X X---- AREA -----X
 FROM GENERATION       5300.0  1589.0R 5533.1       MW     MVAR   40 SWEDEN
 TO LOAD-PQ            2000.0   750.0  2136.0
 TO    3115 SV-N1       -542.0   110.1   553.0     50.59  361.36   40 SWEDEN
 TO    3245 SV-M1        364.3   -79.1   372.8      1.66   22.61   40 SWEDEN
 TO    3300 SV-SW       3477.7   808.0  3570.3    145.14 2184.85   40 SWEDEN

BUS    3100 STRFN         MW     MVAR     MVA   X--- LOSSES ---X X---- AREA -----X
 FROM GENERATION       1500.0  1412.7R 2060.5       MW     MVAR   40 SWEDEN
 TO LOAD-PQ             500.0   100.0   509.9
 TO    3115 SV-N1     -1015.9   207.3  1036.8     34.92  480.03   40 SWEDEN
 TO    3200 KRLSK       998.2   157.0  1010.4     76.76  627.99   40 SWEDEN
 TO    3249 SV-N2     -2755.4   581.1  2816.1     91.71 1251.73   40 SWEDEN
 TO    3359 SV-W       3773.2   367.4  3791.0    139.07 1818.66   40 SWEDEN

BUS    3115 SV-N1         MW     MVAR     MVA   X--- LOSSES ---X X---- AREA -----X
 FROM GENERATION       3570.0   526.0R 3608.5       MW     MVAR   40 SWEDEN
 TO    3000 STCKH       592.5   -48.7   594.5     50.59  361.36   40 SWEDEN
 TO    3100 STRFN      1050.8   197.5  1069.2     34.92  480.03   40 SWEDEN
 TO    3245 SV-M1      1277.9   321.8  1317.8     53.03  883.81   40 SWEDEN
 TO    3249 SV-N2        84.0   -25.6    87.8      0.11    1.42   40 SWEDEN
 TO    6701 NOR400     -262.6    -1.5   262.6      2.78   20.86   67 NOR-NORT
 TO    7100 NO-FIN      827.4    82.6   831.5     70.21  491.48   71 FIN-NORT

BUS    3200 KRLSK         MW     MVAR     MVA   X--- LOSSES ---X X---- AREA -----X
                                                     MW     MVAR   40 SWEDEN
 TO LOAD-PQ             500.0   100.0   509.9
 TO    3100 STRFN      -921.4   313.4   973.2     76.76  627.99   40 SWEDEN
 TO    3300 SV-SW       789.8  -314.1   850.0      9.97  135.61   40 SWEDEN
 TO    3359 SV-W       -368.4   -99.2   381.5      5.58   63.82   40 SWEDEN

BUS    3244 SV-M2         MW     MVAR     MVA   X--- LOSSES ---X X---- AREA -----X
                                                     MW     MVAR   40 SWEDEN
 TO    3245 SV-M1       333.1   -48.9   336.6      0.57    2.26   40 SWEDEN
 TO    6500 MID300     -333.1    48.9   336.6      0.57    5.66   65 NOR-MID

BUS    3245 SV-M1         MW     MVAR     MVA   X--- LOSSES ---X X---- AREA -----X
 FROM GENERATION        780.0   997.5R 1266.2       MW     MVAR   40 SWEDEN
 TO LOAD-PQ            2700.0   500.0  2745.9
 TO    3000 STCKH      -362.6   -25.7   363.5      1.66   22.61   40 SWEDEN
 TO    3115 SV-N1     -1224.9   472.0  1312.7     53.03  883.81   40 SWEDEN
 TO    3244 SV-M2      -332.5    51.2   336.4      0.57    2.26   40 SWEDEN
```

BUS	3249 SV-N2	MW	MVAR	MVA	X--- LOSSES ---X	MW	MVAR	X---- AREA -----X
FROM GENERATION		4750.0	917.5R	4837.8				40 SWEDEN
TO LOAD-PQ		1250.0	300.0	1285.5				
TO	3100 STRFN	2847.2	568.4	2903.4		91.71	1251.73	40 SWEDEN
TO	3115 SV-N1	-83.9	-13.0	84.9		0.11	1.42	40 SWEDEN
TO	3701 SV-N2B	-69.2	-10.1	69.9		0.10	2.44	40 SWEDEN
TO	7100 NO-FIN	805.9	72.1	809.1		66.44	465.06	71 FIN-NORT

BUS	3300 SV-SW	MW	MVAR	MVA	X--- LOSSES ---X	MW	MVAR	X---- AREA -----X
FROM GENERATION		2190.2	3664.4R	4269.1				40 SWEDEN
TO LOAD-PQ		9350.0	1500.0	9469.6				
TO	3000 STCKH	-3332.5	1260.4	3562.9		145.14	2184.85	40 SWEDEN
TO	3200 KRLSK	-779.8	418.2	884.9		9.97	135.61	40 SWEDEN
TO	3359 SV-W	-3047.8	700.4	3127.2		72.45	943.86	40 SWEDEN
TO	8500 SJOLLAND	0.3	-214.6	214.6		0.33	1.29	90 SJELLAND

BUS	3359 SV-W	MW	MVAR	MVA	X--- LOSSES ---X	MW	MVAR	X---- AREA -----X
FROM GENERATION		3500.0	2830.3R	4501.2				40 SWEDEN
TO LOAD-PQ		4500.0	700.0	4554.1				
TO	3100 STRFN	-3634.1	1429.8	3905.3		139.07	1818.66	40 SWEDEN
TO	3200 KRLSK	374.0	89.6	384.6		5.58	63.82	40 SWEDEN
TO	3300 SV-SW	3120.2	226.9	3128.5		72.45	943.86	40 SWEDEN
TO	3360 KONT_135	360.8	183.3	404.7		0.82	3.27	40 SWEDEN
TO	5101 EAST4-A	-610.5	100.4	618.7		5.72	74.55	51 NOR-EAST
TO	5101 EAST4-A	-610.5	100.4	618.7		5.72	74.55	51 NOR-EAST

BUS	3360 KONT_135	MW	MVAR	MVA	X--- LOSSES ---X	MW	MVAR	X---- AREA -----X
								40 SWEDEN
TO LOAD-PQ		360.0	180.0	402.5				
TO	3359 SV-W	-360.0	-180.0	402.5		0.82	3.27	40 SWEDEN

BUS	3701 SV-N2B	MW	MVAR	MVA	X--- LOSSES ---X	MW	MVAR	X---- AREA -----X
								40 SWEDEN
TO	3249 SV-N2	69.3	12.6	70.4		0.10	2.44	40 SWEDEN
TO	6700 NOR300	-69.3	-12.6	70.4		0.05	4.83	67 NOR-NORT

BUS	5100 EAST3	MW	MVAR	MVA	X--- LOSSES ---X	MW	MVAR	X---- AREA -----X
FROM GENERATION		1361.5	1184.4R	1804.6				51 NOR-EAST
TO LOAD-PQ		3437.3	565.0	3483.4				
TO	5101 EAST4-A	483.5	412.4	635.5		0.32	12.32	51 NOR-EAST
TO	5102 EAST4-B	-1235.5	63.5	1237.2		1.22	46.68	51 NOR-EAST
TO	5103 EAST4-C	-419.2	36.0	420.7		0.44	17.70	51 NOR-EAST
TO	5300 HDAL3	-543.2	91.7	550.9		12.35	123.49	53 NOR-HDAL
TO	5500 CNTR3-B	-267.5	0.2	267.5		1.29	10.75	55 NOR-C-B
TO	6500 MID300	-93.8	15.7	95.1		1.36	13.60	65 NOR-MID

BUS	5101 EAST4-A	MW	MVAR	MVA	X--- LOSSES ---X	MW	MVAR	X---- AREA -----X
								51 NOR-EAST
TO	3359 SV-W	616.2	-61.7	619.3		5.72	74.55	40 SWEDEN
TO	3359 SV-W	616.2	-61.7	619.3		5.72	74.55	40 SWEDEN
TO	5100 EAST3	-483.2	-400.1	627.3		0.32	12.32	51 NOR-EAST
TO	5112 SVCHIGH	0.0	-178.6	178.6		0.00	0.00	51 NOR-EAST
TO	5501 CNTR4-C	-749.2	701.9	1026.6		3.74	39.39	55 NOR-C-B

BUS	5102 EAST4-B	MW	MVAR	MVA	X--- LOSSES ---X	MW	MVAR	X---- AREA -----X
								51 NOR-EAST
TO	5100 EAST3	1236.7	-16.8	1236.9		1.22	46.68	51 NOR-EAST
TO	5301 HDAL4	-940.6	36.4	941.3		6.71	96.60	53 NOR-HDAL
TO	6001 WEST400	-296.2	-19.6	296.8		1.78	31.08	60 NOR-S-W

BUS	5103 EAST4-C	MW	MVAR	MVA	X--- LOSSES ---X	MW	MVAR	X---- AREA -----X
								51 NOR-EAST
TO	5100 EAST3	419.6	-18.3	420.0		0.44	17.70	51 NOR-EAST
TO	5301 HDAL4	-419.6	18.3	420.0		3.04	41.29	53 NOR-HDAL

BUS	5111 SVCTERM	MW	MVAR	MVA	X--- LOSSES ---X	MW	MVAR	X---- AREA -----X
FROM GENERATION		0.0	179.7R	179.7				51 NOR-EAST
TO	5112 SVCHIGH	0.0	179.7	179.7		0.00	1.18	51 NOR-EAST

BUS	5112 SVCHIGH	MW	MVAR	MVA	X--- LOSSES ---X	MW	MVAR	X---- AREA -----X
								51 NOR-EAST
TO	5101 EAST4-A	0.0	178.6	178.6		0.00	0.00	51 NOR-EAST
TO	5111 SVCTERM	0.0	-178.6	178.6		0.00	1.18	51 NOR-EAST

BUS	5300 HDAL3	MW	MVAR	MVA	X--- LOSSES ---X	MW	MVAR	X---- AREA -----X
FROM GENERATION		2092.8	-7.0R	2092.8				53 NOR-HDAL
TO LOAD-PQ		164.1	9.2	164.4				
TO	5100 EAST3	555.6	-18.2	555.9		12.35	123.49	51 NOR-EAST
TO	5301 HDAL4	1373.1	1.9	1373.1		3.02	115.01	53 NOR-HDAL

BUS	5301 HDAL4	MW	MVAR	MVA	X--- LOSSES ---X	MW	MVAR	X---- AREA -----X
								53 NOR-HDAL
TO	5102 EAST4-B	947.3	-68.5	949.8		6.71	96.60	51 NOR-EAST
TO	5103 EAST4-C	422.8	-44.6	425.1		3.04	41.29	51 NOR-EAST
TO	5300 HDAL3	-1370.1	113.1	1374.7		3.02	115.01	53 NOR-HDAL

BUS	5400 CNTR3-A	MW	MVAR	MVA	X--- LOSSES ---X	MW	MVAR	X---- AREA -----X
FROM GENERATION		1460.8	104.4R	1464.5				54 NOR-C-A
TO LOAD-PQ		77.1	0.0	77.1				
TO	5401 CNTR4-A	266.8	5.7	266.9		0.23	8.54	54 NOR-C-A
TO	5402 CNTR4-B	55.2	59.7	81.3		0.00	0.10	54 NOR-C-A
TO	5500 CNTR3-B	969.5	1.2	969.5		8.25	102.89	55 NOR-C-B
TO	6000 WEST300	-70.0	22.3	73.5		0.06	0.56	60 NOR-S-W
TO	6100 NWEST3	162.2	15.5	163.0		0.53	5.28	61 NOR-WEST

BUS	5401 CNTR4-A	MW	MVAR	MVA	X--- LOSSES ---X	MW	MVAR	X---- AREA -----X
								54 NOR-C-A
TO	5400 CNTR3-A	-266.6	2.9	266.6		0.23	8.54	54 NOR-C-A
TO	5501 CNTR4-C	400.2	-74.4	407.1		2.43	32.46	55 NOR-C-B
TO	5602 SOUTH4B	414.0	55.3	417.7		2.79	43.65	56 NOR-SOUT
TO	6001 WEST400	-547.7	16.2	547.9		0.90	15.03	60 NOR-S-W

```
BUS   5402 CNTR4-B       MW     MVAR     MVA   X--- LOSSES ---X X---- AREA -----X
                                                     MW     MVAR   54 NOR-C-A
 TO   5400 CNTR3-A     -55.2   -59.6    81.2       0.00    0.10   54 NOR-C-A
 TO   6001 WEST400      55.2    59.6    81.2       0.04    0.61   60 NOR-S-W

BUS   5500 CNTR3-B       MW     MVAR     MVA   X--- LOSSES ---X X---- AREA -----X
 FROM GENERATION       761.7  -635.0R  991.7       MW     MVAR   55 NOR-C-B
 TO LOAD-PQ           1003.4    93.9  1007.8
 TO   5100 EAST3       268.8   -10.8   269.0       1.29   10.75   51 NOR-EAST
 TO   5400 CNTR3-A    -961.3   101.7   966.6       8.25  102.89   54 NOR-C-A
 TO   5501 CNTR4-C     355.7  -950.0  1014.4       0.42   15.70   55 NOR-C-B
 TO   5603 SOUTH3B      95.0   130.3   161.2       1.09   12.22   56 NOR-SOUT

BUS   5501 CNTR4-C       MW     MVAR     MVA   X--- LOSSES ---X X---- AREA -----X
                                                     MW     MVAR   55 NOR-C-B
 TO   5101 EAST4-A     753.1 -1012.2  1261.6       3.74   39.39   51 NOR-EAST
 TO   5401 CNTR4-A    -397.8    46.5   400.5       2.43   32.46   54 NOR-C-A
 TO   5500 CNTR3-B    -355.3   965.7  1029.0       0.42   15.70   55 NOR-C-B

BUS   5600 SOUTH3A      MW     MVAR     MVA   X--- LOSSES ---X X---- AREA -----X
 FROM GENERATION     2187.5   230.0R 2199.6       MW     MVAR   56 NOR-SOUT
 TO LOAD-PQ          2548.1   242.5  2559.7
 TO   1000 WINDFARN -1000.0  -230.0  1026.1       0.00    0.00   10 WINDFARM
 TO   5601 SOUTH4A     13.6   -70.6    71.9       0.00    0.04   56 NOR-SOUT
 TO   5603 SOUTH3B    648.1   294.4   711.9      10.11  111.22   56 NOR-SOUT
 TO   6000 WEST300     -22.4    -6.2    23.2       0.03    0.27   60 NOR-S-W

BUS   5601 SOUTH4A      MW     MVAR     MVA   X--- LOSSES ---X X---- AREA -----X
                                                     MW     MVAR   56 NOR-SOUT
 TO   5600 SOUTH3A     -13.6    70.7    72.0       0.00    0.04   56 NOR-SOUT
 TO   6001 WEST400      13.6   -70.7    72.0       0.02    0.36   60 NOR-S-W

BUS   5602 SOUTH4B      MW     MVAR     MVA   X--- LOSSES ---X X---- AREA -----X
                                                     MW     MVAR   56 NOR-SOUT
 TO   5401 CNTR4-A    -411.3   -97.4   422.6       2.79   43.65   54 NOR-C-A
 TO   5603 SOUTH3B     411.3    97.4   422.6       0.15    5.74   56 NOR-SOUT

BUS   5603 SOUTH3B      MW     MVAR     MVA   X--- LOSSES ---X X---- AREA -----X
                                                     MW     MVAR   56 NOR-SOUT
 TO LOAD-PQ           1143.0   420.5  1217.9
 TO   5500 CNTR3-B     -93.9  -125.8   157.0       1.09   12.22   55 NOR-C-B
 TO   5600 SOUTH3A    -638.0  -203.1   669.5      10.11  111.22   56 NOR-SOUT
 TO   5602 SOUTH4B    -411.1   -91.6   421.2       0.15    5.74   56 NOR-SOUT

BUS   6000 WEST300      MW     MVAR     MVA   X--- LOSSES ---X X---- AREA -----X
 FROM GENERATION     1038.6  -203.2R 1058.3       MW     MVAR   60 NOR-S-W
 TO LOAD-PQ             3.3     0.0     3.3
 TO   5400 CNTR3-A     70.1   -31.9    77.0       0.06    0.56   54 NOR-C-A
 TO   5600 SOUTH3A     22.4   -39.2    45.2       0.03    0.27   56 NOR-SOUT
 TO   6001 WEST400    778.4  -131.0   789.4       0.25    9.37   60 NOR-S-W
 TO   6100 NWEST3     164.4    -1.0   164.4       0.59    6.43   61 NOR-WEST
BUS   6001 WEST400      MW     MVAR     MVA   X--- LOSSES ---X X---- AREA -----X
                                                     MW     MVAR   60 NOR-S-W
 TO   5102 EAST4-B     298.3   -49.3   302.4       1.78   31.08   51 NOR-EAST
 TO   5401 CNTR4-A     548.6   -16.2   548.8       0.90   15.03   54 NOR-C-A
 TO   5402 CNTR4-B     -55.2   -82.6    99.4       0.04    0.61   54 NOR-C-A
 TO   5601 SOUTH4A     -13.6     7.8    15.7       0.02    0.36   56 NOR-SOUT
 TO   6000 WEST300    -778.2   140.4   790.7       0.25    9.37   60 NOR-S-W

BUS   6100 NWEST3       MW     MVAR     MVA   X--- LOSSES ---X X---- AREA -----X
 FROM GENERATION     2158.1   765.2R 2289.7       MW     MVAR   61 NOR-WEST
 TO LOAD-PQ          2483.6   800.1  2609.3
 TO   5400 CNTR3-A    -161.7   -22.3   163.2       0.53    5.28   54 NOR-C-A
 TO   6000 WEST300    -163.9   -12.6   164.3       0.59    6.43   60 NOR-S-W

BUS   6500 MID300       MW     MVAR     MVA   X--- LOSSES ---X X---- AREA -----X
 FROM GENERATION     1390.0   443.6R 1459.1       MW     MVAR   65 NOR-MID
 TO LOAD-PQ          1566.8   227.8  1583.2
 TO   3244 SV-M2      333.6   -44.3   336.6       0.57    5.66   40 SWEDEN
 TO   5100 EAST3       95.2    -3.2    95.2       1.36   13.60   51 NOR-EAST
 TO   6700 NOR300    -605.6   263.2   660.3      35.10  482.56   67 NOR-NORT

BUS   6700 NOR300       MW     MVAR     MVA   X--- LOSSES ---X X---- AREA -----X
 FROM GENERATION     2549.1   559.0R 2609.6       MW     MVAR   67 NOR-NORT
 TO LOAD-PQ          1573.3   364.1  1614.9
 TO   3701 SV-N2B      69.3    12.3    70.4       0.05    4.83   40 SWEDEN
 TO   6500 MID300     640.7   209.1   674.0      35.10  482.56   65 NOR-MID
 TO   6701 NOR400     265.8   -26.5   267.1       0.35    1.41   67 NOR-NORT

BUS   6701 NOR400       MW     MVAR     MVA   X--- LOSSES ---X X---- AREA -----X
                                                     MW     MVAR   67 NOR-NORT
 TO   3115 SV-N1      265.4   -27.9   266.9       2.78   20.86   40 SWEDEN
 TO   6700 NOR300    -265.4    27.9   266.9       0.35    1.41   67 NOR-NORT

BUS   7000 SO-FIN       MW     MVAR     MVA   X--- LOSSES ---X X---- AREA -----X
 FROM GENERATION     5300.0  1016.1R 5396.5       MW     MVAR   70 FIN-SOUT
 TO LOAD-PQ          5600.0  1250.0  5737.8
 TO   7100 NO-FIN    -150.0  -117.0   190.2       3.30   23.59   71 FIN-NORT
 TO   7100 NO-FIN    -150.0  -117.0   190.2       3.30   23.59   71 FIN-NORT

BUS   7100 NO-FIN       MW     MVAR     MVA   X--- LOSSES ---X X---- AREA -----X
 FROM GENERATION     1310.0   683.0R 1477.3       MW     MVAR   71 FIN-NORT
 TO LOAD-PQ          2500.0   400.0  2531.8
 TO   3115 SV-N1     -757.2   308.9   817.8      70.21  491.48   40 SWEDEN
 TO   3249 SV-N2     -739.4   292.9   795.3      66.44  465.06   40 SWEDEN
 TO   7000 SO-FIN     153.3  -159.4   221.2       3.30   23.59   70 FIN-SOUT
 TO   7000 SO-FIN     153.3  -159.4   221.2       3.30   23.59   70 FIN-SOUT

BUS   8500 SJOLLAND     MW     MVAR     MVA   X--- LOSSES ---X X---- AREA -----X
 FROM GENERATION     1000.0   909.8R 1351.9       MW     MVAR   90 SJELLAND
 TO LOAD-PQ          1000.0  1000.0  1414.2
 TO   3300 SV-SW        0.0   -90.2    90.2       0.33    1.29   40 SWEDEN
```

APPENDIX E: DYNAMIC VERIFICATIONS FOR THE ORIGINAL MODEL

ORIGINAL MODEL, BUS FAULT ON BUS 5401

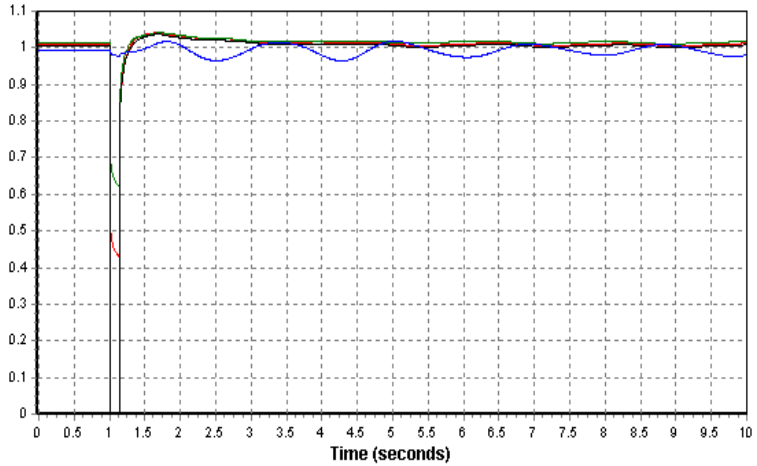

Voltage at the bus 3300 (blue), at the bus 5401(black), at the bus 5600 (green) and at the bus 6000(red) [p.u]

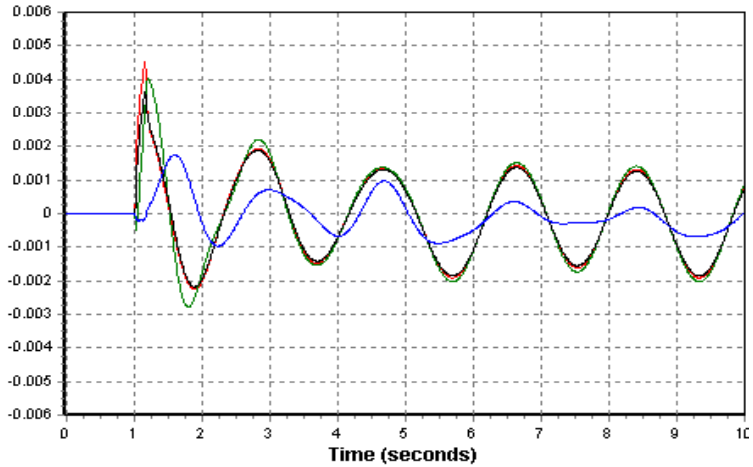

Frequency deviation at the bus 3300 (blue), at the bus 5401(black), at the bus 5600 (green) and at the bus 6000(red) [p.u]

ORIGINAL MODEL, BUS FAULT ON BUS 5600

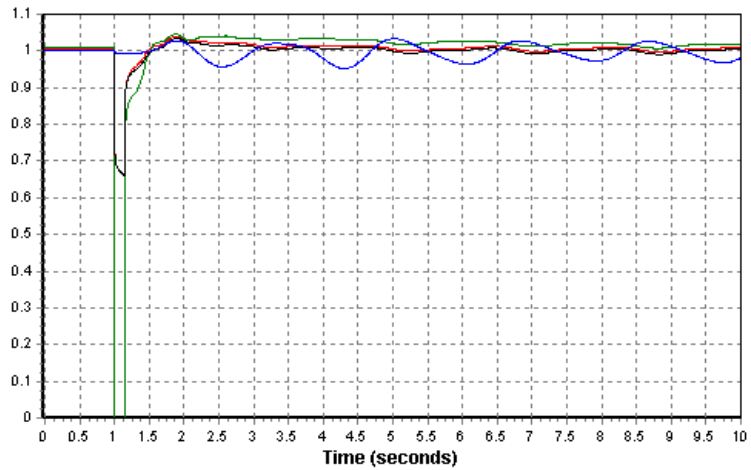

Voltage at the bus 3300 (blue), at the bus 5401(black), at the bus 5600 (green) and at the bus 6000(red) [p.u]

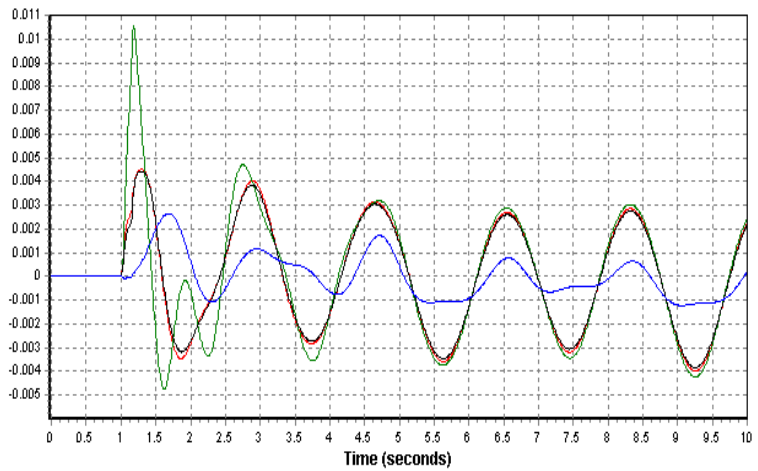

Frequency deviation at the bus 3300 (blue), at the bus 5401(black), at the bus 5600 (green) and at the bus 6000(red) [p.u]

ORIGINAL MODEL, BUS FAULT ON BUS 6000

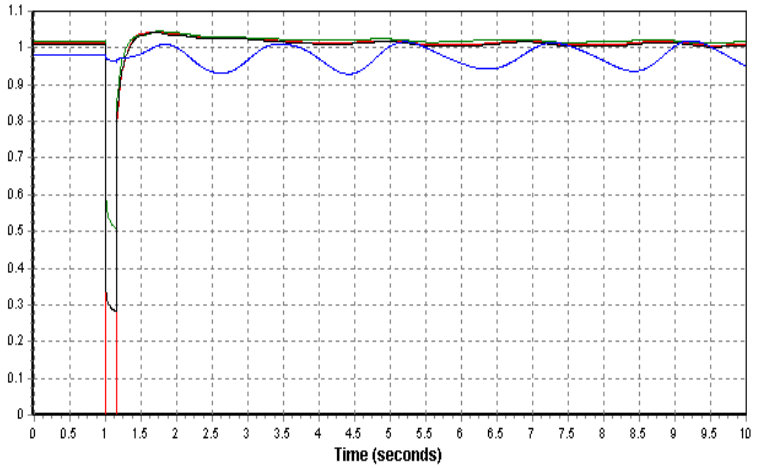

Voltage at the bus 3300 (blue), at the bus 5401(black), at the bus 5600 (green) and at the bus 6000(red) [p.u]

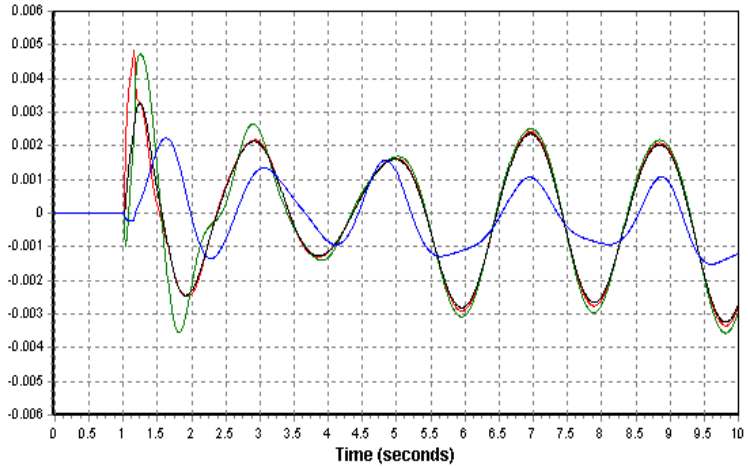

Frequency deviation at the bus 3300 (blue), at the bus 5401(black), at the bus 5600 (green) and at the bus 6000(red) [p.u]

APPENDIX F: DYNAMIC SIMULATION RESULTS

CONFIGURATION 1: HVAC LINK , CONNECTION BUS 6000

Fault 1, bus fault at connection bus 6000

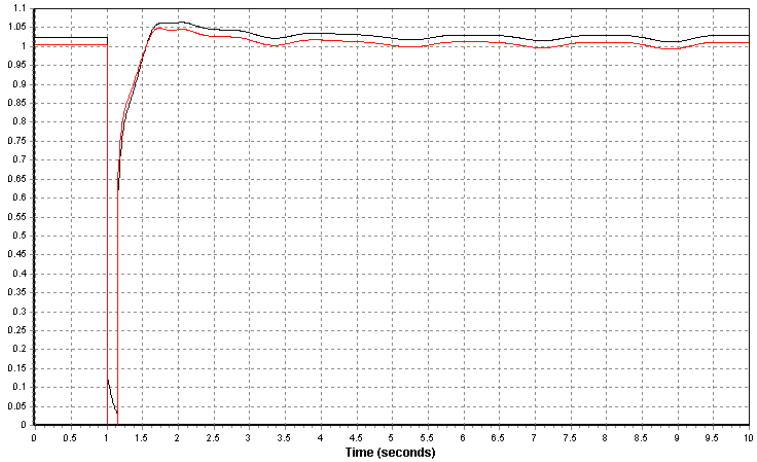

Voltage at offshore bus (black) and onshore bus (red) [p.u]

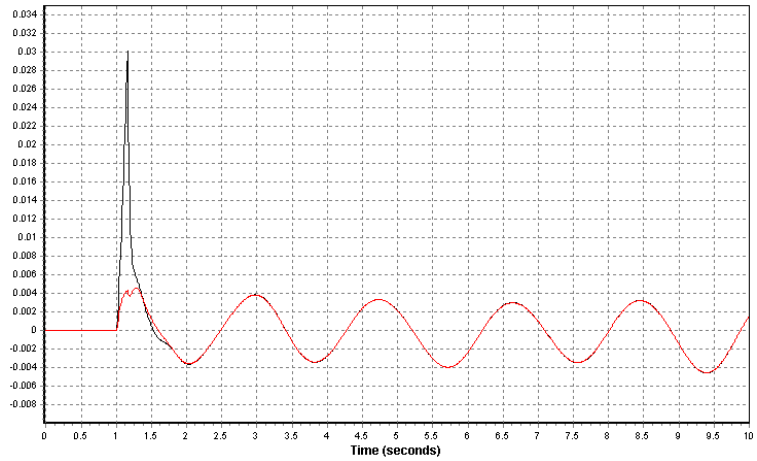

Frequency deviation at bus offshore (black) and onshore bus (red) [p.u]

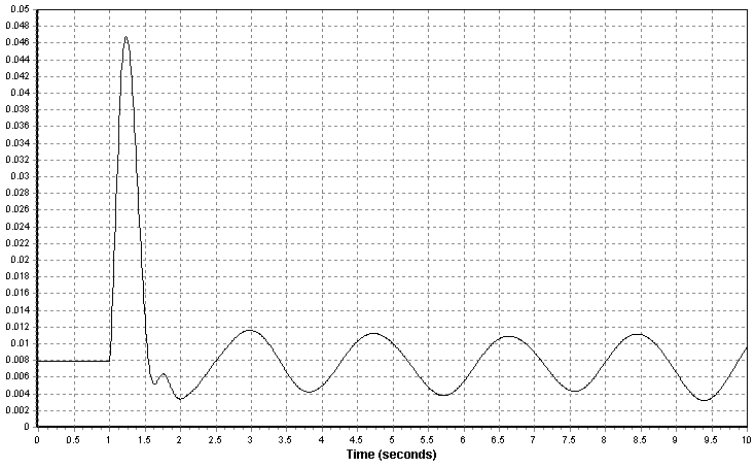

Speed deviation of the wind turbine generator [p.u]

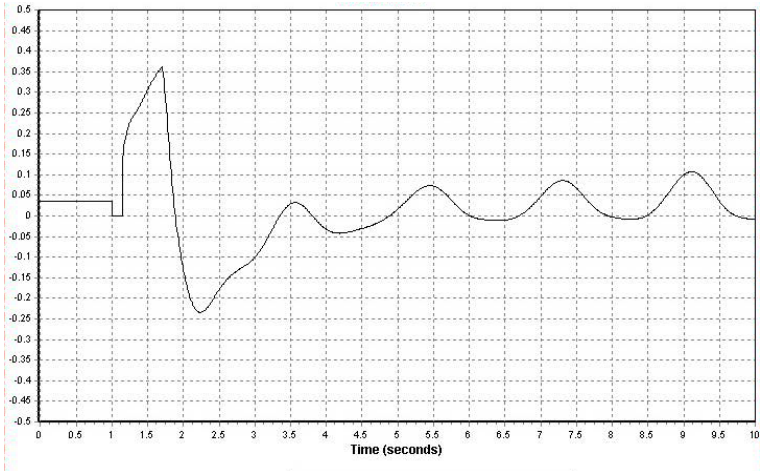

Reactive power from wind farm SVC [p.u].

Fault 2, bus fault at neighbour bus 5400

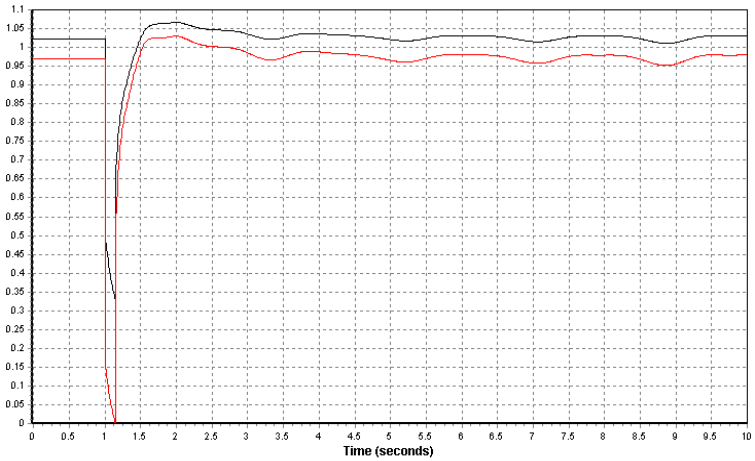

Voltage at offshore bus (black) and onshore bus (red) [p.u]

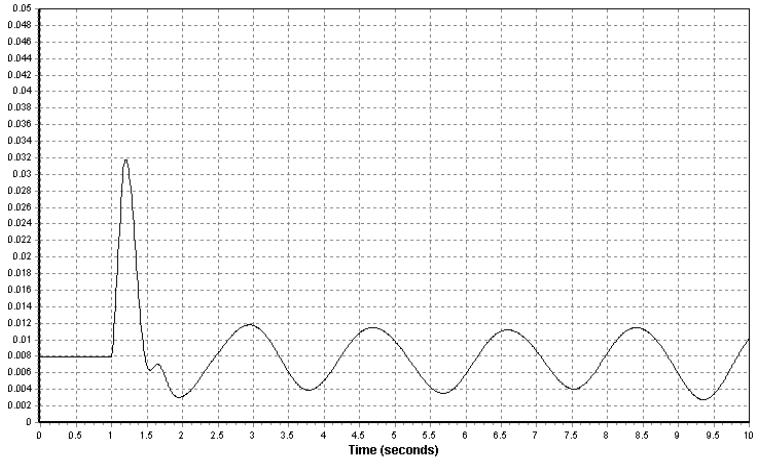

Speed deviation of the wind turbine generator [p.u]

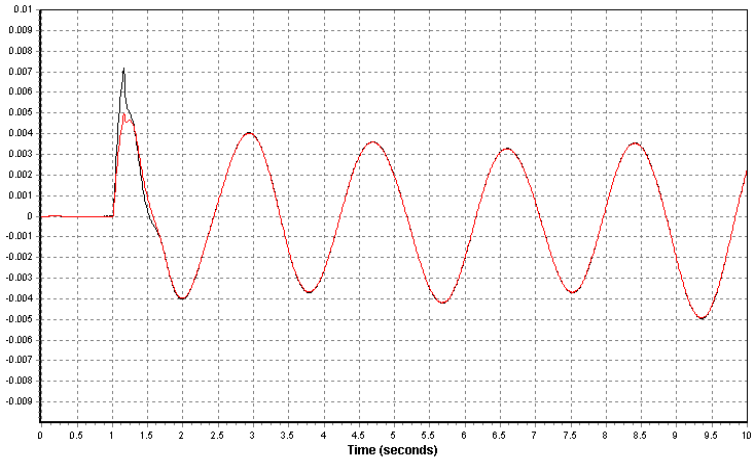

Frequency deviation at bus offshore (black) and onshore bus (red) [p.u]

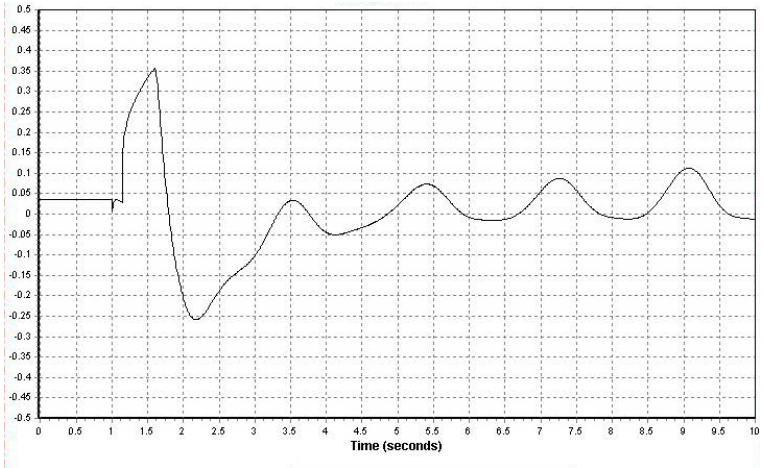

Reactive power from wind farm SVC [p.u]

Fault 3, line fault on the line from bus 6000 to bus 5400

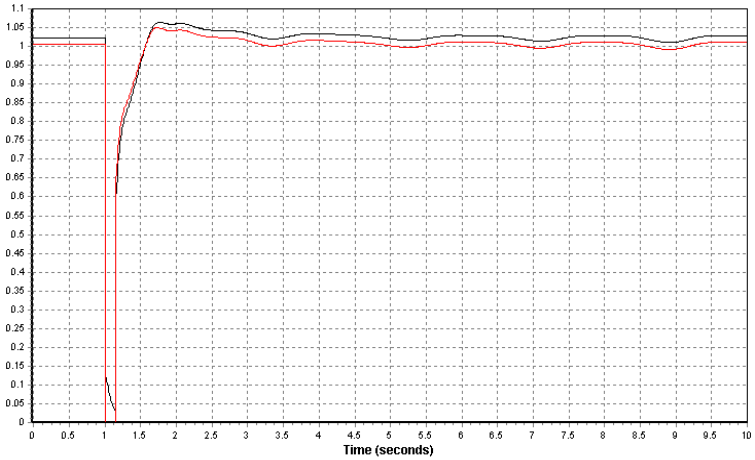

Voltage at offshore bus (black) and onshore bus (red) [p.u]

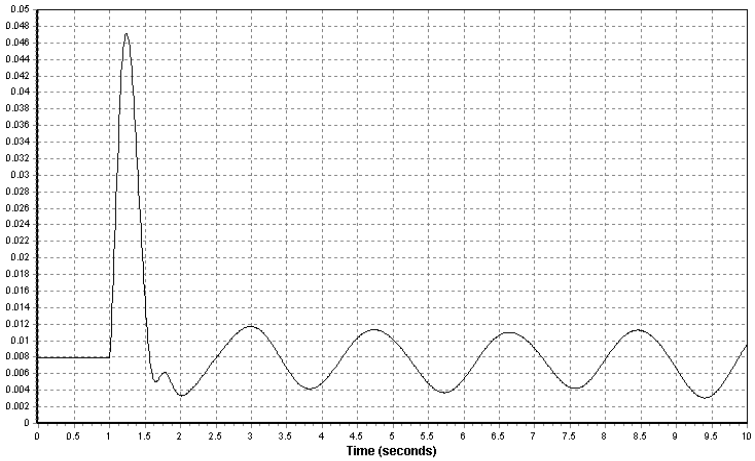

Speed deviation of the wind turbine generator [p.u]

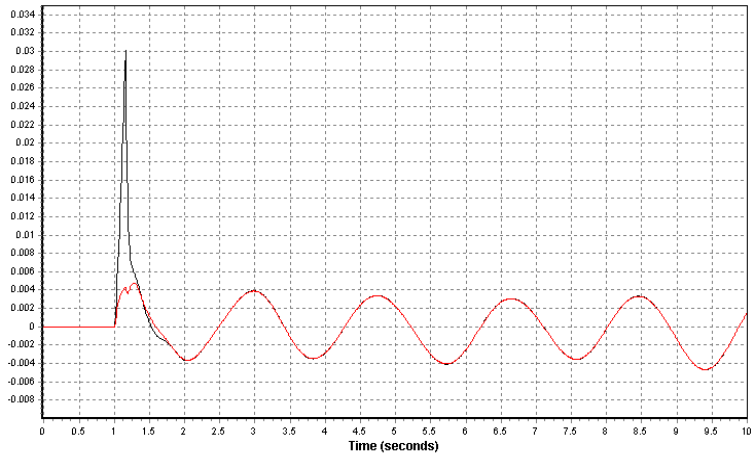

Frequency deviation at bus offshore (black) and onshore bus (red) [p.u]

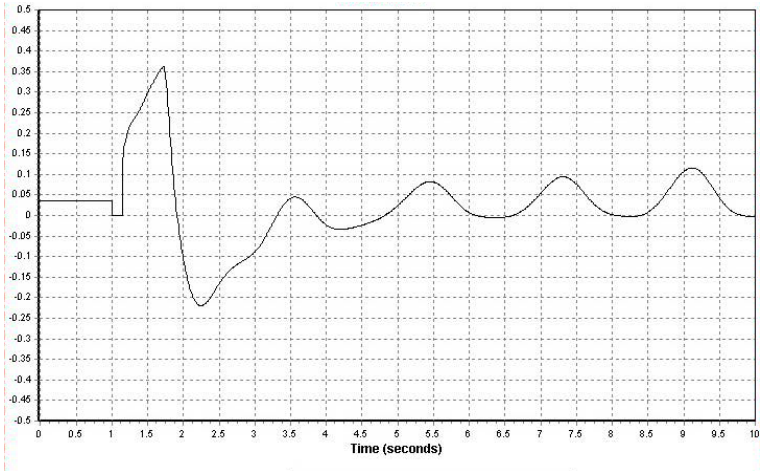

Reactive power from wind farm SVC [p.u]

Fault 4, bus fault on the wind farm bus 1000

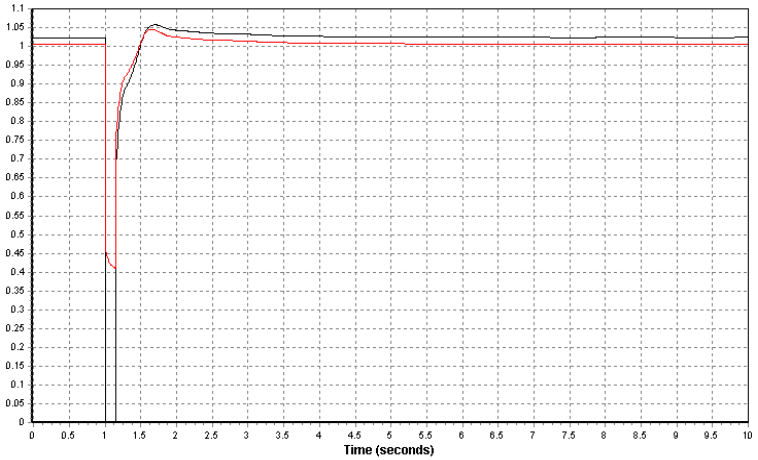

Voltage at offshore bus (black) and onshore bus (red) [p.u]

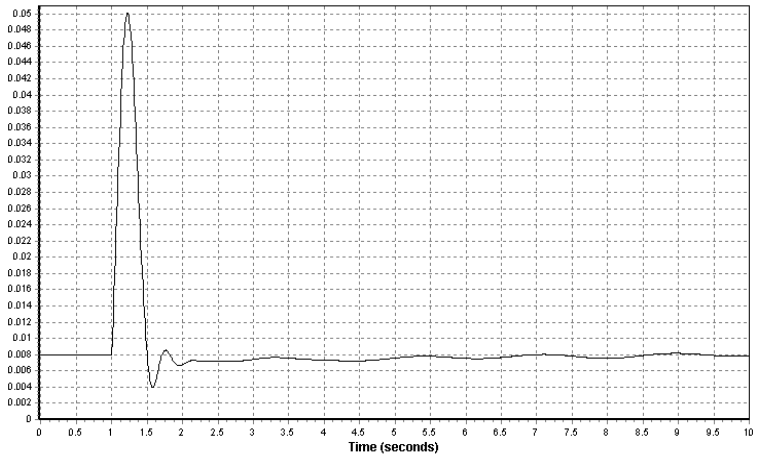

Speed deviation of the wind turbine generator [p.u]

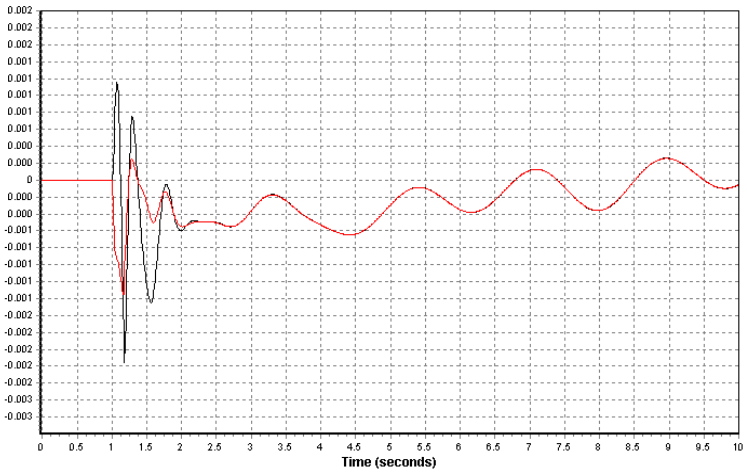

Frequency deviation at bus offshore (black) and onshore bus (red) [p.u]

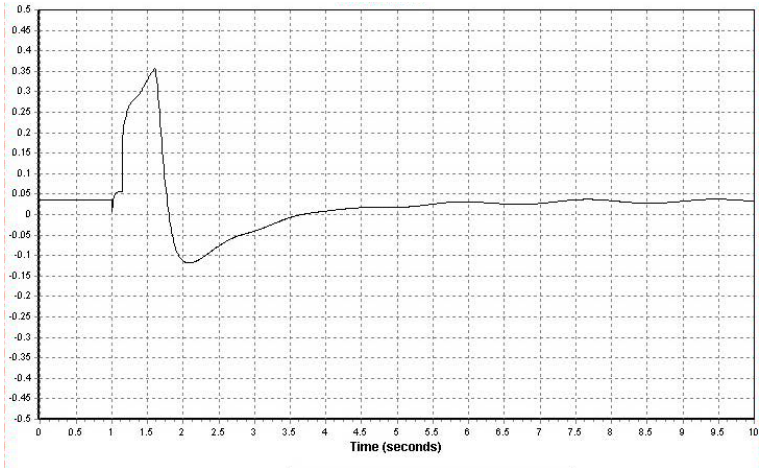

Reactive power from wind farm SVC [p.u]

CONFIGURATION 1 : HVAC LINK , CONNECTION BUS 5600

Fault 1, bus fault at connection bus 5600

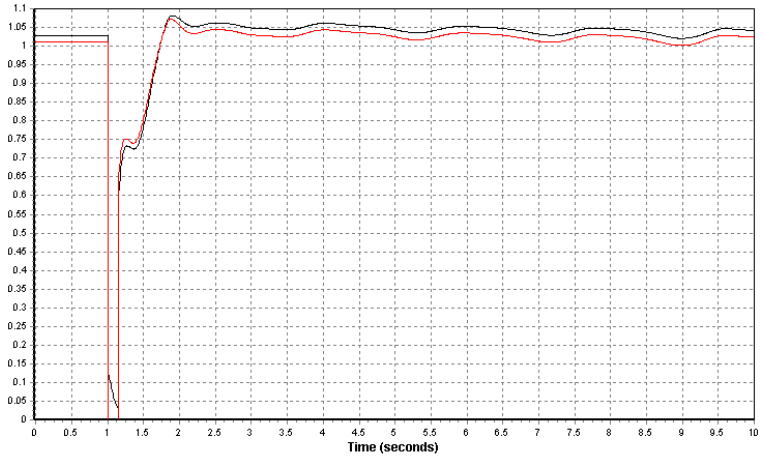

Voltage at offshore bus (black) and onshore bus (red) [p.u]

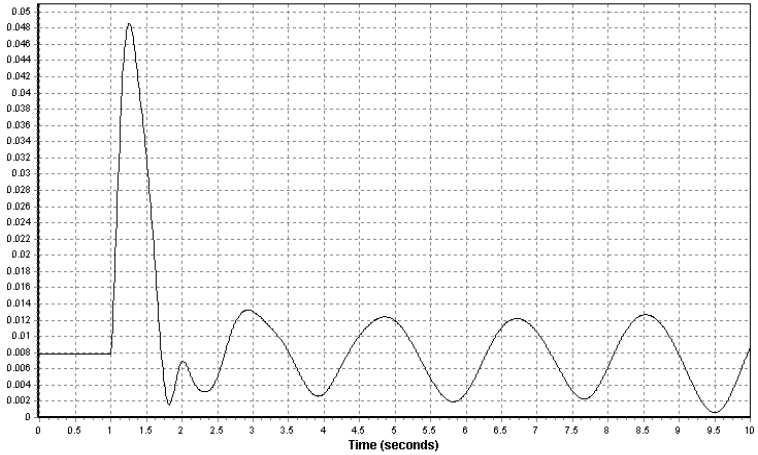

Speed deviation of the wind turbine generator [p.u]

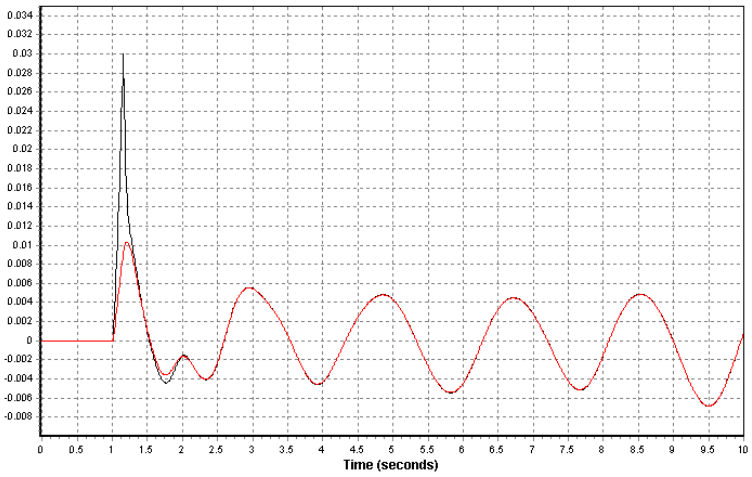

Frequency deviation at bus offshore (black) and onshore bus (red) [p.u]

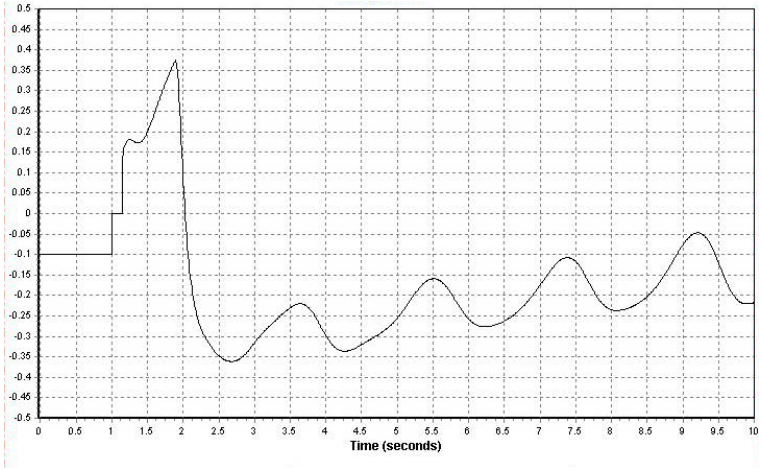

Reactive power from wind farm SVC [p.u]

Fault 2, bus fault at neighbour bus 5603

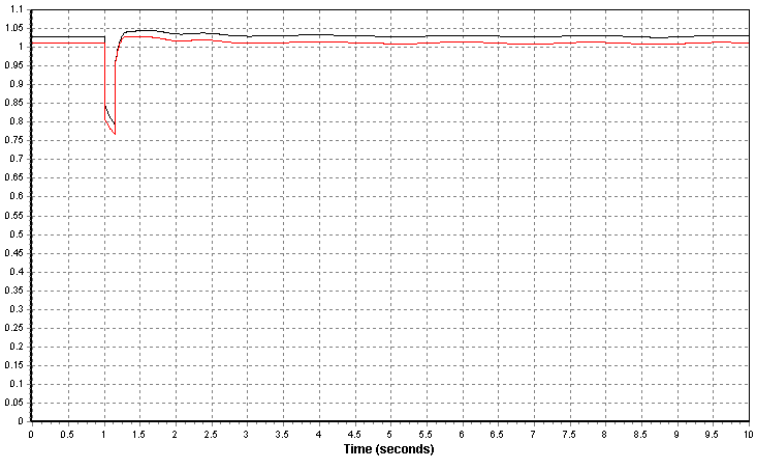

Voltage at offshore bus (black) and onshore bus (red) [p.u]

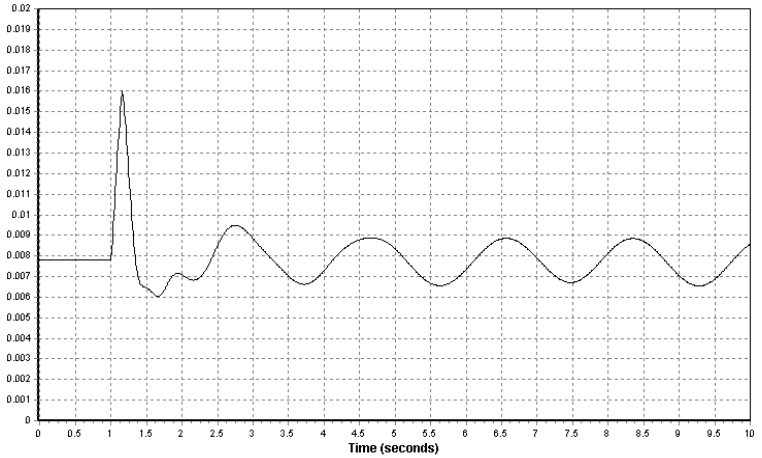

Speed deviation of the wind turbine generator [p.u]

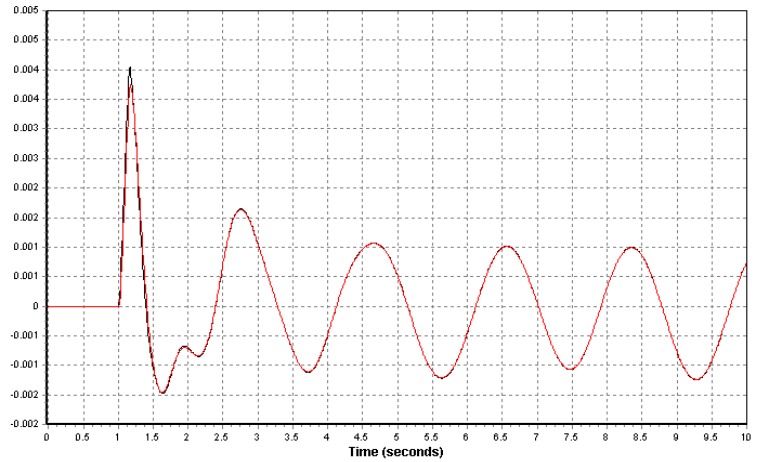

Frequency deviation at bus offshore (black) and onshore bus (red) [p.u]

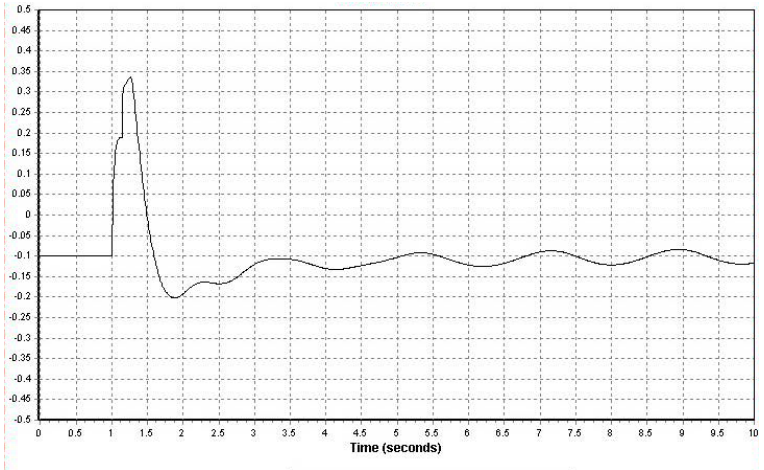

Reactive power from wind farm SVC [p.u]

Fault 3, line fault on the line from bus 5600 to bus 5603

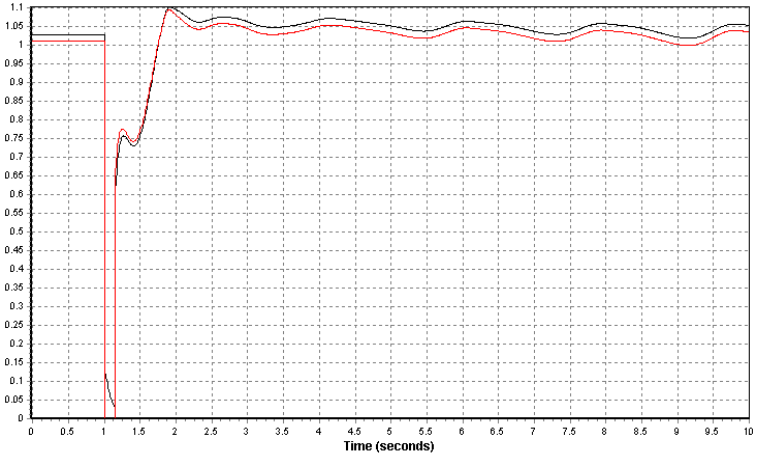

Voltage at offshore bus (black) and onshore bus (red) [p.u]

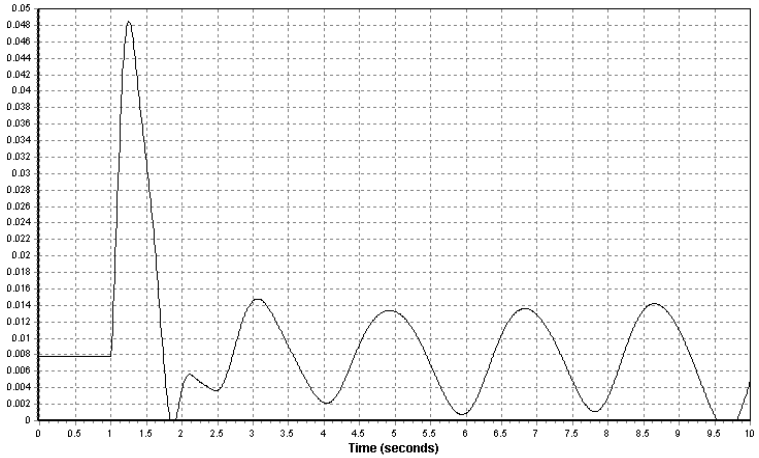

Speed deviation of the wind turbine generator [p.u]

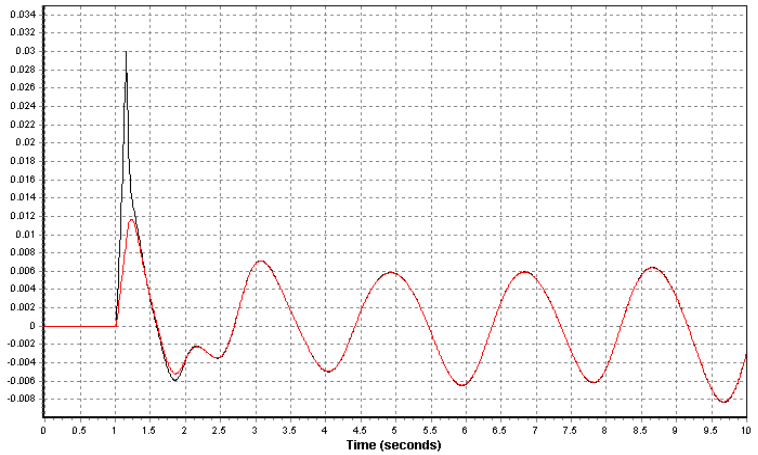

Frequency deviation at bus offshore (black) and onshore bus (red) [p.u]

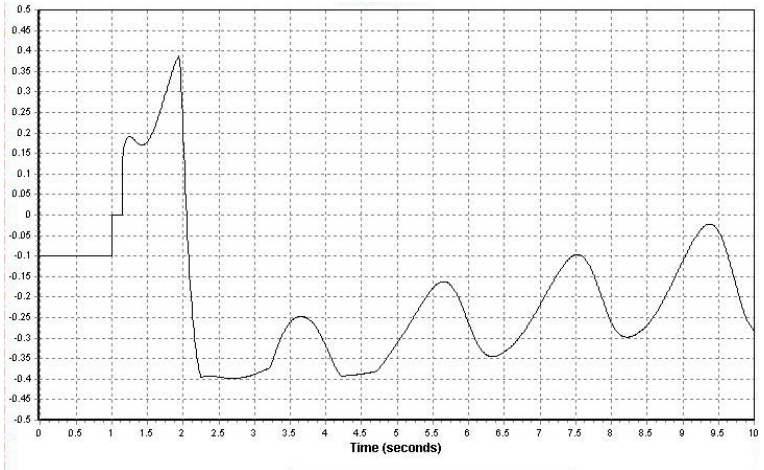

Reactive power from wind farm SVC [p.u]

Fault 4, bus fault on the wind farm bus 1000

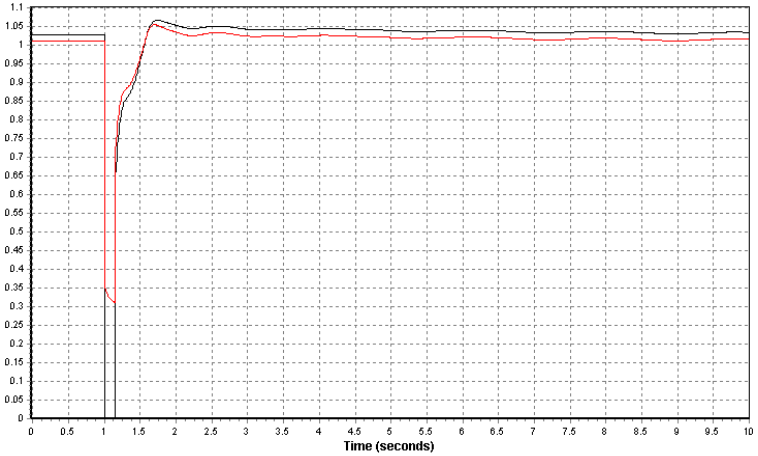

Voltage at offshore bus (black) and onshore bus (red) [p.u]

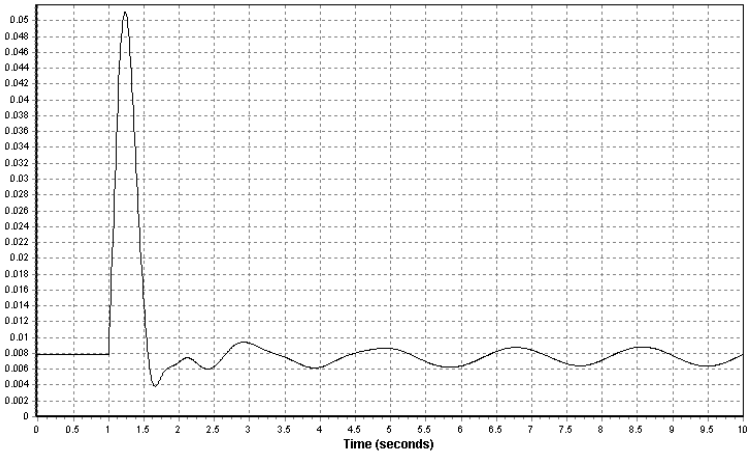

Speed deviation of the wind turbine generator [p.u]

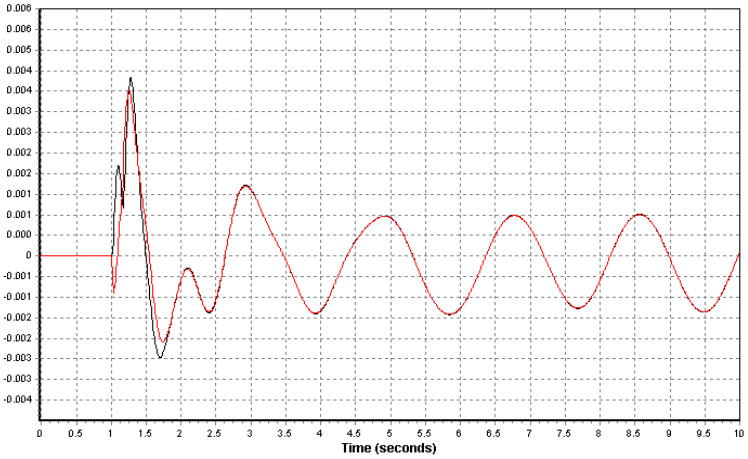

Frequency deviation at bus offshore (black) and onshore bus (red) [p.u]

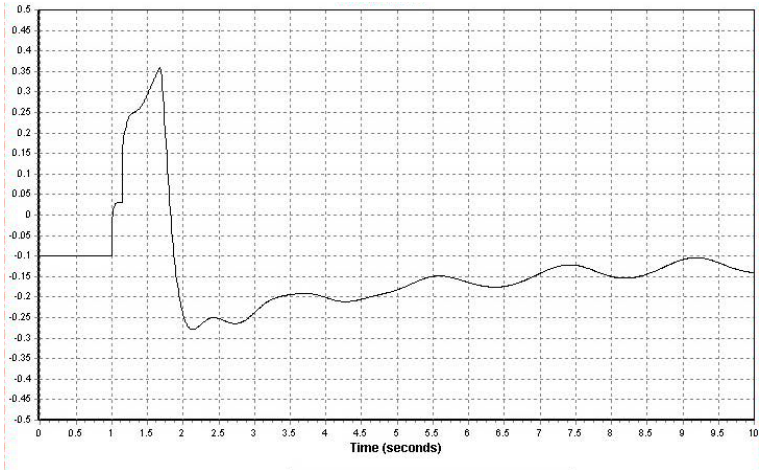

Reactive power from wind farm SVC [p.u]

CONFIGURATION 2 : HVDC LINK , CONNECTION BUS 6000

Fault 1, bus fault at connection bus 6000

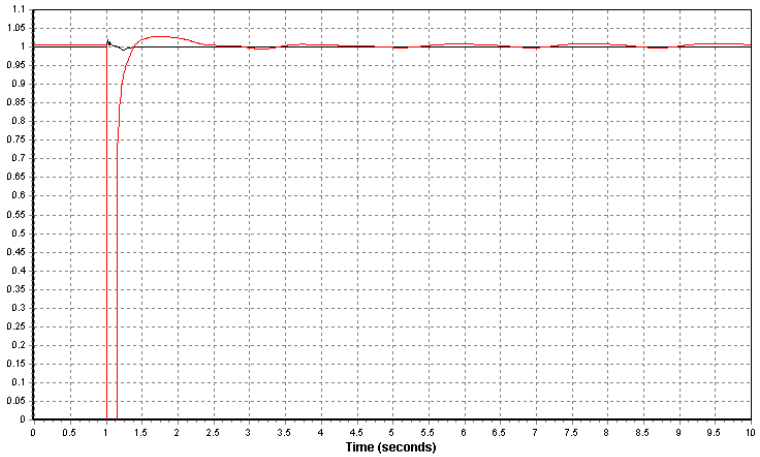

Voltage at offshore bus (black) and onshore bus (red) [p.u]

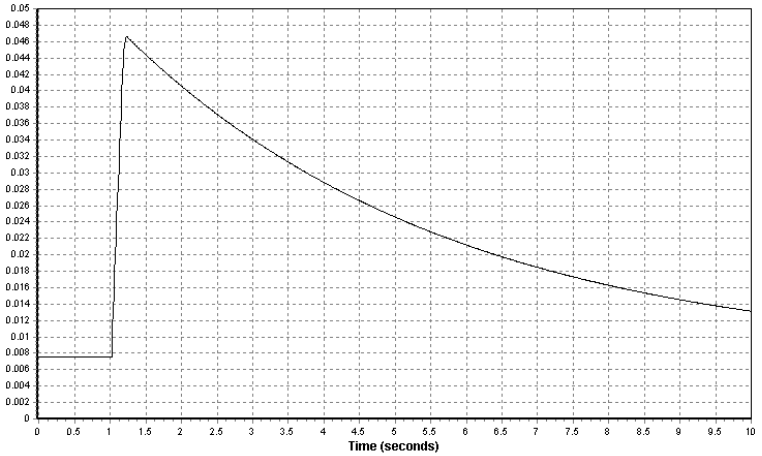

Speed deviation of the wind turbine generator [p.u]

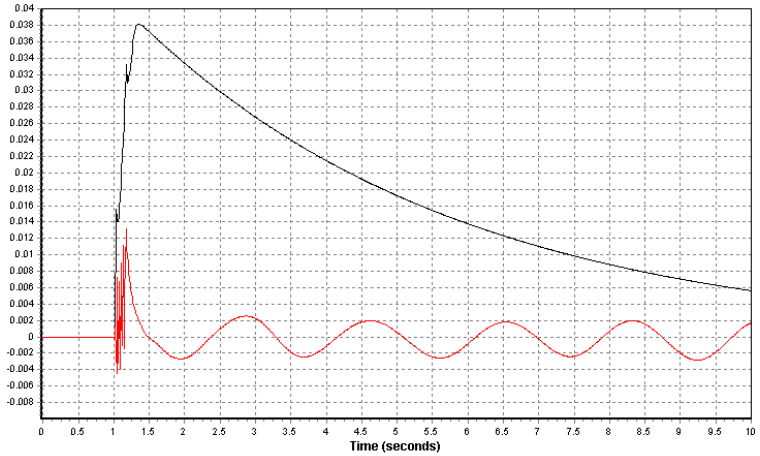

Frequency deviation at bus offshore (black) and onshore bus (red) [p.u]

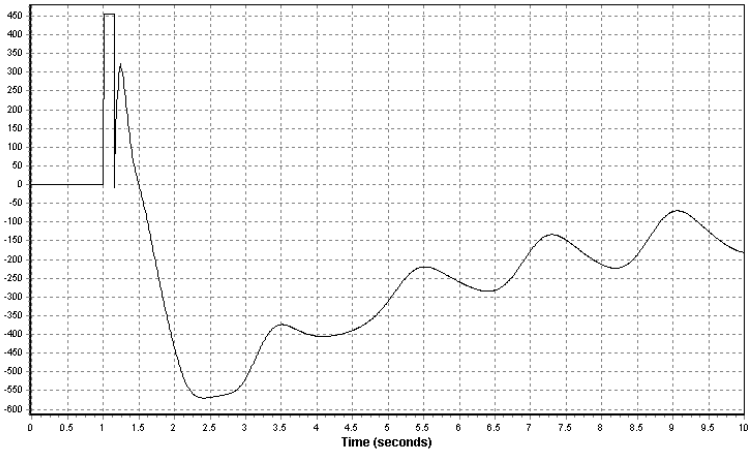

Reactive power from the onshore converter [MVar]

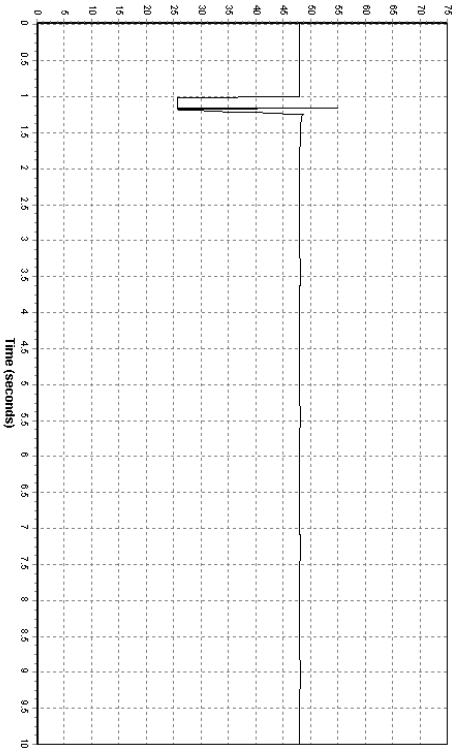

Losses on the DC line [MW]

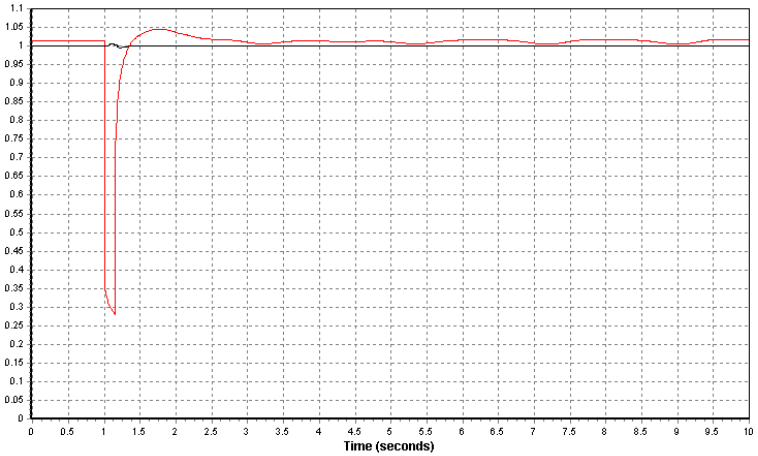

Voltage at offshore bus (black) and onshore bus (red) [p.u]

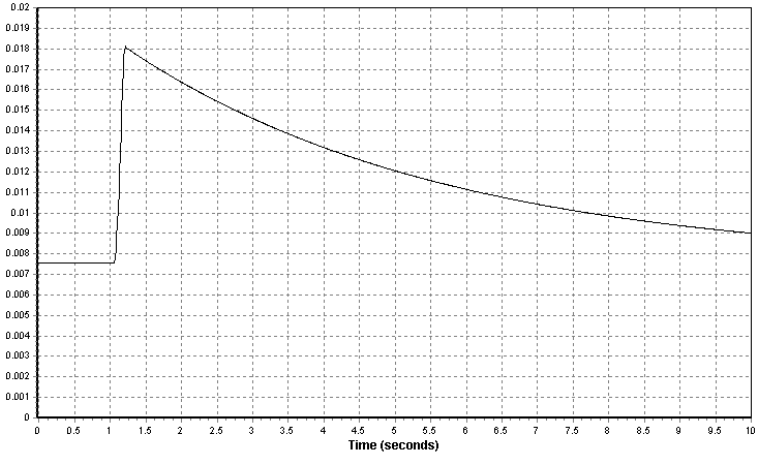

Speed deviation of the wind turbine generator [p.u]

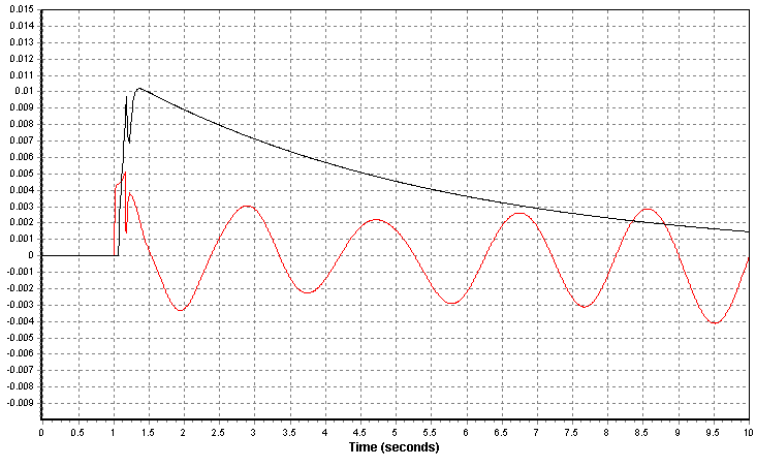

Frequency deviation at bus offshore (black) and onshore bus (red) [p.u]

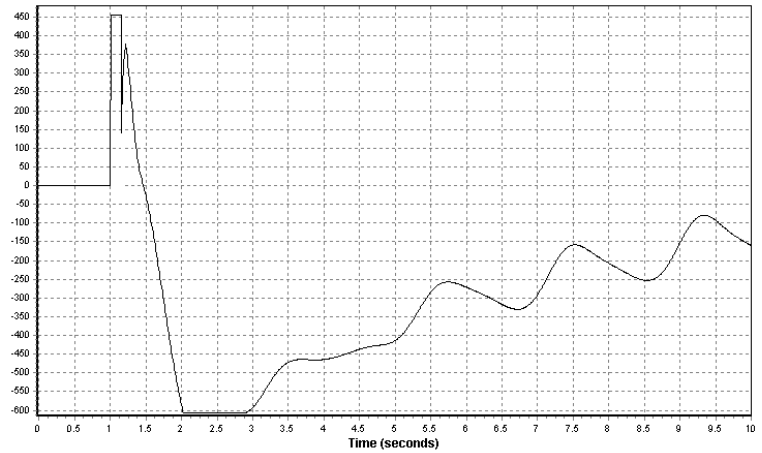

Reactive power from the onshore converter [MVar]

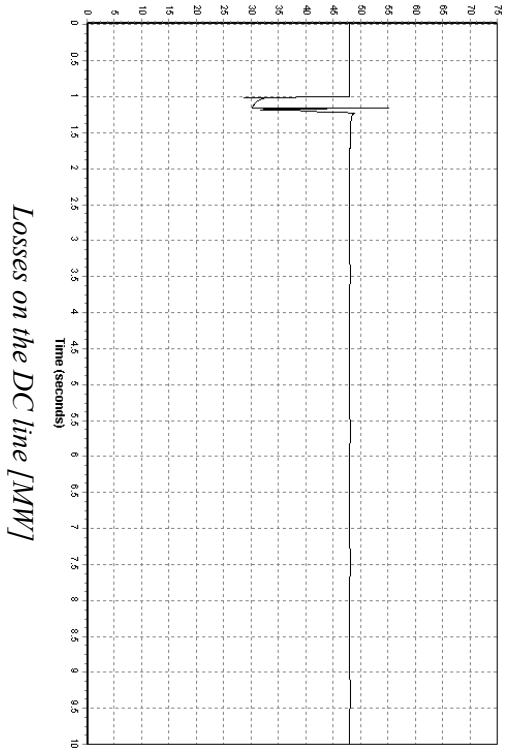

Losses on the DC line [MW]

Fault 3, line fault on the line from bus 6000 to bus 5400

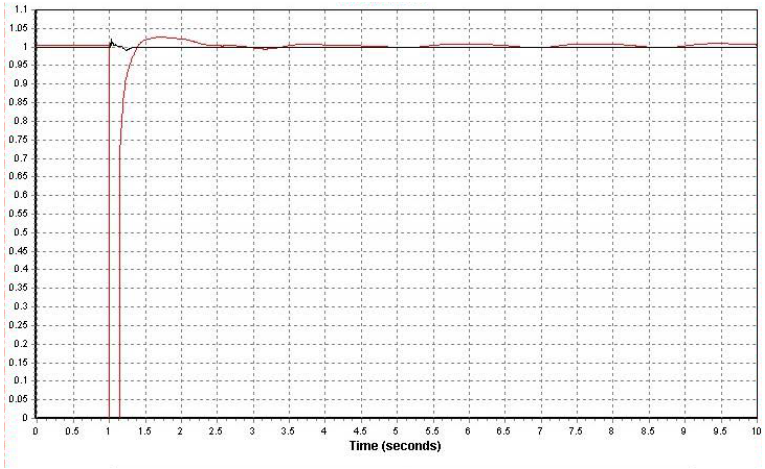

Voltage at offshore bus (black) and onshore bus (red) [p.u]

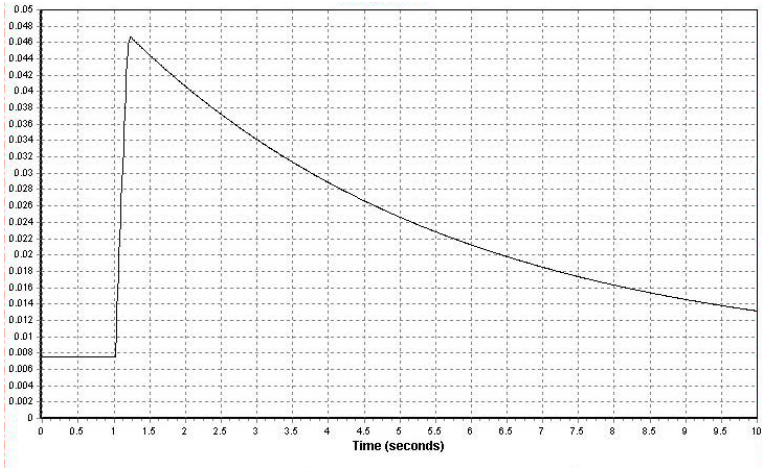

Speed deviation of the wind turbine generator [p.u]

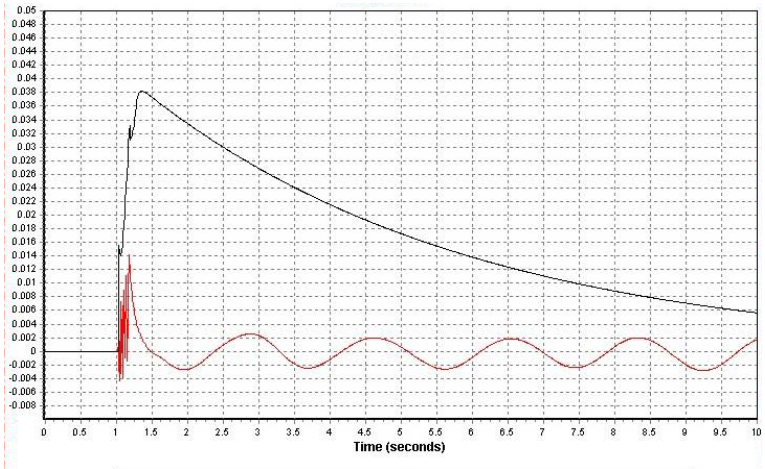

Frequency deviation at bus offshore (black) and onshore bus (red) [p.u]

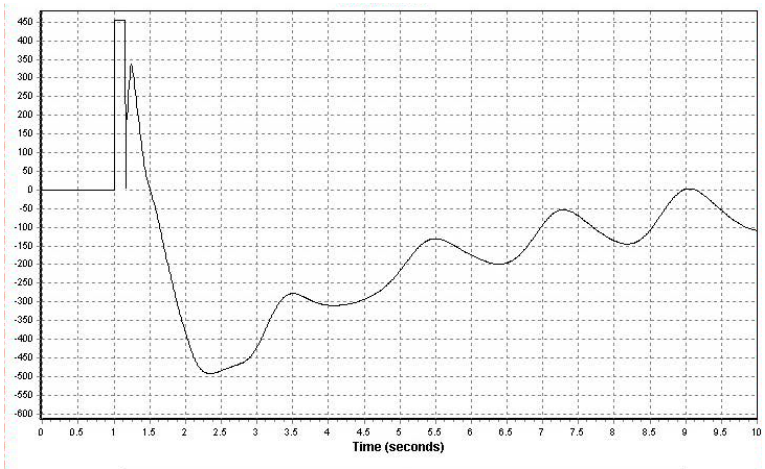

Reactive power from the onshore converter [MVar]

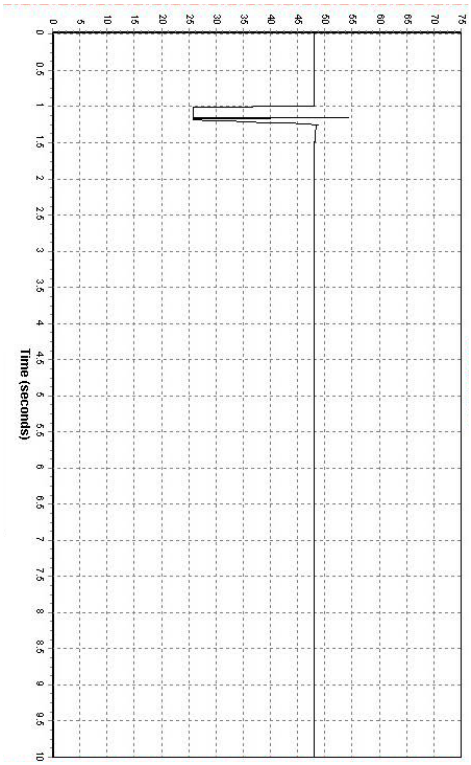

Losses on the DC line [MW]

Fault 4, bus fault on the wind farm bus 1000

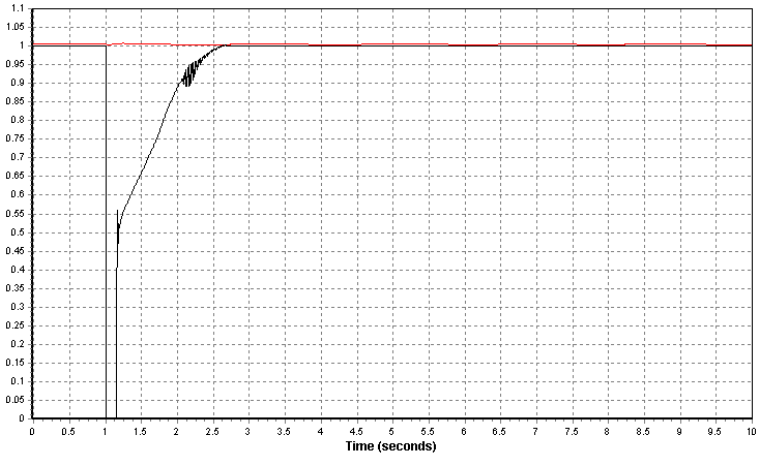

Voltage at offshore bus (black) and onshore bus (red) [p.u]

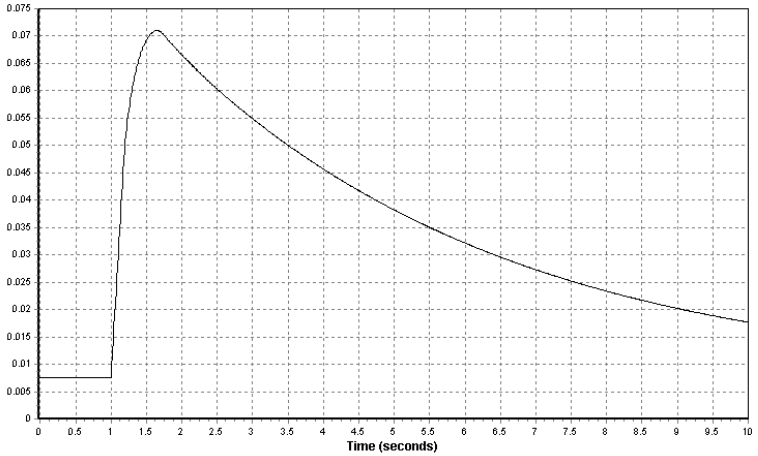

Speed deviation of the wind turbine generator [p.u]

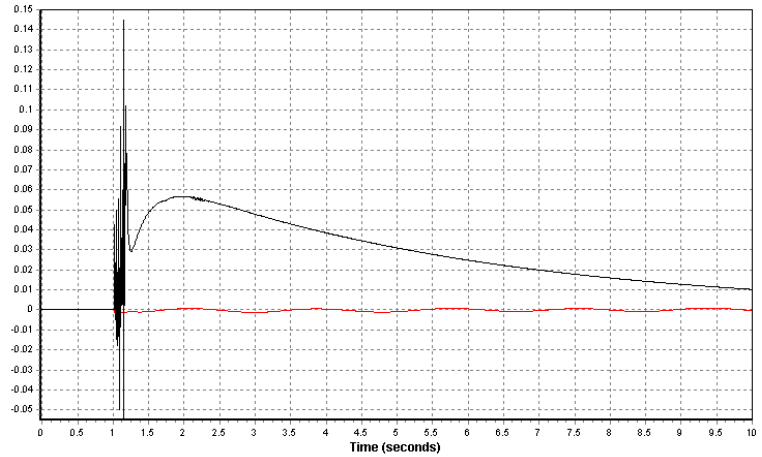

Frequency deviation at bus offshore (black) and onshore bus (red) [p.u]

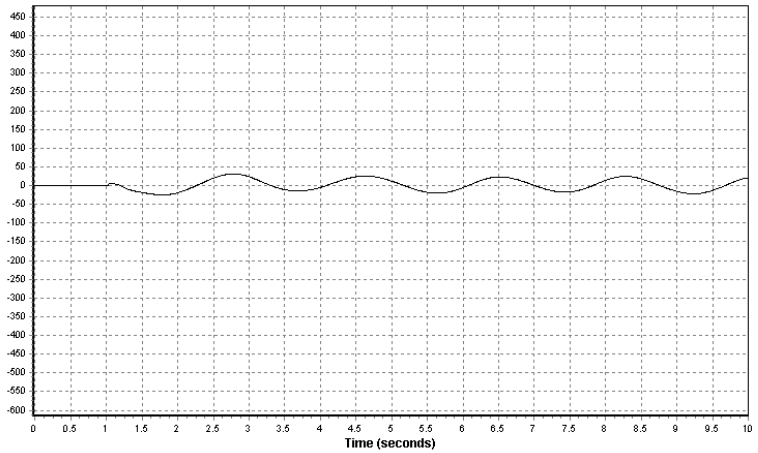

Reactive power from the onshore converter [MVar]

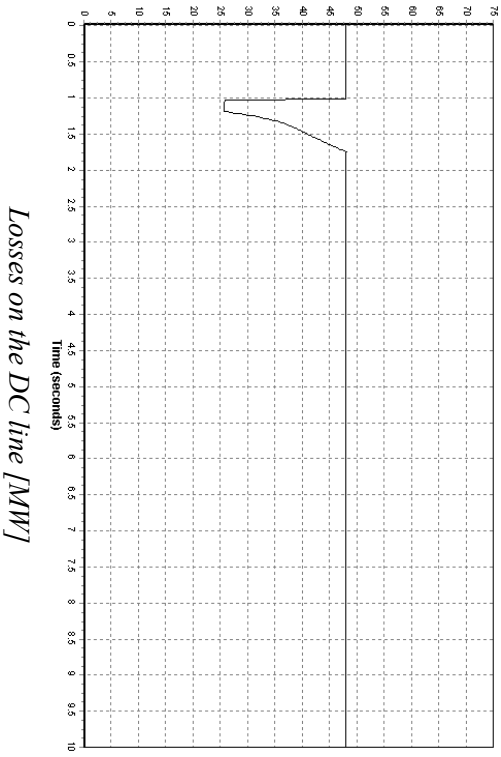

Losses on the DC line [MW]

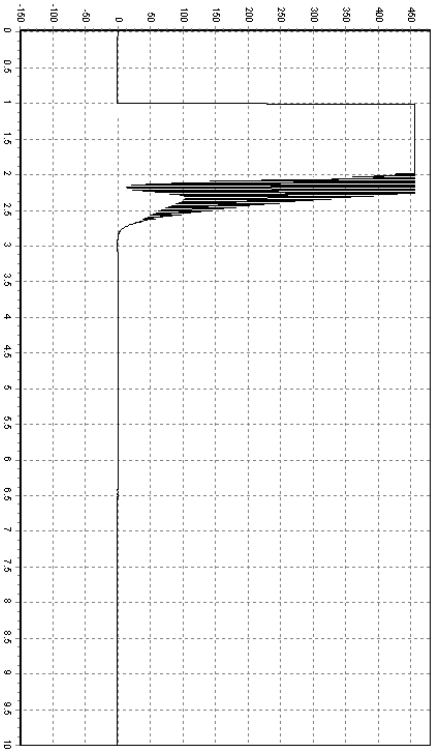

Reactive power from the offshore converter [MVar]

CONFIGURATION 2: HVDC LINK , CONNECTION BUS 5600

Fault 1, bus fault at connection bus 5600

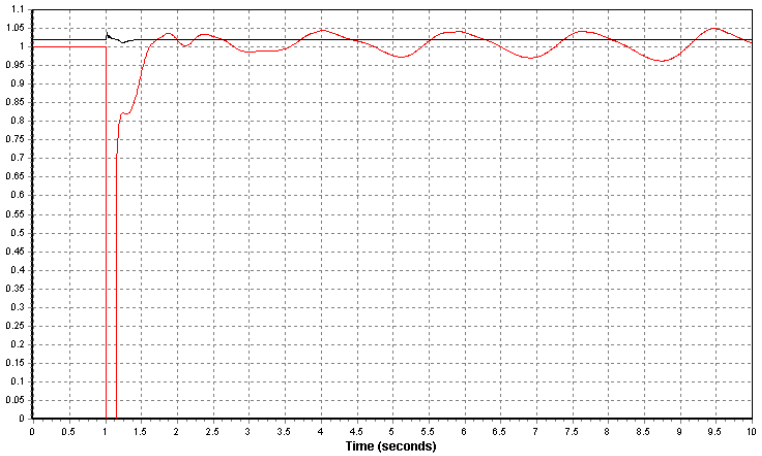

Voltage at offshore bus (black) and onshore bus (red) [p.u]

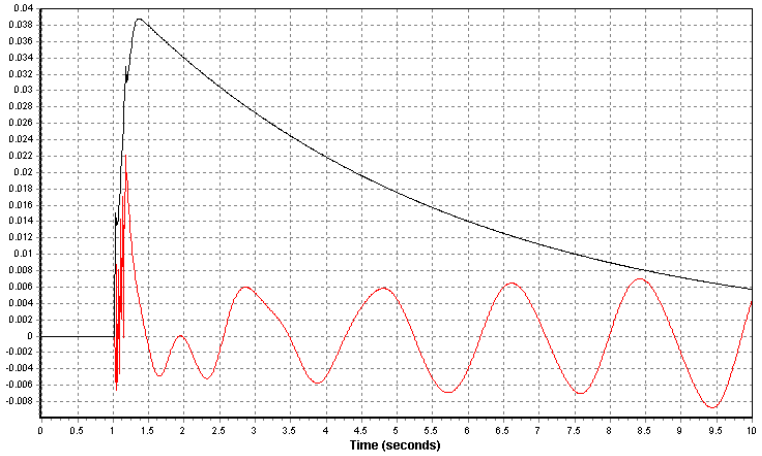

Frequency deviation at bus offshore (black) and onshore bus (red) [p.u]

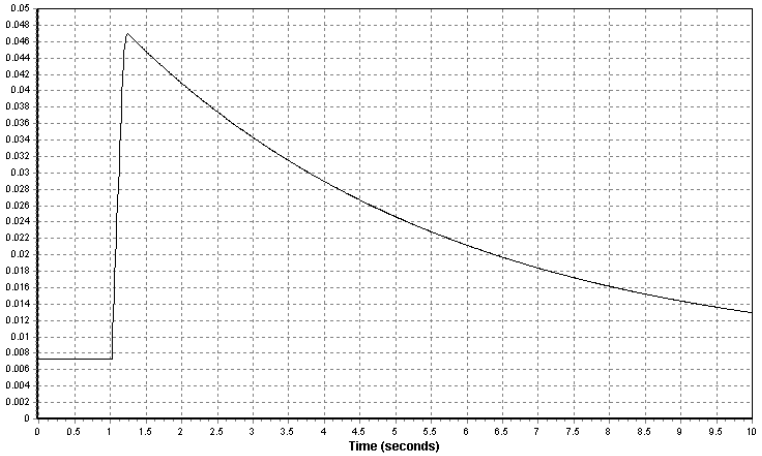

Speed deviation of the wind turbine generator [p.u]

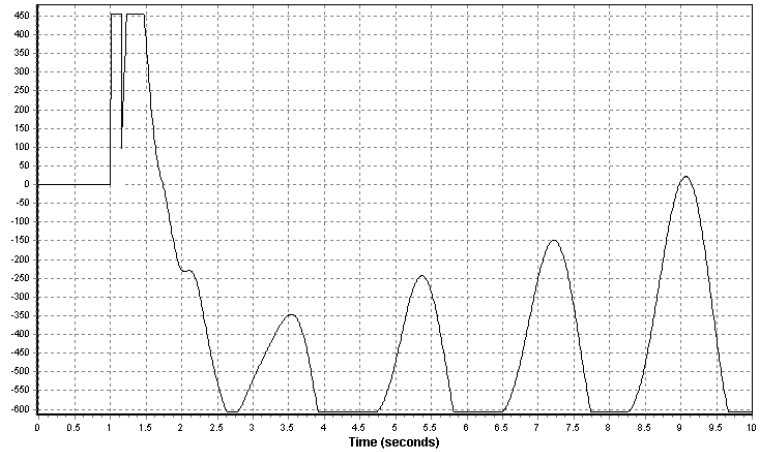

Reactive power from the onshore converter [MVar]

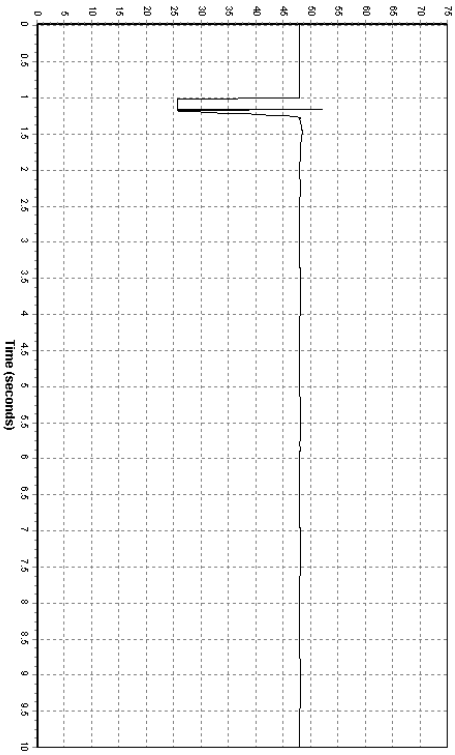

Losses on the DC line [MW]

Fault 2, bus fault at neighbour bus 5603

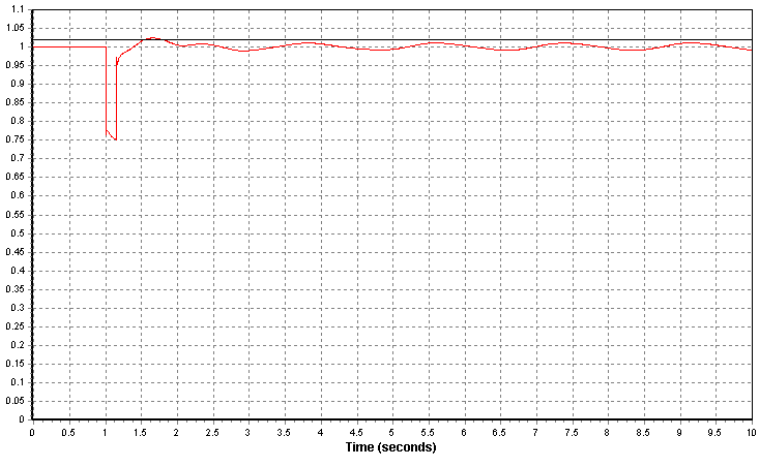

Voltage at offshore bus (black) and onshore bus (red) [p.u]

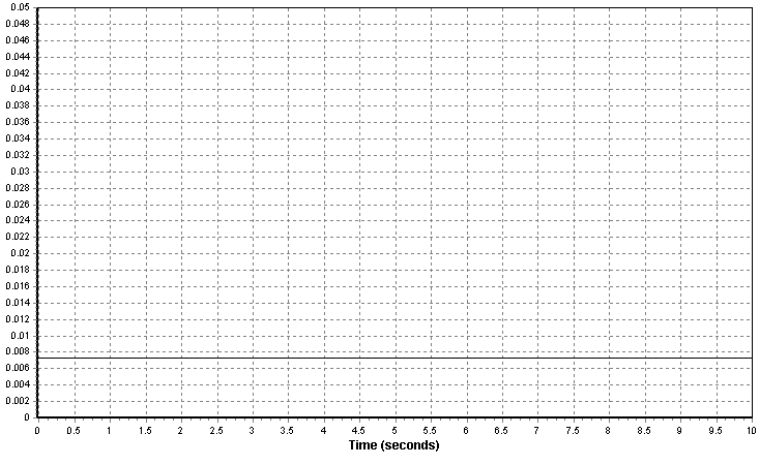

Speed deviation of the wind turbine generator [p.u]

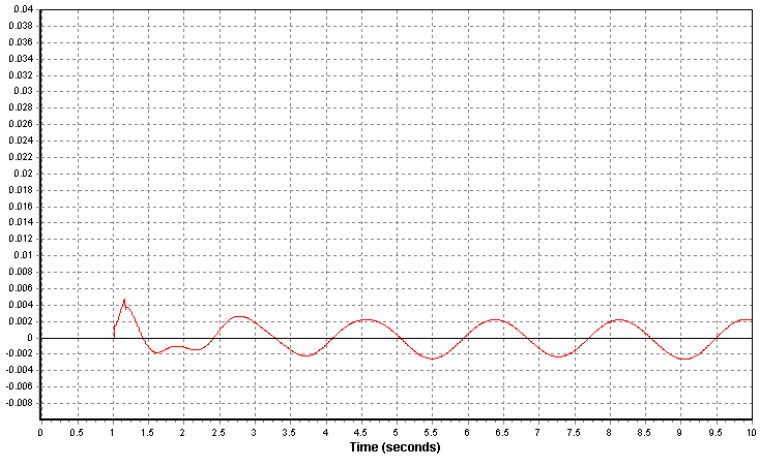

Frequency deviation at bus offshore (black) and onshore bus (red) [p.u]

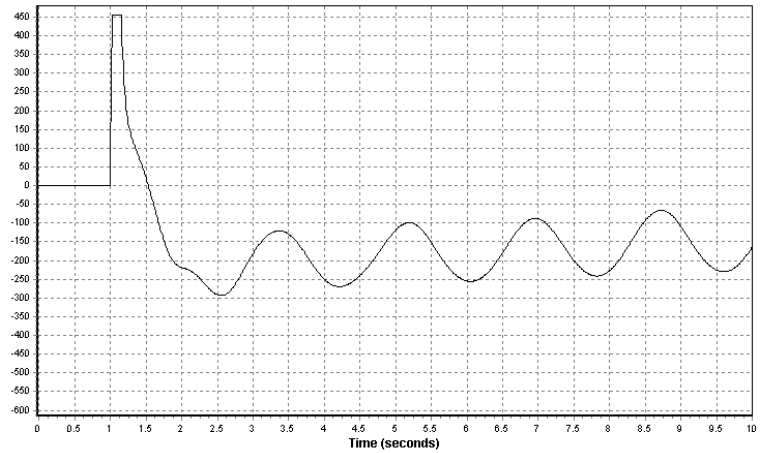

Reactive power from the onshore converter [MVar]

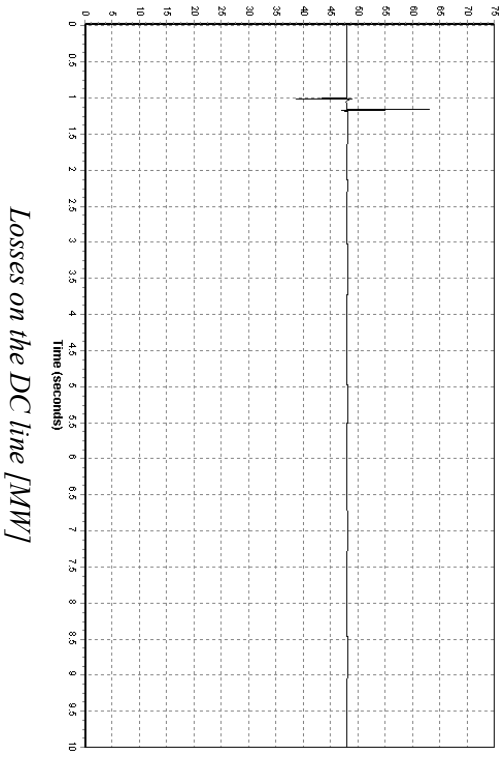

Losses on the DC line [MW]

Fault 3, line fault on the line from bus 5600 to bus 5603

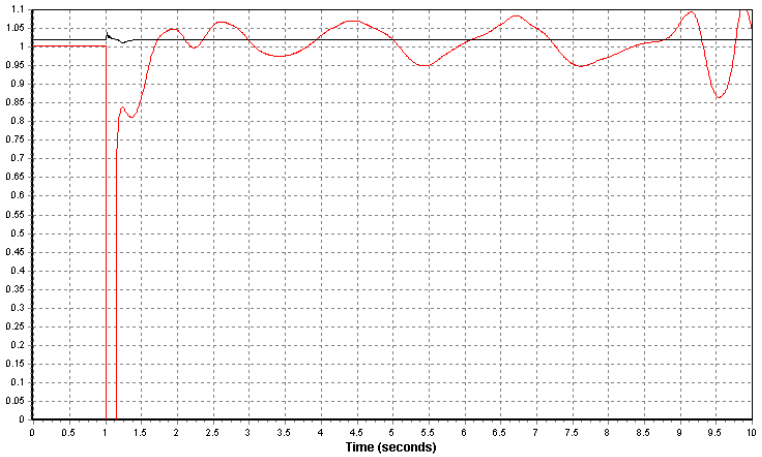

Voltage at offshore bus (black) and onshore bus (red) [p.u]

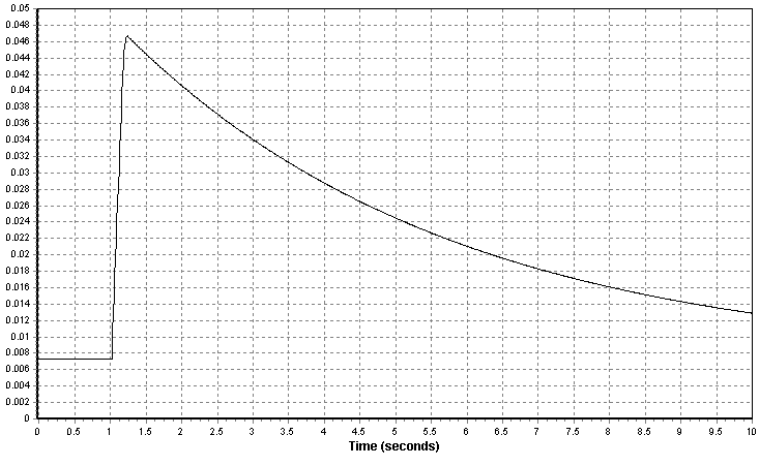

Speed deviation of the wind turbine generator [p.u]

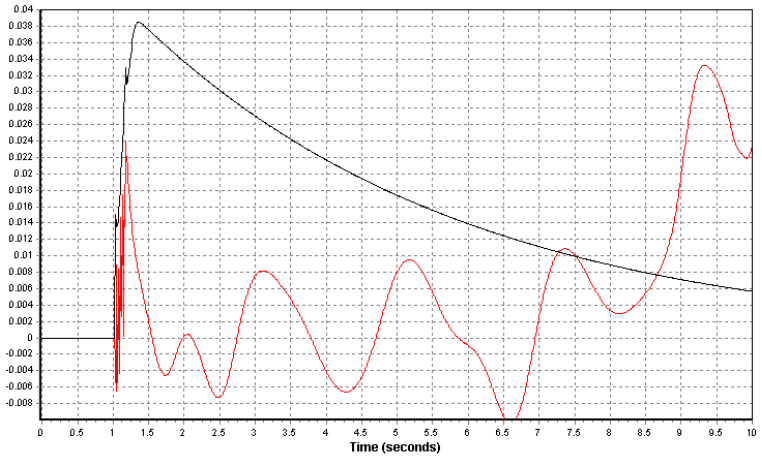

Frequency deviation at bus offshore (black) and onshore bus (red) [p.u]

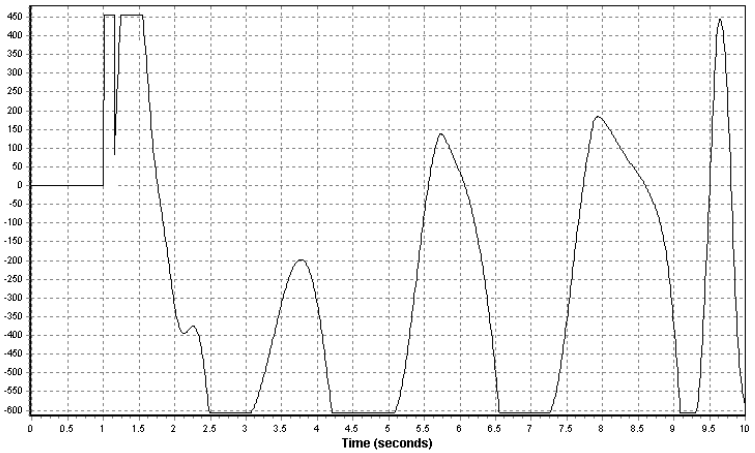

Reactive power from the onshore converter [MVar]

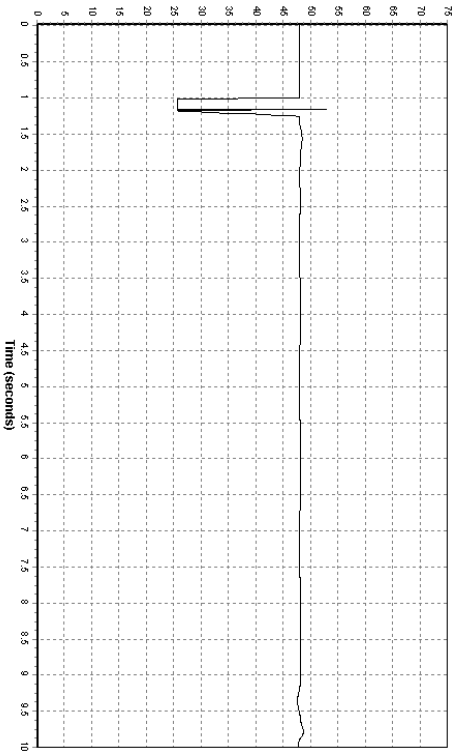

Losses on the DC line [MW]

Fault 4, bus fault on the wind farm bus 1000

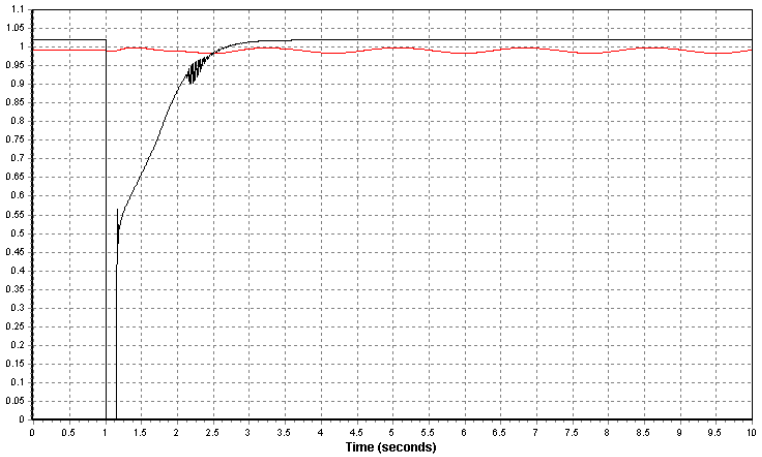

Voltage at offshore bus (black) and onshore bus (red) [p.u]

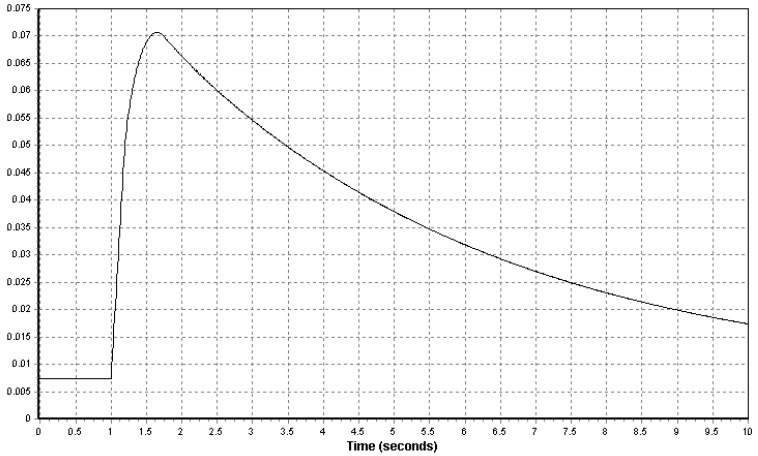

Speed deviation of the wind turbine generator [p.u]

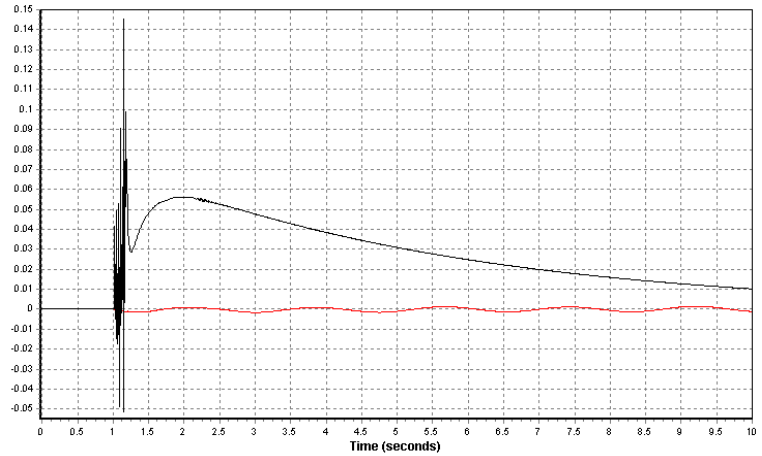

Frequency deviation at bus offshore (black) and onshore bus (red) [p.u]

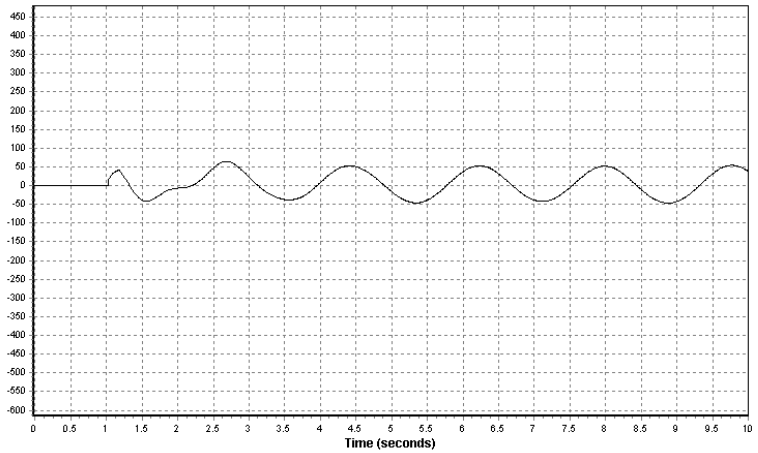

Reactive power from the onshore converter [MVar]

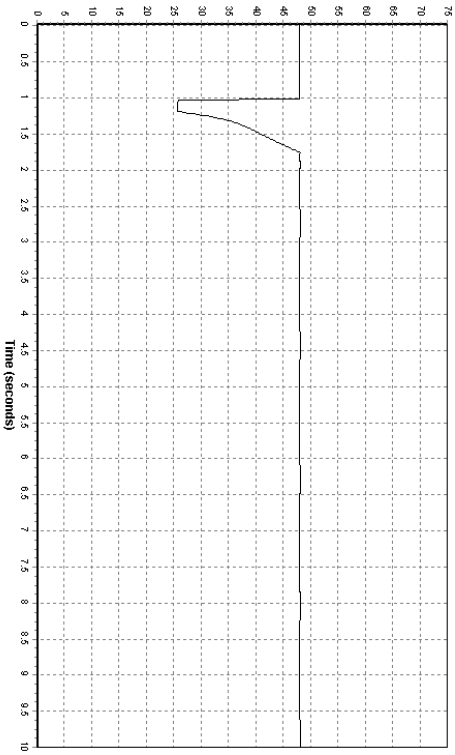

Losses on the DC line [MW]

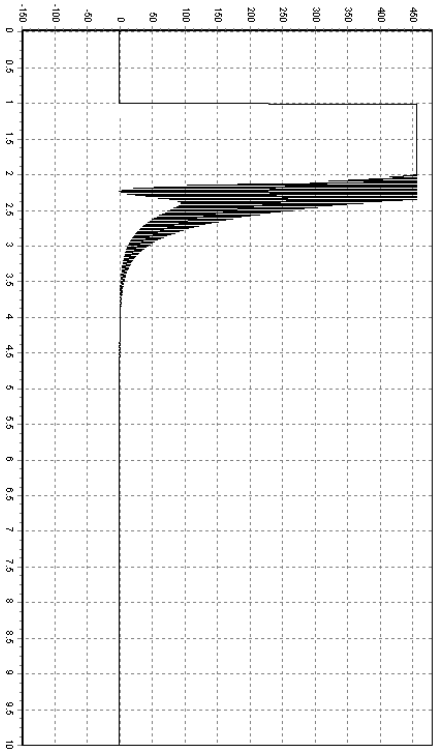

Reactive power from the offshore converter [MVar]

CONFIGURATION 3 : HVDC / HVAC LINK , CONNECTION BUS 6000

Fault 1, bus fault at connection bus 6000

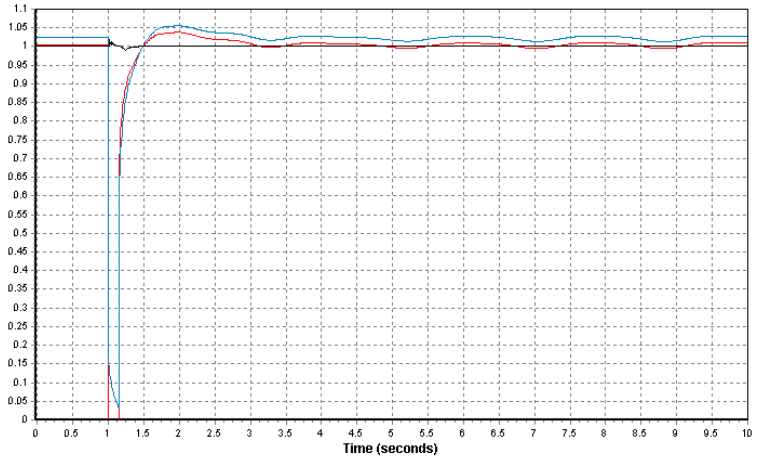

Voltage at offshore HVDC bus (black), offshore HVAC bus (blue) and onshore bus (red) [p.u]

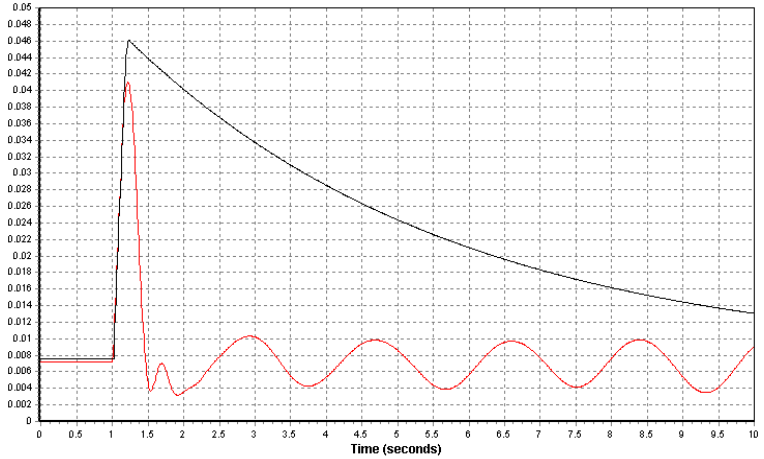

Speed deviation of the HVDC wind turbine generator (black) and the HVAC wind turbine generator (red) [p.u]

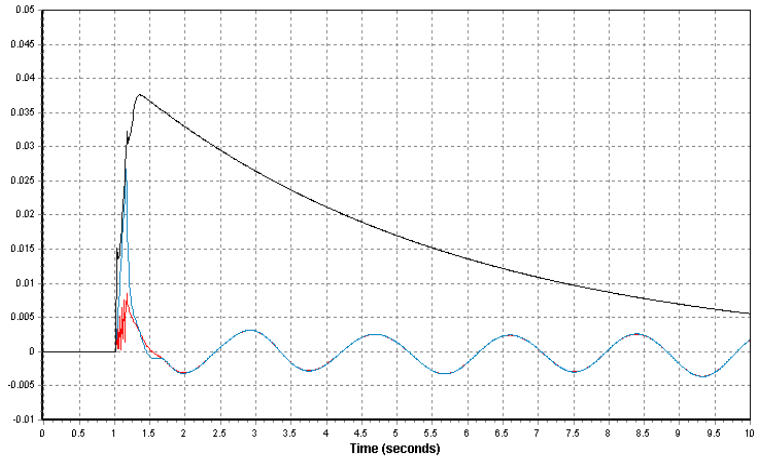

Frequency deviation at offshore HVDC bus (black), offshore HVAC bus (blue) and onshore bus (red)) [p.u]

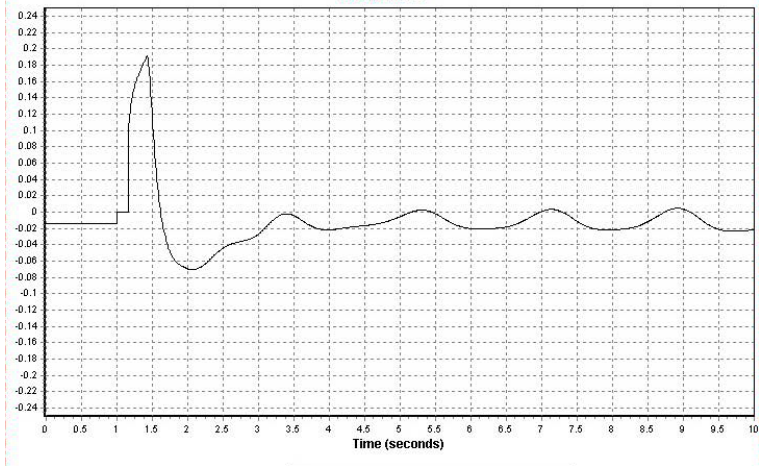

Reactive power from wind farm SVC [p.u]

Reactive power from the onshore converter [MVar]

Losses on the DC line [MW]

Fault 2, bus fault at neighbour bus 5400

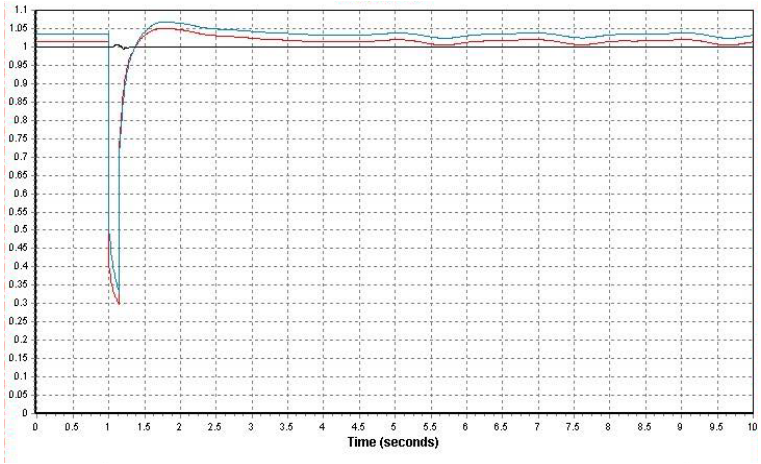

Voltage at offshore HVDC bus (black), offshore HVAC bus (blue) and onshore bus (red) [p.u]

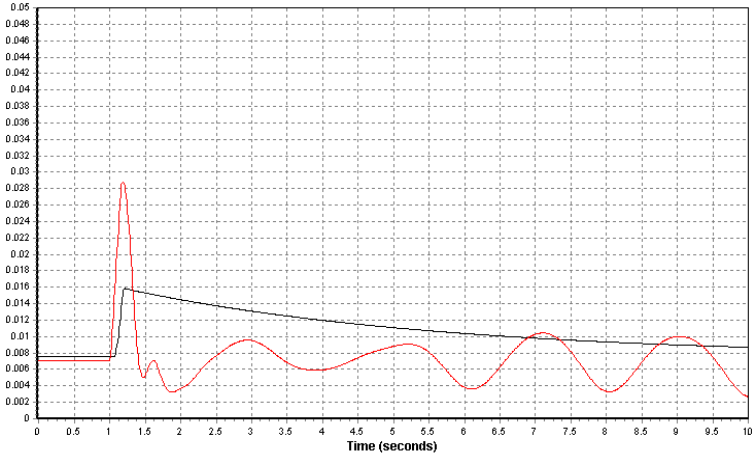

Speed deviation of the HVDC wind turbine generator (black) and the HVAC wind turbine generator (blue) [p.u]

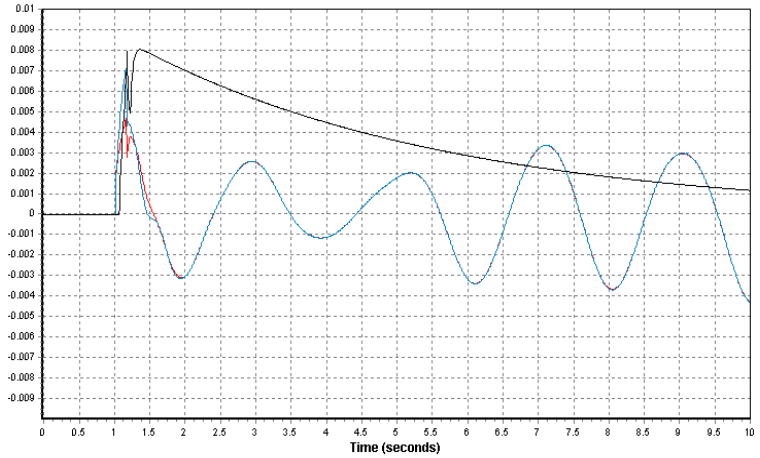

Frequency deviation at offshore HVDC bus (black), offshore HVAC bus (blue) and onshore bus (red)) [p.u]

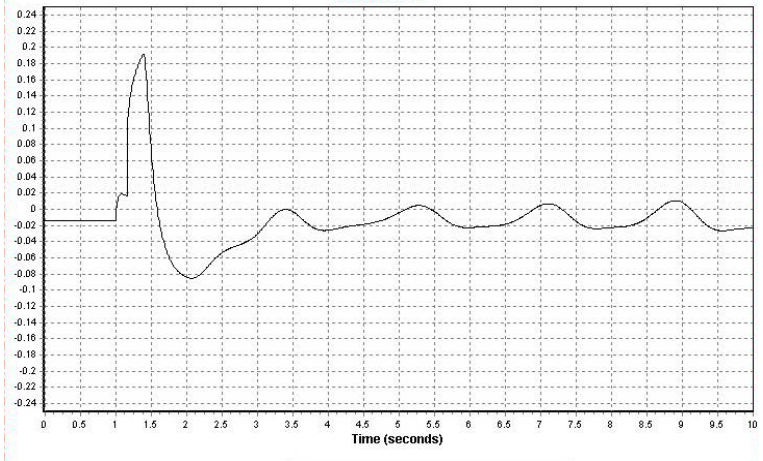

Reactive power from wind farm SVC [p.u]

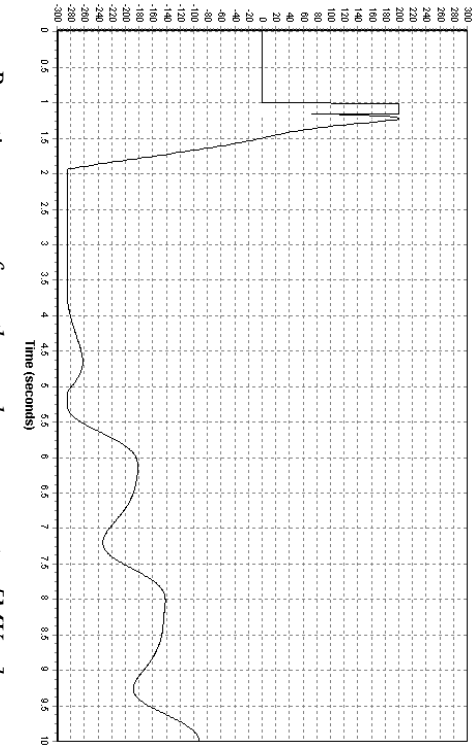

Reactive power from the onshore converter [MVar]

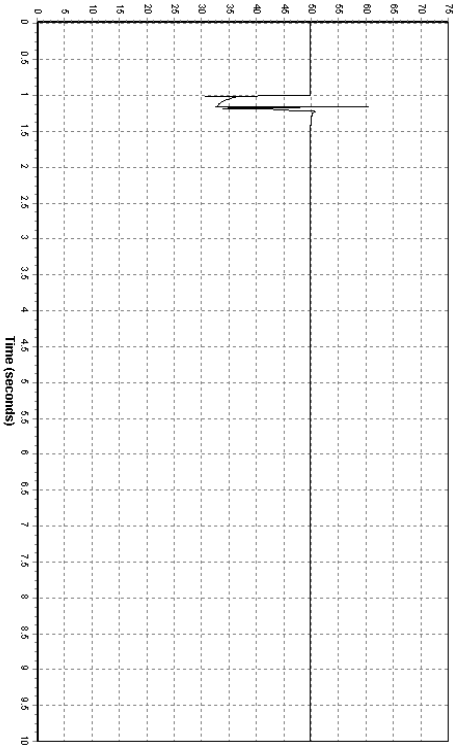

Losses on the DC line [MW]

Fault 3, line fault on the line from bus 6000 to bus 5400

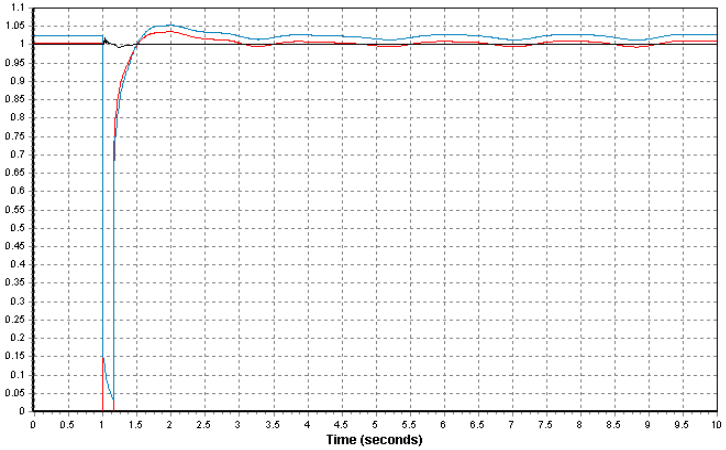

Voltage at offshore HVDC bus (black), offshore HVAC bus (blue) and onshore bus (red) [p.u]

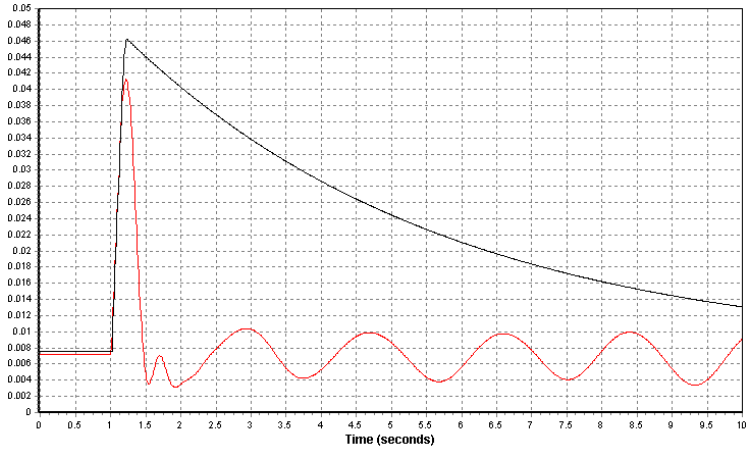

Speed deviation of the HVDC wind turbine generator (black) and the HVAC wind turbine generator (red) [p.u]

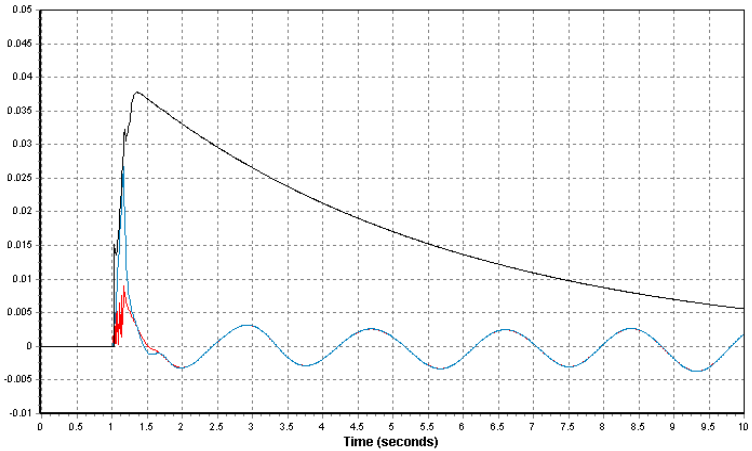

Frequency deviation at offshore HVDC bus (black), offshore HVAC bus (blue) and onshore bus (red)) [p.u]

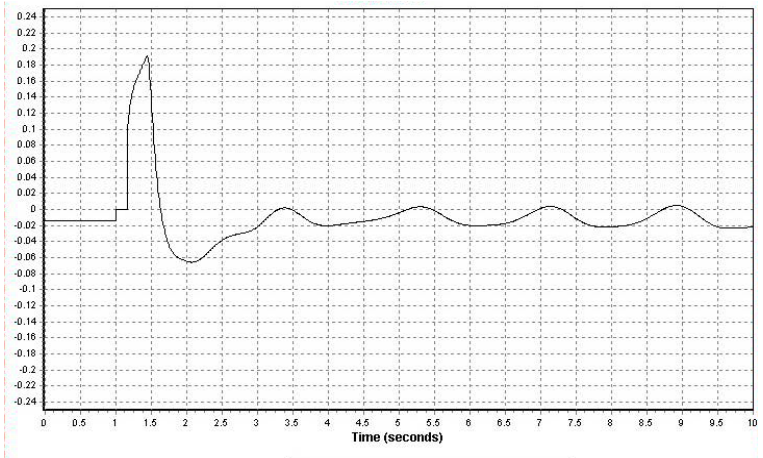

Reactive power from wind farm SVC [p.u]

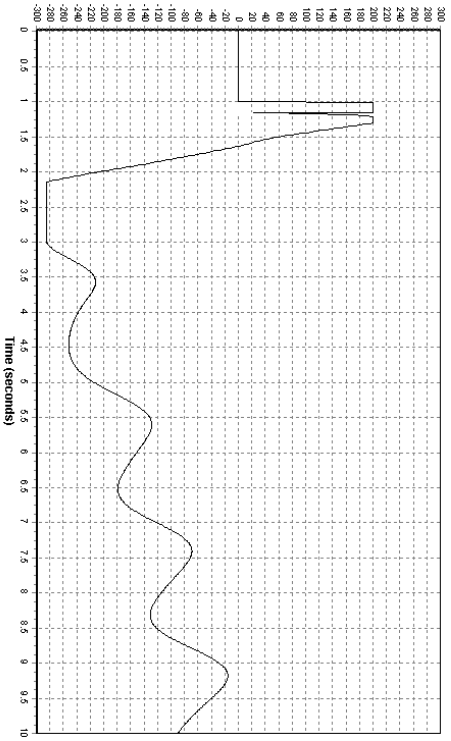

Reactive power from the onshore converter [MVar]

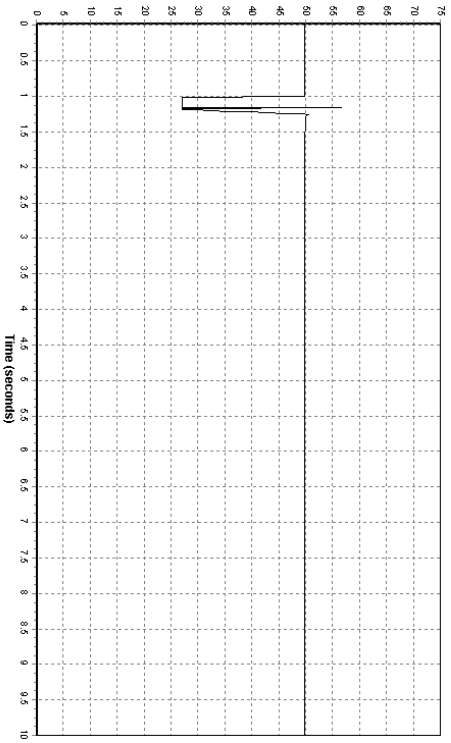

Losses on the DC line [MW]

Fault 4A, bus fault on the HVDC wind farm bus 1100

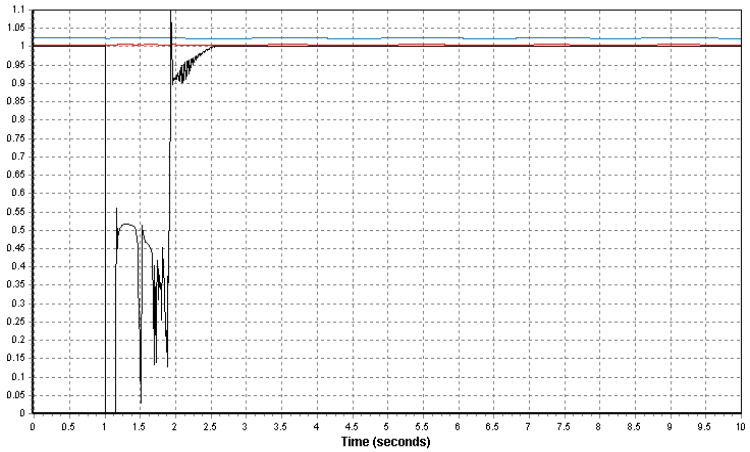

Voltage at offshore HVDC bus (black), offshore HVAC bus (blue) and onshore bus (red) [p.u]

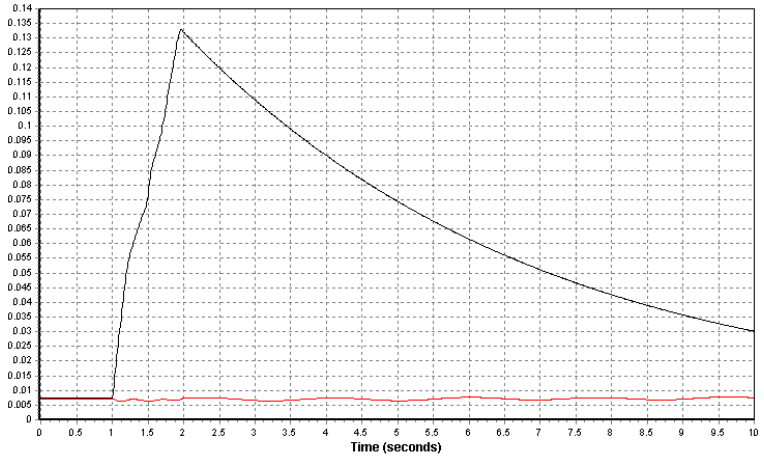

Speed deviation of the HVDC wind turbine generator (black) and the HVAC wind turbine generator (red) [p.u]

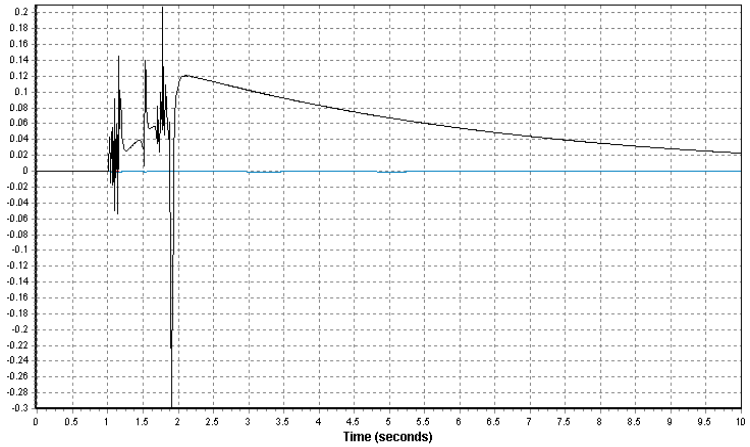

Frequency deviation at offshore HVDC bus (black), offshore HVAC bus (blue) and onshore bus (red)) [p.u]

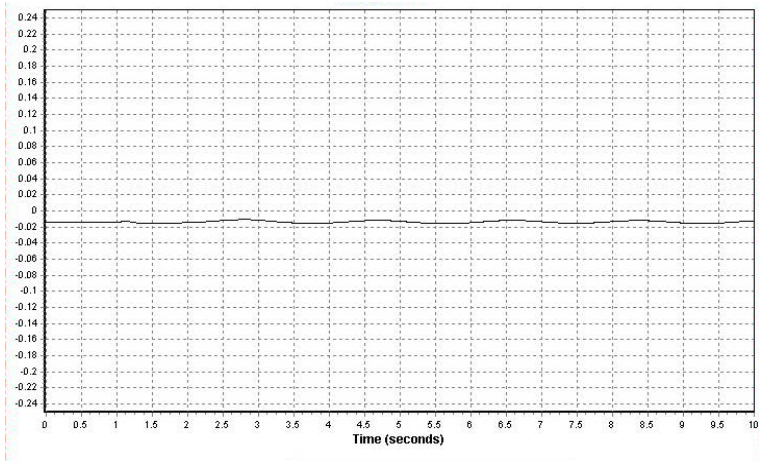

Reactive power from wind farm SVC [p.u]

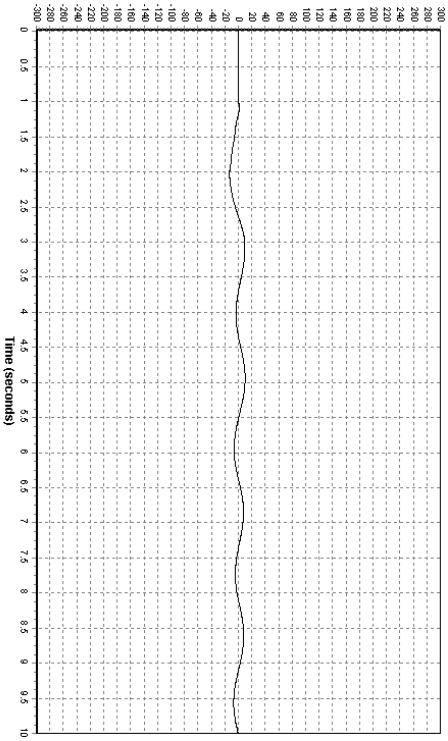

Reactive power from the onshore converter [MVar]

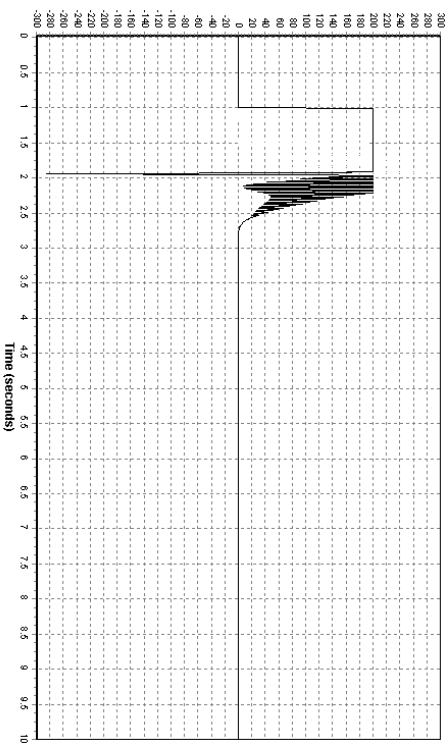

Reactive power from the offshore converter [MVar]

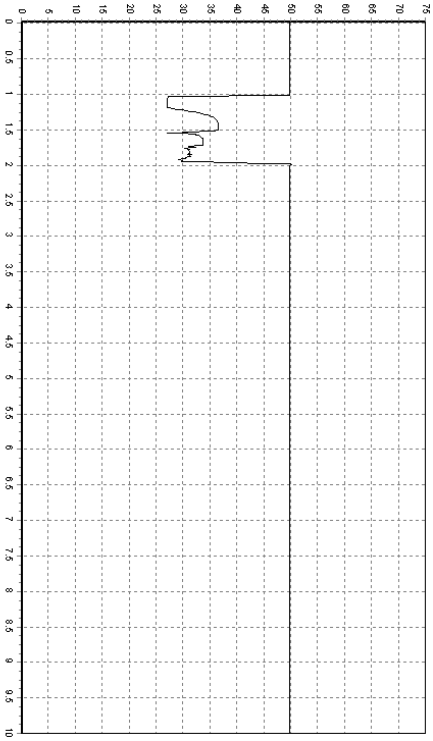

Losses on the DC line [MW]

Fault 4B, bus fault on the HVAC wind farm bus 1200

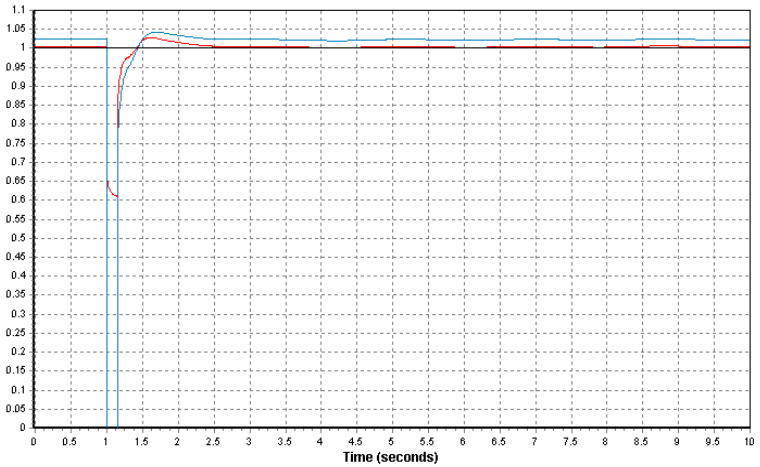

Voltage at offshore HVDC bus (black), offshore HVAC bus (blue) and onshore bus (red) [p.u]

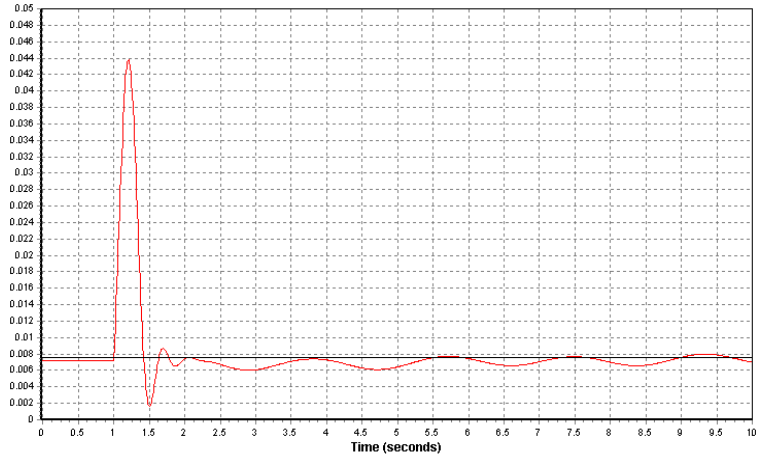

Speed deviation of the HVDC wind turbine generator (black) and the HVAC wind turbine generator (red) [p.u]

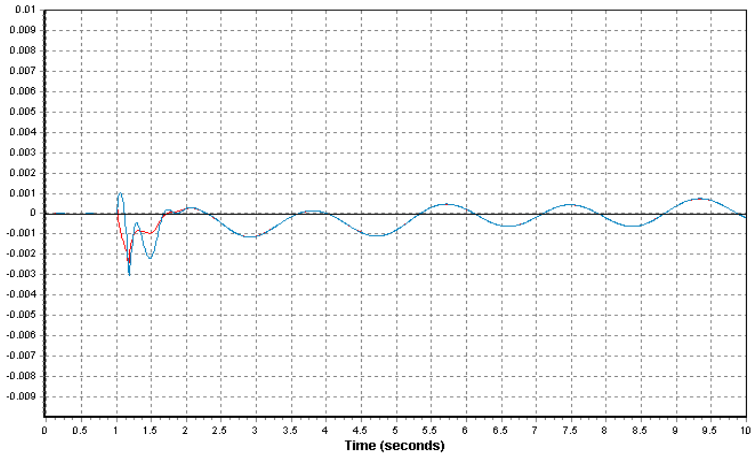

Frequency deviation at offshore HVDC bus (black), offshore HVAC bus (blue) and onshore bus (red)) [p.u]

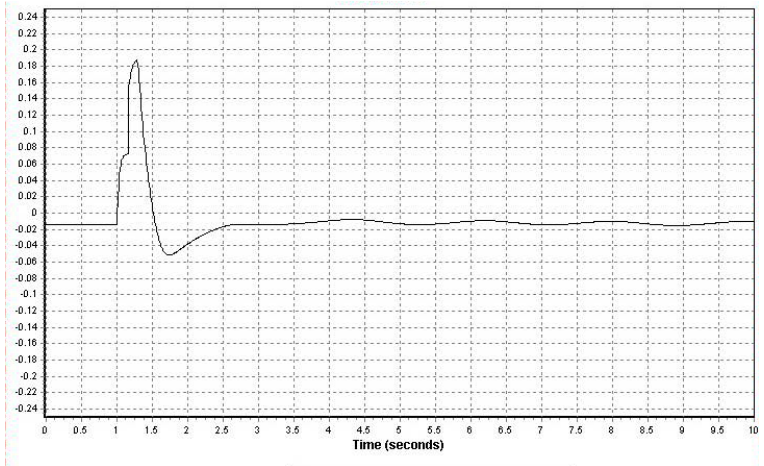

Reactive power from wind farm SVC [p.u]

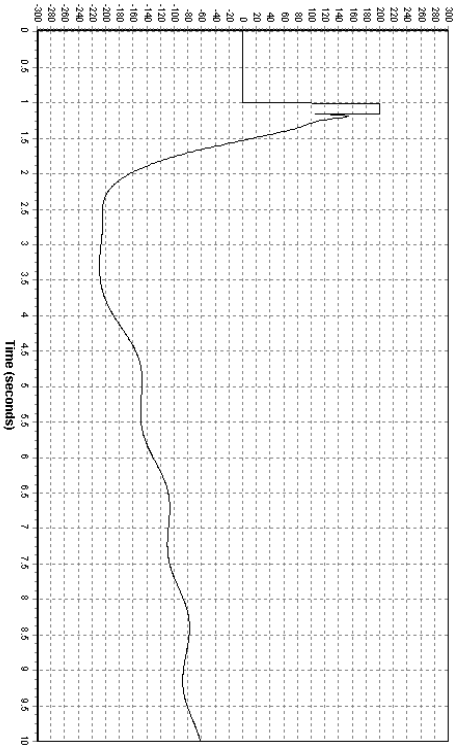

Reactive power from the onshore converter [MVar]

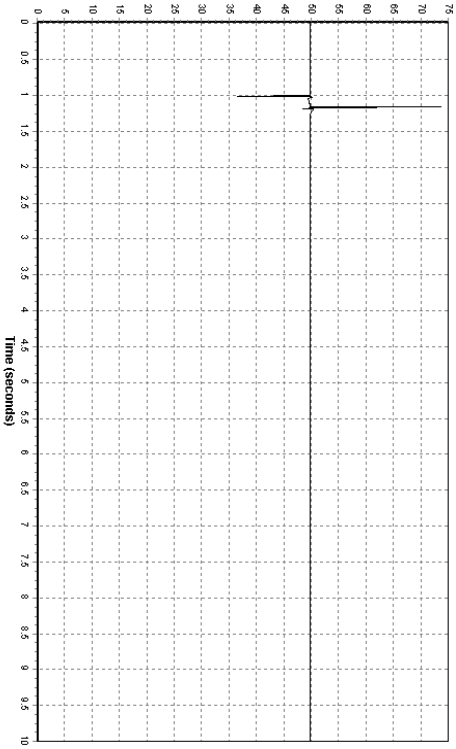

Losses on the DC line [MW]

Fault 4C, bus fault on the HVDC wind farm bus 1100 and on the HVAC wind farm bus 1200

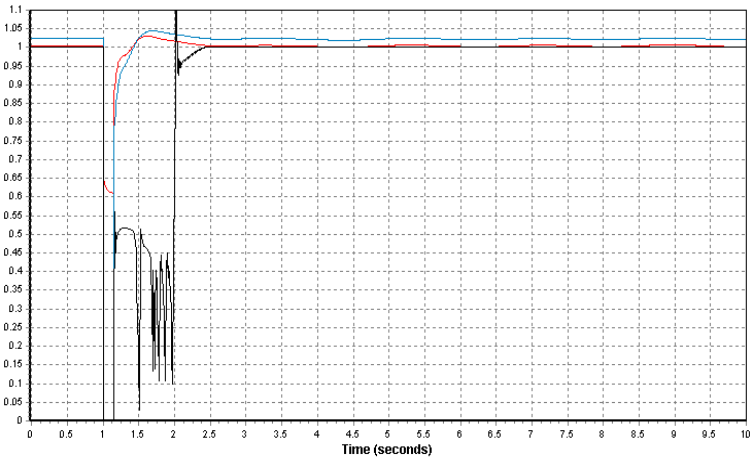

Voltage at offshore HVDC bus (black), offshore HVAC bus (blue) and onshore bus (red) [p.u]

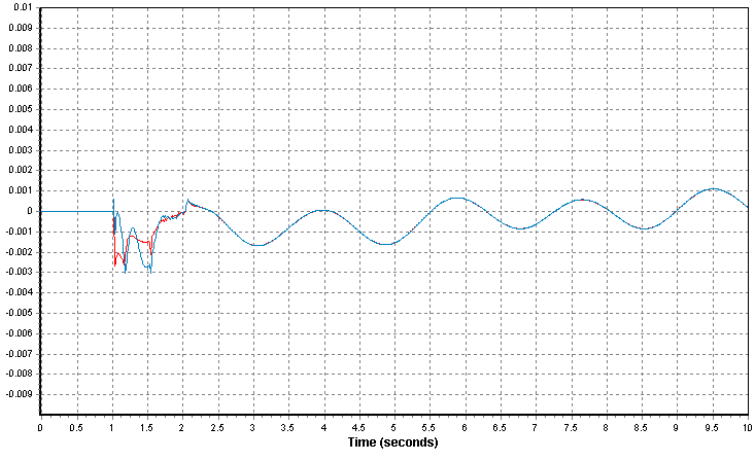

Frequency deviation at offshore HVAC bus (blue) and onshore bus (red)) [p.u]

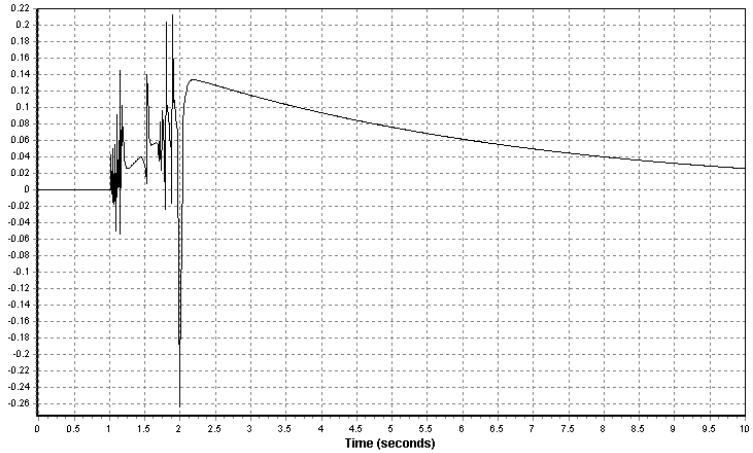

Frequency deviation at offshore HVDC bus (black) [p.u]

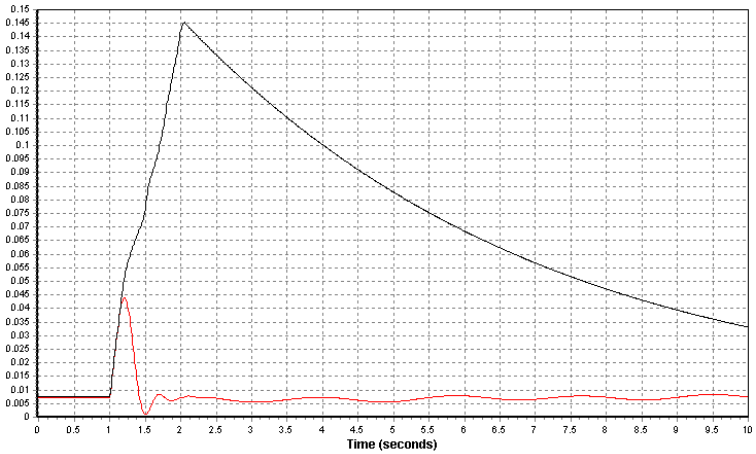

Speed deviation of the HVDC wind turbine generator (black) and the HVAC wind turbine generator (red) [p.u]

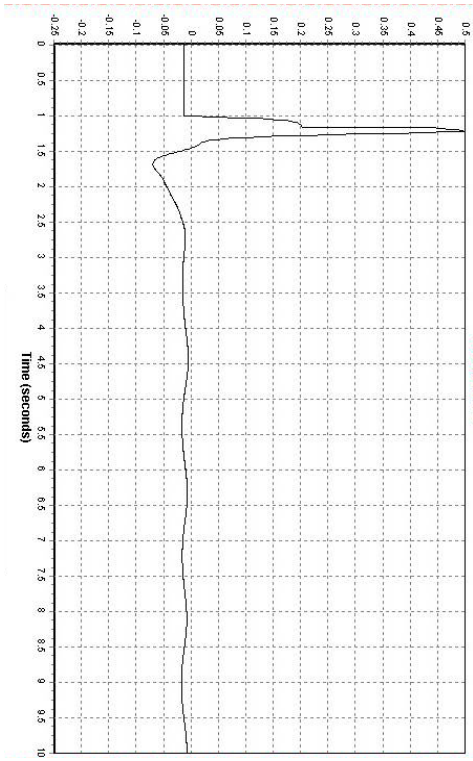

Reactive power from wind farm SVC [p.u]

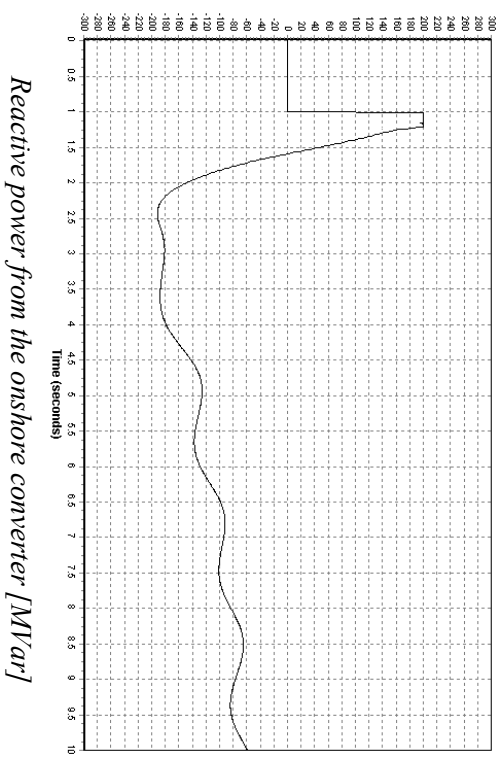

Reactive power from the onshore converter [MVar]

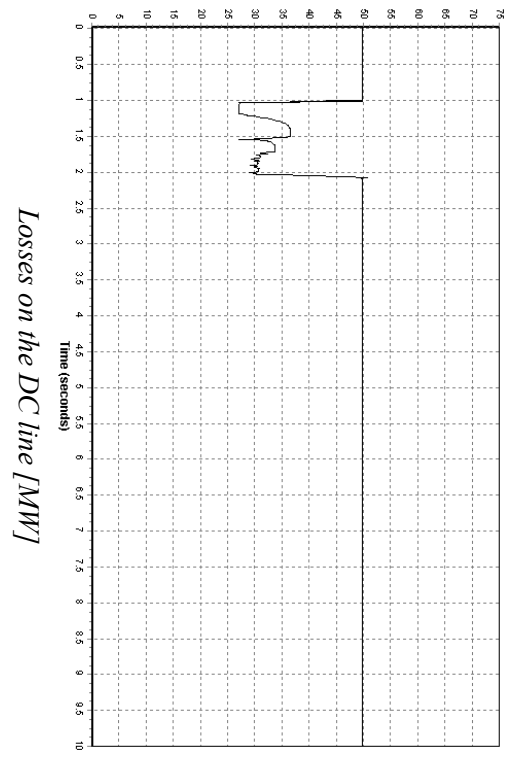

Losses on the DC line [MW]

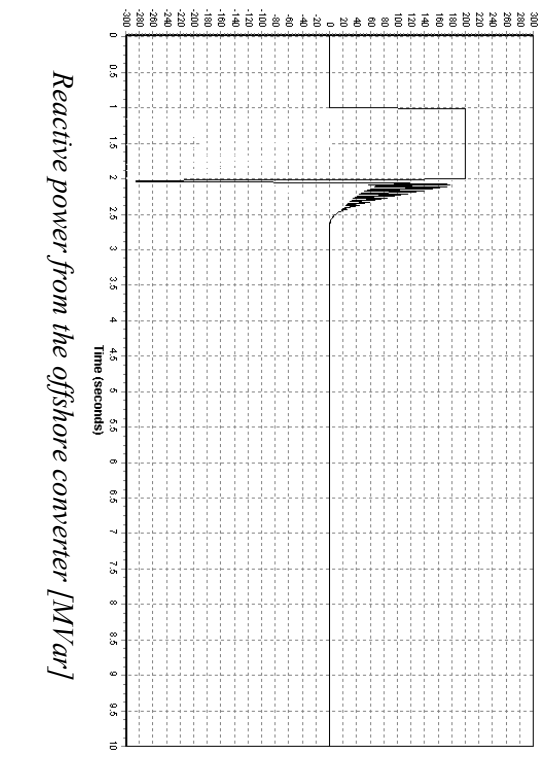

Reactive power from the offshore converter [MVar]

CONFIGURATION 3 : HVDC / HVAC LINK , CONNECTION BUS 5600

Fault 1, bus fault at connection bus 5600

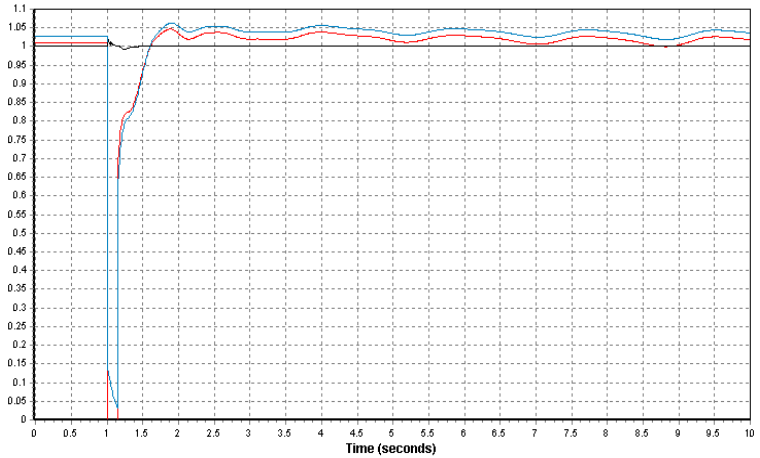

Voltage at offshore HVDC bus (black), offshore HVAC bus (blue) and onshore bus (red) [p.u]

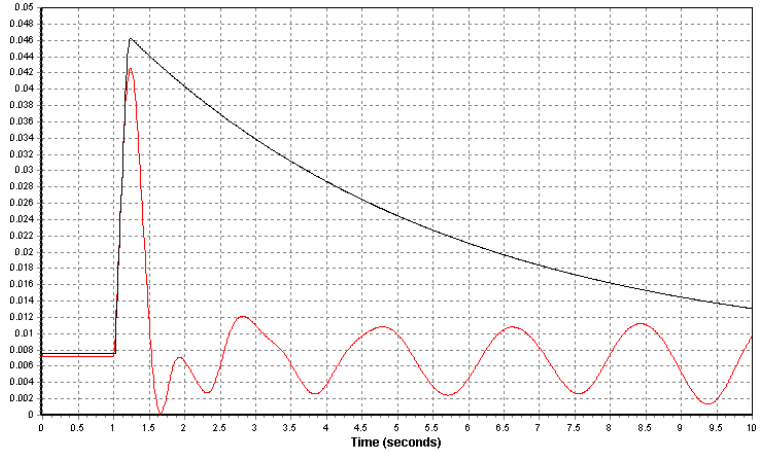

Speed deviation of the HVDC wind turbine generator (black) and the HVAC wind turbine generator (red) [p.u]

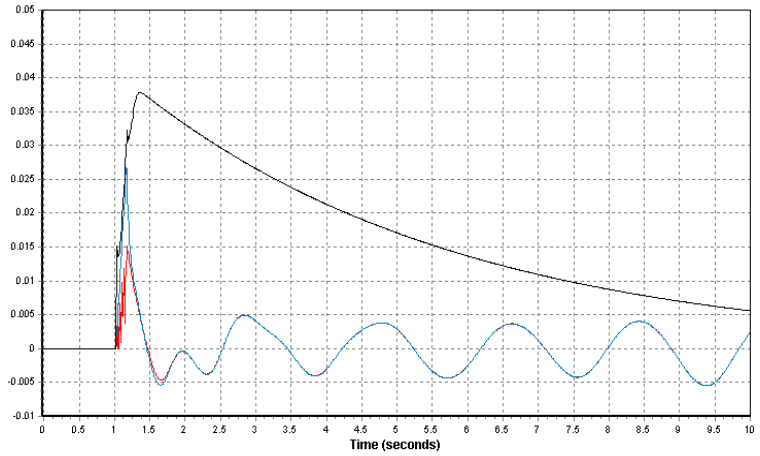

Frequency deviation at offshore HVDC bus (black), offshore HVAC bus (blue) and onshore bus (red)) [p.u]

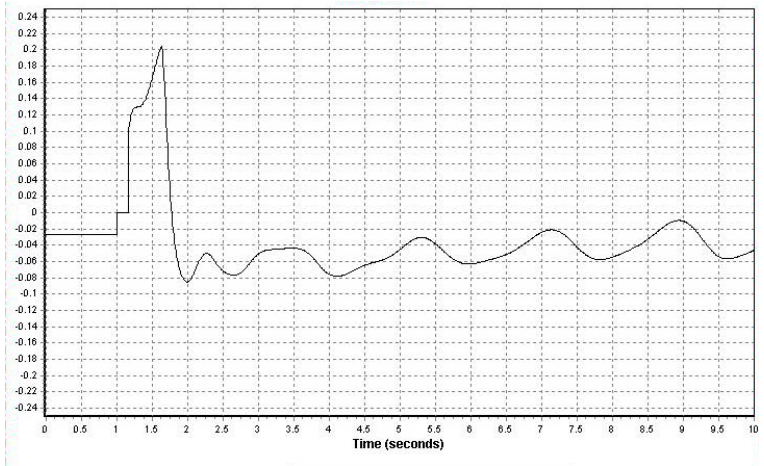

Reactive power from wind farm SVC [p.u]

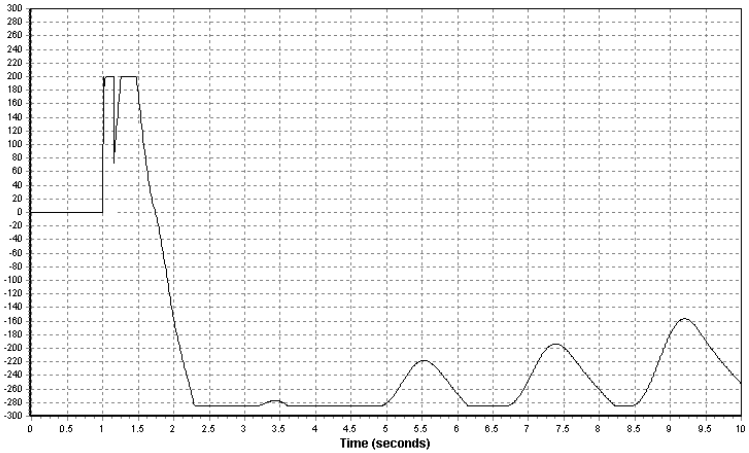

Reactive power from the onshore converter [MVar]

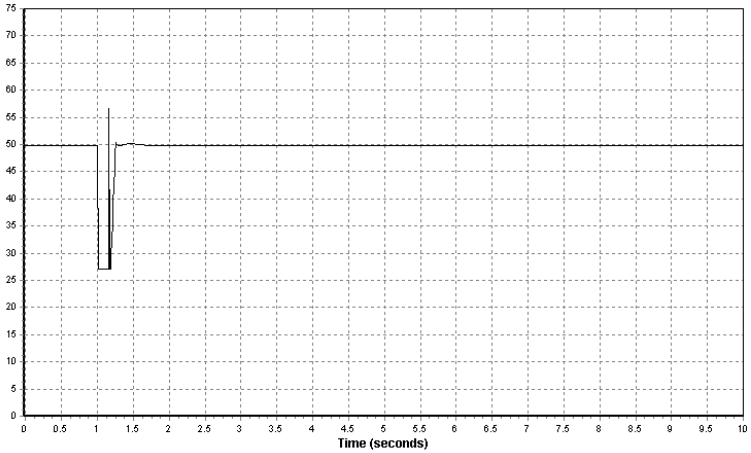

Losses on the DC line [MW]

Fault 2, bus fault at neighbour bus 5603

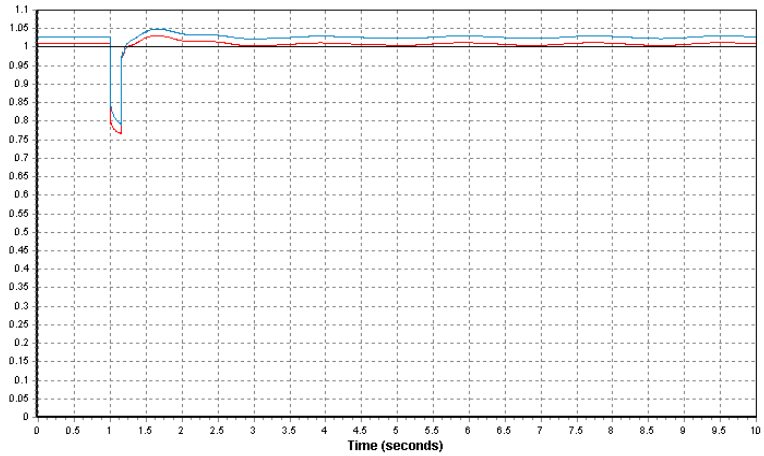

Voltage at offshore HVDC bus (black), offshore HVAC bus (blue) and onshore bus (red) [p.u]

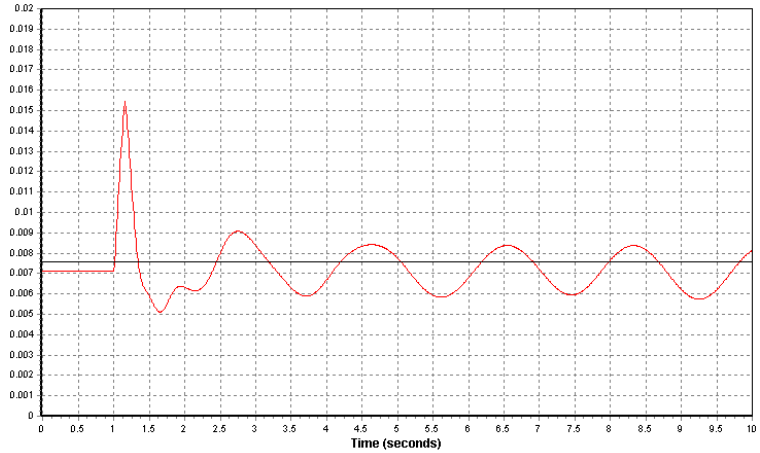

Speed deviation of the HVDC wind turbine generator (black) and the HVAC wind turbine generator (red) [p.u]

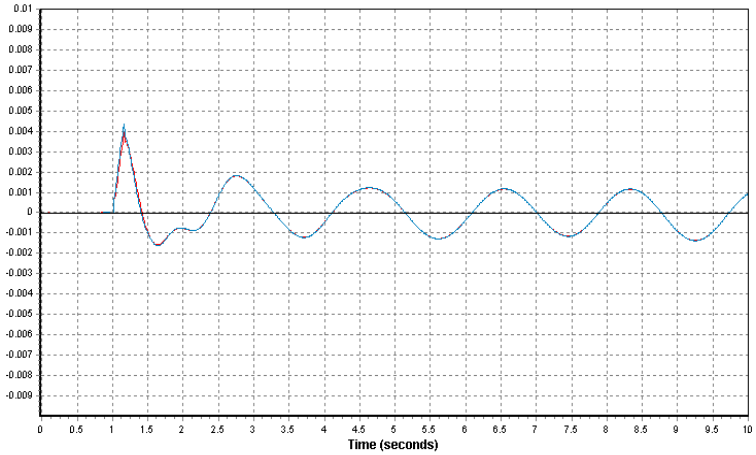

Frequency deviation at offshore HVDC bus (black), offshore HVAC bus (blue) and onshore bus (red)) [p.u]

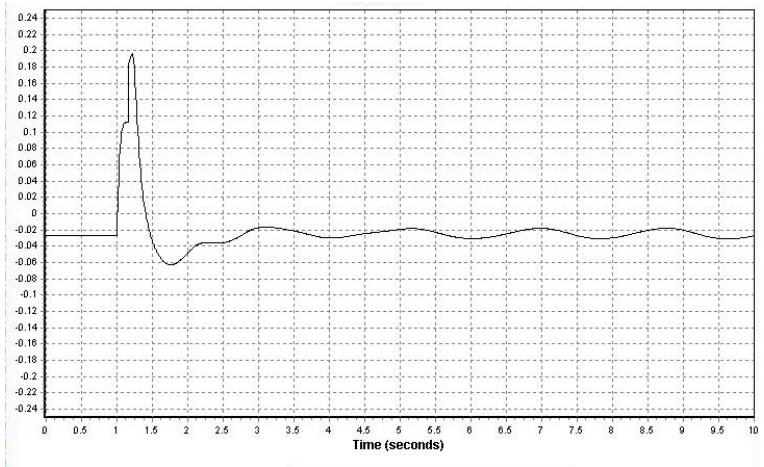

Reactive power from wind farm SVC [p.u]

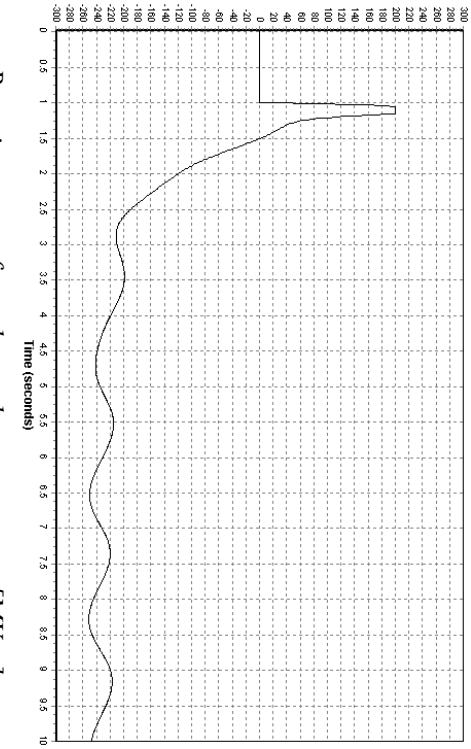

Reactive power from the onshore converter [MVar]

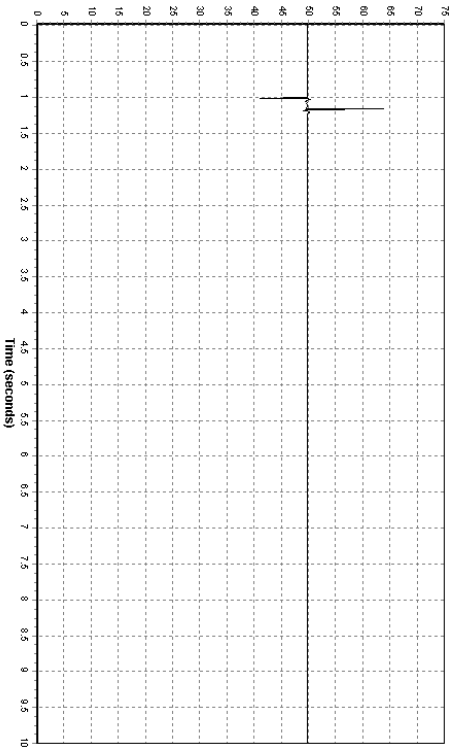

Losses on the DC line [MW]

Fault 3, line fault on the line from bus 5600 to bus 5603

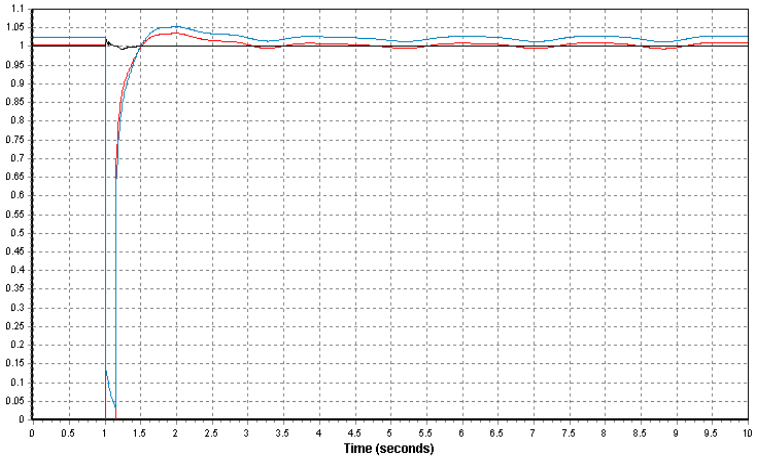

Voltage at offshore HVDC bus (black), offshore HVAC bus (blue) and onshore bus (red) [p.u]

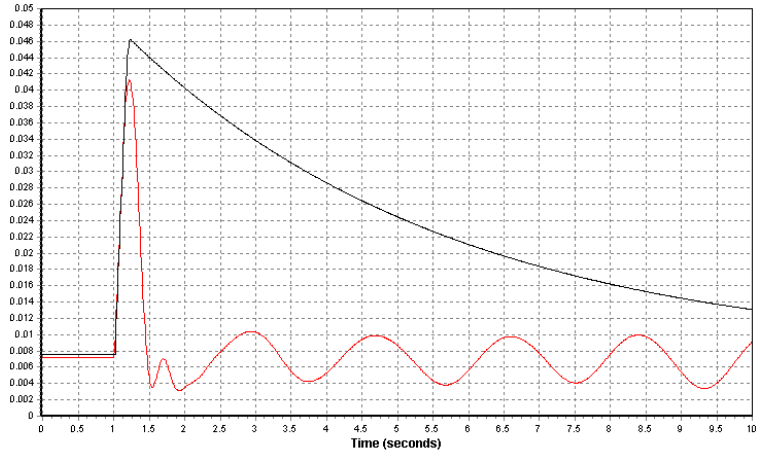

Speed deviation of the HVDC wind turbine generator (black) and the HVAC wind turbine generator (red) [p.u]

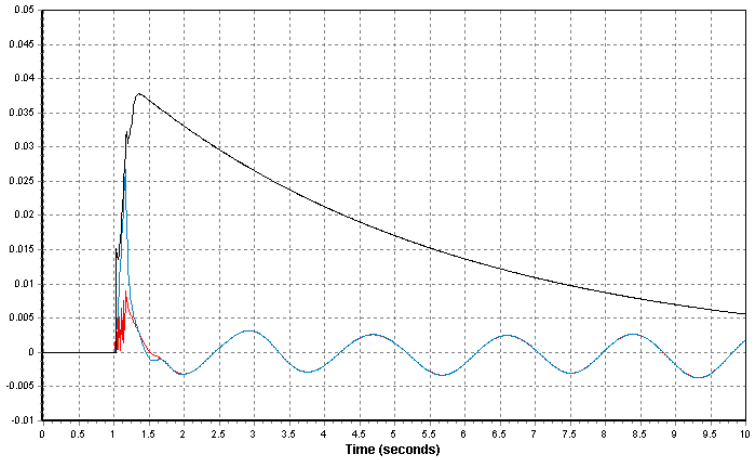

Frequency deviation at offshore HVDC bus (black), offshore HVAC bus (blue) and onshore bus (red)) [p.u]

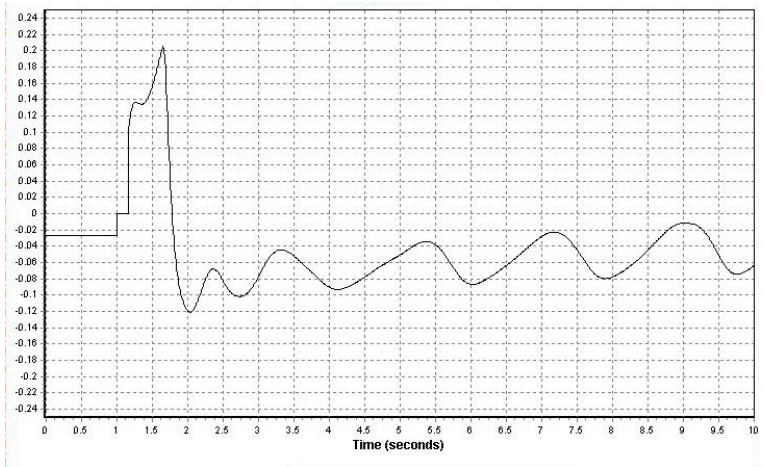

Reactive power from wind farm SVC [p.u]

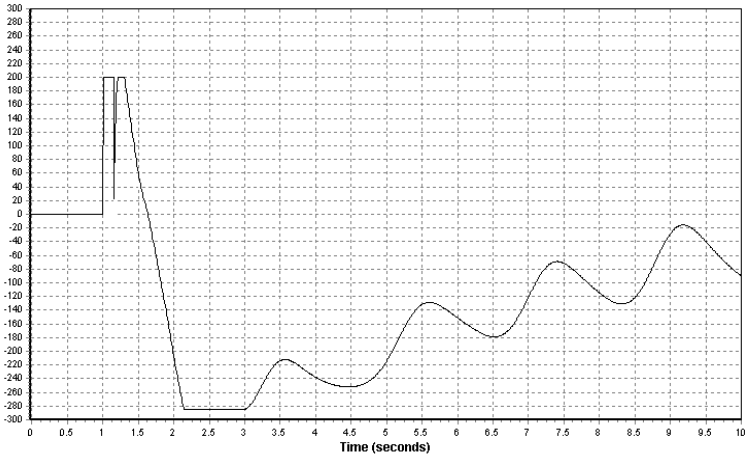

Reactive power from the onshore converter [MVar]

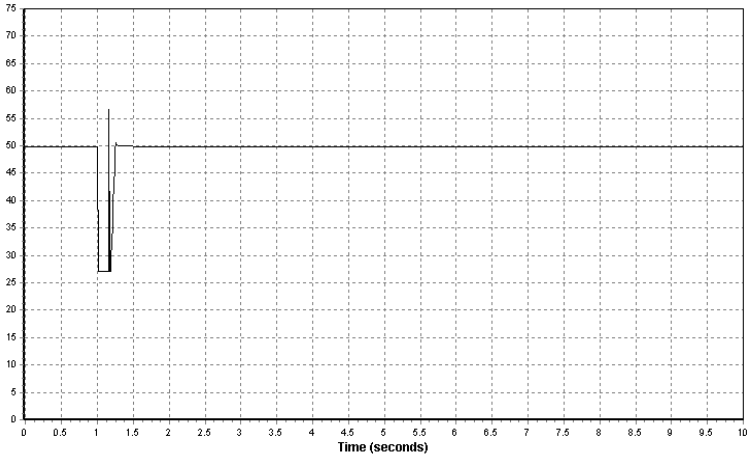

Losses on the DC line [MW]

Fault 4a, bus fault on the HVDC wind farm bus 1100

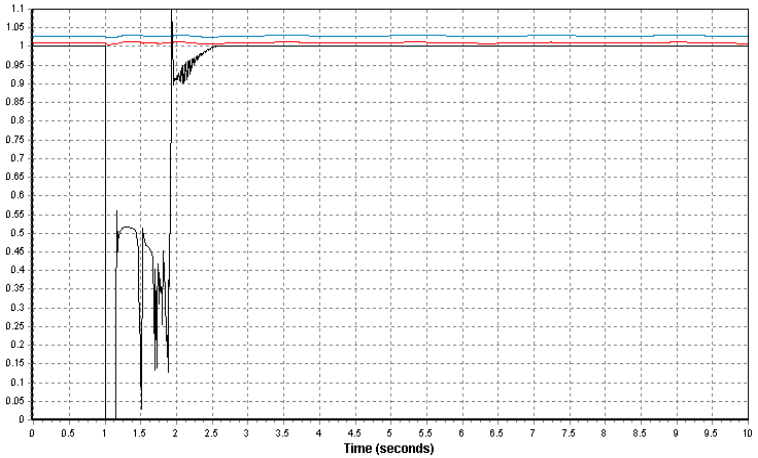

Voltage at offshore HVDC bus (black), offshore HVAC bus (blue) and onshore bus (red) [p.u]

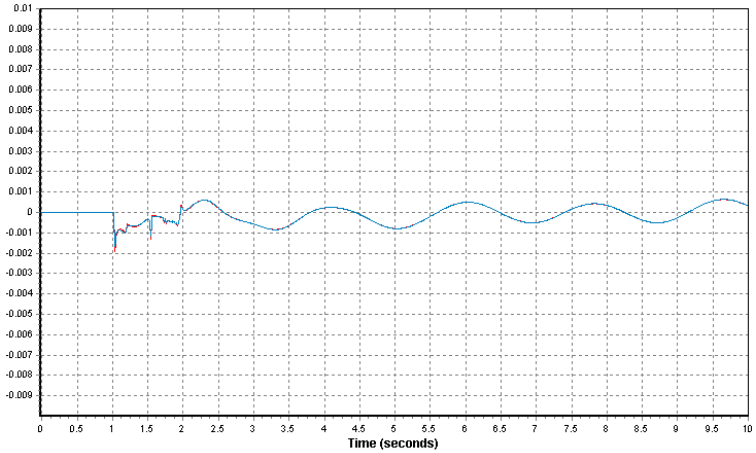

Frequency deviation at offshore HVAC bus (blue) and onshore bus (red)) [p.u]

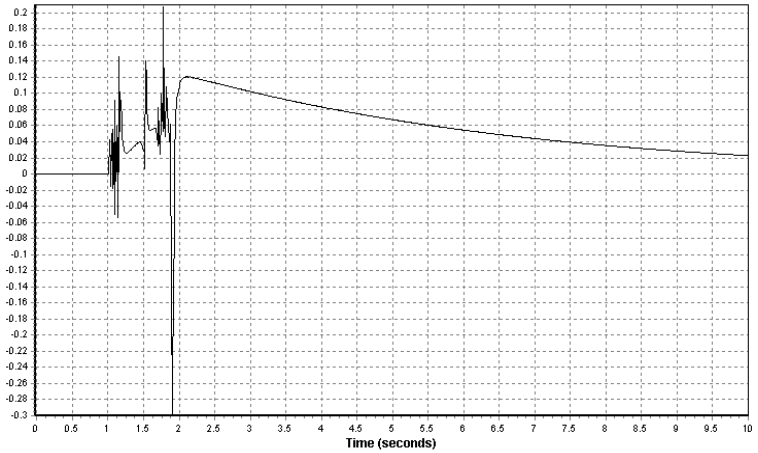

Frequency deviation at offshore HVDC bus (black)) [p.u]

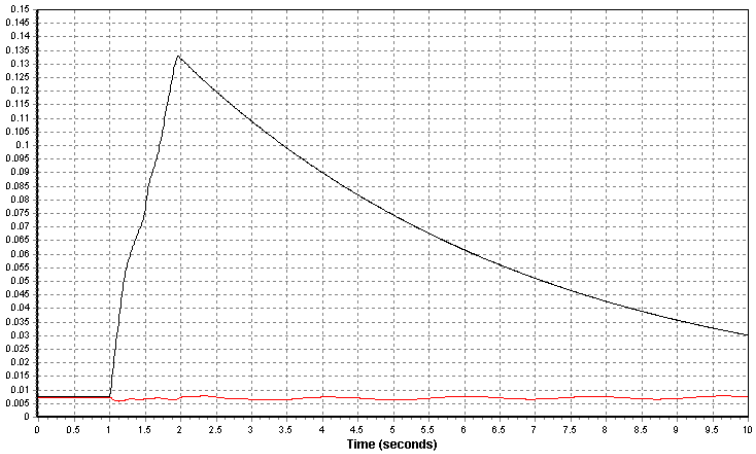

Speed deviation of the HVDC wind turbine generator (black) and the HVAC wind turbine generator (red) [p.u]

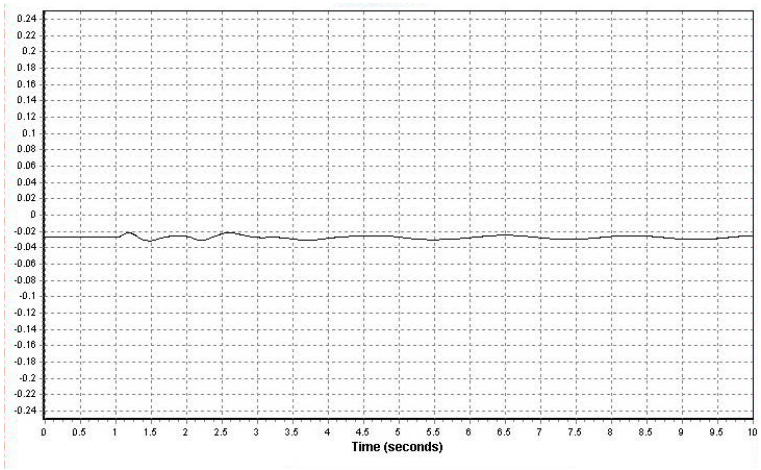

Reactive power from wind farm SVC [p.u]

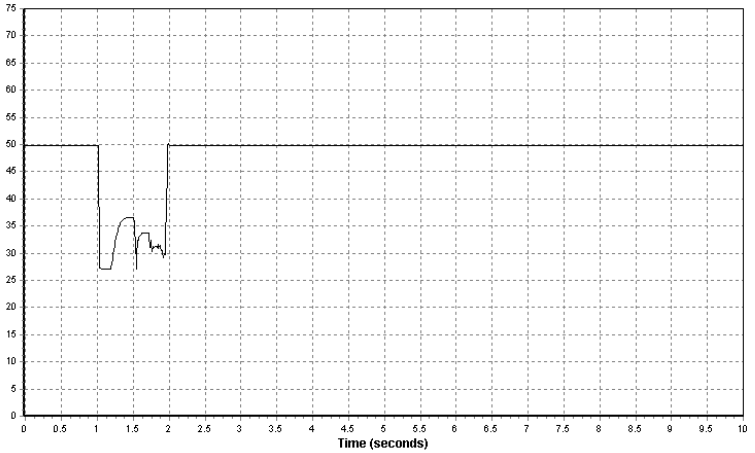

Losses on the DC line [MW]

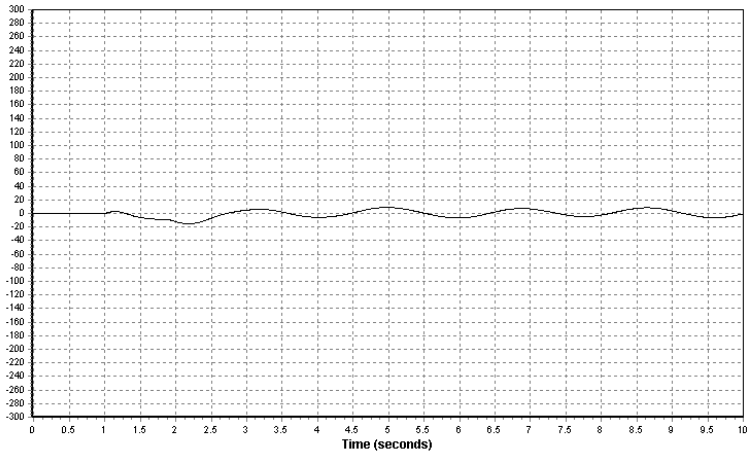

Reactive power from the onshore converter [MVar]

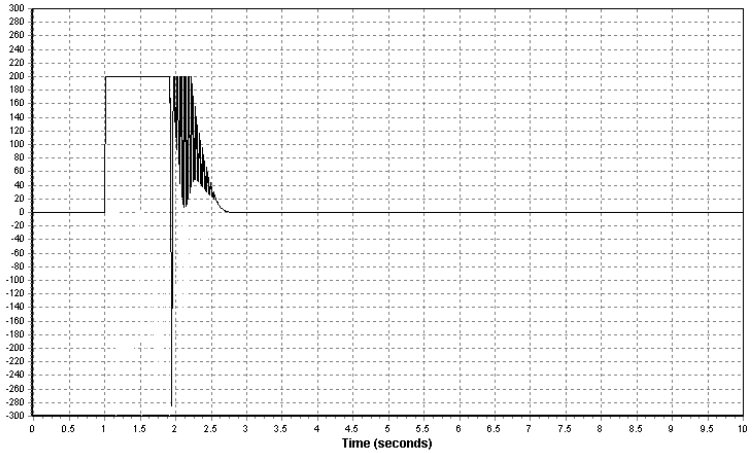

Reactive power from the offshore converter [MVar]

Fault 4b, bus fault on the HVAC wind farm bus 1200

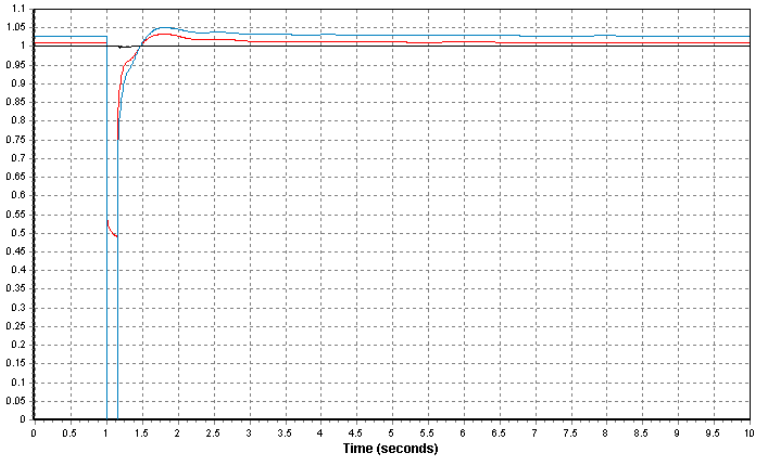

Voltage at offshore HVDC bus (black), offshore HVAC bus (blue) and onshore bus (red) [p.u]

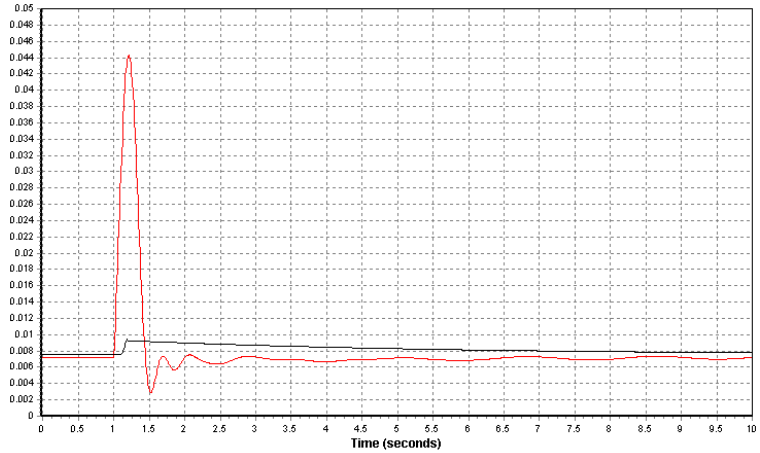

Speed deviation of the HVDC wind turbine generator (black) and the HVAC wind turbine generator (red) [p.u]

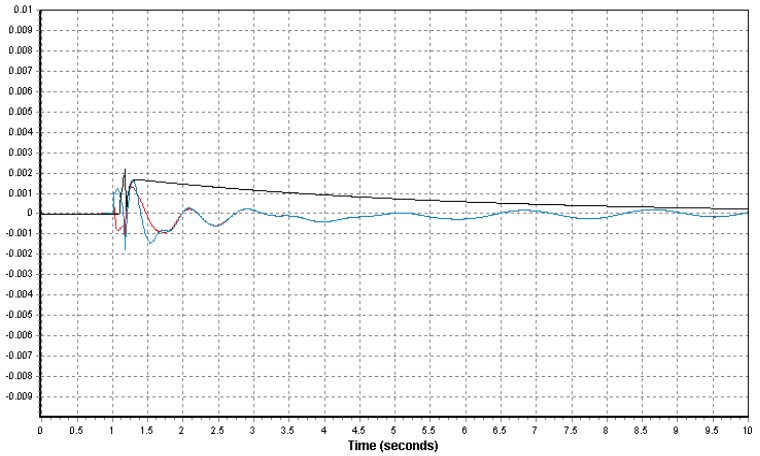

Frequency deviation at offshore HVDC bus (black), offshore HVAC bus (blue) and onshore bus (red)) [p.u]

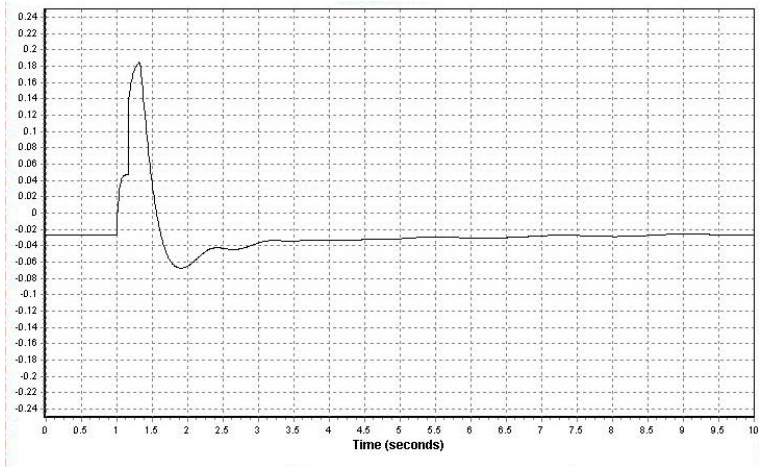

Reactive power from wind farm SVC [p.u]

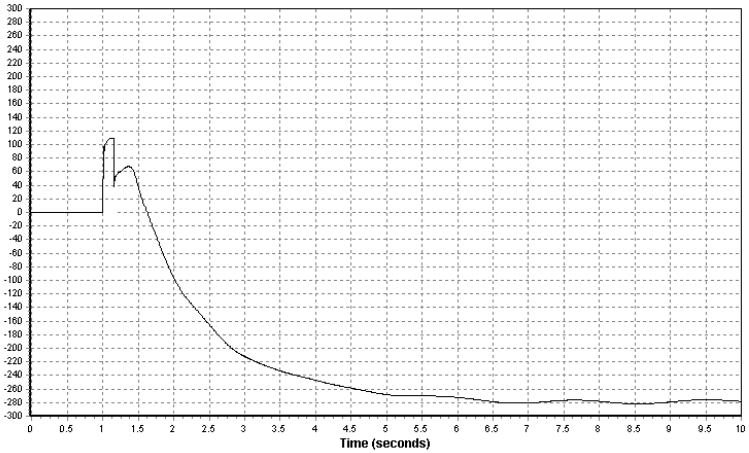

Reactive power from the onshore converter [MVar]

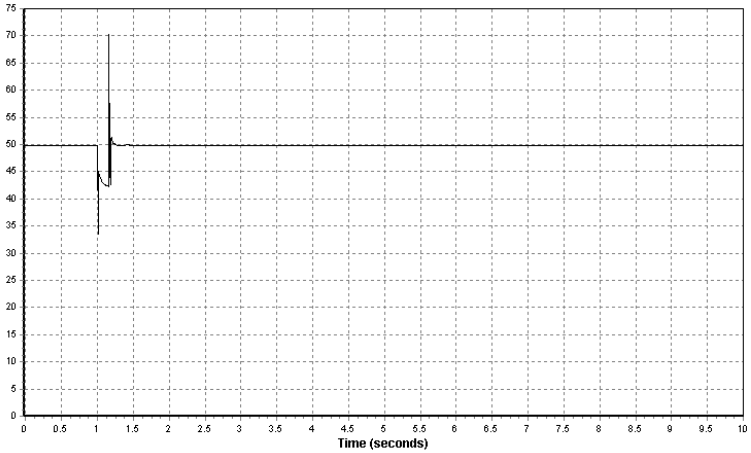

Losses on the DC line [MW]

Fault 4c, bus fault on the HVDC wind farm bus 1100 and on the HVAC wind farm bus 1200

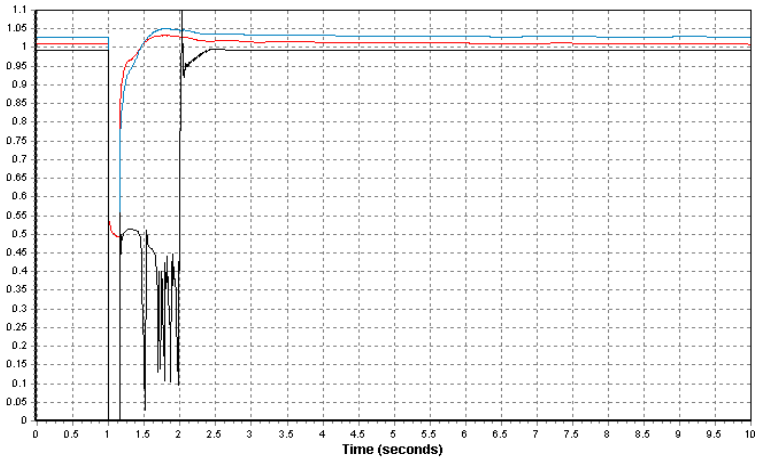

Voltage at offshore HVDC bus (black), offshore HVAC bus (blue) and onshore bus (red) [p.u]

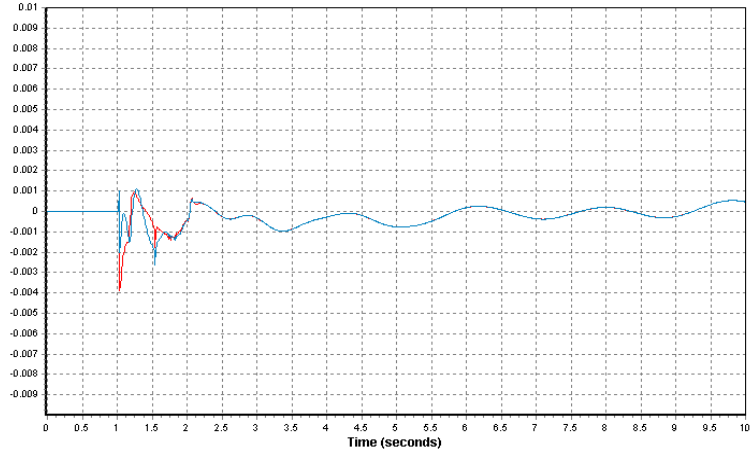

Frequency deviation at offshore HVAC bus (blue) and onshore bus (red)) [p.u]

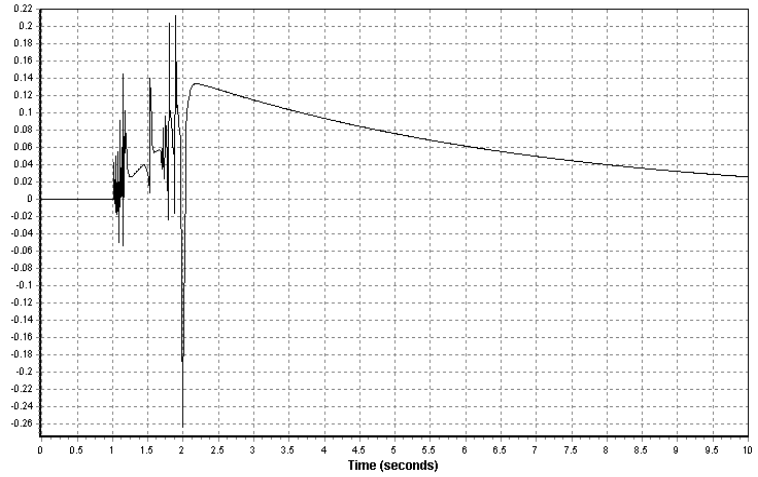

Frequency deviation at offshore HVDC bus (black) [p.u]

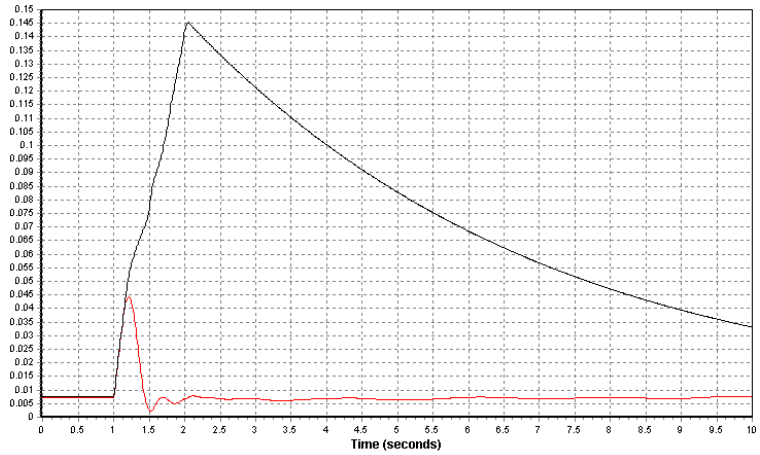

Speed deviation of the HVDC wind turbine generator (black) and the HVAC wind turbine generator (red) [p.u]

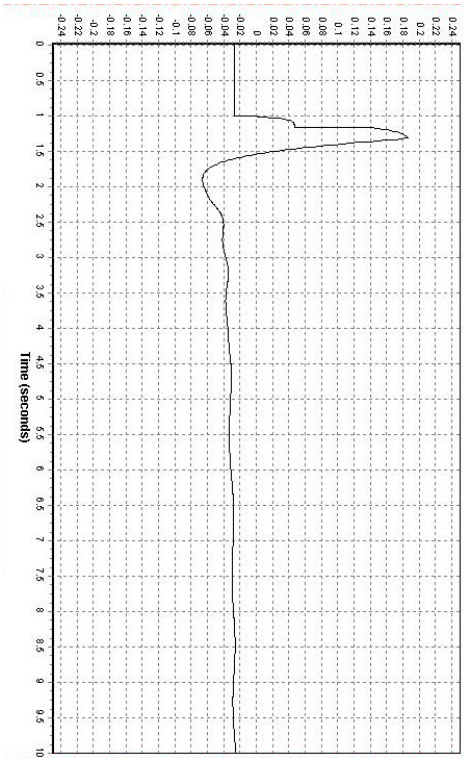

Reactive power from wind farm SVC [p.u]

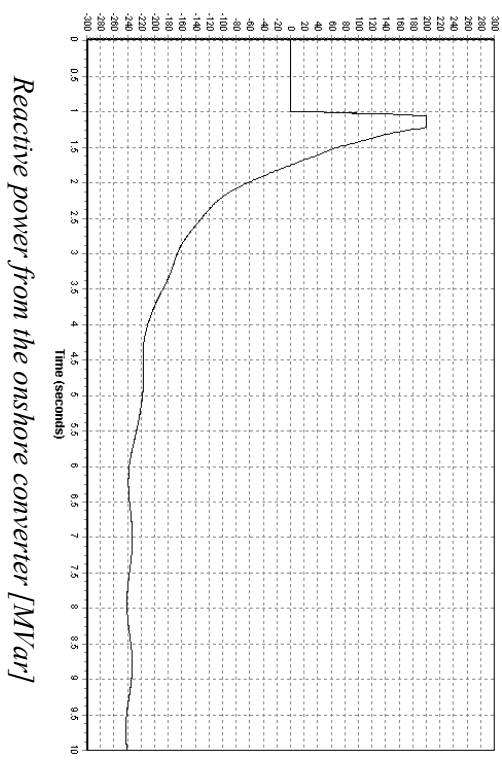

Reactive power from the onshore converter [MVar]

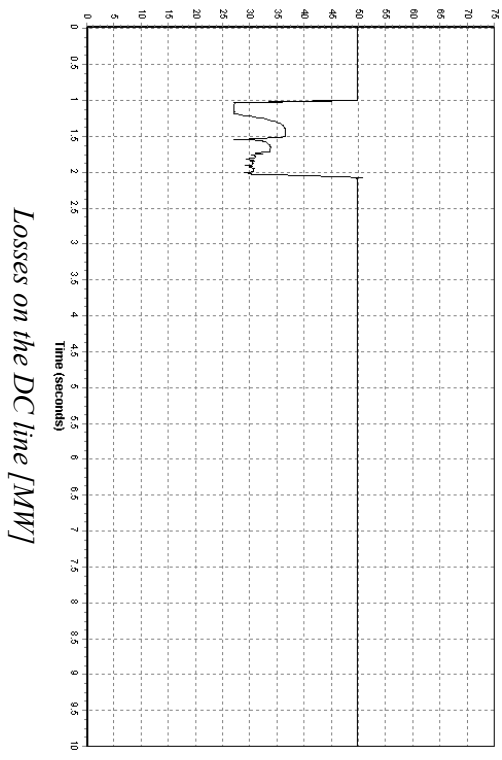

Losses on the DC line [MW]

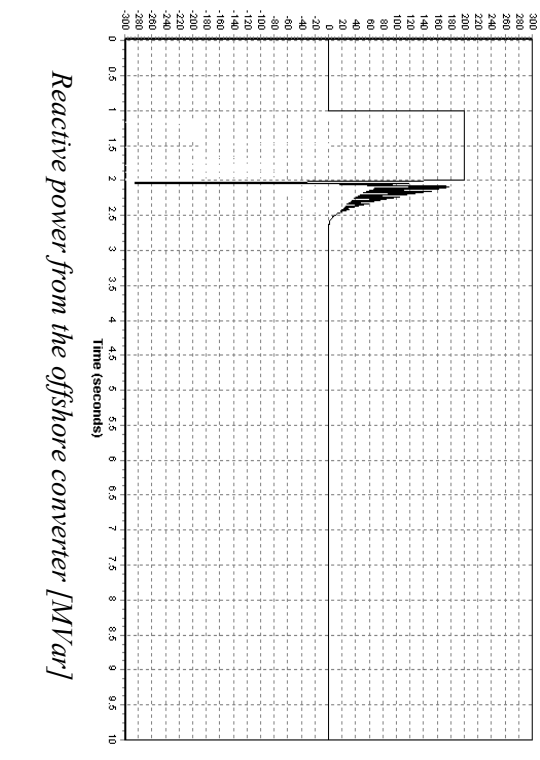

Reactive power from the offshore converter [MVar]

CONFIGURATION 4 : 2 HVAC LINKS CONNECTED TO HVDC, CONNECTION BUS 6000

Fault 1, bus fault at connection bus 6000

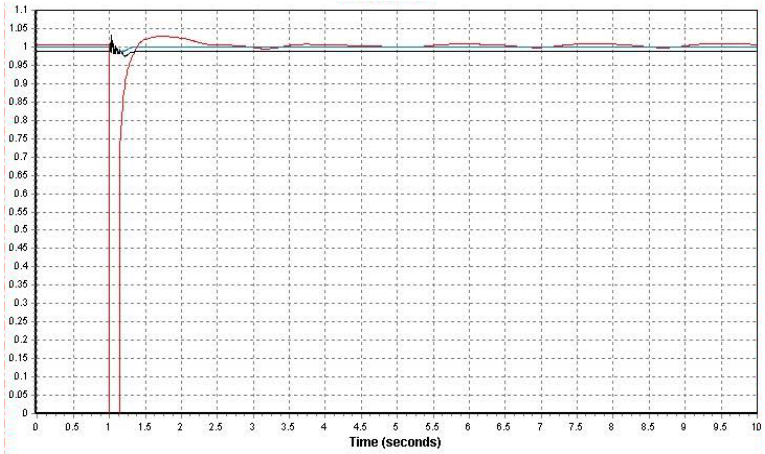

Voltage at offshore HVDC bus (black), at one of offshore wind farm bus (blue) and at the connection bus (red) [p.u]

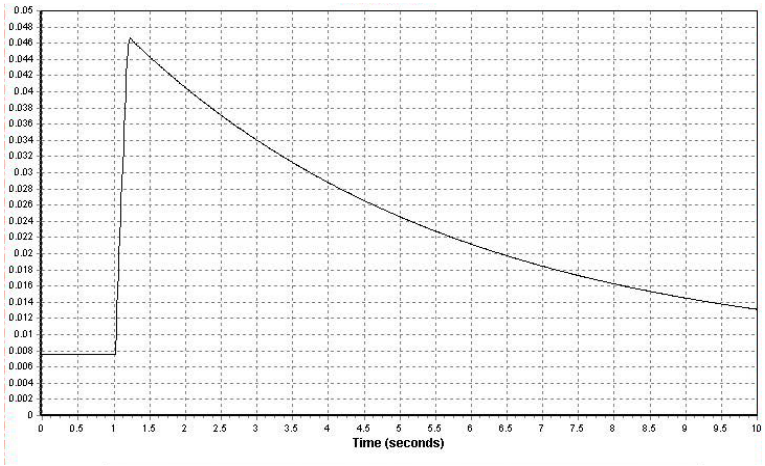

Speed deviation of the wind turbine generators [p.u]

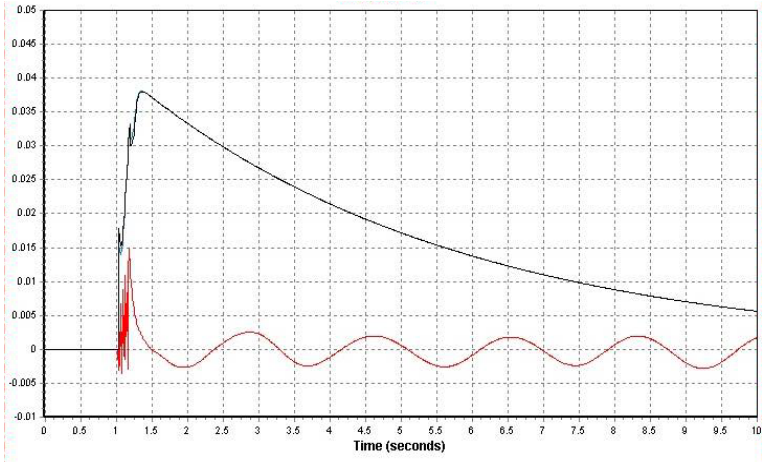

Frequency deviation at offshore HVDC bus (black), at one of offshore wind farm bus (blue) and at the connection bus (red) [p.u]

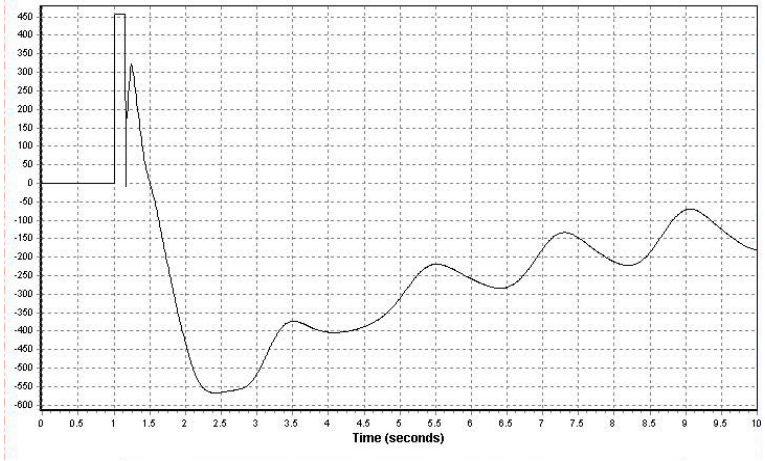

Reactive power from the onshore converter [MVar]

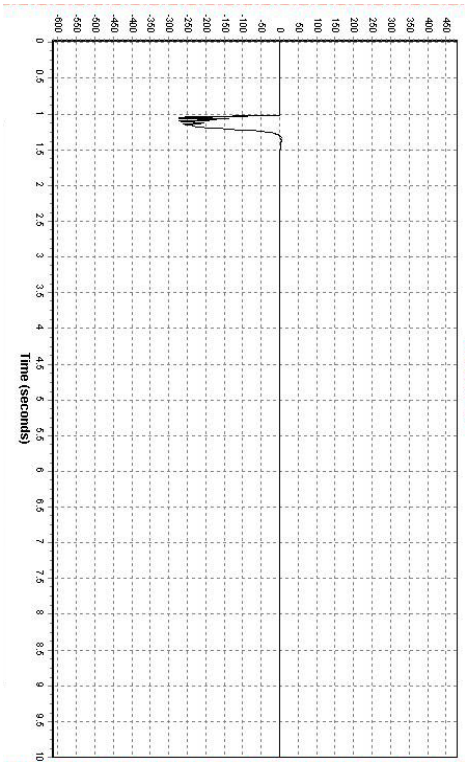

Reactive power from the offshore converter [MVar]

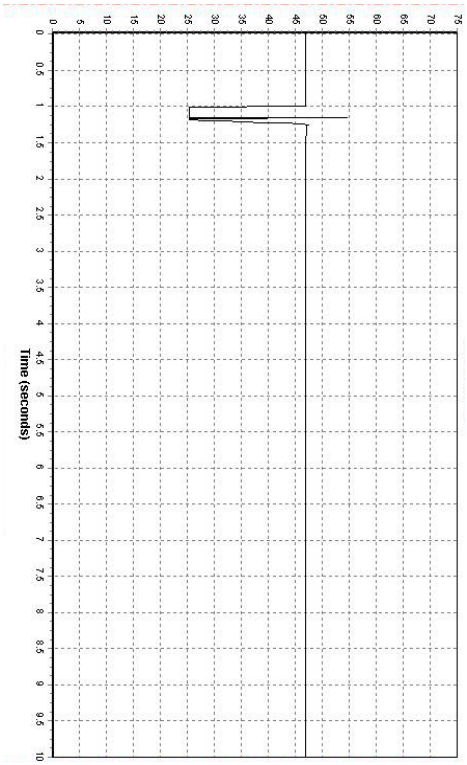

Losses on the DC line [MW]

Fault 2, bus fault at neighbour bus 5400

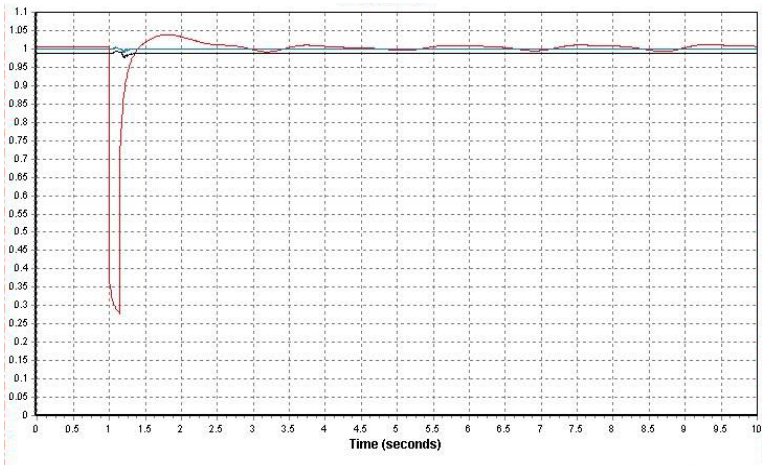

Voltage at offshore HVDC bus (black), at one of offshore wind farm bus (blue) and at the connection bus (red) [p.u]

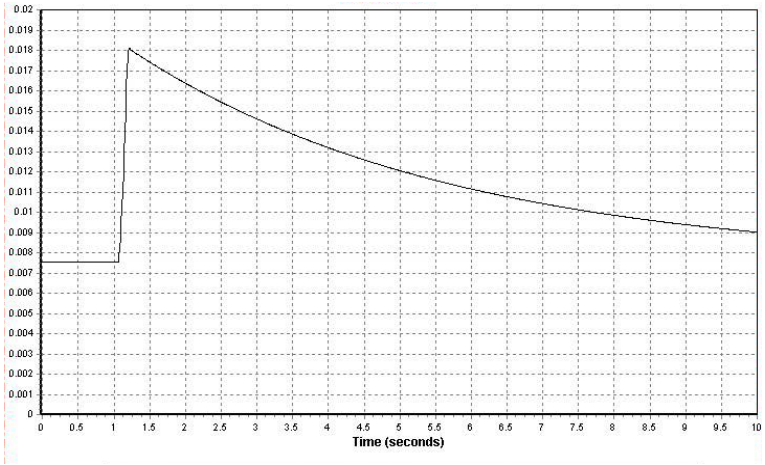

Speed deviation of the wind turbine generators [p.u]

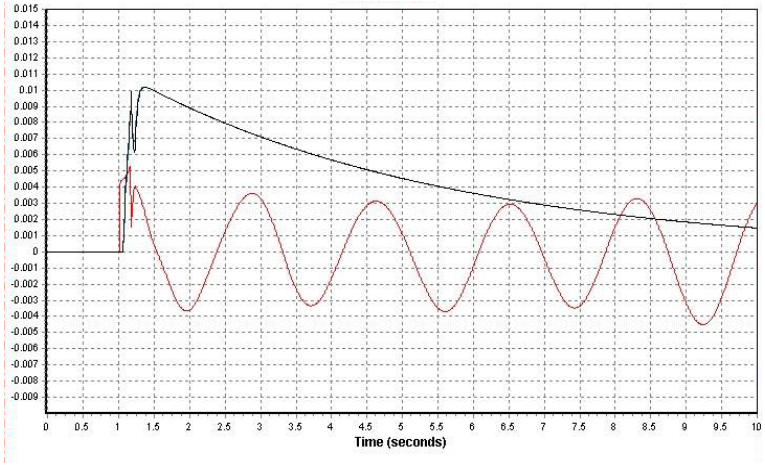

Frequency deviation at offshore HVDC bus (black), at one of offshore wind farm bus (blue) and at the connection bus (red) [p.u]

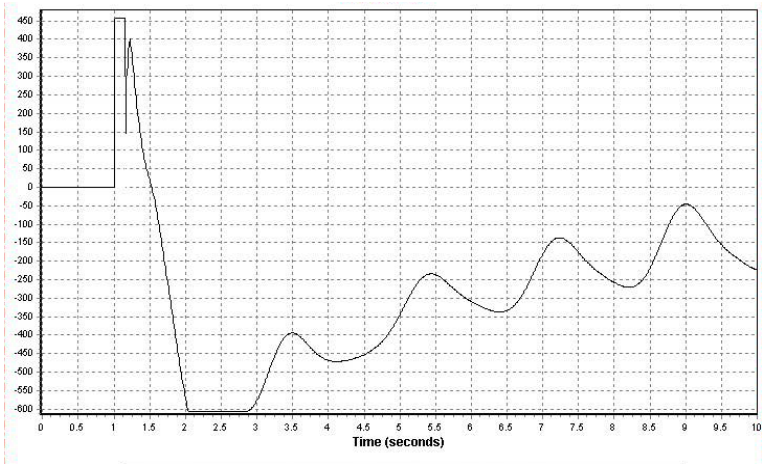

Reactive power from the onshore converter [MVar]

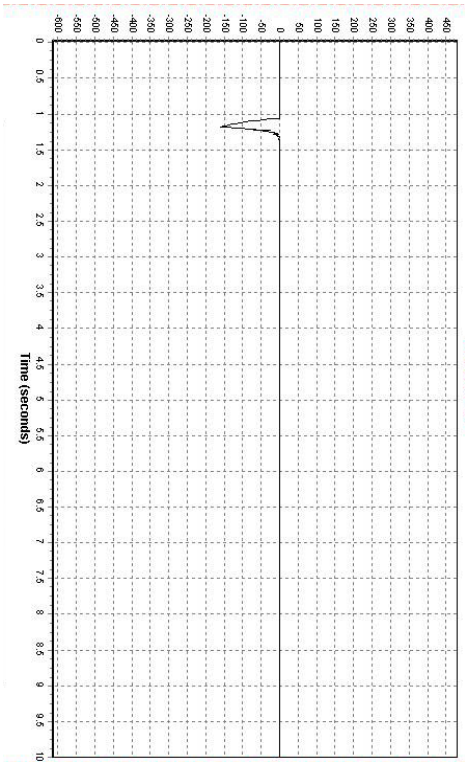

Reactive power from the offshore converter [MVar]

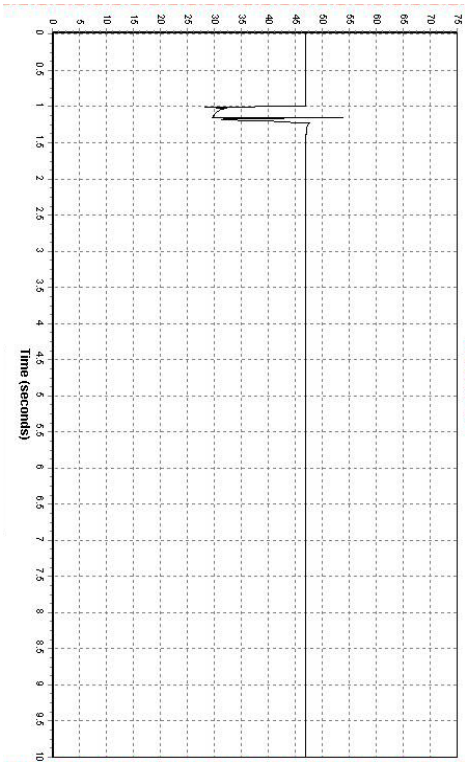

Losses on the DC line [MW]

Fault 3, line fault on the line from bus 6000 to bus 5400

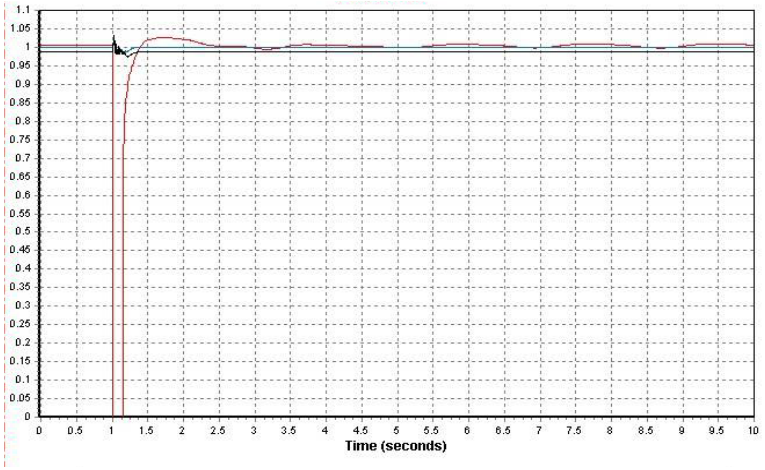

Voltage at offshore HVDC bus (black), at one of offshore wind farm bus (blue) and at the connection bus (red) [p.u]

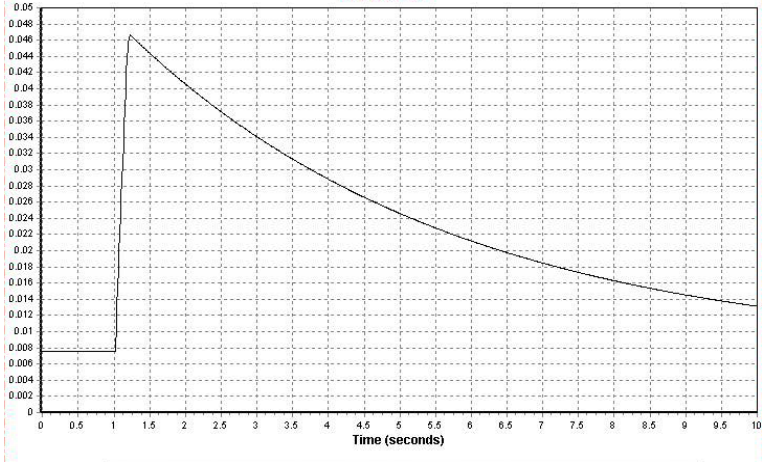

Speed deviation of the wind turbine generators [p.u]

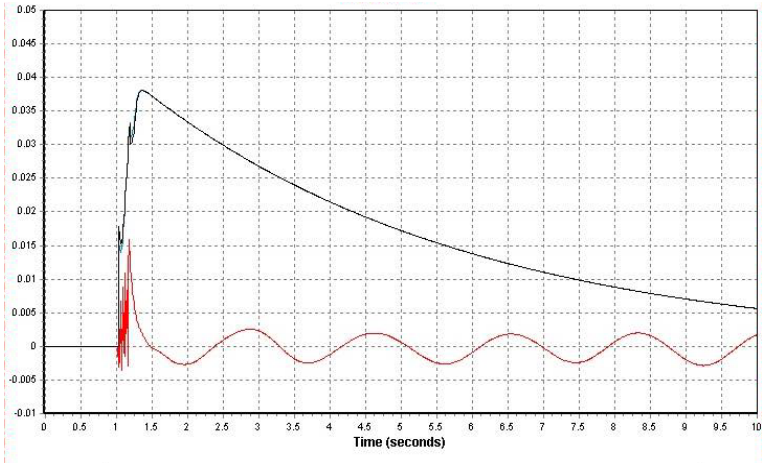

Frequency deviation at offshore HVDC bus (black), at one of offshore wind farm bus (blue) and at the connection bus (red) [p.u]

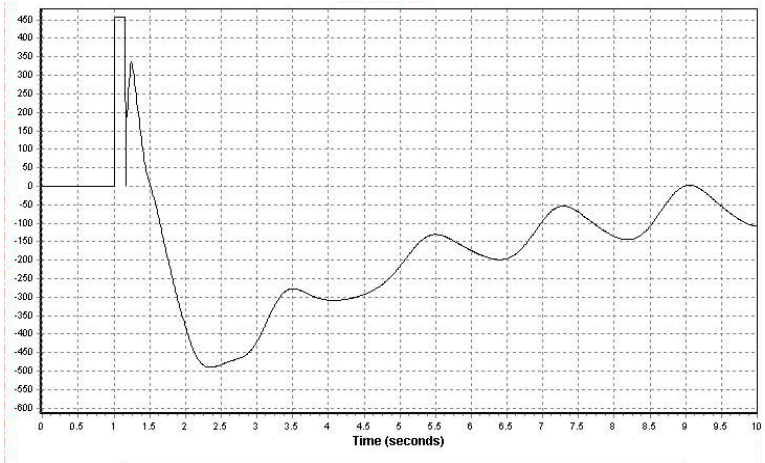

Reactive power from the onshore converter [MVar]

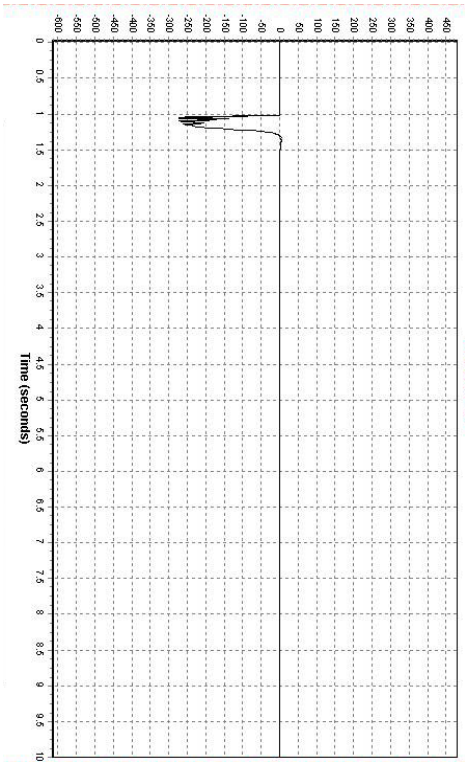

Reactive power from the offshore converter [MVar]

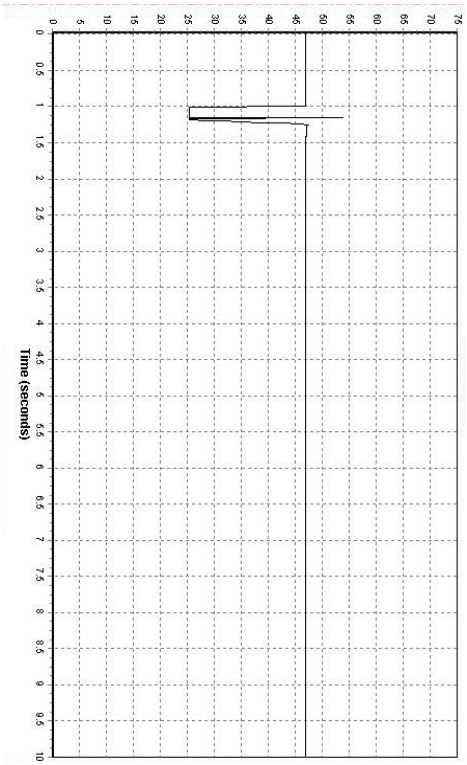

Losses on the DC line [MW]

CONFIGURATION 4 : 2 HVAC LINKS CONNECTED TO HVDC, CONNECTION BUS 5600

Fault 1, bus fault at connection bus 5600

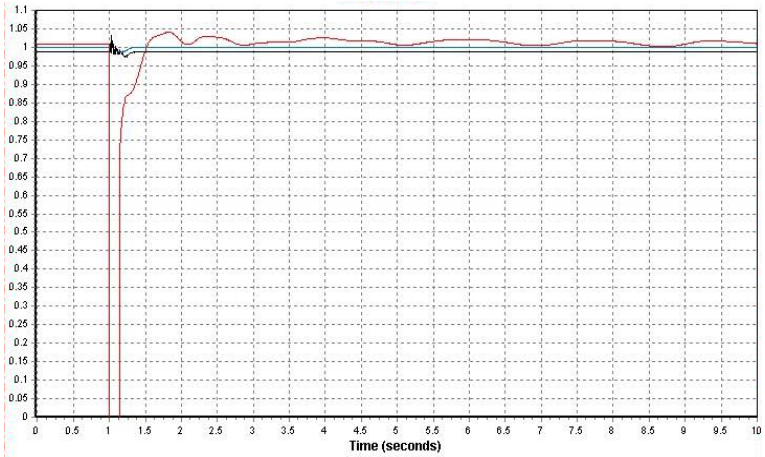

Voltage at offshore HVDC bus (black), at one of offshore wind farm bus (blue) and at the connection bus (red) [p.u]

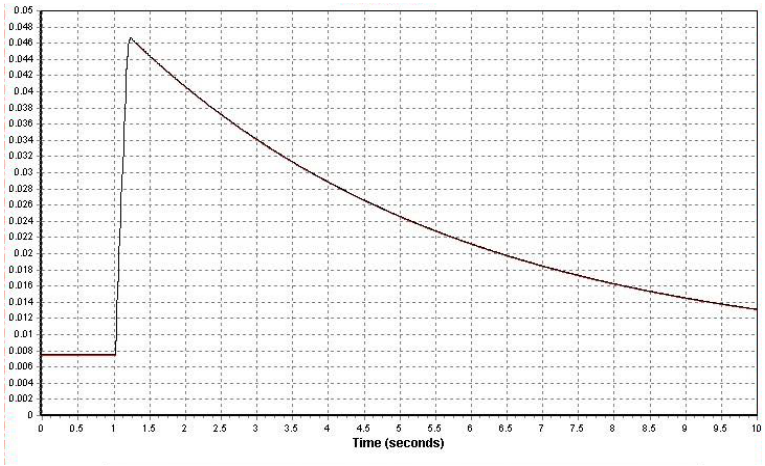

Speed deviation of the wind turbine generators [p.u]

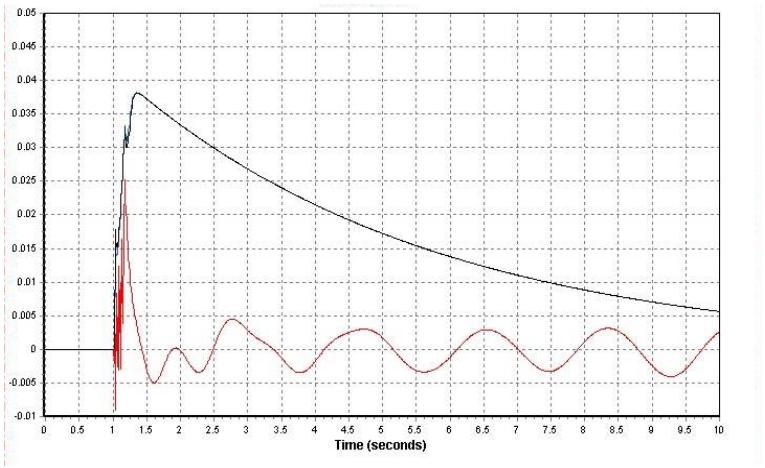

Frequency deviation at offshore HVDC bus (black), at one of offshore wind farm bus (blue) and at the connection bus (red) [p.u]

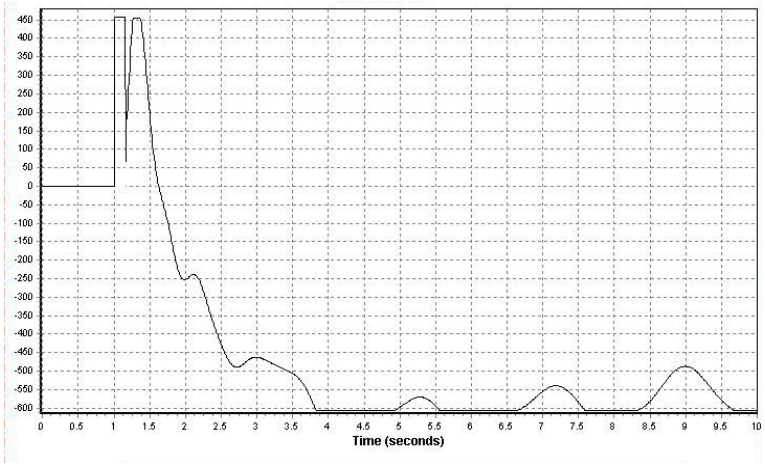

Reactive power from the onshore converter [MVar]

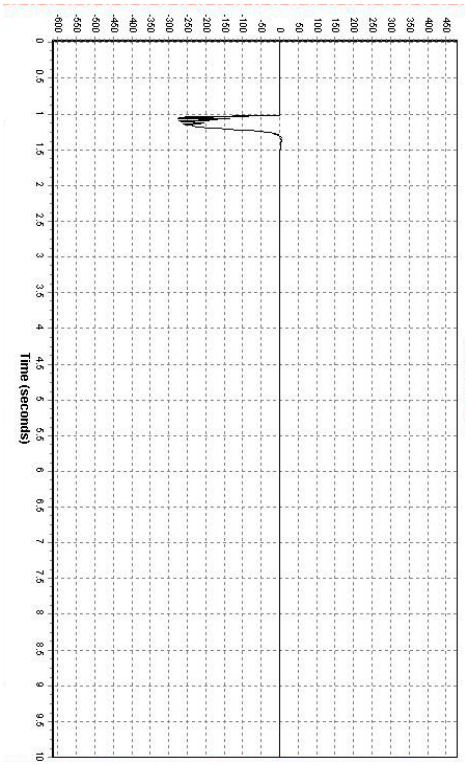

Reactive power from the offshore converter [MVar]

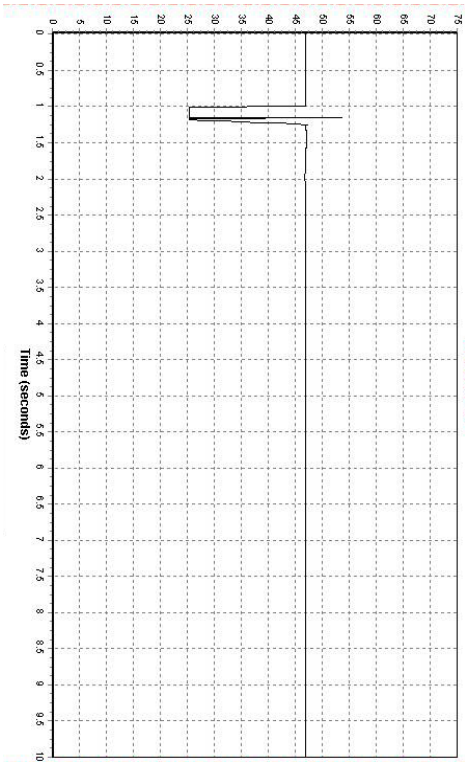

Losses on the DC line [MW]

Fault 2, bus fault at neighbour bus 5603

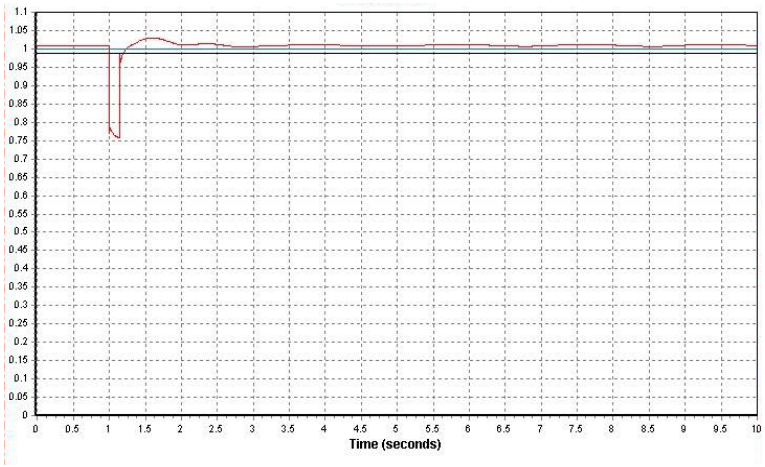

Voltage at offshore HVDC bus (black), at one of offshore wind farm bus (blue) and at the connection bus (red) [p.u]

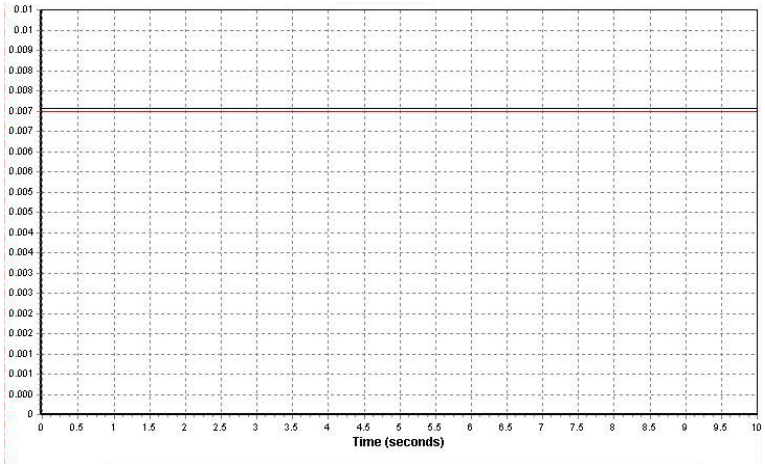

Speed deviation of the wind turbine generators [p.u]

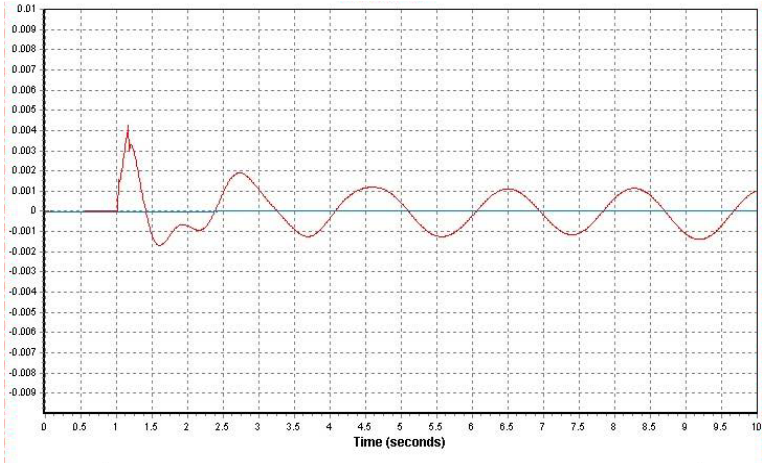

Frequency deviation at offshore HVDC bus (black), at one of offshore wind farm bus (blue) and at the connection bus (red) [p.u]

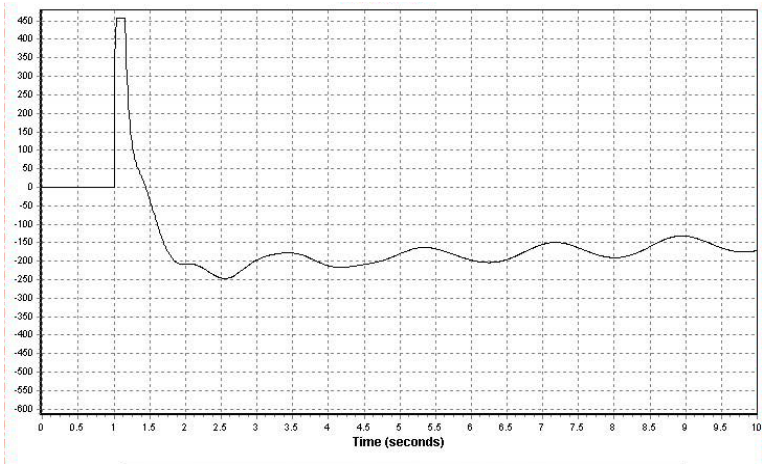

Reactive power from the onshore converter [MVar]

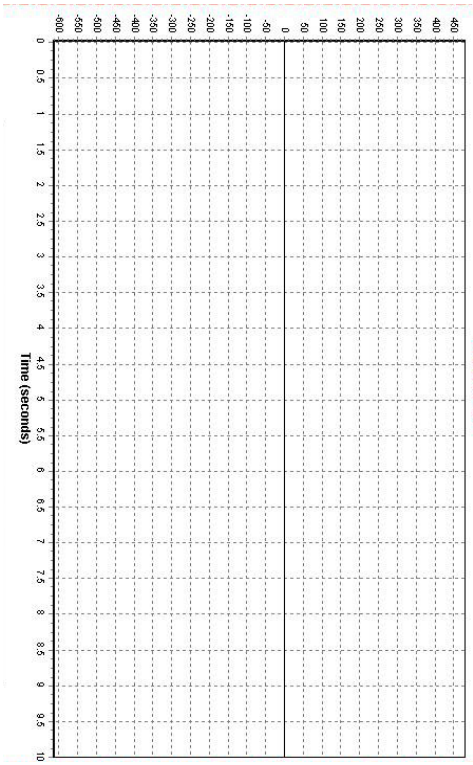

Reactive power from the offshore converter [MVar]

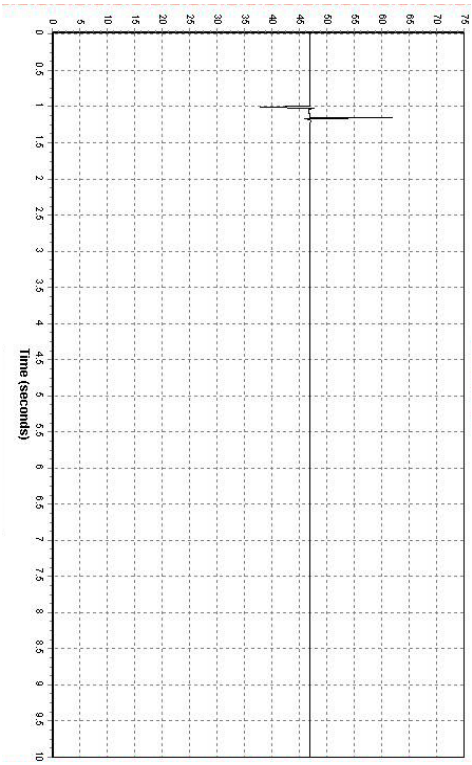

Losses on the DC line [MW]

Fault 3, line fault on the line from bus 5600 to bus 5603

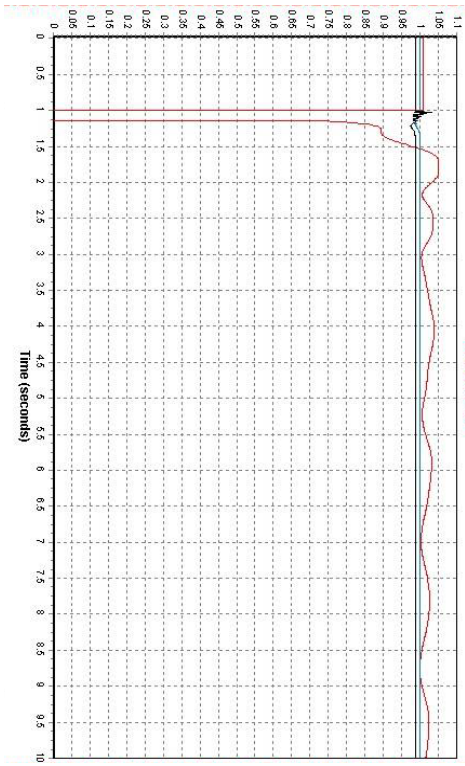

Voltage at offshore HVDC bus (black), at one of offshore wind farm bus (blue) and at the connection bus (red) [p.u]

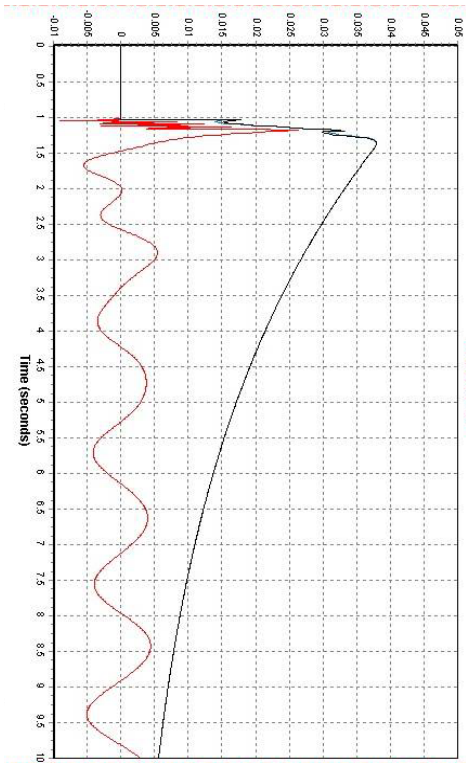

Frequency deviation at offshore HVDC bus (black), at one of offshore wind farm bus (blue) and at the connection bus (red) [p.u]

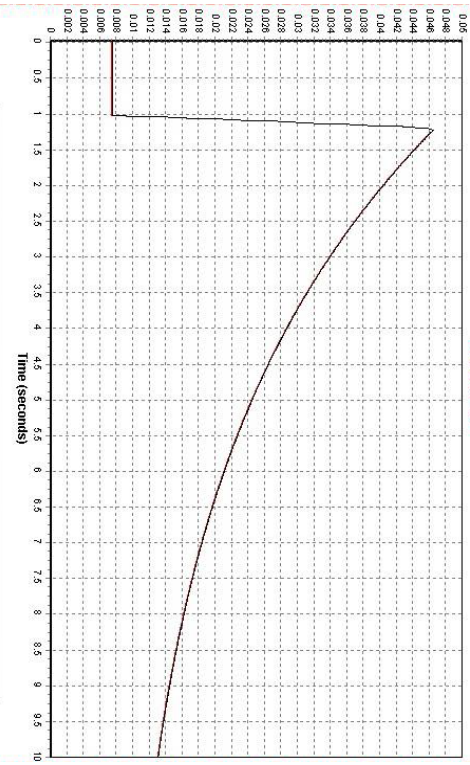

Speed deviation of the wind turbine generators [p.u]

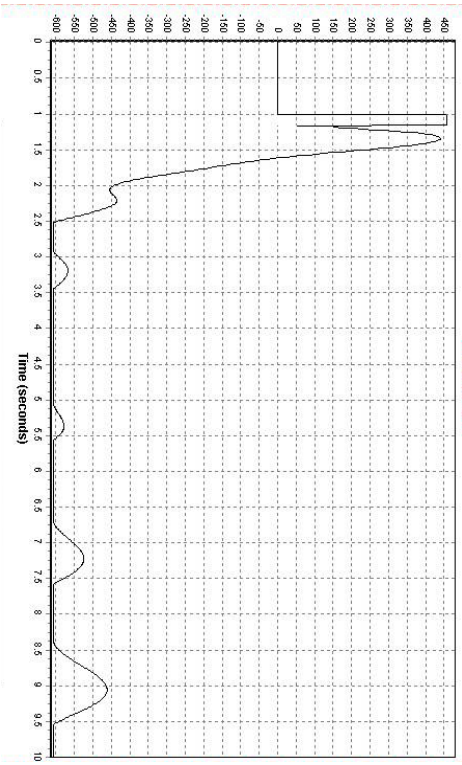

Reactive power from the onshore converter [MVar]

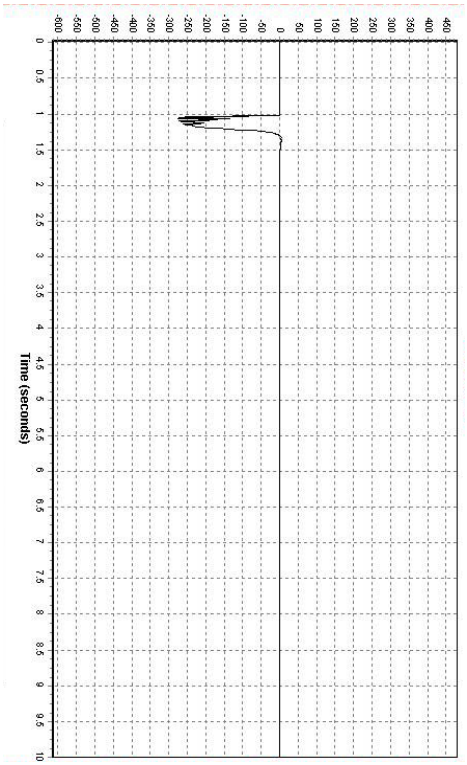

Reactive power from the offshore converter [MVar]

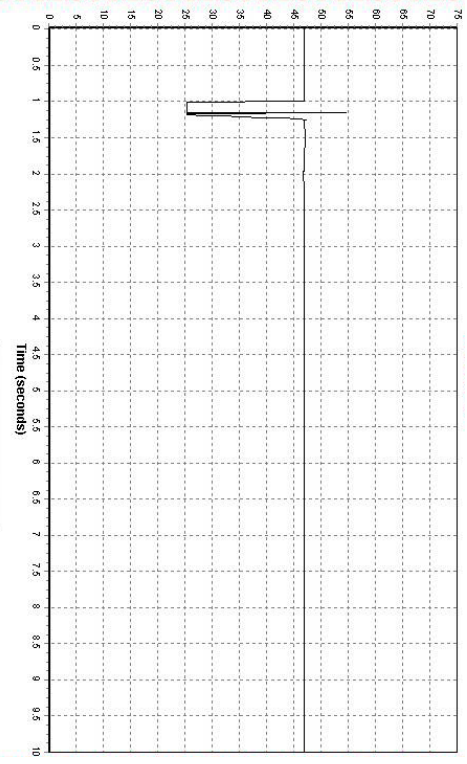

Losses on the DC line [MW]

CONFIGURATION 4 : 2 HVAC LINKS CONNECTED TO HVDC WITH A SVC CONNECTED AT THE OFFSHORE STATION, CONNECTION BUS 6000

Fault 4a, bus fault on one wind farm bus 1100

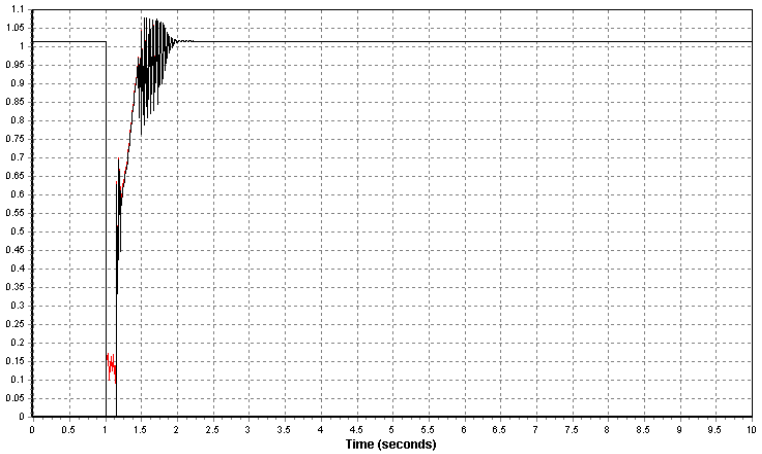

Voltage at the bus of the wind farm1 (black) and at bus of the wind farm 2 (red) [p.u]

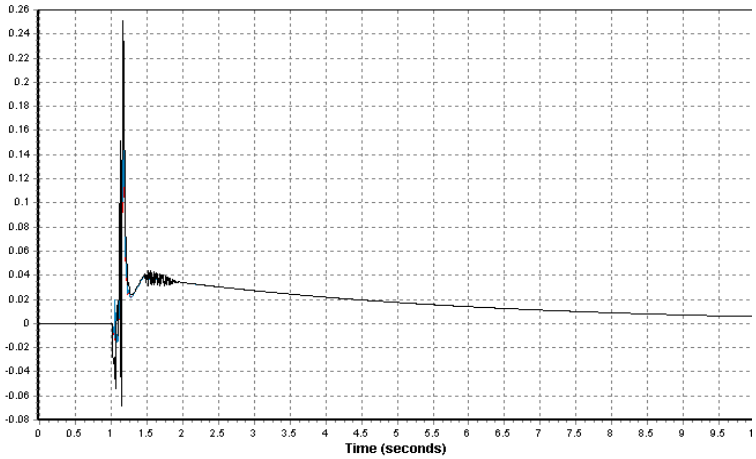

Frequency deviation at the wind farm 1 (blue),at the wind farm 2 (red) and at the offshore converter (black) [p.u]

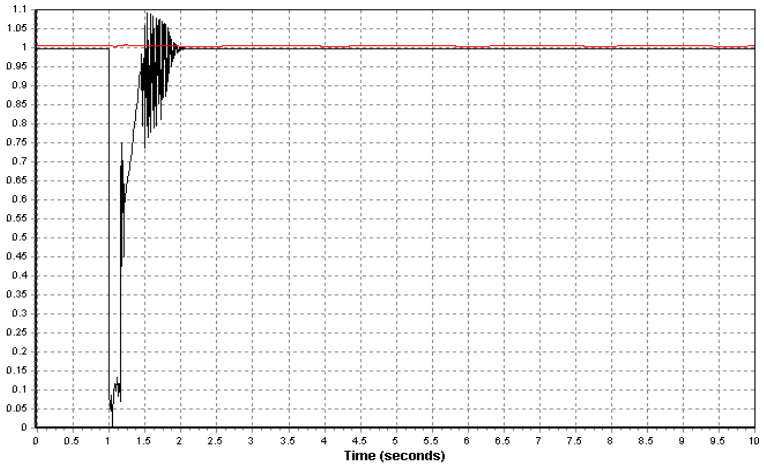

Voltage at the offshore converter (black) and at the connection point (red) [p.u]

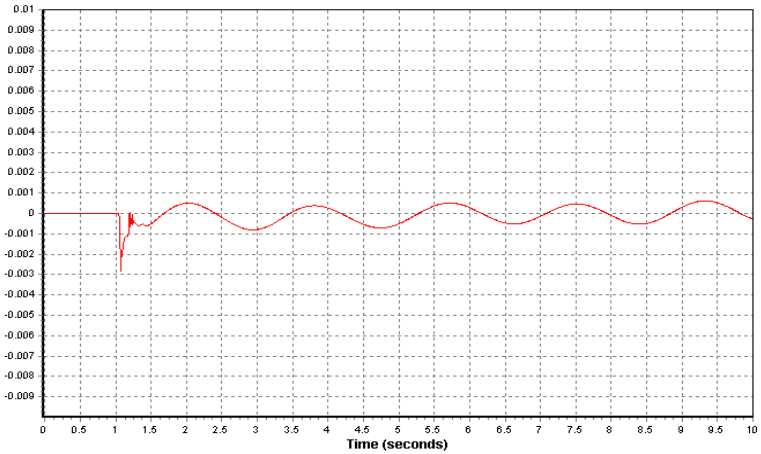

Frequency deviation at the connection bus(red) [p.u]

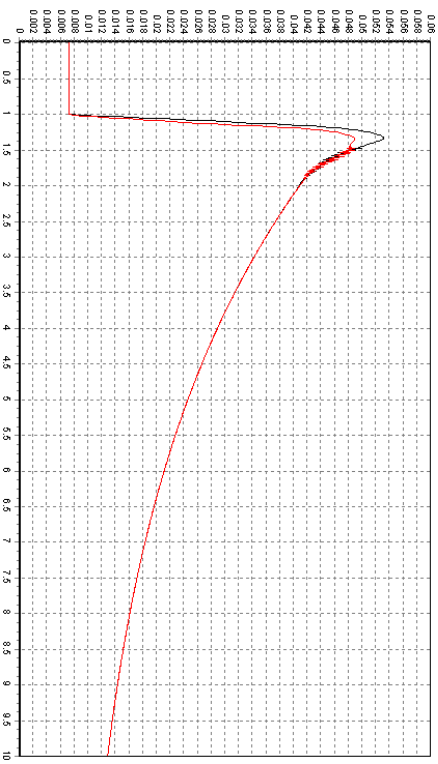

Speed deviation of the wind turbine 1 (black) and wind turbine 2 (red) [p.u]

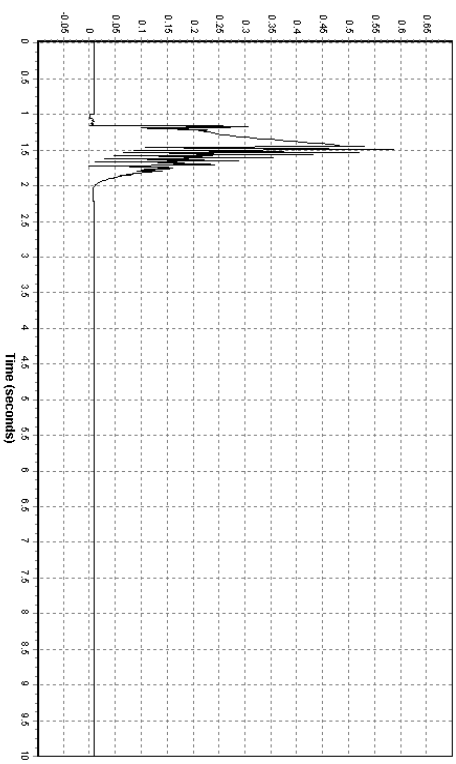

Reactive power from the SVC [p.u]

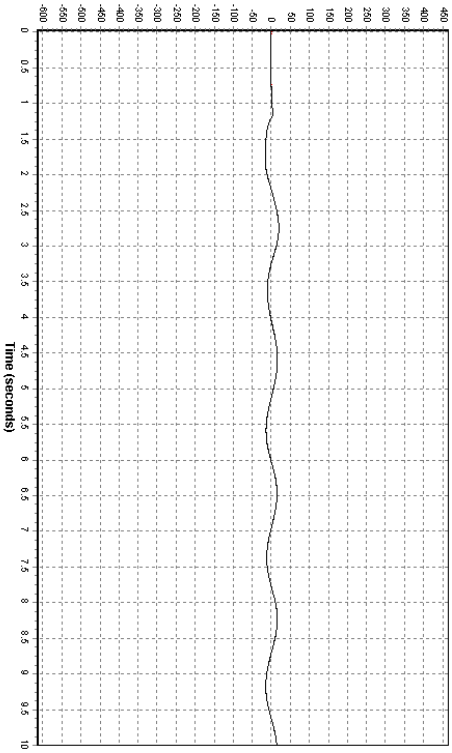

Reactive power from the onshore converter [MVar]

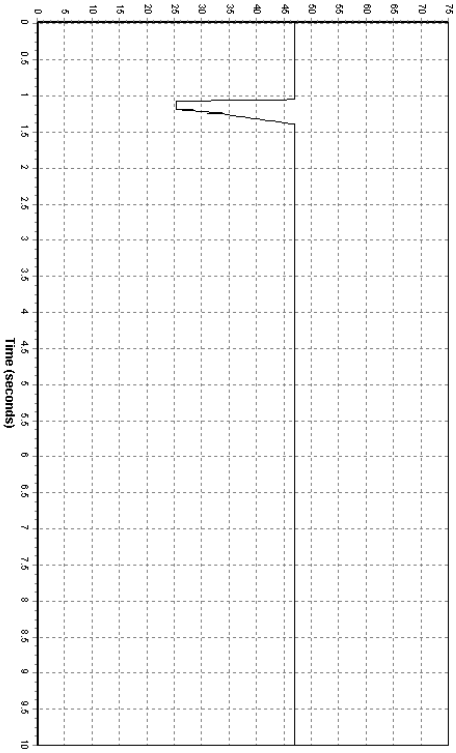

Losses on the DC line [MW]

Reactive power from the offshore converter [MVar]

Fault 4b, bus fault on the offshore converter bus

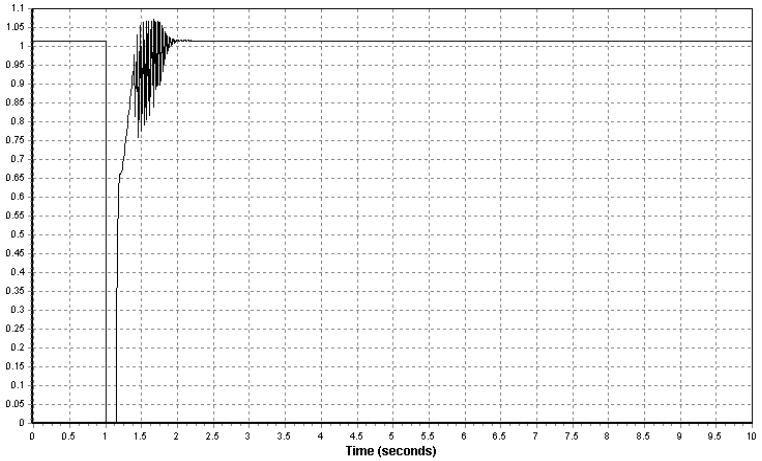

Voltage at the bus of the wind farm1 (black) and at bus of the wind farm 2 (red) [p.u]

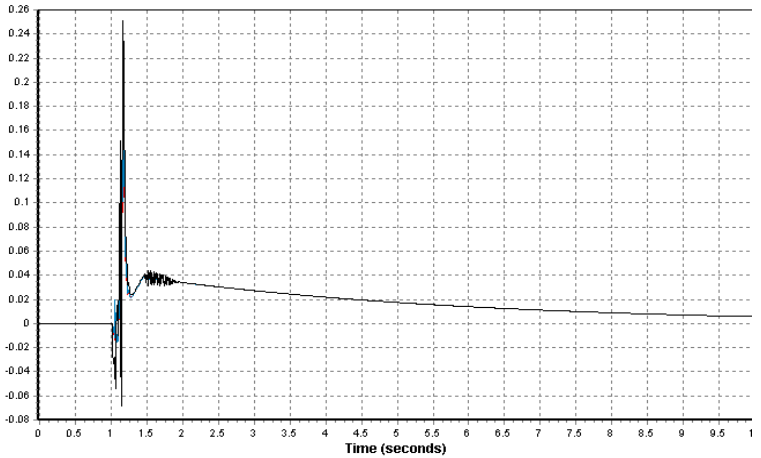

Frequency deviation at the wind farm 1 (blue), at the wind farm 2 (red) and at the offshore converter (black) [p.u]

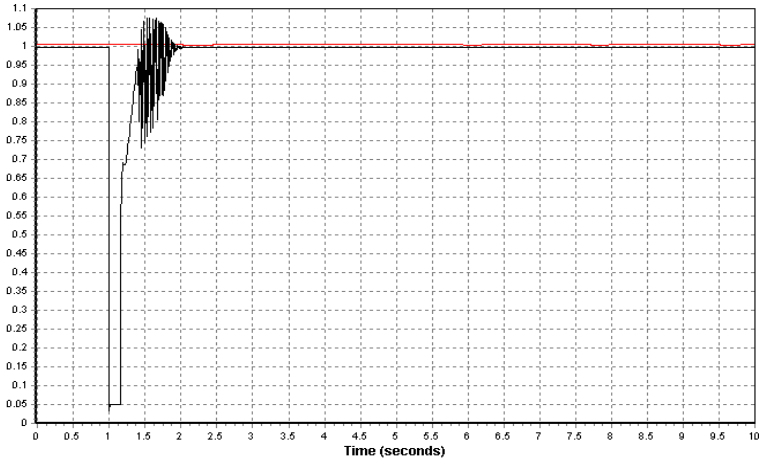

Voltage at the offshore converter (black) and at the connection point (red) [p.u]

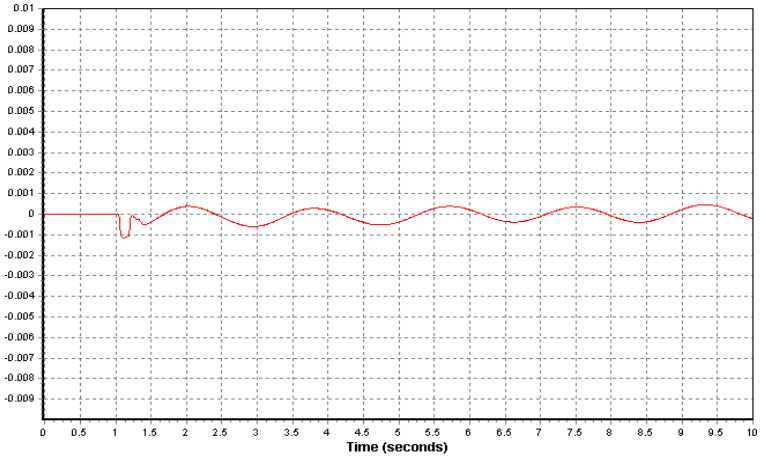

Frequency deviation at the connection bus(red) [p.u]

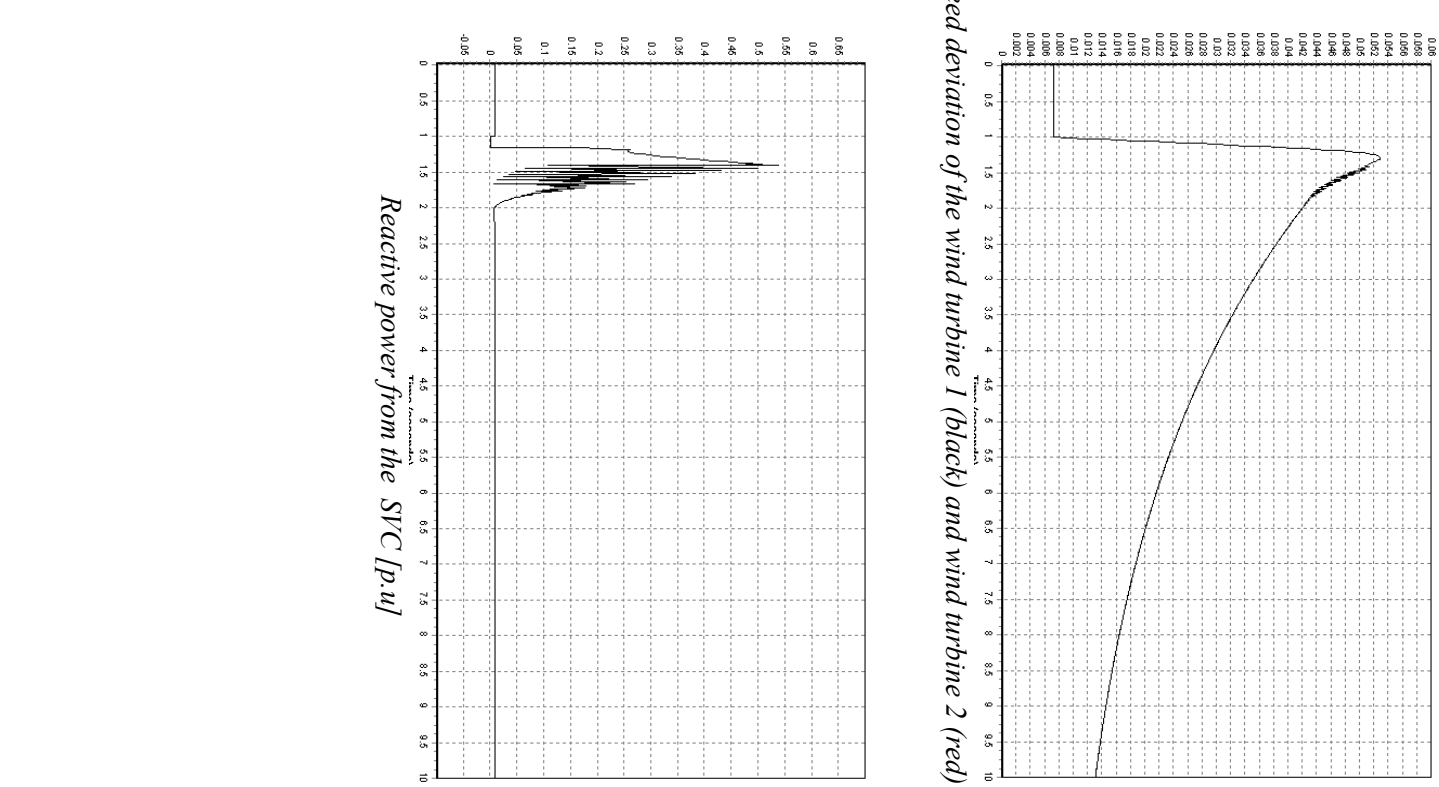

Speed deviation of the wind turbine 1 (black) and wind turbine 2 (red) [p.u]

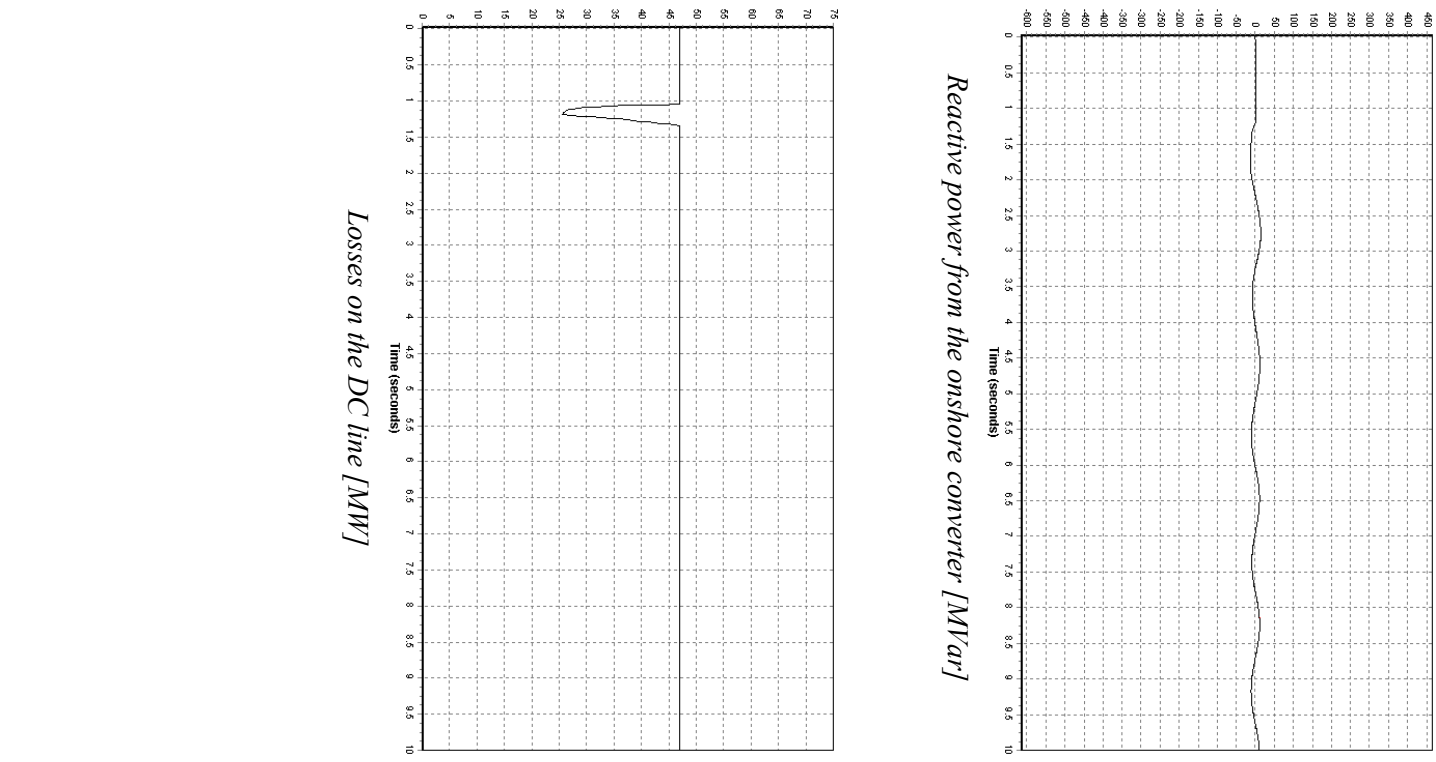

Reactive power from the onshore converter [MVar]

Reactive power from the SVC [p.u]

Losses on the DC line [MW]

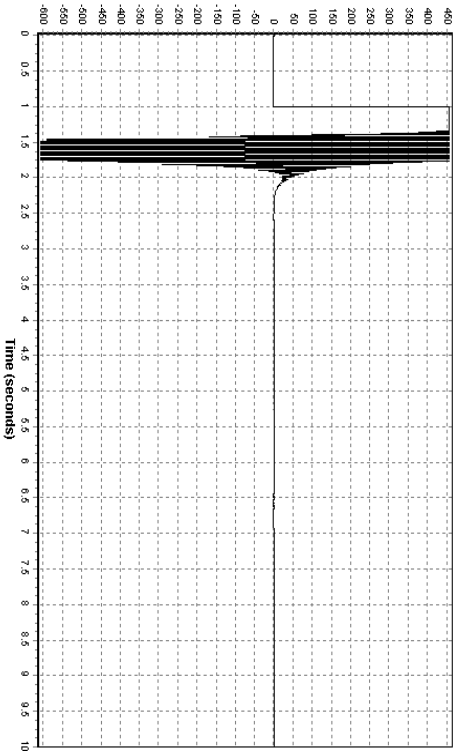

Reactive power from the offshore converter [MVar

CONFIGURATION 4 : 2 HVAC LINKS CONNECTED TO HVDC WITH A SVC CONNECTED AT THE OFFSHORE STATION, CONNECTION BUS 5600

Fault 4a, bus fault on one wind farm bus 1100

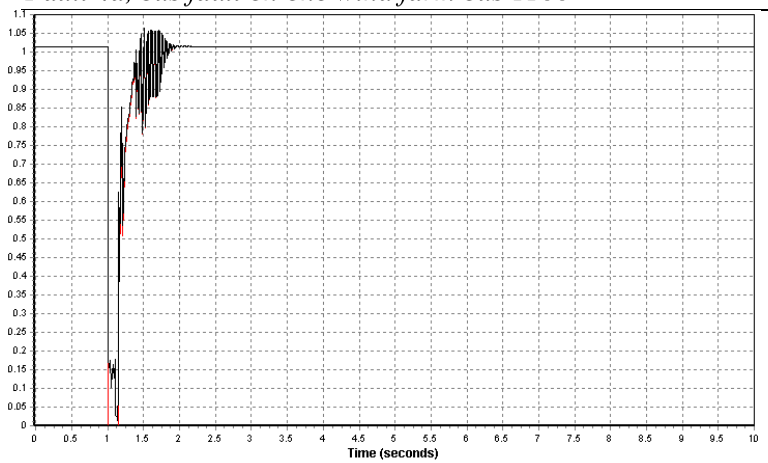

Voltage at the bus of the wind farm1 (black) and at bus of the wind farm 2 (red) [p.u]

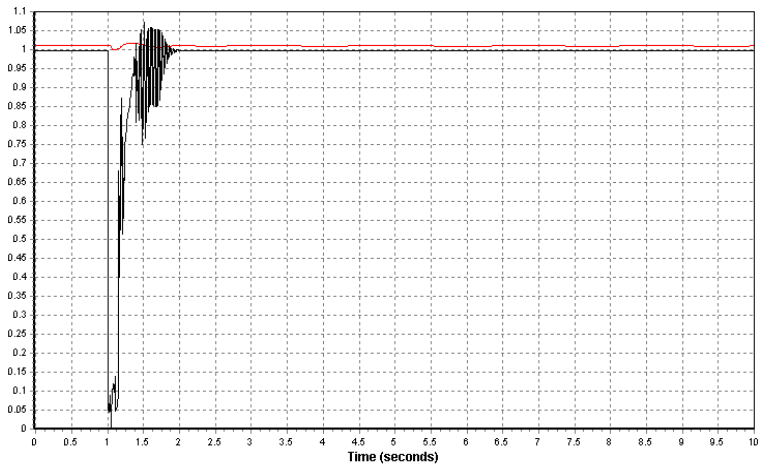

Voltage at the offshore converter (black) and at the connection point (red) [p.u]

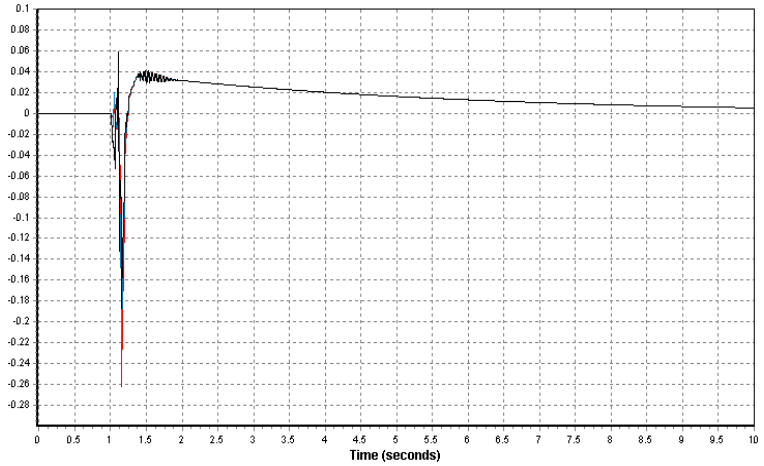

Frequency deviation at the wind farm 1 (blue),at the wind farm 2 (red) and at the offshore converter (black) [p.u]

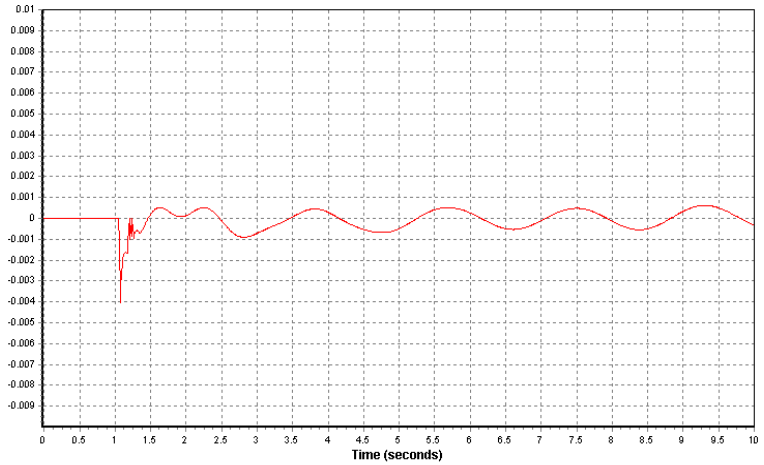

Frequency deviation at the connection bus(red) [p.u]

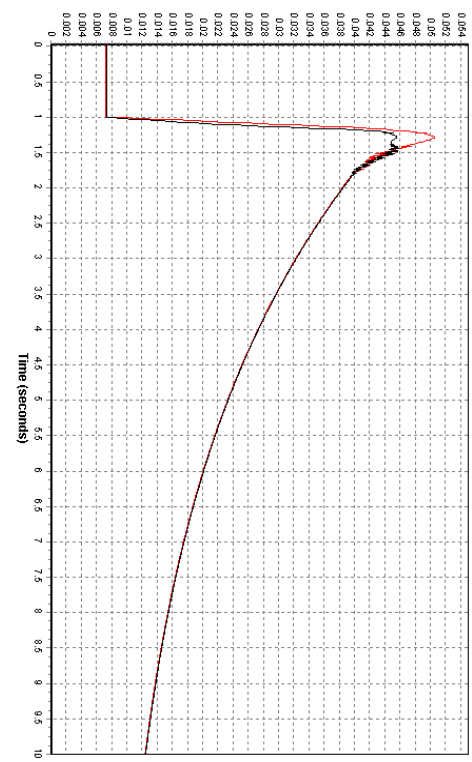

Speed deviation of the wind turbine 1 (black) and wind turbine 2 (red) [p.u]

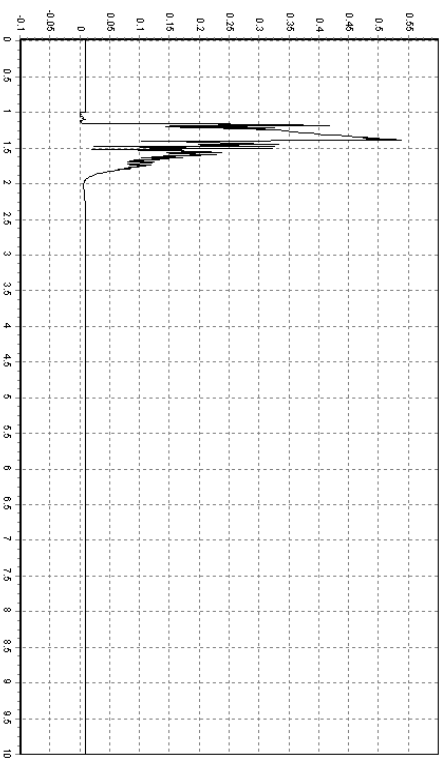

Reactive power from the SVC [p.u]

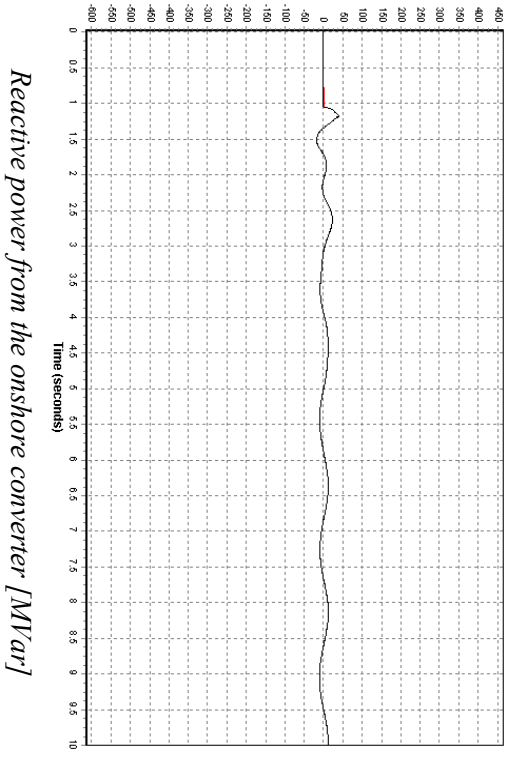

Reactive power from the onshore converter [MVar]

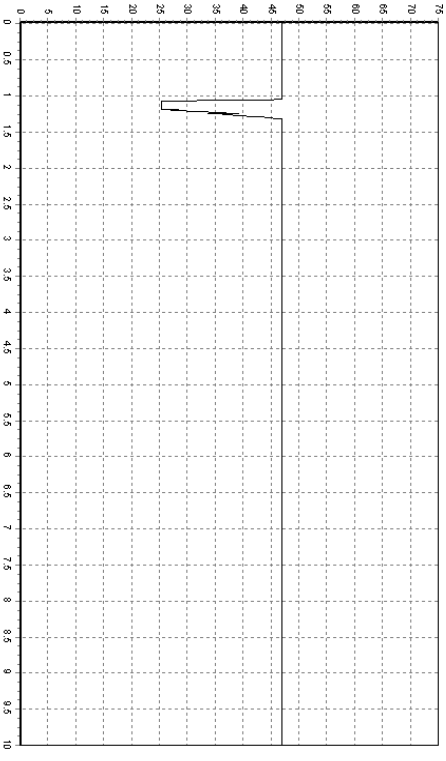

Losses on the DC line [MW]

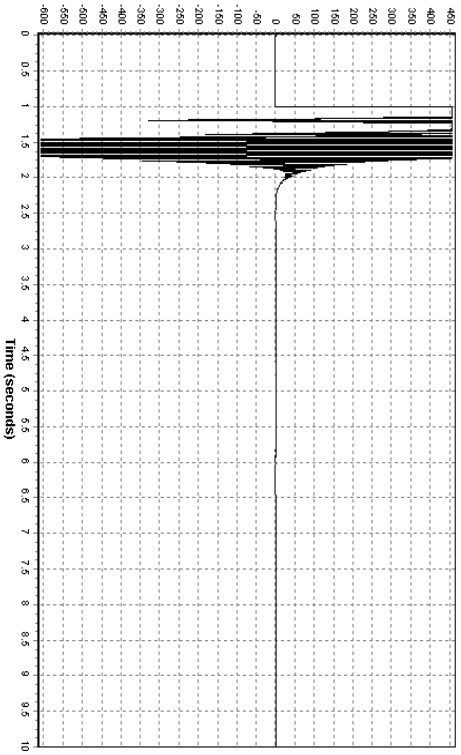

Reactive power from the offshore converter [MVar]

Fault 4b, bus fault on the offshore converter bus

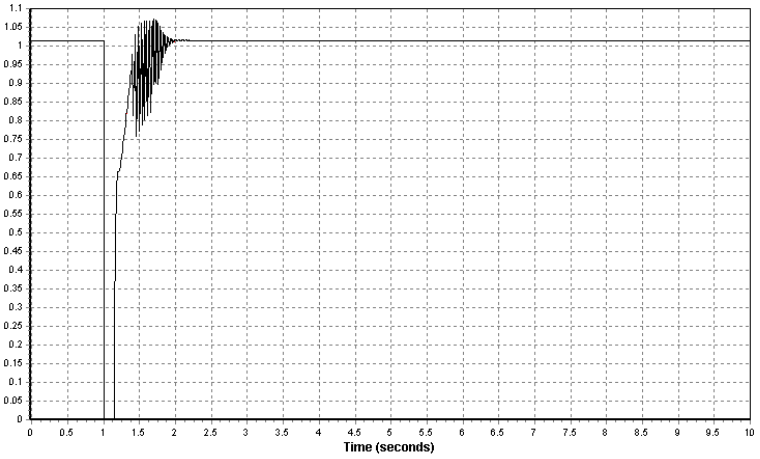

Voltage at the bus of the wind farm1 (black) and at bus of the wind farm 2 (red) [p.u]

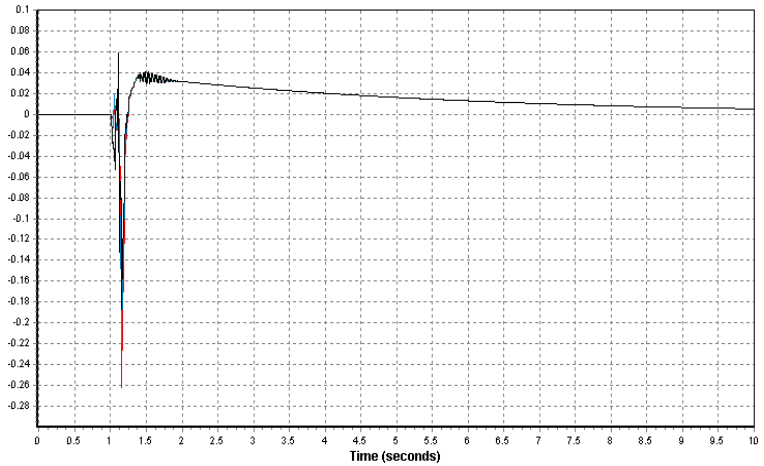

Frequency deviation at the wind farm 1 (blue),at the wind farm 2 (red) and at the offshore converter (black) [p.u]

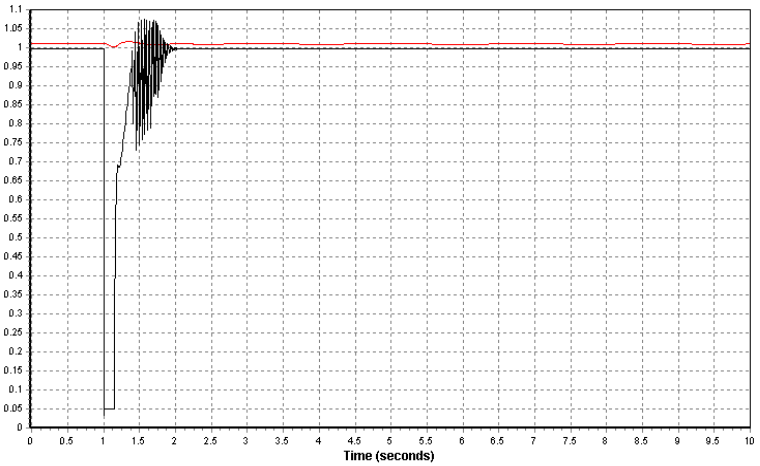

Voltage at the offshore converter (black) and at the connection point (red) [p.u]

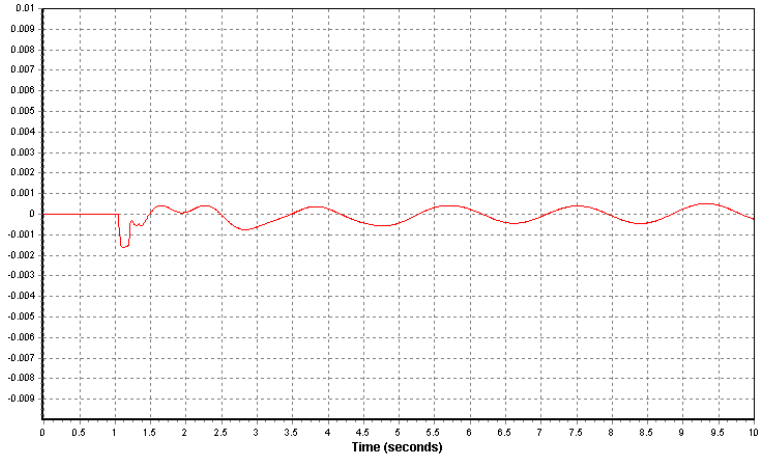

Frequency deviation at the connection bus(red) [p.u]

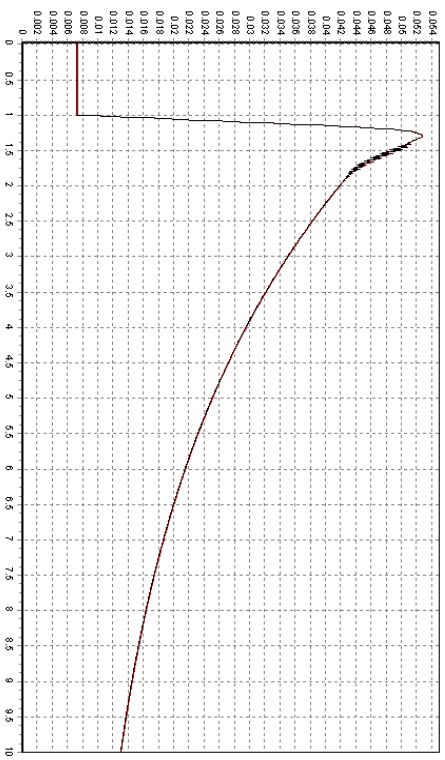

Speed deviation of the wind turbine 1 (black) and wind turbine 2 (red) [p.u]

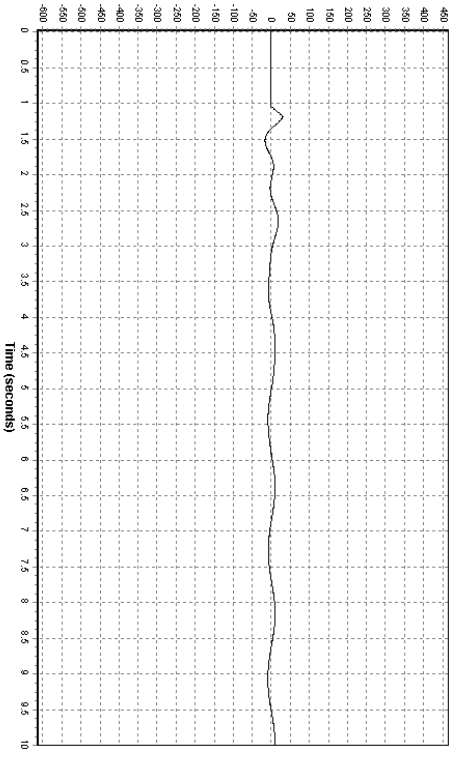

Reactive power from the onshore converter [MVar]

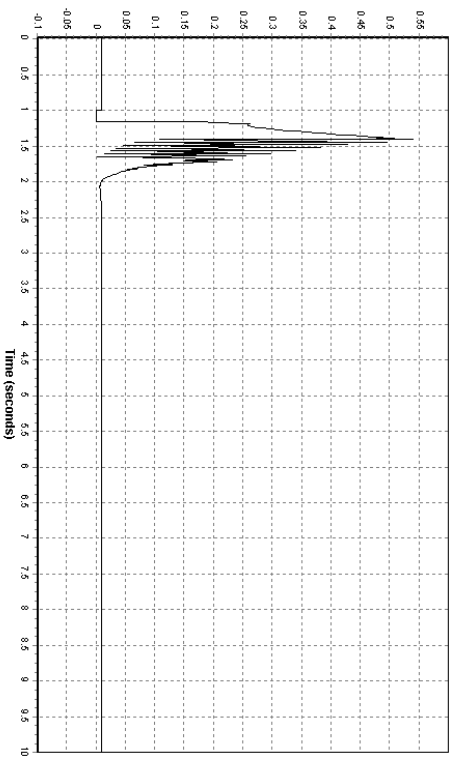

Reactive power from the SVC [p.u]

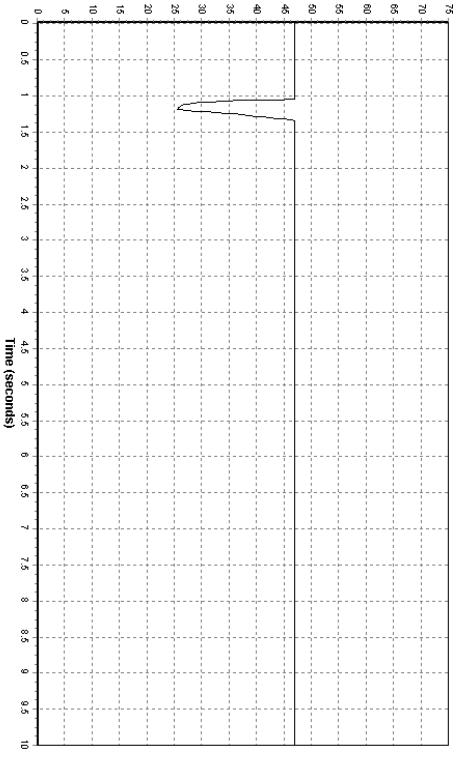

Losses on the DC line [MW]

Reactive power from the offshore converter [MVar]